



INSTITUTO
SUPERIOR
TÉCNICO

UNIVERSIDADE TÉCNICA DE LISBOA
INSTITUTO SUPERIOR TÉCNICO

**Nitrogen- and oxygen-based chelating ligands:
tris(pyrazolyl)methane and salicylamidate ligands**

Riccardo Wanke
(Licenciado)

Dissertação para obtenção do Grau de Doutor em Química

Orientador: Doutor Armando José Latourrette de Oliveira Pombeiro

Co-orientador: Doutora Luísa Margarida Dias Ribeiro de Sousa Martins

Júri

Presidente: Presidente do Conselho Científico do IST

Vogais: Doutor Armando José Latourrette de Oliveira Pombeiro

Doutor José do Rosário Acenso

Doutora Maria de Fátima Costa Guedes da Silva

Doutor João Paulo Nuner Cabral Telo

Doutora Luísa Margarida Dias Ribeiro de Sousa Martins

Julho de 2010

Nitrogen- and oxygen-based chelating ligands:

tris(pyrazolyl)methane and salicylamidate ligands

Table of contents

General Introduction	1
<hr/>	
Scorpionates Ligands: tris(pyrazolyl)methane	2
Characteristics	2
Functionalization	4
Salicylamidate based ligands	6
Characteristics	6
Functionalization	8
References	12
1 Scorpionates ligands	17
<hr/>	
Abstract	18
1.1 Introduction	19
1.2 Tpm: chemical properties	22
1.2.1 Tp and Tpm: differences and analogies	22
1.2.2 Tpm: stability	23
1.2.3 Tpm: characteristics	26
1.2.4 Tpm: the pyrazolyl ring	27
1.2.5 Tpm: the central carbon	32
1.3 Carbon functionalization of Tpm	34
1.3.1 The tris(pyrazolyl)methanesulfonate: Tpm _s	35
1.3.2 Tris-2,2,2-(1-pyrazolyl)ethanol (2): the hydroxy derivative	38
1.3.2.1 Reactivity of tris-2,2,2-(1-pyrazolyl)ethanol.	41
1.3.2.1.1 Substitution of the hydroxy group	41
1.3.2.1.2 Alkylation of tris-2,2,2-(1-pyrazolyl)ethanol.	43

1.3.2.1.3 Benzyl and 4-pyridyl derivative of tris-2,2,2-(1-pyrazolyl)ethanol	44
1.4 Carbon functionalization via radical pathway	46
1.4.1 Identification of the radical $\cdot\text{C}(\text{pz}^{\text{Me}_2})_3$, (7 ⁺)	48
1.4.2 Reactivity of $\cdot\text{C}(\text{pz}^{\text{Me}_2})_3$	53
1.4.3 Characterisation of $\text{C}(\text{pz}^{\text{Me}_2})_4$ (8)	54
1.4.4 Future studies on the radical pathway	56
1.5 Appendix 1.A: synthesis of other Tpm derivatives	58
1.5.1 Sterically hindered Tpm^{tBu} and Tpm^{iPr}	58
1.5.2 Polysulfonated derivative of Tpm: toward water solubility	58
1.5.3 Tpm derivatives incorporating new functional groups at the central carbon	59
1.6 Appendix 1.B: Dendritic-Tpm ligands	63
References	68
2 Cu^I complexes of Li(Tpms^{Ph})	75
<hr/>	
Abstract	76
2.1 Introduction	78
2.2 Syntheses of Tpm^{Ph} and $\text{Li}(\text{Tpms}^{\text{Ph}})$ and metal complexes	80
2.2.1 Syntheses of the sterically hindered scorpionates Tpm^{Ph} and $\text{Li}(\text{Tpms}^{\text{Ph}})$	80
2.2.2 Syntheses of the Cu ^I complexes $[\text{Cu}(\text{Tpms}^{\text{Ph}})\text{L}]$ [$\text{L} = \text{MeCN}$ (20), PTA (21), HMT (22)] and $[\text{Cu}(\text{Tpms}^{\text{Ph}})(\text{mPTA})][\text{PF}_6]$ (23)	81
2.3 X-ray molecular structures of complexes $[\text{Cu}(\text{Tpms}^{\text{Ph}})\text{L}]$ [$\text{L} = \text{MeCN}$ (20), PTA (21), HMT (22)] and $[\text{Cu}(\text{Tpms}^{\text{Ph}})(\text{mPTA})][\text{PF}_6]$ (23)	84
2.4 NMR solution studies	91
2.5 Cu-Tpms^{Ph} complexes (20)-(23): overview	95
2.6 Appendix 2.A: study of the Cu^I-Tpms^{Ph} system on the activation of nitriles, isonitriles and carbon monoxide	98
2.6.1 Syntheses of $[\text{Cu}(\text{Tpms}^{\text{Ph}})(\text{CyNC})]$ (24) and $[\text{Cu}(\text{Tpms}^{\text{Ph}})(\text{XyNC})]$ (25) (CyNC = cyclohexyl isocyanide; XyNC = 2,6-dimethylphenyl isocyanide) and their reactivity toward nucleophiles: 3-iminoisoindolin-1-one and methylamine	98

2.6.2 Synthesis of [Cu(Tpms ^{Ph})(CO)] (27) and its unexpected instability	102
2.7 Appendix 2.B: dioxygen coordination at the ‘Cu^I-Tpms^{Ph}’ system	104
2.8 Appendix 2.C: catalytic studies of [Cu(Tpms^{Ph})(MeCN)] (20)	108
References	111

3 Toward an extra coordinating site: TpmPy and TpmPy^{Ph}

117

Abstract	118
3.1 Introduction	119
3.2 TpmPy (3) and TpmPy^{Ph} (19)	121
3.3 Coordination chemistry of (3) and (19)	123
3.3.1 Reaction of (3) with Fe ^{II}	123
3.3.2 Reactions of (3) and (19) with Ni ^{II} , Zn ^{II} and V ^{III}	128
3.3.3 Reactions of (3) and (19) with Pd ^{II}	133
3.4 Applications of (3) and (19) to the synthesis of bimetallic complexes	138
3.5 Pyridyl-functionalized scorpionates: overview	141
References	143

4 Salicylamidate ligands: a new N₂O class of chelating phenol ligands

147

Abstract	148
4.1 New class of salicylamidate ligands	149
4.2 H-bonded salicylamidate ligands	152
4.2.1 Synthesis and characterisation of phenolates [NBu ₄][^{OHNH} L] (42), [NBu ₄][^{NHMe} L] (43) and [NBu ₄][^{NMe2} L] (44)	154
4.2.1.1 X-ray structures	155
4.2.1.2 ¹ H-NMR spectra.	157

4.2.1.3 IR spectra	159
4.2.1.4 Electrochemistry	160
4.2.1.5 EPR spectra	163
4.2.1.6 UV/vis spectra	165
4.2.2 Overview	166
4.2.4 Conclusions	170
References	171
5 Salicylamidate ligands: coordination chemistry	175
<hr/>	
Abstract	176
5.1 Introduction	177
5.2 Polianionic ligands	178
5.3 Ni^{II}-complex	179
5.3.1 Synthesis and characterisation of [NBu ₄] ₂ [Ni ₂ (^{OHNH} L) ₂]	179
Scheme 5.3. Synthesis of [NBu ₄] ₂ [Ni ₂ (^{OHNH} L) ₂] (47)	179
5.3.2 Oxidation of [NBu ₄] ₂ [Ni ₂ (^{OHNH} L) ₂]	181
5.3.2.1 Electrochemical studies of [NBu ₄] ₂ [Ni ₂ (^{OHNH} L) ₂]	182
5.3.2.2 Generation of (47 ⁺) and (47 ⁺⁺)	185
5.3.2.3 Electronic structures of (47 ⁺) and (47 ⁺⁺)	186
5.4 Overview	193
References	196
6 Experimental data	197
<hr/>	
6.1 Synthetic procedures	198
6.2 Crystallographic data	239
6.3 Electrochemical experiments	243
6.3.1 Cyclic Voltammetry	243
Apparatus	243
Internal standard:	243

General Procedure:	243
Reversibility tests:	244
6.3.2 Coulometry:	245
6.3.3 Electrochemical results	246
6.3.3.1 Results of reversibility studies of the oxidation/reduction processes for (42 ⁻), (43 ⁻) and (44 ⁻)	250
6.3.3.2 Reversibility of the oxidation/reduction process of Fc ^{0/+} (ferrocene/ferrocinium)	251
6.3.3.3 Reversibility of the oxidation/reduction process of (42 ⁻)/(42 [•])	252
6.3.3.4 Reversibility of the oxidation/reduction processes of (43 ⁻)/(43 [•]) and (43 ⁻)/(44 [•])	255
6.4 EPR conditions	258
6.5 Computational data	259
6.6 Catalytic studies	261
6.7 Compounds	263
References	280

Acknowledgements

I would like to thank

prof. Armando J. L. Pombeiro
dr. Luísa M. D. R. S. Martins

dr. M. Fátima C. Guedes da Silva
dr. Piotr Smoleński
dr. Maxim L. Kuznetsov
dr. João Paulo N. C. Telo
dr. Konstantin V. Luzyanin
Ricardo Fernandes
dr. M. Conceição Oliveira
dr. Alexandra M. Antunes
Stefano Lancianesi
dr. Paul Servin
prof. Anne-Marie Caminade
Group V

FCT for grant (SFRH/BD/23187/2005)

AQUACHEM network (Marie Curie Actions) (MRTN-CT-2003-503864)

very special thanks to

Dr. Laurent Benisvy
Antje Disterheft

Abbreviations

Ac = acetate
Ar = aryl
Bpa = bis(pyrazolyl)acetate
BuLi = *n*butyl lithium
bipy = 2,2-bipyridyl
Bn = benzyl
Bp = bis(pyrazolyl)borate
Bp* = bis(3,5-dimethylpyrazolyl)borate
CH₂Cl₂ = dichloromethane
CH₃Cl = chloroform
COD = 1,5-cyclo-octadiene
Cp = cyclopentadienyl
Cp* = pentamethylcyclopentadienyl
Cy = cyclohexyl
 δ = chemical deviation from tetramethylsilane
DCC = dicyclohexylcarbodiimide
DEAD = diethylazodicarboxylate
DMAD = dimethylacetylenedicarboxylate
DMF = dimethylformamide
DMSO = dimethylsulfoxide
E = potential (volt)
EDA = ethyl diazoacetate
EPR = electronic paramagnetic resonance
eq. = equivalent or equivalents
ESR = electronic spin resonance
Et = ethyl
Et₂O = diethyl ether
F = Faraday constant
FAB = fast atomic bombardment
Fc = ferrocene
Fc⁺ = ferrocinium
GAO = galactose oxidase
GC = gas chromatography
Hex = hexyl
HF-EPR = high frequency electronic paramagnetic resonance
HMT = hexamethylenetetramine
Hpz = pyrazole
Hpz^{Me} = 3,5-dimethylpyrazole
Hpz* = general pyrazole
I = current (ampère)
I = nuclear angular momentum
IR = infrared
*i*Pr = *isopropyl*
LG = leaving group
m/z = mass/charge

mPTA = *N*-methyl-1,3,5-triaza-7-phosphaadamantane
Me = methyl
Ms = mesyl, methanesulfonyl
 ν = frequency
NBS = *N*-bromosuccinimide
NHE = normal hydrogen electrode
NIR = near infrared
OTf = trifluoromethanesulfonate
OTs = tosylate
PCET = proton-coupled electron transfer
Ph = phenyl
ppm = part per million
PTA = 1,3,5-triaza-7-phosphaadamantane
py = pyridine
pz = pyrazolyl
pz^{Me} = 3,5-dimethylpyrazolyl
Q = charge (coulomb)
RNR = ribonucleotide reductase
S = electronic spin momentum
*t*Bu = *tert*butyl
TBDMS = *tert*butyl dimethyl silyl
TEMPO = 2,2,6,6-tetramethyl-1-piperidinyloxy
Terpy = 2,2',6',2''-terpyridine
TFA = trifluoro acetic acid
TON = turnover number
THF = tetrahydrofuran
TMEDA = tetramethylethylenediamine
Tp = tris(pyrazol-1-yl)borate
Tp^{Me} = tris(3,5-dimethylpyrazol-1-yl)borate
Tp* = substituted tris(pyrazol-1-yl)borate
Tpm = tris(pyrazolyl)methane
Tpm^{Me} = tris(3,5-dimethylpyrazol-1-yl)methane
Ts = tosyl, *p*-toluenesulfonyl
Tyr = tyrosyl
Tyr⁻ = tyrosylate
Tyr[•] = tyrosyl radical
wu = work up
Xy = xylyl (2,6-dimethylphenyl)

Resumo

O estudo da química de coordenação de novos ligandos quelantes é um tema fundamental e atrai a atenção de muito grupos científicos com interesse em diferentes disciplinas da química. Os escorpionatos e os salicilamidatos são dois exemplos importantes de tipos de ligandos quelantes ocupando uma posição relevante em muitas áreas da investigação. O trabalho pretende estudar a síntese e a química de coordenação de novos derivados destes ligandos com uma funcionalidade altamente orientada. Os capítulos 1 e 4 descrevem respectivamente as investigações sobre as propriedades químicas e a reactividade dos escorpionatos tris(pirazolil)metano (Tpm) e dos ligandos salicilamidatos. Os capítulos 2 e 3 reportam os estudos da química de coordenação de novos derivados do Tpm (*i.e.* Li(Tpms^{Ph}), TpmPy and TpmPy^{Ph}). Os correspondentes complexos metálicos têm características únicas que são favoráveis à activação de moléculas, em catálise (Li(Tpms^{Ph})) e em química supramolecular (TpmPy and TpmPy^{Ph}). Nos capítulos 4 e 5 são descritas as sínteses, as propriedades e a química de coordenação duma nova classe de ligandos salicilamidatos que apresentam grupos fenóis, fenolatos ou radicais fenoxilo, com um potencial perfil para uso como compostos biomiméticos.

Palavras-chave: *ligandos quelatos, escorpionatos, funcionalizações, indução estereoquímica, flexibilidade de coordenação, radicais fenoxilo.*

Abstract

The study of the coordination chemistry of new chelating ligands is a fundamental domain and attracts the attention of many research groups with interests in different chemical areas. The tripodal scorpionates and the N,O-based salicylamidates are two relevant examples of types of chelating ligands and hold a primary role in many areas of chemistry. The present work directs on the synthesis and coordination chemistry of new derivatives of these compounds with highly oriented functions. Hence, chapters 1 and 4 describe the investigation carried out on the chemical properties and reactivity of the tris(pyrazolyl)methane scorpionate (Tpm) and the salicylamidate ligands, respectively. Chapters 2 and 3 report the coordination chemistry of new Tpm derivatives (*i.e.* Li(Tpms^{Ph}), TpmPy and TpmPy^{Ph}). The corresponding complexes possess peculiar characteristics with important features for activation of small molecules, catalysis (Li(Tpms^{Ph})) and supramolecular chemistry (TpmPy and TpmPy^{Ph}). In the chapters 4 and 5 are described the syntheses, the properties and the coordination chemistry of a new class of salicylamidate ligands bearing phenols, phenolates and their oxidized forms (*i.e.* phenoxyl radicals), contributing to their potential biomimetic use.

Key-words: *chelating ligands, scorpionates, functionalizations, steric inducement, coordination flexibility, phenoxyl radicals.*

Chapters' Structure

The work has been organized into five main chapters:

- Chapters 1-3: Scorpionate ligands
- Chapters 4, 5: Salicylamidate ligands
- Chapter 6: Experimental Data

I adopted a procedure to simplify the reading: every chapter incorporates a short *abstract*, a general *introduction*, a *discussion* of the results and –in some cases- a conclusive *overview* to summarize the results.

The chapters contain some concluding sections identified as “**Appendixes**”, where are described several supplementary studies, correlated to the topic. I decided to move these sections to focus the attention on the difference between (i) those subjects that were extensively explored and took the main part of time and (ii) those studies that resulted incomplete and not adequately developed or not strictly related to the theme.

I remain conscious of the utility and the value of unsuccessful results, nevertheless this choice has the unique purpose to make the reading clearer more coherent.

Chapter 1 is exclusively focused on the functionalization of Tpm ligand, starting from the study of the chemical characteristics of the molecule (*i.e.* structure, stability, solubility, reactivity, effect of substituents, ...). This chapter would have the aspiration to summarize all the experimental observations, the empirical studies and the analyses collected during these years on the chemistry of Tpm into a unique text, joining them together with the scientific results obtained and the examples reported in literature, to achieve a review of this class ligands and its potential applications.

Chapter 2 reports the coordination chemistry of a new Tpm derivative (*i.e.* Li(Tpms^{Ph})) toward copper(I) centers.

Chapter 3 describes the coordination chemistry of two new Tpm derivatives, bearing an extra pendant (*i.e.* Tpm^{Py}, and TpmPy^{Ph}) able to coordinate toward different metal centers.

Chapter 4 introduces a new class of salicylamide ligands and, similarly to Tpm ligands, describes their chemical properties and functionalizations. Analogously to Chapter 1, this chapter is exclusively focused on the chemistry of these ligands (*i.e.* organic) and on the study of the important features of some specifically designed derivatives.

Chapter 5 gives an account of the first studies of coordination chemistry of the salicylamidate ligand toward nickel centers and concentrates on the potential bioinorganic characteristics of these complexes.

Chapter 6 includes all experimental data, procedures, crystallographic data, electrochemical, theoretical and catalytic studies together with the pictures of all numbered compounds.

Additionally, this thesis, at the first and last pages, incorporates two **Schemes** (*i.e.* chapters 1-3 and 4-5) where the main studies are shown.

“There is no greater impediment to progress in the sciences than the desire to see it take place too quickly.” G. C. Lichtenberg (1742-1799)

“Hay que hacer investigación, crítica literaria, ensayos de interpretación, panfletos divulgativos si así la ocasión lo requiriera, pero no este híbrido entre fantaciencia y novela negra inconclusa, [...]” 2666, R. Bolaño (1953-2003)

General Introduction

The study of chelating ligands is undoubtedly one of the most significant fields of chemical research. The investigation of chelating molecules to a metal center reached fundamental results for the development of the overall scientific knowledge in chemistry.

While the term “*ligand*” was first used by Stock in 1916 and used in scientific journal in 1948;^{1,2} the term “*chelate*” was first applied³ in 1920 indicating those groups “which function as two associating units and fasten to the central atom so as to produce heterocyclic rings” (Figure 1).

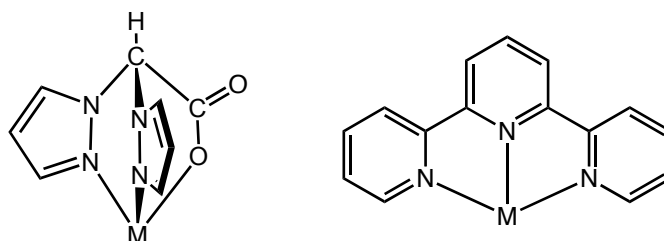


Figure 1. Representation of the usual coordination mode of two chelating ligands: **Bpa**, bis(pyrazolyl)acetate (left), **Terpy**, terpyridine (right).

From there, the designation of these compounds has been subjected to a progressive refinement: the introduction of several descriptive concepts, such as “denticity”, “hapticity”, “macrocyclic”, “bridging” and “bi-, tri-, poli-, ambidentate ligand”, contributes to clarify and differentiate many categories of chelating ligands and promote the genesis of peculiar disciplines and research areas. In fact, around the wide subject of chelating ligands many branches of investigation have grown, such as:

- thermodynamics (stabilization of chelation and macrocyclic effects);
- reaction mechanisms (fluxionality and flexibility of ligands);
- theoretical studies (electron donor ability and ionic nature of the ligands);
- coordination chemistry (ligand exchange reactions);
- biomimetic models and catalysis;
- solid supported and supramolecular chemistries.

Reedijk and co-workers, recently, emphasized⁴ the importance of ligand design in coordination chemistry in order to achieve successfully specific desired functions in many research fields. In fact, it is commonly recognized that specific functionalization or derivatisation of a species is a powerful strategy to enhance its reactivity. Many areas of research base their development on this approach; for instance, in medicinal chemistry the functionalization of a lead compound has been shown to improve its biological activity.

I have used a similar approach toward two tridentate ligands which possess different characteristics and I have studied their functionalization for the exploration of highly oriented coordination chemistry, what may confer new properties to the material.

Scorpionates Ligands: tris(pyrazolyl)methane

Characteristics

The scorpionate ligands constitute one of the most known class of chelating ligands. They consist in pyrazole-based ligands, know as poly(pyrazolyl)ligands, which are formed from two or more N-deprotonated pyrazole rings bound to a main group atom through one of the ring nitrogens.

The designation of these ligands came from its peculiar coordination mode: with the three nitrogen atoms of the corresponding pyrazolyl rings able to occupy three facially adjacent vacant positions of the coordination sphere of a metal center. This configuration (*i.e. fac*-chelation) mimics the analogue position of the scorpion that uses the three stings (two pincers and one claw) to attack its prey. A similar analogy has been described for another class of chelating ligand, the pincer ligands. The latter are, in fact, characterized by their peculiarity to bind two or three adjacent coplanar positions of the coordination sphere of a metal center. Differently, the scorpionate ligands extend their coordination ability out of a planar dimension, employing the third 'arm' to a facially capping coordination (Figure 2).

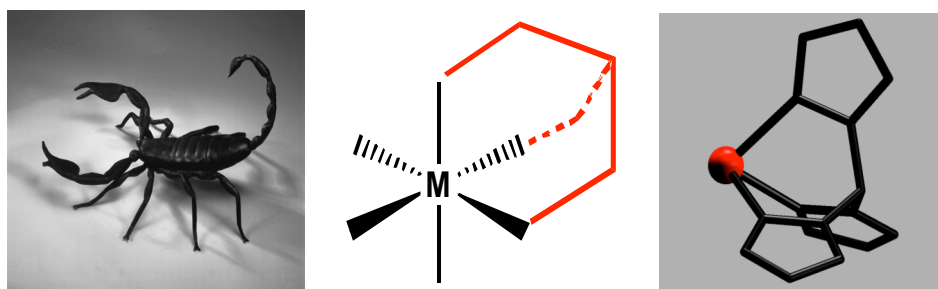


Figure 2. Illustration of a parallel between the scorpion and the tris(pyrazolyl) ligands.

The boron derivatives, hydrotris(pyrazolyl)hydroborates, **Tp**,⁵ have become one of the most highly studied class of ligands⁶⁻¹⁴ and they have been used to synthesize complexes of most metals of the periodic table.¹⁵

It is commonly agreed to compare¹⁶⁻¹⁹ the main characteristics of Tp ligand with other face-capping ligands, in particular taking into account the parallel between tris(pyrazolyl)borate (Tp) and cyclopentadienyl (Cp⁻) and considering that at least three important features are common: they are both mononegative, six electron donor and occupy three coordination positions (*i.e.* face-capping chelating ligand). The carbon analogue to Tp, known as hydrotris(pyrazolyl)methane, **Tpm**, maintains the tripodal face capping aspect and the same electrodonor ability, but differs from the others in the charge that holds (Figure 3).

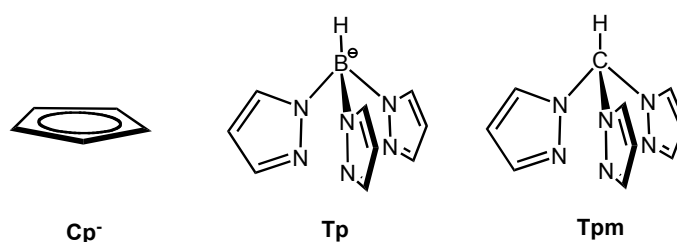


Figure 3. Cyclopentadienyl Cp⁻, Tris(pyrazolyl)borate Tp, and tris(pyrazolyl)methane Tpm.

Tpm is, then, a tridentate ligand able to coordinate metal centers in a N₃-chelating mode; nevertheless it is also reported²⁰ that, in some cases, Tpm (and Tp) could afford different coordination modes, adapting their geometry to the demands of the metal center, binding in a κ²-mode (*i.e.* bidentate)²¹ or acting as a bridging ligand.²²

As will be described in Chapter 1, the relatively more complicated synthesis of Tpm in comparison to that of Tp analogues, is the main reason of the underdeveloped research on this class of ligands, and encourages to explore a variety of functionalizations.

Functionalization

The large numbers of works^{15,16} concerning the derivatisation of Tp ligands have already demonstrated that the diversification of these ligands is an important topic and allows to direct the design of the derivatives toward highly specific applications.

Starting from the study of its properties and reactivity, several positions of the scorpionate molecule are commonly recognized of a great significance for functionalization. Two main points of functionalization could be identified: the apical position and the heterocyclic ring (Figure 4), and through the modification of these sites it is possible to achieve unique effects on the coordination behavior of the corresponding ligand.

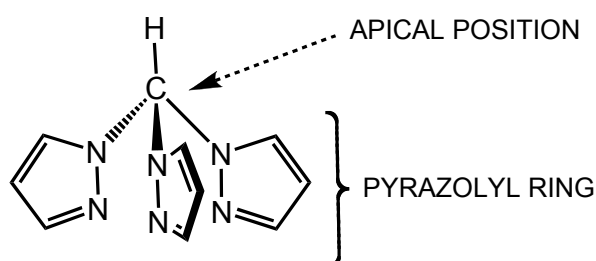
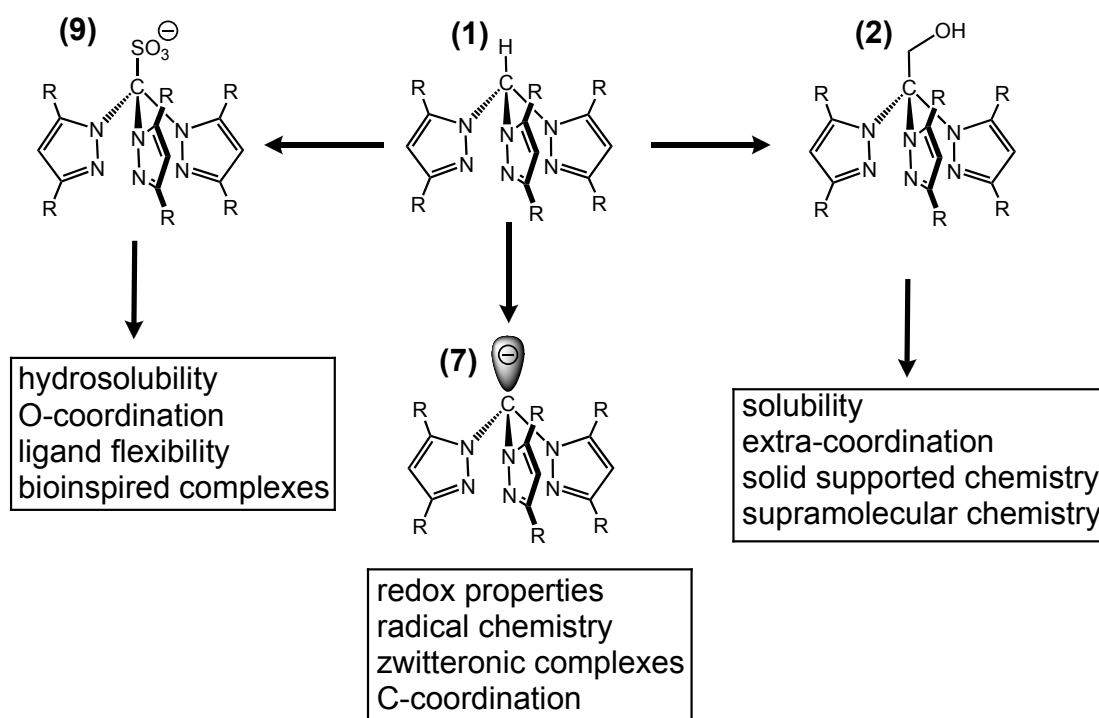


Figure 4. The two main sites for the functionalization of Tpm.

In particular, the **functionalization at 3, 4 and 5-positions of pyrazolyl rings** has been extensively studied for Tp and represents an important topic for many researchers.²³⁻²⁵ for instance the study of the roles of bulky substituents at 3 or 5-positions of pyrazolyl rings will be object of discussion in Chapter 1 and held a considerable part of work for this thesis.

Recently, it has been recognized that synthetic progress toward the functionalization of the **central methine carbon** atom at the apical position of Tpm derivatives would be considerably advantageous,²⁶ and the modifications of the

backbone can influence the properties of the complexes, as well as permitting their attachment on a solid support.²⁷



Scheme 1. Examples of deprotonation and functionalization of Tpm.

The substitution at the central methine carbon atom can be achieved by reacting a suitable electrophile with the carbanion $\text{C}^-(\text{pz})_3$ (Scheme 1, (7)) formed by deprotonation of Tpm.²⁶⁻³⁰ Recently, this anionic derivative has attracted a growing interest³¹ and a significant part of this thesis discusses the nature of this carbanion.

An important carbon-functionalized derivative of Tpm is the sulfonated analogue, tris(pyrazolyl)methanesulfonate, **Tpms**²⁹ (Scheme 1, (9), R = H). The latter has captured the attention of many groups³²⁻³⁶ for its high stability and hydrosolubility. Moreover the additional sulfonate group could be involved in the coordination to metal, converting the N_3 -type Tpm^{R} ligand, in a more versatile Tpms^{R} able to coordinate as either a tripodal or a bipodal ligand (*i.e.* with N_3^- , N_2O^- , N_2^- or NO -coordination modes, see Figure 5).^{32-34,36} In Chapter 2, this flexibility of Tpms has been studied and appears to be related both to the nature of the metal center and the other ligands.

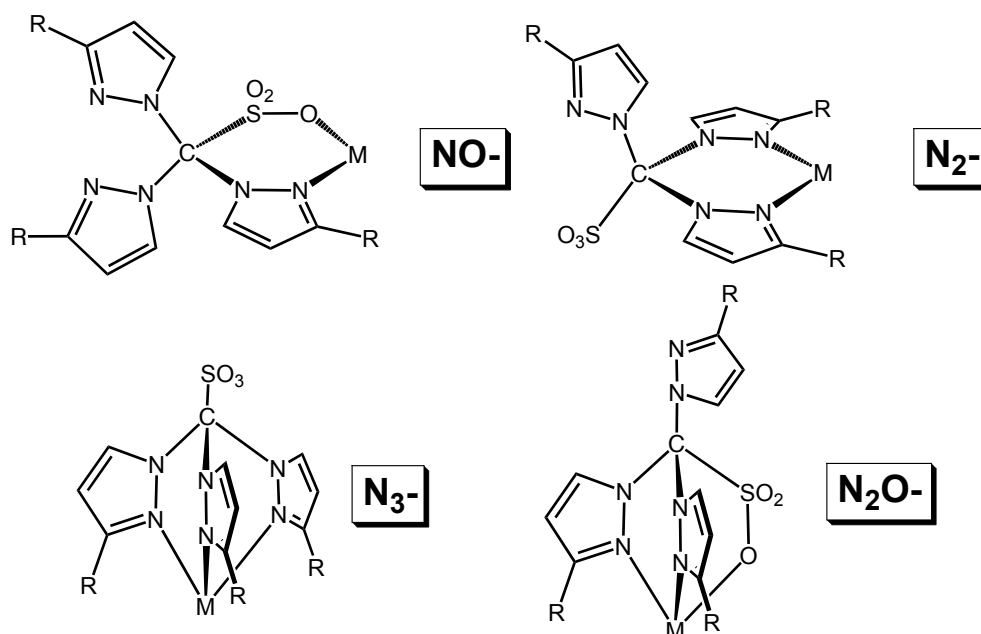


Figure 5 Coordination modes of $Tpms^R$ ligand.

An important derivative of Tpm is the **2,2,2-tris(pyrazolyl)ethanol** (Scheme 1, **(2)**, R = H). The latter compound represents, in fact, a sort of ‘chemical scaffold’ for the development of a synthetic plan for further functionalizations. This compound could, indeed, react with a large variety of species and this topic has been object^{26,28,37-41} of wide investigation in the last years in coordination chemistry and inspired many sections of this thesis: the prospects to extend the ‘denticity’ (Chapter 3) and to radically modify the properties of the molecule, *i.e.* anchoring it to a dendritic (Chapter 1) or solid support, have recently opened the research toward new fields of application.^{27,42}

Salicylamidate based ligands

Characteristics

A large variety of chemical and biochemical redox processes are based on phenol oxidation, being a common intermediate in several enzymatic pathways.⁴³⁻⁴⁷ In general, phenols constitute an important class of antioxidants that inhibit the oxidative degradation of organic materials including a large number of biological aerobic organisms and commercial products.⁴⁸⁻⁵³



Phenols realize this by hydrogen-atom transfer to peroxy radicals, converting them to hydroperoxides much faster than the radical attacks an organic substrate, forming the corresponding **phenoxyl radicals** species (eq. 1). The latter are, in fact, intermediates in a large variety of thermochemical, photochemical and biochemical processes.⁵⁴ Furthermore, the proton-coupled electron transfer (PCET) oxidations of phenols to phenoxyl radicals are of particular importance⁵⁵ in biological systems because of the widespread involvement of tyrosyl radicals (*i.e.* Tyr[•]) in enzymatic mechanisms: they contribute for an important catalytic function in the enzyme ribonucleotide reductase (RNR) and also in photosystem II.

For these reasons, there is a growing interest in the chemistry of phenol-based ligands (Figure 6). These ligands are characterised by a large number of categories that have many different features: from the simple bidentate ligands to tetradentate and crown ligands. These differences hold, indeed, a complex variety of properties and applications.

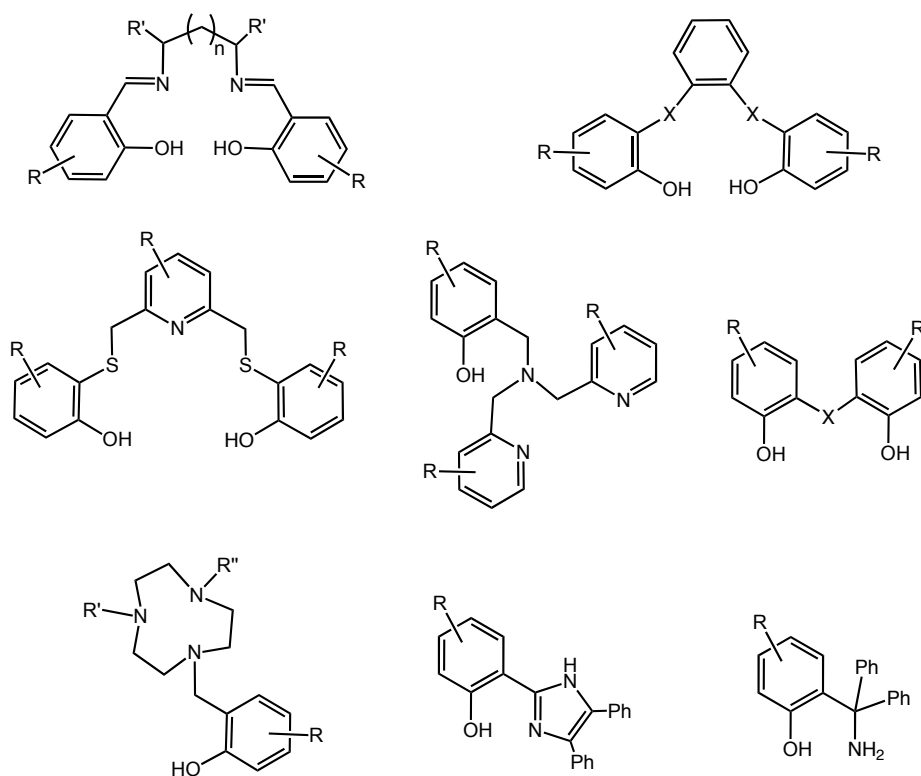


Figure 6. Different phenol-based chelating ligands.

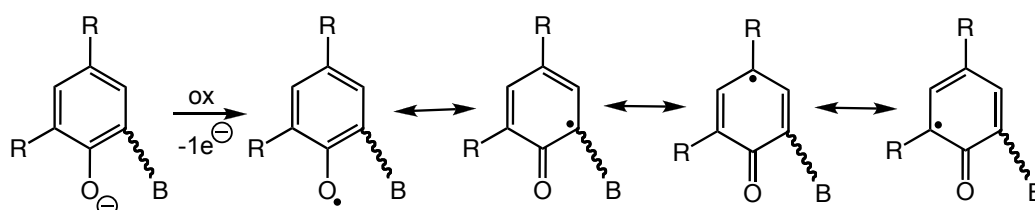
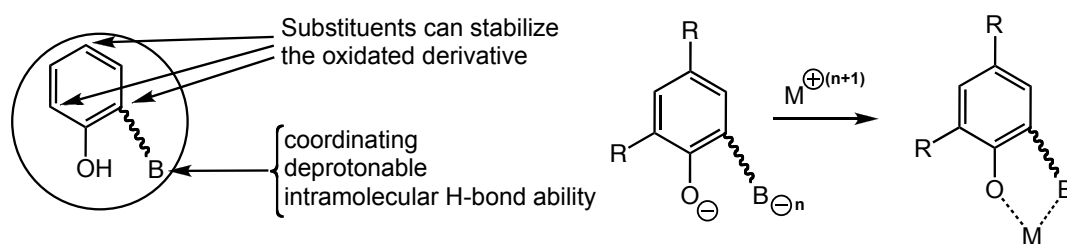
This study focus the attention toward a highly oriented class of phenol ligands that can incorporate two or more deprotonable sites able to coordinate and then stabilise a high oxidation state of a metal ion. In fact, there is an increasing attraction on the design and synthesis of bioinspired chelating ligands able to form stable complexes with a metal center in different oxidation states. Actually, the Cu^{II}/Cu^I phenol-based mechanisms of galactose oxidase (*i.e.* GAO) is one of the most studied⁵⁶ examples of an enzymatic process that uses a metal-mediated mechanism (*i.e.* involving copper-tyrosyl radical unit) to bind and activate O₂ and oxidize organic substrates.

Strictly connected to this topic, the copper-catalysed alcohol oxidation has become of a great interest⁵⁷ and an extremely wide variety of synthetic systems incorporating organic radical and copper complexes have been studied for this reaction.

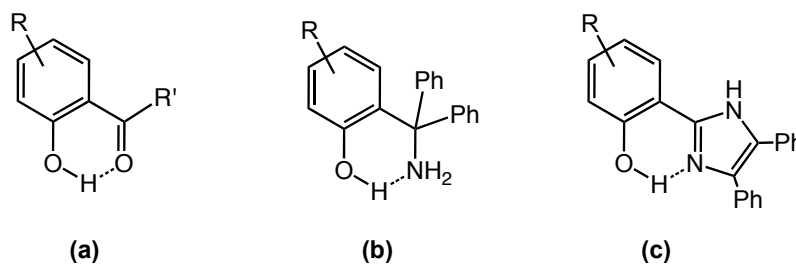
Functionalization

A variety of phenol-based ligands shows a wide panorama of derivatives, but the highly focused selectivity of their applications helps to select the most interesting functionalization. In order to fortify the ligand to oxidative degradation, it has been reported that 2, 4 and 6 alkyl substituents at the phenol ring confer stability against the decomposition of the oxydized derivative (Figure 7).⁵⁸

Furthermore, the ability of phenols to form H-bonds has been object of a comprehensive research⁵⁹ and the extensive work done^{55,60} on the intramolecular H-bonded phenols has clarified the description of important enzymatic mechanisms. Among the different systems, 2-nitrophenols⁶¹ and especially salicylic acid derivatives⁶² (*i.e.* 2-hydroxy benzoyl compounds, Figure 7 compound **(a)**) have been the favourite models, although other derivatives employing a nitrogen-assisted H-bond (compound **(b)** and **(c)**, Figure 7) have been studied.⁵⁵



Examples of intramolecular H-bonded phenols



Possible equilibria for oxidized derivatives of intramolecular H-bonded phenols:

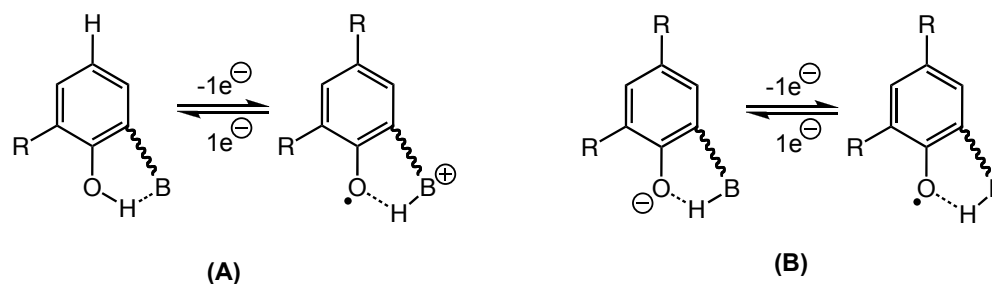
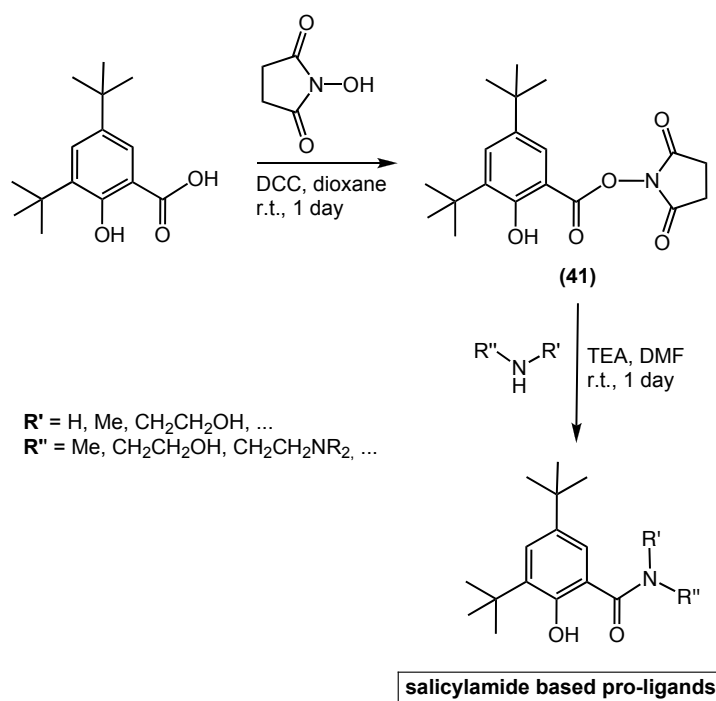


Figure 7. Schematic representation of main features of phenol chelating ligands examined by this study.

The production of chemical analogues of tyrosyl radical (*i.e.* phenoxyl radical) in various local environments is of much current theoretical and experimental interest;⁶³ in particular the studies of the influence of intramolecular H-bonding to phenol and its corresponding phenoxyl radical, are essential to understand the physico-chemical properties of a biological system. It has been reported⁶⁴ that these

H-bonded classes of compounds undergo a reversible one-electron oxidation to form a phenoxyl radical that incorporate the intramolecular H-bond (Equilibria **(A)** and **(B)**, Figure 7): as previously mentioned, the proton-coupled electron transfer (PCET) generated from direct oxidation of phenol is one of the highly studied processes in the biological systems.

The work of this thesis focused the attention on the salicylamidate derivatives (Chapter 4) that present an amidic moiety at 2-position of the phenol ring. In addition, Kanamori et al.⁶⁵ have recently reported that relatively strong (phenolate)O⁻⋯H-N(amide) H-bonding occurs in salicylamidate and isophthalate compounds. These results have prompted us to design and synthesize several unprecedented H-bonded (or not) *o,p*-*t*Bu-protected salicylamidate compounds.

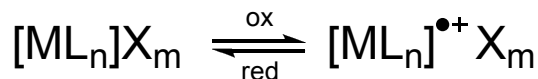


Scheme 2. Synthesis of salicylamide pro-ligands of this thesis

This class of ligands⁶⁶ holds peculiar properties and represents a sort of framework for theoretical studies, coordination chemistry, electrochemistry and bioinorganic chemistry (Scheme 2).

In particular, the coordination chemistry (Chapter 5) of this new class of ligands is a theme of primary interest toward the metal centers that, widely present in Nature, occupy a central role in different enzymes and catalytic systems (*i.e.* Cu, Fe,

Zn, Ni...). Furthermore, a proper effort should be devoted to investigate the capacity of the resulting metal complexes to sustain the oxidative conditions, being a reversible redox system (Scheme 3).



Scheme 3 Schematical representation of a reversible redox metal complex

In general, the study of electronic structures of oxidized species of various metal-phenolate complexes is the starting point to assess them as good candidates for further applications in biomimetic systems. The electronic characteristics of these paramagnetic derivatives have been shown⁶⁷⁻⁶⁹ to be dependent on the nature metal ions but also on the nature of the coordinated phenolate moiety (Chapter 5).⁶⁷

The investigation of new chelating ligands and their corresponding metal complexes occupies a crucial place in the comprehensive panorama of chemical research. The study of these two different classes of chelating ligands (*i.e.* scorpionate and salicylamidate ligands) shows how important is the analysis of their chemical properties and reactivity to design the synthesis of new derivatives.

These examples demonstrate that the possible functionalizations of the starting ligands drive to different potential applications.

References

- [1] Irving, H.; Williams, R. J. P., *Nature* **1948**, *162*, 746.
- [2] Brock, W. H.; Jensen, K. A.; Jorgensen, C. K.; Kauffman, G. B., *Polyhedron* **1983**, *2*, 1.
- [3] Morgan, G. T.; Drew, H. D. K., *Journal of the Chemical Society* **1920**, *117*, 1456.
- [4] Elsevier, C. J.; Reedijk, J.; Walton, P. H.; Ward, M. D., *Dalton Trans.* **2003**, 1869.
- [5] Trofimenko, S., *J. Am. Chem. Soc.* **1967**, *89*, 3170.
- [6] Calabrese, J. C.; Trofimenko, S., *Inorg. Chem.* **1992**, *31*, 4810.
- [7] Carmona, D.; Lahoz, F. J.; Atencio, R.; Edwards, A. J.; Oro, L. A.; Lamata, M. P.; Esteban, M.; Trofimenko, S., *Inorg. Chem.* **1996**, *35*, 2549.
- [8] Kitajima, N.; Tolman, W. B., Coordination Chemistry with Sterically Hindered Hydrotris(pyrazolyl)borate ligands organometallic and bioinorganic perspectives. In *Progress in Inorganic Chemistry, Vol 43*, John Wiley & Sons Inc: New York, 1995; Vol. 43, pp 419.
- [9] Schneider, J. L.; Carrier, S. M.; Ruggiero, C. E.; Young, V. G.; Tolman, W. B., *J. Am. Chem. Soc.* **1998**, *120*, 11408.
- [10] Vahrenkamp, H., *Acc. Chem. Res.* **1999**, *32*, 589.
- [11] Thompson, J. S.; Harlow, R. L.; Whitney, J. F., *J. Am. Chem. Soc.* **1983**, *105*, 3522.
- [12] Dias, H. V. R.; Fianchini, M., *Angew. Chem., Int. Ed.* **2007**, *46*, 2188.
- [13] Trofimenko, S.; Calabrese, J. C.; Thompson, J. S., *Angew. Chem., Int. Ed.* **1989**, *28*, 205.
- [14] Rheingold, A. L.; Haggerty, B. S.; Trofimenko, S., *Angew. Chem., Int. Ed.* **1994**, *33*, 1983.
- [15] Pettinari, C., *Scorpionates II: Chelating Borate Ligands*. Imperial College Press London, 2008
- [16] Trofimenko, S., *Chem. Rev.* **1993**, *93*, 943.
- [17] Trofimenko, S., *Adv. Chem. Ser.* **1976**, 289.
- [18] Trofimenko, S., *Prog. Inorg. Chem.* **1986**, *34*, 115.

- [19] Brunker, T. J.; Cowley, A. R.; O'Hare, D., *Organometallics* **2002**, *21*, 3123.
- [20] Macchioni, A.; Bellachioma, G.; Cardaci, G.; Gramlich, V.; Ruegger, H.; Terenzi, S.; Venanzi, L. M., *Organometallics* **1997**, *16*, 2139.
- [21] Trofimenko, S., *J. Am. Chem. Soc.* **1970**, *92*, 5118.
- [22] Ellis, D. D.; Jeffery, J. C.; Jelliss, P. A.; Kautz, J. A.; Stone, F. G. A., *Inorg. Chem.* **2001**, *40*, 2041.
- [23] Trofimenko, S.; Calabrese, J. C.; Thompson, J. S., *Inorg. Chem.* **1987**, *26*, 1507.
- [24] Trofimenko, S.; Calabrese, J. C.; Domaille, P. J.; Thompson, J. S., *Inorg. Chem.* **1989**, *28*, 1091.
- [25] Zhao, N.; Bullinger, J. C.; Van Stipdonk, M. J.; Stern, C. L.; Eichhorn, D. M., *Inorg. Chem.* **2008**, *47*, 5945.
- [26] Reger, D. L.; Semeniuc, R. F.; Little, C. A.; Smith, M. D., *Inorg. Chem.* **2006**, *45*, 7758.
- [27] Sanchez-Mendez, A.; Ortiz, A. M.; de Jesus, E.; Flores, J. C.; Gomez-Sal, P., *Dalton Trans.* **2007**, 5658.
- [28] Reger, D. L.; Grattan, T. C.; Brown, K. J.; Little, C. A.; Lamba, J. J. S.; Rheingold, A. L.; Sommer, R. D., *J. Organomet. Chem.* **2000**, *607*, 120.
- [29] Klaui, W.; Berghahn, M.; Rheinwald, G.; Lang, H. R., *Angew. Chem., Int. Ed.* **2000**, *39*, 2464.
- [30] Bigmore, H. R.; Dubberley, S. R.; Kranenburg, M.; Lawrence, S. C.; Sealey, A. J.; Selby, J. D.; Zuideveld, M. A.; Cowley, A. R.; Mountford, P., *Chem. Commun.* **2006**, 436.
- [31] Breher, F.; Grunenberg, J.; Lawrence, S. C.; Mountford, P.; Ruegger, H., *Angew. Chem., Int. Ed.* **2004**, *43*, 2521.
- [32] Klaui, W.; Berghahn, M.; Frank, W.; Reiss, G. J.; Schonherr, T.; Rheinwald, G.; Lang, H., *Eur. J. Inorg. Chem.* **2003**, 2059.
- [33] Papish, E. T.; Taylor, M. T.; Jernigan, F. E.; Rodig, M. J.; Shawhan, R. R.; Yap, G. P. A.; Jove, F. A., *Inorg. Chem.* **2006**, *45*, 2242.
- [34] Chenskaya, T. B.; Berghahn, M.; Kunz, P. C.; Frank, W.; Klaui, W., *J. Mol. Struct.* **2007**, *829*, 135.
- [35] Smolenski, P.; Dinoi, C.; da Silva, M.; Pombeiro, A. J. L., *J. Organomet. Chem.* **2008**, *693*, 2338.
- [36] Wanke, R.; Smolenski, P.; da Silva, M.; Martins, L.; Pombeiro, A. J. L., *Inorg. Chem.* **2008**, *47*, 10158.

- [37] Reger, D. L.; Semeniuc, R. F.; Smith, M. D., *Inorg. Chem.* **2001**, *40*, 6545.
- [38] Reger, D. L.; Semeniuc, R. F.; Smith, M. D., *J. Chem. Soc., Dalton* **2002**, 476.
- [39] Reger, D. L.; Semeniuc, R. F.; Smith, M. D., *J. Organomet. Chem.* **2003**, *666*, 87.
- [40] Reger, D. L.; Gardinier, J. R.; Bakbak, S.; Semeniuc, R. F.; Bunz, U. H. F.; Smith, M. D., *New J. Chem.* **2005**, *29*, 1035.
- [41] Reger, D. L.; Semeniuc, R. F.; Captain, B.; Smith, M. D., *Inorg. Chem.* **2005**, *44*, 2995.
- [42] Reger, D. L.; Foley, E. A.; Watson, R. P.; Pellechia, P. J.; Smith, M. D.; Grandjean, F.; Long, G. J., *Inorg. Chem.* **2009**, *48*, 10658.
- [43] Que, L.; Tolman, W. B., *Nature* **2008**, *455*, 333.
- [44] *The Chemistry of Phenols*. John Wiley & Sons, Ltd 2003.
- [45] Stubbe, J.; van der Donk, W. A., *Chem. Rev.* **1998**, *98*, 705.
- [46] Pesavento, R. P.; Van Der Donk, W. A., Tyrosyl radical cofactors. In *Advances in Protein Chemistry, Vol 58*, 2001; Vol. 58, pp 317.
- [47] Cukier, R. I.; Nocera, D. G., *Annu. Rev. Phys. Chem.* **1998**, *49*, 337.
- [48] *Free Radicals in Biological Medicine*. Oxford Science Publications: 1999.
- [49] Mason, K. E., *Vitamin E. Basic and Clinical Nutrition*. New York, 1980; Vol. 1.
- [50] Burton, G. W.; Joyce, A.; Ingold, K. U., *Arch. Biochem. Biophys.* **1983**, *221*, 281.
- [51] Evans, H. M.; Bishop, K. S., *Science* **1922**, *56*, 650.
- [52] *Natural Antioxidants. Chemistry, Health Effects, and Applications*. AOCS Press: Champaign, Illinois, 1997.
- [53] *Biological Oxidants and Antioxidants. Molecular Mechanisms and Health Effects*. Champaign, Illinois, 1998.
- [54] Chaudhuri, P.; Wieghardt, K., Phenoxy radical complexes. In *Progress in Inorganic Chemistry, Vol. 50*, 2001; Vol. 50, pp 151.
- [55] Rhile, I. J.; Markle, T. F.; Nagao, H.; DiPasquale, A. G.; Lam, O. P.; Lockwood, M. A.; Rotter, K.; Mayer, J. M., *J. Am. Chem. Soc.* **2006**, *128*, 6075.
- [56] Thomas, F., *Eur. J. Inorg. Chem.* **2007**, 2379.

- [57] Gamez, P.; Aubel, P. G.; Driessen, W. L.; Reedijk, J., *Chem. Soc. Rev.* **2001**, *30*, 376.
- [58] Altwicker, E. R., *Chem. Rev.* **1967**, *67*, 475.
- [59] *The Chemistry of Phenols, Chapter 8*. John Wiley & Sons, Ltd 2003; p 529.
- [60] Benisvy, L.; Bittl, R.; Bothe, E.; Garner, C. D.; McMaster, J.; Ross, S.; Teutloff, C.; Neese, F., *Angew. Chem., Int. Ed.* **2005**, *44*, 5314.
- [61] Caminati, W.; Velino, B.; Danieli, R., *J. Mol. Spectrosc.* **1993**, *161*, 208.
- [62] Palomar, J.; De Paz, J. L. G.; Catalan, J., *Chem. Phys.* **1999**, *246*, 167.
- [63] Benisvy, L.; Hammond, D.; Parker, D. J.; Davies, E. S.; Garner, C. D.; McMaster, J.; Wilson, C.; Neese, F.; Bothe, E.; Bittl, R.; Teutloff, C., *J. Inorg. Biochem.* **2007**, *101*, 1859.
- [64] Rhile, I. J.; Mayer, J. M., *J. Am. Chem. Soc.* **2004**, *126*, 12718.
- [65] Kanamori, D.; Furukawa, A.; Okamura, T.; Yamamoto, H.; Ueyama, N., *Organic & Biomolecular Chemistry* **2005**, *3*, 1453.
- [66] Jimenez, C. A.; Belmar, J. B., *Tetrahedron* **2005**, *61*, 3933.
- [67] Rotthaus, O.; Jarjays, O.; Del Valle, C. P.; Philouze, C.; Thomas, F., *Chem. Commun.* **2007**, 4462.
- [68] Shimazaki, Y.; Yajima, T.; Tani, F.; Karasawa, S.; Fukui, K.; Naruta, Y.; Yamauchi, O., *J. Am. Chem. Soc.* **2007**, *129*, 2559.
- [69] Benisvy, L.; Kannappan, R.; Song, Y.-F.; Milikisyants, S.; Huber, M.; Multikainen, I.; Turpeinen, U.; Gamez, P.; Bernasconi, L.; Baerends, E. J.; Hartl, F.; Reedijk, J., *Eur. J. Inorg. Chem.* **2007**, 637.

1 Scorpionates ligands

Table of contents

Abstract	18
1.1 Introduction	19
1.2 Tpm: chemical properties	22
1.2.1 Tp and Tpm: differences and analogies	22
1.2.2 Tpm: stability	23
1.2.3 Tpm: characteristics	26
1.2.4 Tpm: the pyrazolyl ring	27
1.2.5 Tpm: the central carbon	32
1.3 Carbon functionalization of Tpm	34
1.3.1 The tris(pyrazolyl)methanesulfonate: Tpm _s	35
1.3.2 Tris-2,2,2-(1-pyrazolyl)ethanol (2): the hydroxy derivative	38
1.3.2.1 Reactivity of tris-2,2,2-(1-pyrazolyl)ethanol	41
1.3.2.1.1 Substitution of the hydroxy group	41
1.3.2.1.2 Alkylation of tris-2,2,2-(1-pyrazolyl)ethanol	43
1.3.2.1.3 Benzyl and 4-pyridyl derivative of tris-2,2,2-(1-pyrazolyl)ethanol	44
1.4 Carbon functionalization via radical pathway	46
1.4.1 Identification of the radical $\cdot\text{C}(\text{pz}^{\text{Me}2})_3$, (7 ⁺)	48
1.4.2 Reactivity of $\cdot\text{C}(\text{pz}^{\text{Me}2})_3$	53
1.4.3 Characterisation of $\text{C}(\text{pz}^{\text{Me}2})_4$ (8)	54
1.4.4 Future studies on the radical pathway	56
1.5 Appendix 1.A: synthesis of other Tpm derivatives	58
1.5.1 Sterically hindered Tpm ^{<i>t</i>Bu} and Tpm ^{<i>i</i>Pr}	58
1.5.2 Polysulfonated derivative of Tpm: toward water solubility	58
1.5.3 Tpm derivatives incorporating new functional groups at the central carbon	59
1.6 Appendix 1.B: Dendritic-Tpm ligands	63
References	68

Abstract

The coordination chemistry of hydrotris(pyrazolyl)methane (Tpm) (and derived species), the carbon analogue of tris(pyrazolyl)borate (Tp), is relatively much less studied in comparison to its boron-analogue. One reason for the limited research in this area is that the syntheses, with the exception of Tpm itself, are more difficult than those of the corresponding tris(pyrazolyl)borates. Recently, important progresses have been done in this field and some researchers developed an extensive knowledge on the preparation of derivatives of Tpm.

The study of chemical properties of the starting pro-ligand (*i.e.* stability, geometry, solubility, coordination ability...) is a key point to define the different synthetic strategies to functionalize the lead compound and achieve unique derivatives.

Two main synthetic routes have been highlighted: **(i)** The functionalization of pyrazolyl rings pass through the synthesis of differently substituted pyrazoles and provides different classes of Tpm derivatives where the substituents at the pyrazolyl rings can lead to significant modifications of the stability, solubility and coordination properties. In particular, the 5- and 3-functionalizations have been studied and the resulting ligands hold important functions that could open to a large variety of applications. **(ii)** The activation of the central methine carbon of Tpm has a high synthetic potential and is the most important topic in this field. In the last decades, the proliferation of works reporting new Tpm derivatives functionalized at the apical carbon is a real demonstration of the relevance of this theme. A multi-directions synthetic plan has been designed and carried out providing a large variety of Tpm analogues with different chemical properties: within these compounds, several derivatives display unique peculiarities that have been studied in the next chapters.

In the last sections of the chapter (1.5 and 1.6) several new possible functionalizations of Tpm ligand have been explored and indicate perspectives for future work in this area.

1.1 Introduction

The pyrazole-based poly(pyrazolyl) ligands are formed from two or more N-deprotonated pyrazole rings bound to a main group atom through one of the ring nitrogens (Figure 1.1).

First introduced by Trofimenko in 1967,¹ hydrotris(pyrazolyl)borates, **Tp**, have become one of the most widely exploited and highly studied class of ligands in inorganic,²⁻⁴ bioinorganic,⁵⁻⁹ organometallic^{10,11} and coordination chemistries,^{12,13} and they have been used to synthesize complexes of most metals of the periodic table. The Tp ligand is uninegative, six-electron donor and, analogously to cyclopentadienide ligand (Cp^-), is a face-capping chelating ligand. The carbon analogue to Tp, known as hydrotris(pyrazolyl)methane, **Tpm**, is a neutral chelating ligand bearing three N-pyrazolyl rings bound to a central carbon (Figure 1.1). Tpm is, then, a potentially tridentate ligand able to coordinate metal centers in a N_3 -chelating mode; nevertheless it is also reported¹⁴ that Tpm (and Tp) could exhibit other coordination modes (*e. g.* κ^2 -metal complexes in a square planar geometry).

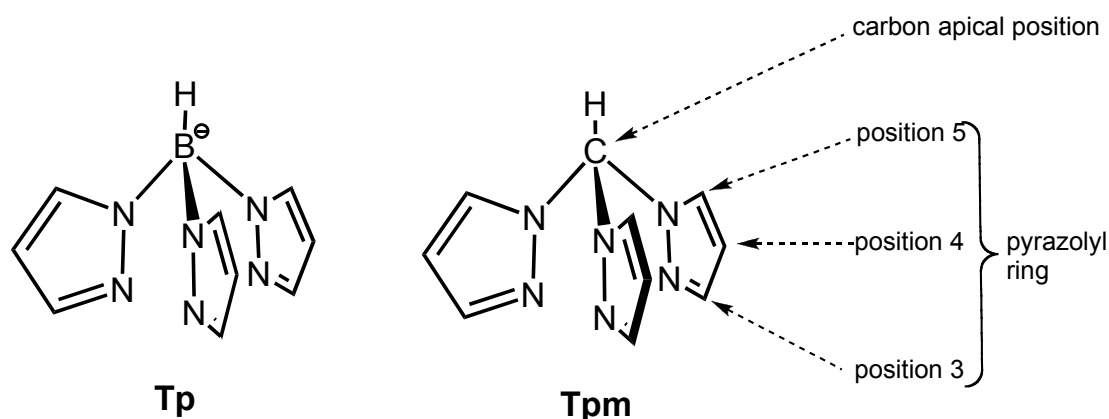
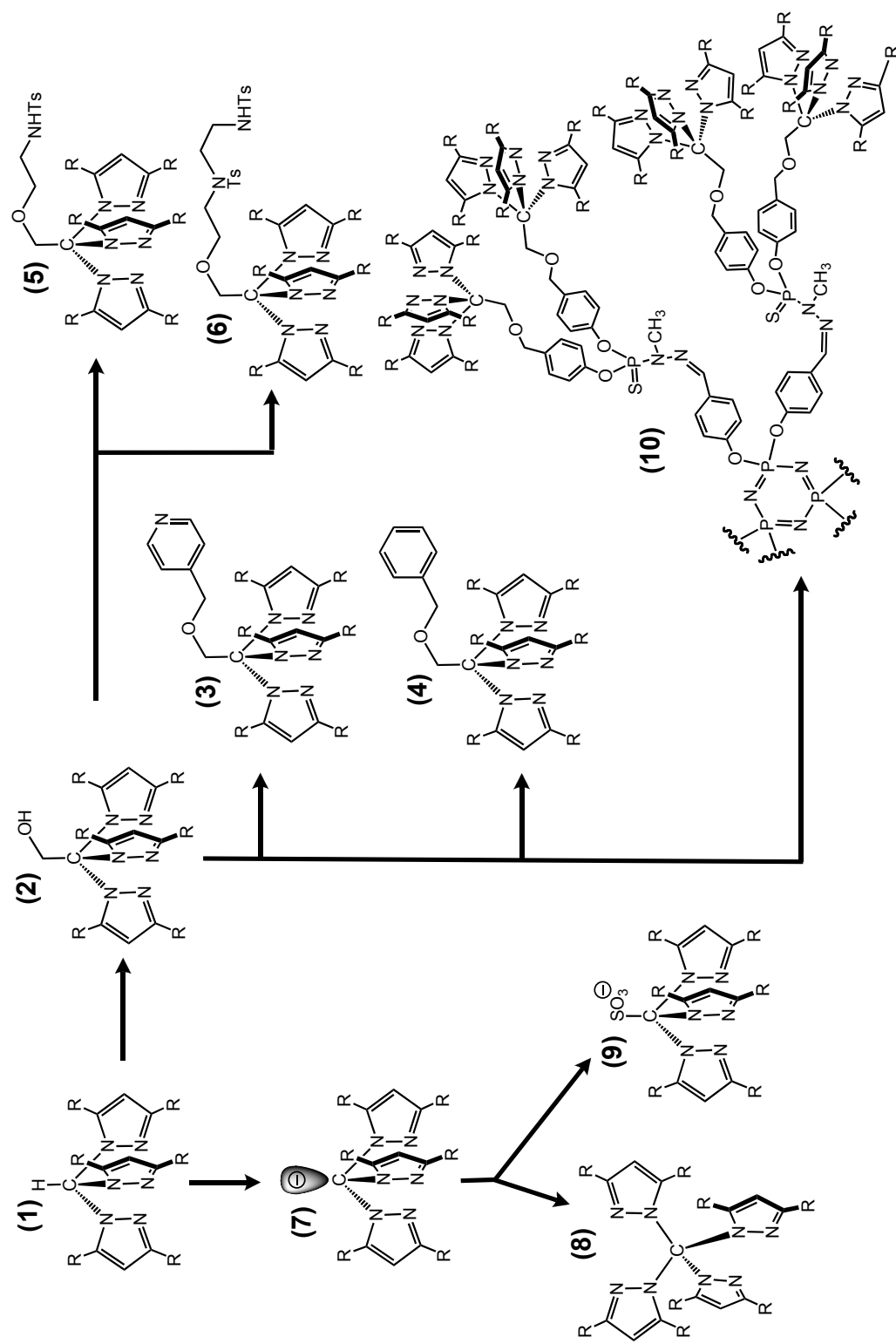


Figure 1.1 Hydrotris(pyrazolyl)borate (Tp), and hydrotris(pyrazolyl)methane (Tpm).

The large variety^{15,16} of Tp derivatives indicates how wide and explored is the research in this field; the synthetic functionalization of tris(pyrazolyl)borate is until now an intensively studied domain. In particular, due to its handy synthesis, the functionalization of 3, 4 and 5-substituted tris(pyrazolyl)borate has been an important

topic for many researchers.¹⁷⁻²⁰ On the contrary, the relatively less reactive Tpm led to an underdeveloped panorama of its derivatives.

The aim of this chapter is to describe in every respect all the investigations developed during these years for the functionalization of Tpm (Scheme 1.1), the illustration of Tpm characteristics (Sections 1.2.2 and 1.2.3), the description of Tpm functionalization at a pyrazolyl ring (Section 1.2.4) and at the central methine carbon (Sections 1.2.5, 1.3 and 1.4). At the end of the Chapter are described –as Appendixes– the studies that have not been completed so far and those that led to unsuccessful results (Sections 1.5 and 1.6).



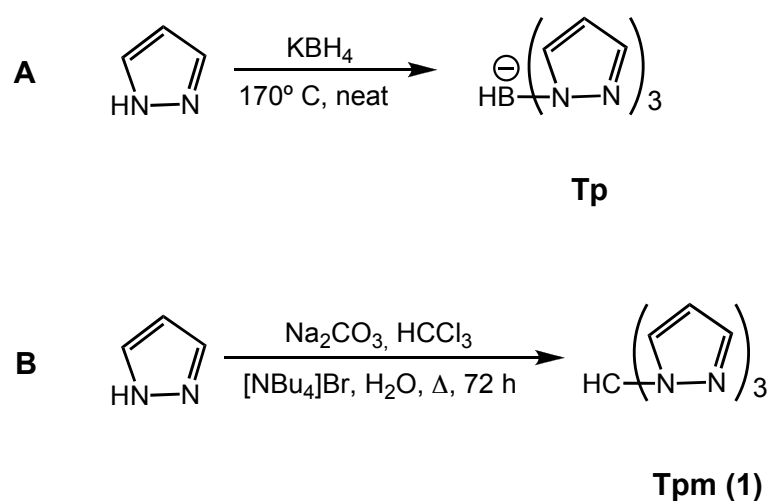
Scheme 1.1 General scheme for syntheses of derivatives of Tpm.

1.2 Tpm: chemical properties

1.2.1 Tp and Tpm: differences and analogies

Taking into account the different preparation methods of Tpm and Tp, it is simple to notice how the synthesis of tris(pyrazolyl)borate and of its derivatives is undoubtedly easier and more versatile than those of its carbon analogue, Tpm.

In fact, the Tp preparation proceeds with H₂ formation from reaction between the highly reactive potassium borohydride and pyrazole.¹⁵ On the contrary the synthesis of Tpm (Scheme 1.2, **(1)**) proceeds through the deprotonation of pyrazole to pyrazolate and the successive nucleophilic substitution at a chloroform molecule. This difference of the synthetic process is even more evident in the case of preparation of 3-, 4- or 5-substituted tris(pyrazolyl) species:¹⁶ where the synthesis of a tris(3,5-diphenylpyrazolyl)borate, Tp^{Ph2}, proceeds regularly as described,¹⁵ the preparation, carried out in this study, of its carbon analogue does not occur (see Section 1.5.1). Moreover, it has been reported¹ that a vigilant control of temperature in the Tp synthesis is required to avoid the formation of the ‘over-substituted’ product, tetrakis(pyrazolyl)borate; whereas (as it is explained in Section 1.4) the synthesis of tetrakis(pyrazolyl)methane, using carbon tetrachloride, does not seem to proceed easily.



Scheme 1.2 Synthesis of hydrotris(pyrazolyl)borate (Tp, reaction A) and of hydrotris(pyrazolyl)methane (Tpm (1), reaction B).

Different attempts to improve the Tpm synthesis have been reported, starting from the 1937 Hückel's preparation,²¹ and clarify that the best yield²² is earned in biphasic conditions: using a large excess of a mild base (*i.e.* Na₂CO₃) to deprotonate the pyrazole and refluxing the resulting mixture for over 70 h. In fact, the use of a stoichiometric amount of a strong base to remove the N-pyrazolyl proton does not lead to the desired product, since it has been proved that strongly basic conditions could launch into a series of side-reactions, starting from the decomposition of the chloroform molecule to lose HCl and form the reactive dichloro carbene²³ that reacts with the unsubstituted pyrazole to yield ring expansion reactions.²⁴

In its reviews, Trofimenko lists and compares^{15,25-27} the characteristics of Tp ligand with other face-capping ligands, in particular by taking into account the parallel between tris(pyrazolyl)borate (Tp) and cyclopentadienide (Cp⁻) and showing that at least three important features are common: they are both mononegative, six electron donors and tend to occupy three coordination positions. The Tpm ligand (**1**) tends to maintain the tripodal face capping aspect and the same electron-donor ability, but differs from the others for the charge that holds. In particular cases, the neutral nature of Tpm changes drastically its properties (in comparison to Tp) by promoting or hampering the coordination to the metal center, as will be shown in next chapters.

1.2.2 Tpm: stability

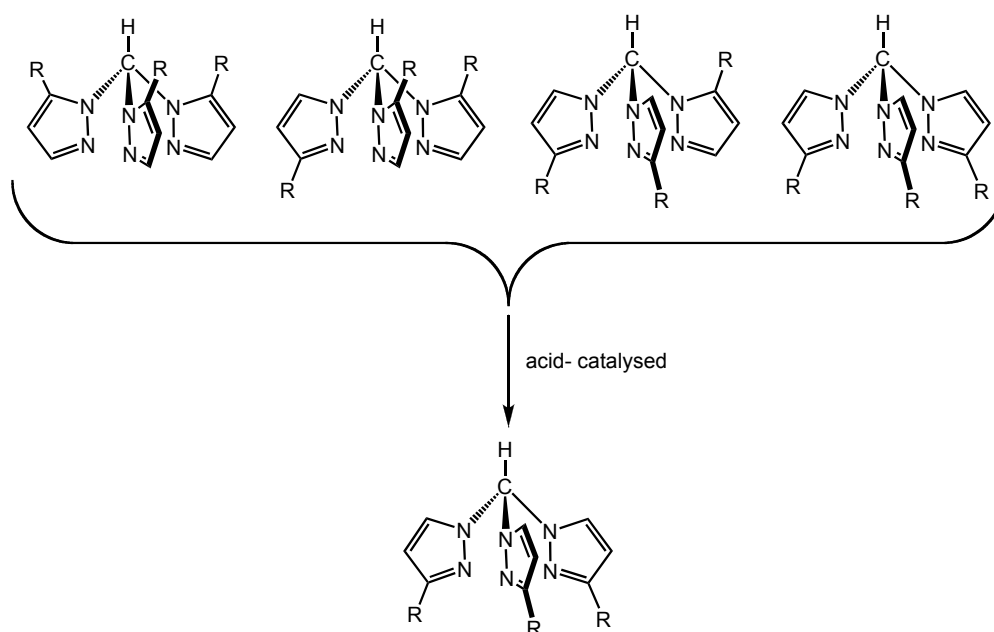
An important advantage of Tpm and its derivatives is their substantial stability in air. This behavior is very useful when Tpm is prepared in a large scale, stored and used for further functionalization. In fact, it has been possible to keep the compound for months in air without any decomposition. Nevertheless, its storage under inert atmosphere avoids the absorption of humidity, since it is slightly hygroscopic after several weeks. However, it has been sufficient to dry it under vacuum for a few hours to remove the absorbed water.

The synthesis²² of Tpm does not need chromatographic purification: the compound is effectively crystallized from diethyl ether. Moreover, different methods to increase the yield and the efficiency of the synthesis have been tested, especially with a view to further synthetic steps of functionalization: (i) crushing of crude product with diisopropylether leads to a white off powder in higher yield and in a

appreciable purity for further reactions; (ii) chromatographic purification (acetone/pentane) of crystallisation's mother liquor furnishes a considerable amount of Tpm in very good purity.

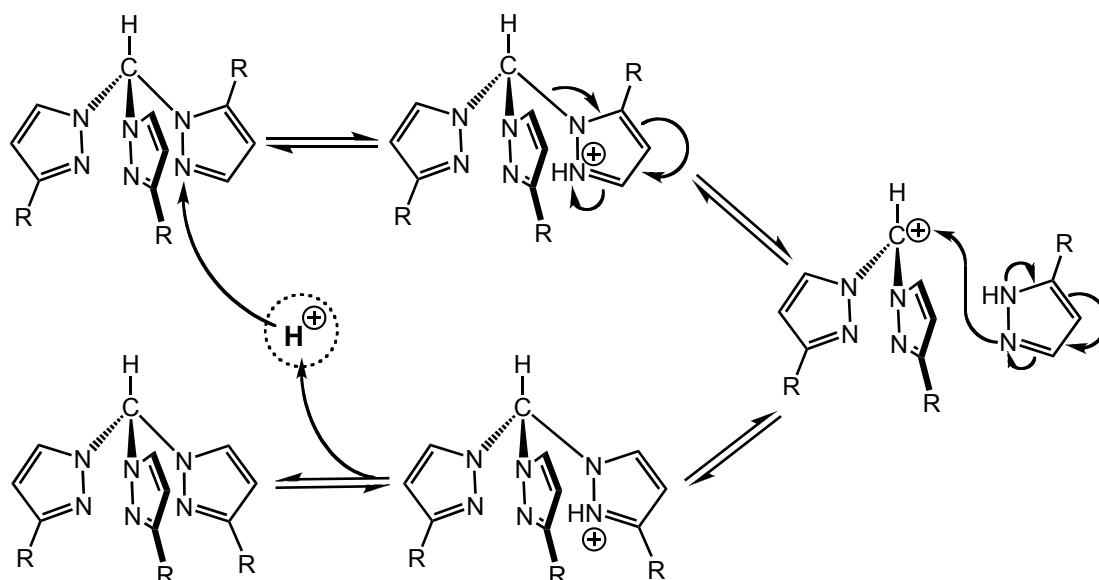
Tpm is well soluble and stable in all common organic solvents (CH_2Cl_2 , CHCl_3 , CH_3CN , THF, MeOH, EtOH, ...), but does not exhibit high solubility in water ($S_{25^\circ\text{C}} \approx 15.5 \text{ mg}\cdot\text{mL}^{-1}$, see also Section 1.3.1).

Several attempts of functionalization that required different pH conditions, have shown that hydrotris(pyrazolyl)methane is goodly stable in a wide range of pH. While remains stable in mild acidic range of pH (*i.e.* acetic acid), decomposition occurs in case of strong acidic conditions (conc. HBr, HCl, HNO_3 ...; see below and Scheme 1.4). This characteristic has hampered the synthesis of some new derivatives that needed these strong conditions during the preparation (Sections 1.3.2.3 and 1.5). The instability in strong acidic media has been exploited in cases of substituted Tpm. In fact, it is reported that the synthesis²⁸ of 3-substituted Tpm derivatives involves the treatment of the crude mixture with a catalytic amount of *p*-toluensulfonic acid: the mixture of regioisomers, formed after the first synthetic step, converts to a single regioisomer where the steric interactions are minimized (Scheme 1.3).



Scheme 1.3 Acid-catalyzed conversion of unsymmetrical Tpm to a single regioisomer.

It is possible to propose herein that, in this acid-catalysed equilibrating condition, the protonation of the pyrazolyl ring could favour a retro-alkylation process to restore the free pyrazole. The latter is able to react with the carbon-cation, forming the sterically favourable regioisomer (Scheme 1.4).



Scheme 1.4 Proposed mechanism, in this study, for acid-catalyzed conversion of 3-substituted *Tpm*.

During the preparation of tris(3-phenylpyrazolyl)methane and tris(3-*tert*butylpyrazolyl)methane, trifluoroacetic acid (TFA) has been successfully used instead of *p*-toluenesulfonic acid (Table 1.1, compounds **(12)** and **(13)**).

Furthermore, a radical decomposition of tris(pyrazolyl)methane has been investigated in this thesis, and it has been verified that when *Tpm* is oxidized at the central carbon to a radical species, it can undergo a decomposition via homolytic breaking of C-pz (pz = pyrazolyl ring) single bond and restore the starting pyrazole ring within other byproduct.²⁹ This behavior has been the object of an extensive study in this work and will be discussed in Section 1.4.

1.2.3 Tpm: characteristics

The tripodal tris(pyrazolyl) ligand is characterized by its three pyrazolyl rings, connected together through a central methine carbon. Thus, the molecule, with the exception of not-symmetrical Tpm that bears pyrazolyl rings differently substituted (*i.e.* known as *heteroscorpionates*), has a C_{3V} symmetry and the corresponding N_3 -coordinated metal complexes maintain this symmetry.³⁰⁻³²

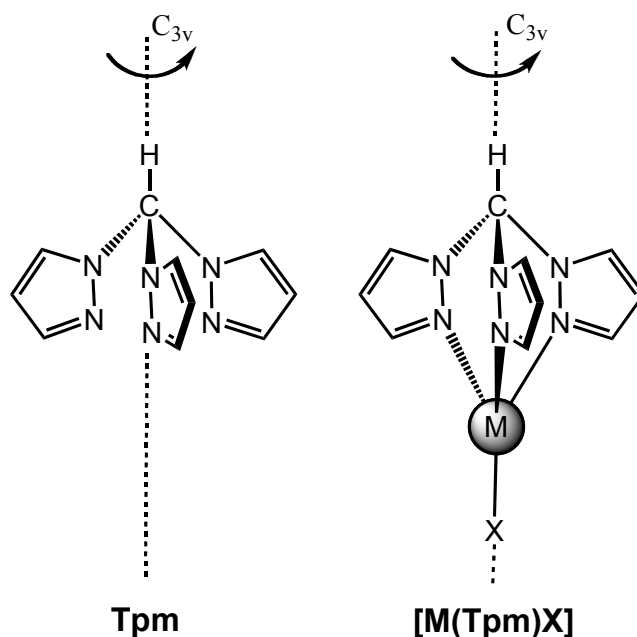


Figure 1.2 The C_{3V} symmetry for Tpm and for a N_3 -coordinated Tpm metal complex of general formula $[M(Tpm)X]$.

The C_{3V} axis crosses the central methine carbon and the planes of pyrazolyl rings are parallel to this axial orientation. It is reported that, in the corresponding metal complexes, the pyrazolyl ring could (in some cases)³³ bend relatively to C_{3V} axis. This torsion angle could depend on some steric interactions³⁴ and electronic spin state^{31,32} of the metal center (*i.e.* Fe^{II} , d^6 , low spin (LS) or high spin (HS), see also Chapter 3, Section 3.3.1). Therefore, this symmetrical property furnishes important advantages in some spectroscopical studies. Proton and carbon NMR experiments³⁵, in fact, are affected by this feature: the three pyrazolyl rings are equivalent in NMR spectra and the 3, 4 and 5-positions of the heterocyclic ring could be definitely identified (Figure 1.3). Furthermore, the N-alkylation of the pyrazolyl ring alters the

positions 3 and 5 of the ring that appear, in the $^1\text{H-NMR}$ spectra, shifted from the free pyrazole: the δ 7.63 ppm value associated to the 3,5-H protons of the free pyrazole, splits to 7.68 and 7.59 ppm for 3-H and 5-H protons of pyrazolyl ring of **(1)**, respectively.

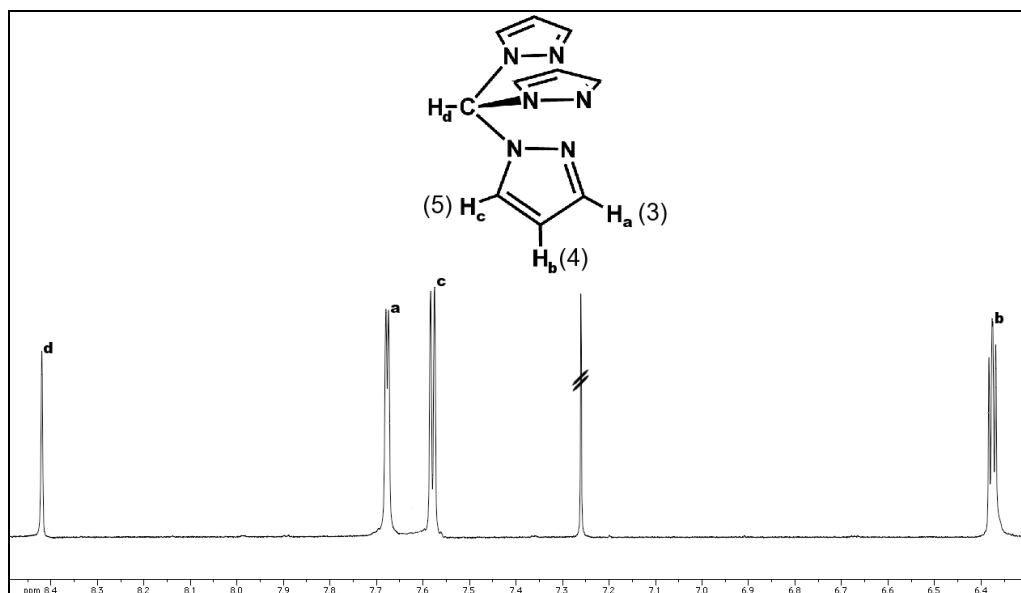


Figure 1.3 $^1\text{H-NMR}$ (CDCl_3) spectrum of Tpm, **(1)**.

1.2.4 Tpm: the pyrazolyl ring

As previously mentioned the pyrazolyl ring of Tpm shows interesting properties and peculiar characteristics.

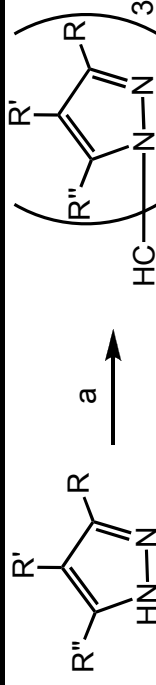
In the $^1\text{H-NMR}$ spectrum, the 3- and 5-positions are differentiated and typically for N-alkylated pyrazole the 5-position is unshielded to lower field, whereas the 3- moves to higher field; consequently the $^1\text{H-NMR}$ signal of the proton at position 4 duplicates its multiplicity. The coupling constant is not affected and maintains its typical value (from 1.7 to 2.6 Hz) of the free pyrazole.

The pyrazolyl ring ligated to the central methine carbon maintains the principal properties of a free heterocyclic ring, but as it is expected the functionalization on the ring results much more complicated than in the pyrazole itself. For instance, the electrophilic substitutions (*i.e.* sulfonation, nitration...) at the 3-, 4- or 5-carbon atoms are not known and it is predictable that the reaction conditions (strong acidic) could lead to decomposition of the Tpm, itself. Therefore,

the functionalization of Tpm, at the pyrazolyl ring, cannot be achieved starting from the Tpm, but (as widely explored^{17,18} for Tp) has been carried out²² for this study, on the pyrazole that has been successively assembled to the desired scorpionate. The latter step has been, then, modified according to the nature of substituents on the pyrazole ring (see Table 1.1).

Table 1.1 Syntheses of pyrazolyl-substituted Tpm used in this work.

Compound	n.	R	R'	R''	a	ref
Tpm	(1)	H	H	H	1) Na ₂ CO ₃ (6 eq), [NBu ₄]Br, H ₂ O; 2) CHCl ₃ (excess), Δ, 72 h	22
Tpm ^{Me2}	(11)	Me	H	Me	same as Tpm; work up (wu): crushing in <i>i</i> Pr ₂ O and chromatographic purification (pentane/acetone)	22
Tpm ^{Ph}	(12)	Ph	H	H	1) Na ₂ CO ₃ (6 eq), [NBu ₄]Br, H ₂ O; 2) CHCl ₃ (12 eq), Δ, 84 h; 3) TFA, toluene, Δ, 15 h; wu: neutralisation with NaHCO ₃ , crushing in <i>i</i> Pr ₂ O	34
Tpm ^{<i>t</i>Bu}	(13)	<i>t</i> Bu	H	H	(3- <i>t</i> Bu-pyrazole prepared from 3,3-dimethyl-2-butanone, ethyl formate and hydrazine) ¹⁷ ; 1) Na ₂ CO ₃ (6 eq), [NBu ₄]Br, H ₂ O; 2) CHCl ₃ (12 eq), Δ, 84h; 3) TFA, toluene, Δ, 15 h; wu: neutralisation with NaHCO ₃ , column (pentane/acetone).	22
Tpm ^{<i>i</i>Pr}	(14)	<i>i</i> Pr	H	H	(3- <i>i</i> Pr-pyrazole prepared from 3-methyl-2-butanone, ethyl formate and hydrazine) ¹⁸ ; 1) Na ₂ CO ₃ (6 eq), [NBu ₄]Br, H ₂ O; 2) CHCl ₃ (12 eq), Δ, 84 h; 3) TFA, toluene, Δ, 15 h; wu: neutralisation with NaHCO ₃ , column (pentane/acetone).	22
Tpm ^{Ph2}	(15)	Ph	H	Ph	1) Na ₂ CO ₃ (6 eq), [NBu ₄]Br, H ₂ O; 2) CHCl ₃ (12 eq), Δ, 90 h. (Note: ¹ H-NMR of crude mixture presents starting material (28%) and some byproducts from decomposition (46%).	this work, p.14



In particular, purification methods of Tpm^{Me_2} (**11**) were modified from the published procedure.²² In fact, alternatively to the sublimation of unreacted 3,5-dimethylpyrazole and successive chromatographic purification, a faster crushing in diisopropyl ether gave the desired product in good purity and reasonable yield. On the other hand, a direct chromatographic purification (acetone/pentane) removed the starting material providing the desired Tpm^{Me_2} in good yield and purity.

The 3-substituted Tpm prepared and used in this work (*i.e.* Tpm^{Ph} (**12**) and Tpm^{tBu} (**13**)) were synthesized by modifying³⁴ the known procedure:²² as previously mentioned, trifluoroacetic acid (TFA) was used instead of *p*-toluene sulphonic acid to convert the mixture of regioisomers to the single more stable regioisomer and, for Tpm^{Ph} , has been possible to avoid chromatographic purification by collecting the product after crushing in *iPr*₂O (diisopropyl ether). Moreover, during the preparation, it has been observed that progressive addition of lower amounts of HCCl_3 to the reaction mixture provides a better yield. For the less reactive 3-substituted pyrazoles the use of a large excess of chloroform could lead to a low efficient synthesis: the sequential addition of small quantities (2 x 6 eq) of HCCl_3 in the biphasic vigorously stirred mixture favours the complete substitution of the three chlorine atoms and minimizes the formation of mono- and bis-adducts (Figure 1.4). In fact, besides the latter being more reactive to substitution than chloroform itself, the steric hindrance hampers the third nucleophilic substitution at the central carbon and the absence of a large excess of chloroform in the reaction mixture favours this process.

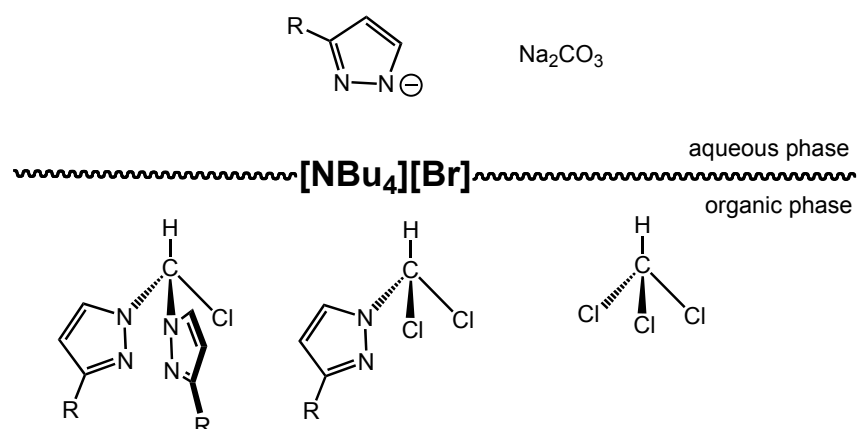


Figure 1.4 Schematic representation of reaction mixture of 3-substituted Tpm synthesis ($R = \text{Ph}$ (**12**), $t\text{Bu}$ (**13**)).

The synthesis of Tpm^{Ph_2} (**15**) has been attempted by modifying the starting procedure, but the product was formed together with a considerable amount of starting material and byproducts. The excessive steric hindrance of the starting 3,5-diphenylpyrazole is the main reason of the low efficiency of the reaction. The final product should exhibit interesting properties in terms of steric modulation of the reactivity of the apical side of the ligand for the stabilisation of anionic derivatives (see Section 1.4).

In general, it is expected that ring substituents would have an effect on the electronic and donor/acceptor properties of the ligand. Nevertheless, Reger and co-workers reported²² that this influence is minimal. At the same time, it is possible to define separately the effect of the substituents at the pyrazolyl ring (Figure 1.5):

-position 3: the major contribution of the substituents at this position is of steric nature. These groups, in fact, are facially oriented toward the coordination to the metal center and hold an important role for the modulation of Tpm derivative coordination chemistry.^{18,34,36} In the case of bulky substituents (*i.e.* *i*Pr, Ph and *t*Bu), the ligand is forced to engage a definite coordination geometry. In particular, for those metals with an high affinity for the octahedral N_6 -coordination mode (*i.e.* Fe^{II}), this steric limitation obliges them to abandon the typical full-sandwich coordination of two of such type of ligands: $[\text{ML}_2]\text{X}$, (L = Tpm derivative). Moreover, it has been reported³⁷⁻³⁹ that substituents at 3-position could be directly involved in the coordination to the metal center. Many relevant applications in bioinorganic chemistry are also known,^{38,40-42} specifically due to this modulation effect on the coordination chemistry of metal centers with biological interest (*i.e.* Cu, Fe, Zn,...). Furthermore, it has been proved that the bulky substituents at the 3-position could also enhance the thermodynamic and hydrolytic stability of the corresponding complexes.

-position 4: substituents in this position of the pyrazolyl ring are not common for Tp or Tpm derivatives^{43,44}, and this type of functionalization is not exhaustively studied probably because of its minor influence on the coordination properties of the scorpionate. In fact, substituents at position 4 are directed neither toward the metal center nor toward the apical position. This ‘meridian’ orientation is, indeed, more related to electronic effect on the heterocyclic ring and do not interfere with the coordination ability of the scorpionate ligand.

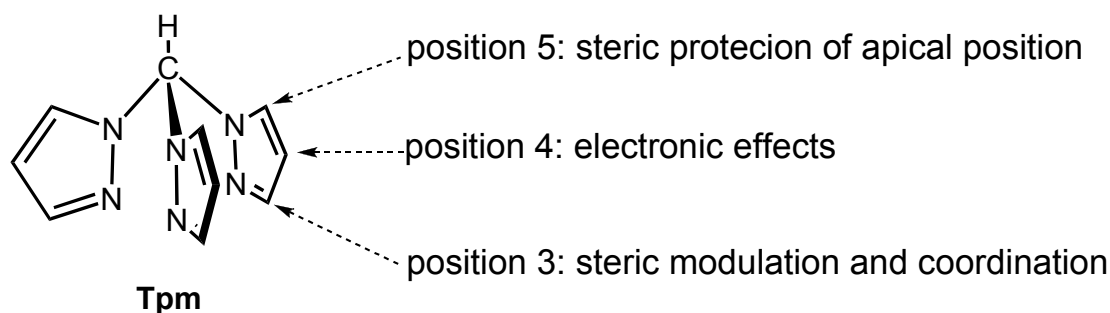


Figure 1.5 Schematic representation of Tpm with highlighted positions.

-position 5: the greater difficulty to prepare Tpm derivatives bearing bulky substituents in position 5 compared to Tp analogues (see Section 1.2.1) is indicative of the steric interactions existing in this type of compound. As mentioned in previous Sections, the low versatility of the Tpm synthesis has driven to a limited investigation on its 5-substituted derivatives. With the exception of methyl and *iso*-propyl substituents,⁴⁵⁻⁴⁷ no bulkier groups have been introduced at position 5. Herein, the groups can modulate the ‘opposite face’ of the scorpionate ligand⁴⁸ and recently many works report important improvements in this field.^{29,49,50} A detailed study of steric effect of 5-substituents is presented in Section 1.4.

The synthesis of other Tpm derivatives, not further explored, will be discussed in Section 1.5: Appendix A. They constitute a crucial point for the exhaustive description of the chemical properties of the Tpm ligand, cover an important set of reactions and demonstrate how extensive could be the investigation in this field.

1.2.5 Tpm: the central carbon

The other important point of the molecule is undoubtedly the central methine carbon. This highly activated tertiary carbon is reasonably stable (see Section 1.2.2), in spite of the electron withdrawing effect of the three pyrazolyl rings. The ¹³C-NMR spectrum of Tpm, in fact, confirms that this methine moiety is affected by the heterocyclic rings: the resonance corresponding to the central carbon appears at δ 100 ppm. Also the proton directly connected to it reflects this effect: its resonance is observed at δ 8.58 ppm in the ¹H-NMR spectrum (Figures 1.3 and 1.6) implying the ‘acidic’ nature of this proton. Nevertheless, the downshifting in chemical shifts could

also be due to a spatial effect of pyrazolyl rings: the hydrogen atom is inside the aromatic ‘cone’ effect of the three rings that could, in principle, affect the central proton atom lowering its resonance.

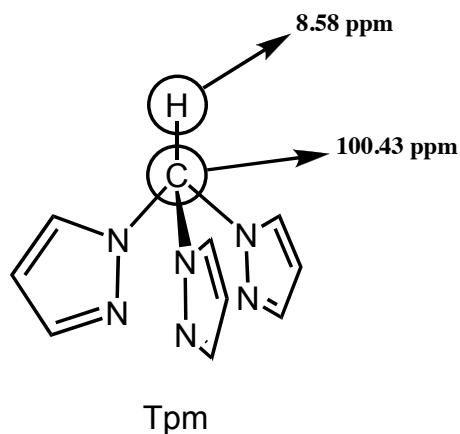


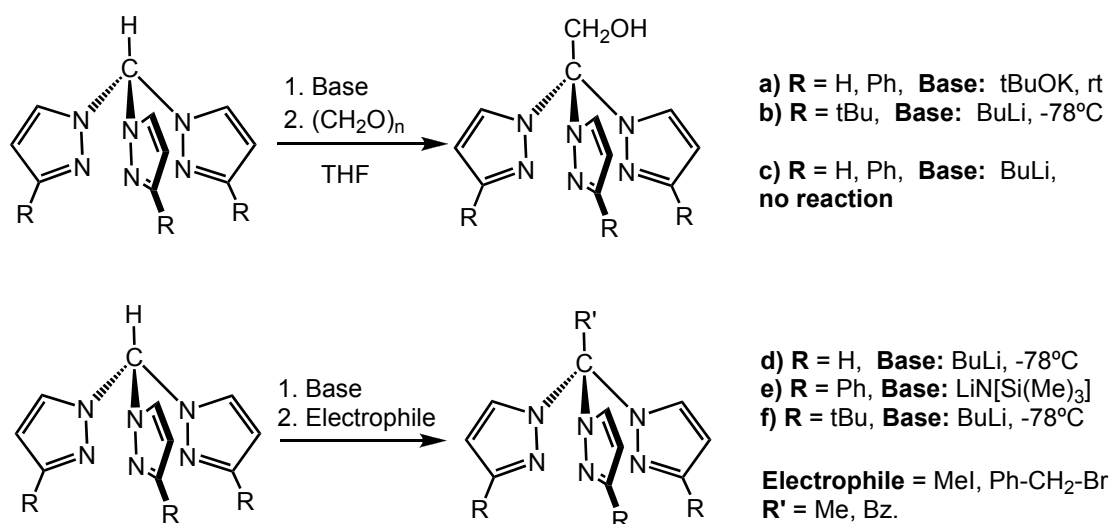
Figure 1.6 ^1H and ^{13}C -NMR δ values for proton and carbon of the central unit of Tpm.

The deprotonation of the methine C has been, in fact, widely explored⁵¹⁻⁵⁴ and object of an intense research in synthetic and organometallic chemistry. Recently,^{55,56} this functionalization of Tpm ligand appeared with a great relevance in multidisciplinary aspects of chemistry (*i.e.* dendrimers, supramolecular and solid supported chemistries...) and many applications in those fields are in fast progress and expansion.

Different parts of this work have included the deprotonation process of the apical proton of Tpm and its derivatives and will be extensively discussed in the next sections.

1.3 Carbon functionalization of Tpm

As mentioned in the previous paragraph, the removal of the apical proton of Tpm leads easily to the corresponding carbanion. The deprotonation could be achieved by different strong bases, such as butyl lithium, sodium hydride, sodium ethoxide or potassium methoxide.^{51,57} It has been carefully described, by Reger, that the choice of a suitable base could be a crucial step for the success of the reaction. Where *n*BuLi is an appropriate base for the methylation of the central carbon, the same base could not be used with paraformaldehyde, (CH₂O)_n, to functionalize by the hydroxymethylene moiety (Scheme 1.5, examples **c** and **d**).



Scheme 1.5 Examples of deprotonation followed by functionalization of Tpm.

The reason of these interesting differences stays in the nature of the carbanion that is generated: the strong lithiation of the central carbon of Tpm is carried out in 'controlled condition' at -78° C and gives rise to a highly reactive species able to react with strong electrophiles (*i.e.* methyl iodide) at low temperature. On the other hand, the mild deprotonation of an alkoxide base (*i.e.* potassium *tert*butoxide) and successive nucleophilic substitution by paraformaldehyde is performed at room temperature for 12 h. Furthermore, it has been demonstrated that, besides the strength of the base, an important effect could be also played by the counter-ion. It was shown,⁵⁸ in fact, that the yields of the deprotonation-Lewis acid substitution improved

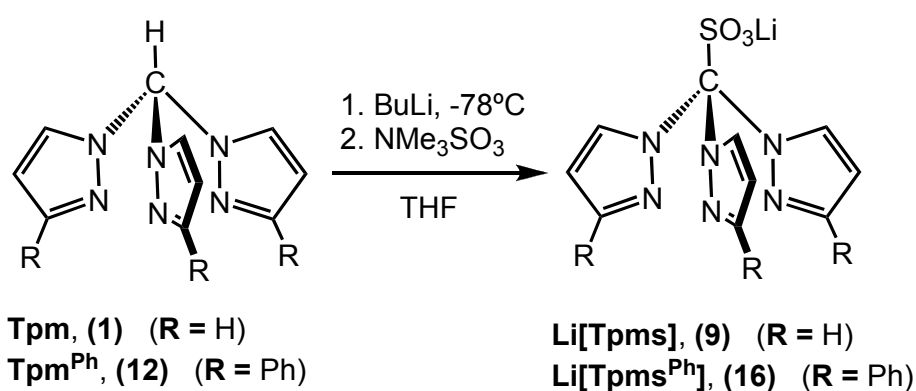
when the ligand was first complexed to a transition metal. In addition, an extensive description of the role of lithium ion (*i.e.* Li^+) in the deprotonation by BuLi, is given in Section 1.4, where the unexpected stability of the carbanion of tris(3,5-dimethylpyrazolyl)methane is explained.

As shown in Scheme 1.1, that summarizes the major synthetic routes studied in this work, the next Sections will describe the most important functionalizations of the central methine carbon developed herein.

1.3.1 The tris(pyrazolyl)methanesulfonate: Tpms

First reported by Kläüi,⁵² in 2000, tris(pyrazolyl)methanesulfonate, Tpms, has rapidly gained a considerable significance on the scorpionate chemistry and many works^{34,59-65} actually relate to this sulfonate functionalization of central methine carbon.

This derivative of Tpm has been prepared by the known procedure (Scheme 1.6) where the adduct NMe_3SO_3 is used as a source of the sulfonate moiety.



Scheme 1.6 Synthesis of $\text{Li}[\text{Tpms}]$ (**9**) ($R = \text{H}$) and $\text{Li}[\text{Tpms}^{\text{Ph}}]$ (**16**), ($R = \text{Ph}$).

The sulfonate compounds synthesized and used in this work are $\text{Li}[\text{Tpms}]$ (**9**) and its unprecedented phenyl analogue $\text{Li}[\text{Tpms}^{\text{Ph}}]$ (**16**) (Scheme 1.6). The synthesis of the latter has been optimized to reach reasonable yield and purity (see Chapter 3).

In contrast to Tpm, the sulfonate derivative is highly soluble in water and moderately soluble in alcohols. Moreover, $\text{Li}[\text{Tpms}]$ is stable over a wide range of pH values in aqueous solution: at pH 0 only small amounts of pyrazole (see Section 1.2.2) can be detected even after several weeks and in basic conditions (pH 13) no

signs of decomposition occur. This feature turned out to be decisive in many areas, since the corresponding water soluble metal complexes represent a favorable class of compounds to be tested in catalysis and bioinorganic chemistry in aqueous media.

It is reported that several 3-substituted Tpm compounds have been functionalized as sulfonates. In particular, sterically hindered derivatives (*i.e.* bearing *i*Pr, *t*Bu and Ph at position 3 of the pyrazolyl ring) have been the object of an extensive investigation.^{34,59,61,63} These bulky substituted tris(pyrazolyl)methanesulfonates, in fact, hold at least four main fascinating characteristics:

(i) modulate the coordination properties of the ligand, bearing steric groups at position 3 of the pyrazolyl ring, *i.e.* avoid the “sandwich” adduct and tune the coordination ability of the resulting metal complex to small molecules,^{34,66-69} such as nitriles, isonitriles, CO,...; this behavior has been studied for new copper complexes in Chapter 2.

(ii) the sulfonate moiety increases the solubility in polar organic solvents and the water solubility; as an example, Li[Tpms^{Ph}] (**16**), prepared in this work, shows a high solubility in water ($S_{25^{\circ}\text{C}} \approx 90 \text{ mg}\cdot\text{mL}^{-1}$) in spite of the presence of phenyl substituents.

(iii) the sulfonate group could be involved in the coordination to metal, converting the N₃-type Tpm^R ligand in a more versatile Tpms^R, able to act as either a tripodal or a bipodal ligand (*i.e.* with N₃-, N₂O-, N₂- or NO-coordination modes, see Figure 1.7).^{34,59,63,64} This flexibility is the central topic of Chapter 2.

(iv) the anionic nature of the sulfonate derivative could undoubtedly modify its coordination properties in comparison to the neutral precursor, Tpm. As will be discussed further, the Tpms coordination chemistry is in general more favoured toward monocationic metal ions (*i.e.* Cu^I) compared to Tpm ligand; the formation of neutral adduct could be, in many cases, an important driving force.

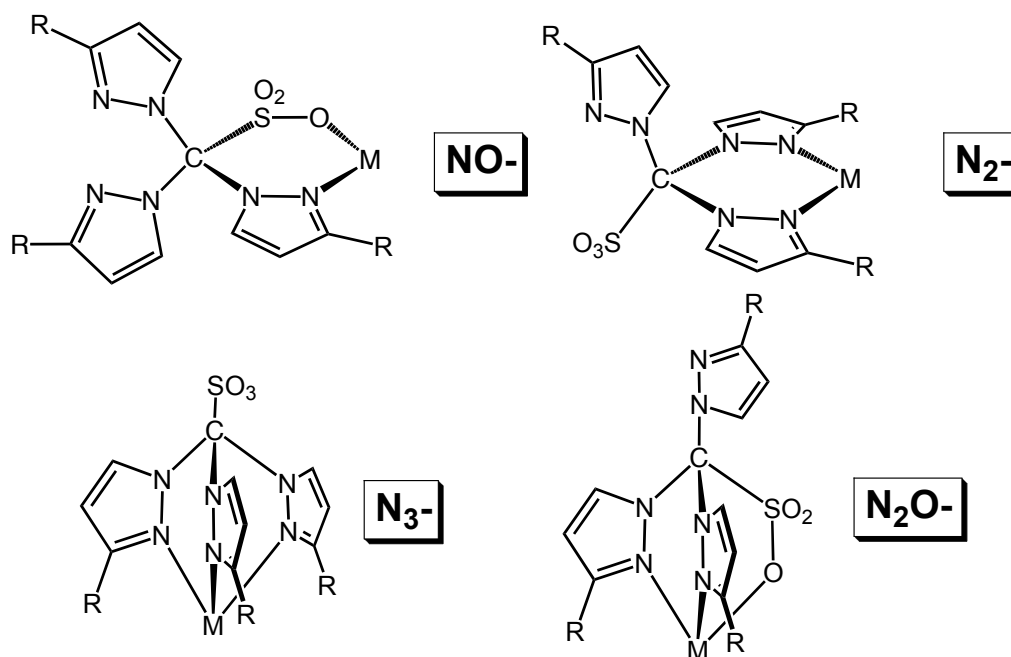


Figure 1.7 Coordination modes of $Tpms^R$ ligand.

A great interest has been devoted^{59,70,71} to the thallium analogue of $Li[Tpms]$. In fact, a simple metathesis reaction of $Li[Tpms]$ with an suitable metal salt gives the corresponding tris(pyrazolyl)sulfonate salt (e.g. $K[Tpms]$ is prepared from reaction with potassium carbonate). The facile removal of thallium salts is the reason of the great interest around the preparation of $Tl[Tpms]$, that is a ‘perfect’ starting material for complexation reaction.

Moreover, it is interesting to consider an additional role of metal cation in the chemical properties of the sulfonate derivative. It is appropriate, in fact, to consider the sulfonates $Li(Tpms^R)$ as lithium complexes. In fact, besides the reported formation of the N_3 -adduct $[(\kappa^3-Tpms^R)Li]$ (see next Section 1.4), the lithium ion usually forms intermolecular $Li \cdots OS$ interactions⁶⁴ that furnish interesting data on IR ν_{SO} and ν_{CS} (Figure 1.8).

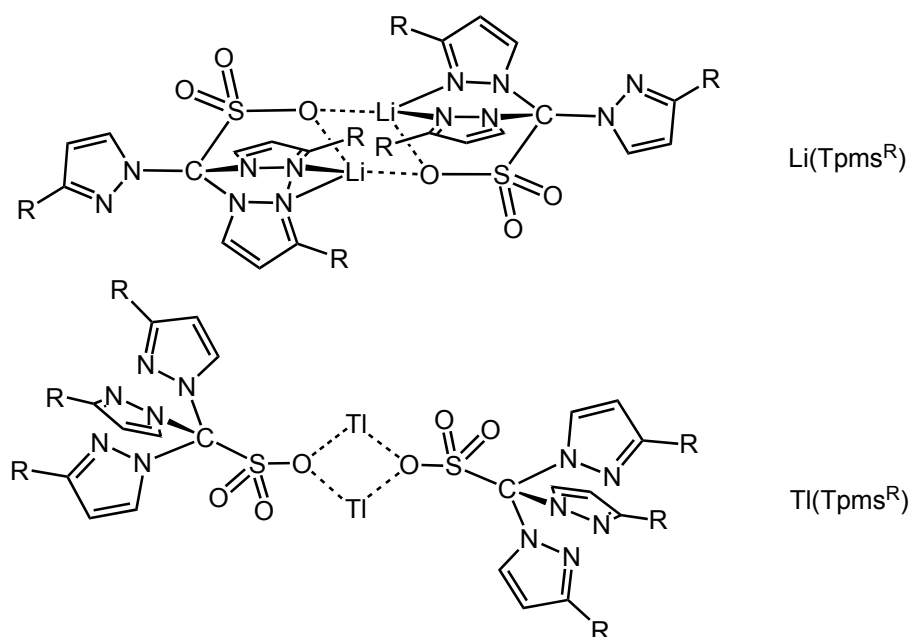


Figure 1.8 Representation of the complexes present in solid state and in solution for $\text{Li}(\text{Tpms}^{\text{R}})$ and $\text{Tl}(\text{Tpms}^{\text{R}})$.

Moreover, it is intriguing to notice the difference among $^1\text{H-NMR}$ resonances of $\text{Li}(\text{Tpms})$ (**9**) in different solvents (*i.e.* δ 7.91, 8.11, 7.62 for 3-H(pz) in MeOD, DMSO and D_2O , respectively; see Experimental Part) that in some cases could be involved in several intermolecular interactions (see also Section 2.5).

In addition to the previously mentioned Tpms species, attempts have been carried out to sulfonate the central carbon of other derivatives of Tpm. In fact, the reactivity of the tris(3,5-dimethylpyrazolyl)methane, Tpm^{Me_2} (**11**) has been unsuccessfully tested in the sulfonation reaction. An exhaustive description of the reasons of the inertness of this 3,5-disubstituted Tpm derivative and, in general, of all 5-substituted tris(pyrazolyl)methane ligands, can be found in Section 1.4.

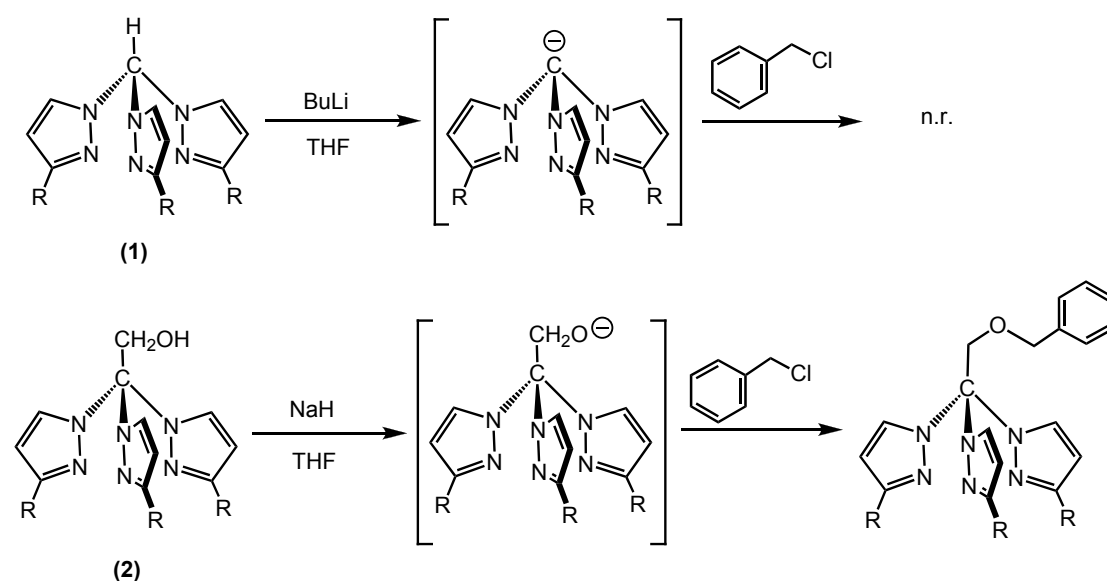
1.3.2 Tris-2,2,2-(1-pyrazolyl)ethanol (**2**): the hydroxy derivative

One of the most important Tpm derivatives for the development of a synthetic plan of functionalization is the hydroxy-methylene derivative, the tris-2,2,2-(1-pyrazolyl)ethanol, $\text{HOCH}_2\text{C}(\text{pz})_3$ (pz = pyrazolyl ring), (Scheme 1.1, (**2**)).

Scheme 1.5 has shown how the preparation of this derivative passes through a mild deprotonation of the apical methine carbon and the successive nucleophilic

attack to paraformaldehyde to yield the alcohol derivative. Tris-2,2,2-(pyrazol-1-yl)ethanol (**2**) has a pronounced affinity to all common organic solvents and its stability is comparable to that of Tpm itself.

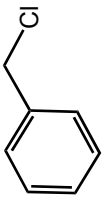



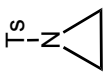

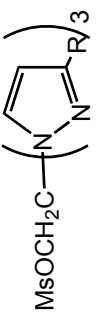
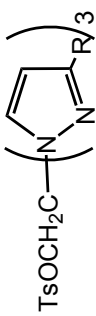
The hydroxy group of (**2**) is an important functional group for further functionalizations of the molecule and it is easily predictable that the reactivity of alkoxide prepared upon deprotonation of the starting material is a more versatile scaffold than the carbanion derived from Tpm (Scheme 1.7).

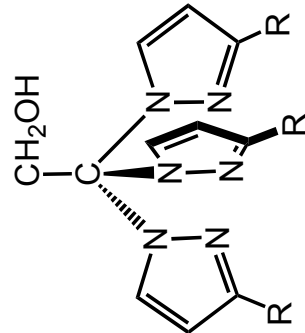


Scheme 1.7 Different reactivity of Tpm (**1**) and tris-2,2,2-(1-pyrazolyl)ethanol, (**2**).

The alkoxide could, indeed, react with a large variety of species and this topic has been the object of a wide investigation in the last years in coordination chemistry.^{22,51,72-79} In this work, compound (**2**) has been used as a building block for the synthesis of new Tpm derivatives: in Table 1.2 the new classes of prepared ligands are schematically presented.

Table 1.2 Functionalization of tris-2,2,2-(pyrazolyl)ethanol (2) carried out in this thesis.

base	electrophile	product	notes
			Section 1.3.2.3
NaH			Section 1.3.2.3 Chapter 3
			Section 1.3.2.2
	$N_3P_3-G_{c0}^{(a)}$	$N_3P_3-G_{c1}^{(a)}$	Section 1.6
-	MsCl		Section 1.3.2.1
-	TsCl		Section 1.3.2.1

^(a) Phosphorus dendrimer, see Section 1.6.

1.3.2.1 Reactivity of tris-2,2,2-(1-pyrazolyl)ethanol.

The hydroxy group of **(2)** could be easily deprotonated with sodium hydride, in a classical procedure of deprotonation of alkyl alcohols.⁷² The sodium salt of tris-2,2,2-(1-pyrazolyl)ethanol (*i.e.* NaOCH₂C(pz)₃) is usually used instantaneously for the next step with a suitable electrophile to give the desired product.

It has been possible to isolate the alkoxide, after evaporation of the solvent (THF) and crushing in dry pentane of the residue. The pale yellow solid could be stored under dinitrogen at room temperature for days.

Several coordination reactions of the salt derivative to a metal center have been attempted, revealing an oxidising nature of the derivative: reaction with an Fe^{II} salt led to formation of a mixture of unidentified Fe^{III} byproducts.

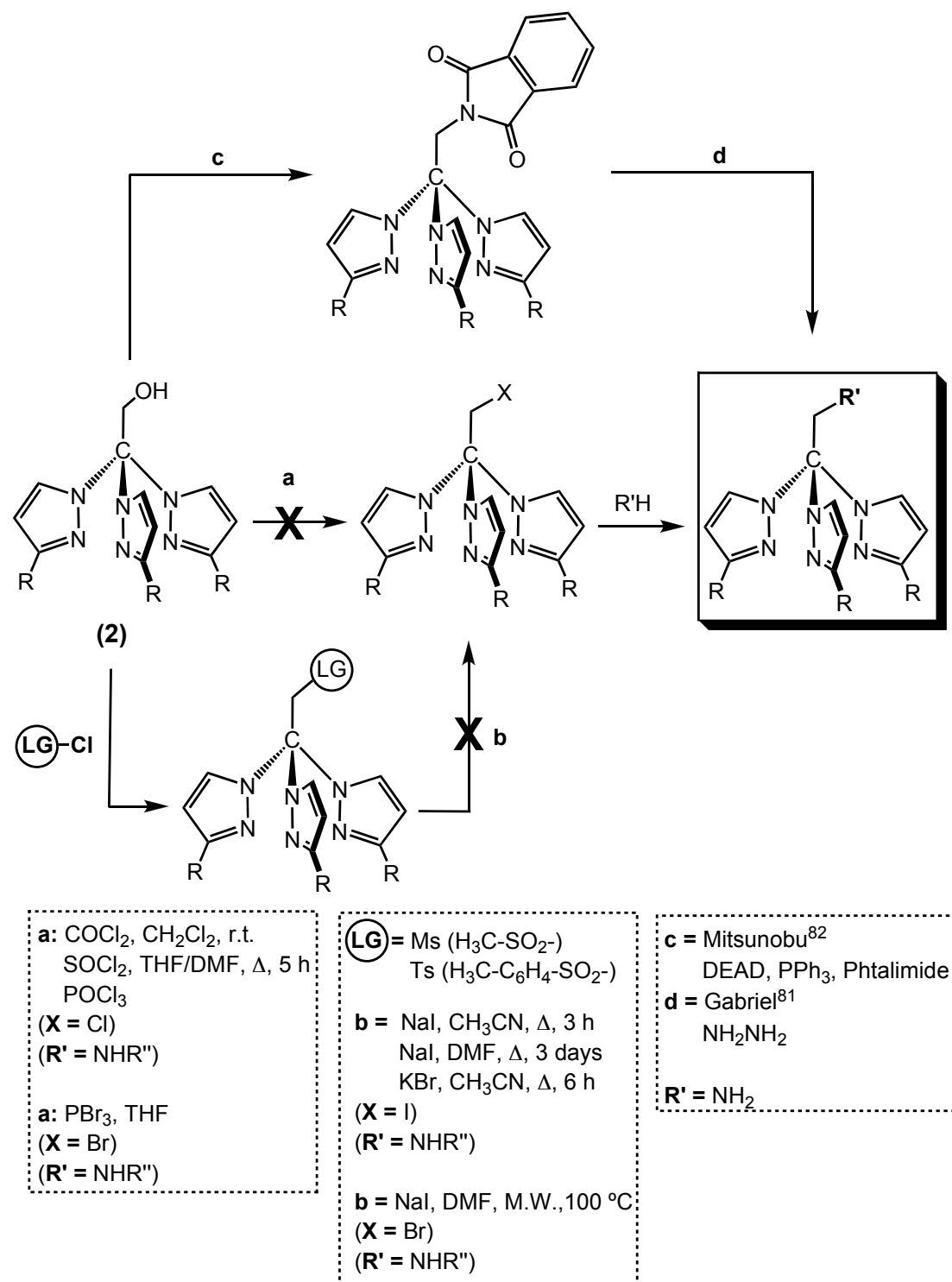
1.3.2.1.1 Substitution of the hydroxy group

One of the main purposes of this research project was to functionalize the Tpm with hydrophilic moieties, in order to increase the water solubility of the compound and of the corresponding metal complexes. Starting from **(2)**, a new strategy to prepare the amino-analogue has been planned (Scheme 1.8). Different synthetic pathways have been studied to substitute the –OH group for an –NHR moiety that holds important features in terms of hydrosolubility (*i.e.* the protonable group increases drastically the hydrophilicity of the compound), coordination chemistry and further functionalization (*i.e.* reaction with electrophiles, N-alkylation,...).

Any effort to replace the hydroxy group by an halogen has been unsuccessful (Scheme 1.8, Step **a**): simple chlorination, in mild conditions (*i.e.* oxalyl chloride, dichloromethane, room temperature) or in drastic conditions (*i.e.* thionyl chloride, neat, reflux) did not occur. Similarly, bromination –*via* phosphorus tribromide- led to decomposition of the scorpionate scaffold to restore free pyrazole. All processes act in strong acidic range of pH (*i.e.* HCl or HBr is formed) and this could lead to a partial decomposition of the compounds (see Section 1.2.2).

The activation of the –OH moiety to generate an efficient leaving group (Scheme 1.8, **LG**) has been performed: mesylation or thiosylation of tris-2,2,2-(1-pyrazolyl)ethanol yields easily the desired product. The latter, surprisingly, appears highly stable⁸⁰ and every attempt (Scheme 1.8, Step **b**) to replace the mesylate (or

thiosylate) group failed. Harsh reaction conditions (*i.e.* NaI excess, DMF, 3 days, reflux) leave the compound unchanged with traces of the desired product.



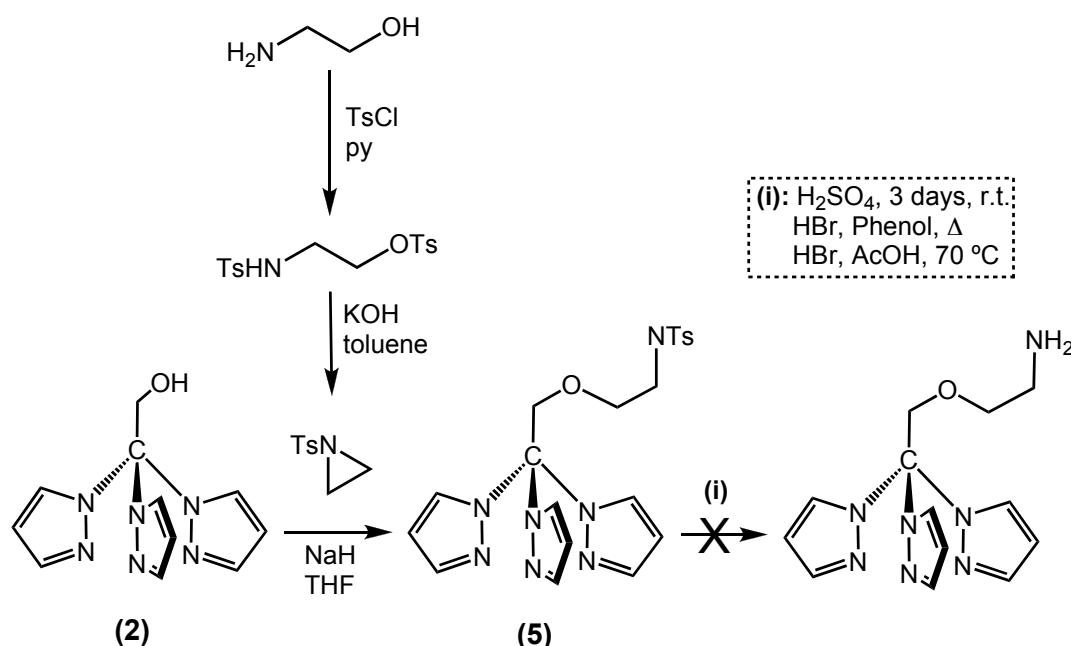
Scheme 1.8 Synthetic plan for the synthesis of amino-based Tpm derivatives.

The unexpected stability of the mesylate derivative of tris-2,2,2-(1-pyrazolyl)ethanol could be partially explained considering the steric hindrance of the three pyrazolyl rings around the methylene moiety, they can obstruct the access to substitution that should occur *via* a S_{N2} mechanism.

To work out this obstacle, another pathway has been carried out. The substitution of hydroxyl group for a primary amine (*i.e.* $-NH_2$) could be accomplished through the Mitsunobu/Gabriel synthesis.^{81,82} This procedure provides the best results, although the final yield and purity of the amino derivative are not satisfactory to extend the process for the large-scale synthesis of the new Tpm derivative.

1.3.2.1.2 Alkylation of tris-2,2,2-(1-pyrazolyl)ethanol.

At the same time, another functionalization of tris-2,2,2-(1-pyrazolyl)ethanol (**2**) has been developed in order to connect an amino group to the scorpionate scaffold. As an alternative to the previous synthesis (Section 1.3.2.2), the alkylation of the hydroxy group with thiosylated-aziridine could provide a derivative of Tpm bearing a longer alkyl chain with amino termination (Scheme 1.9, compound **5**).



Scheme 1.9 Synthetic pathway for the synthesis of 2-(tris-2,2,2-(pyrazolyl)ethoxy)ethanamine.

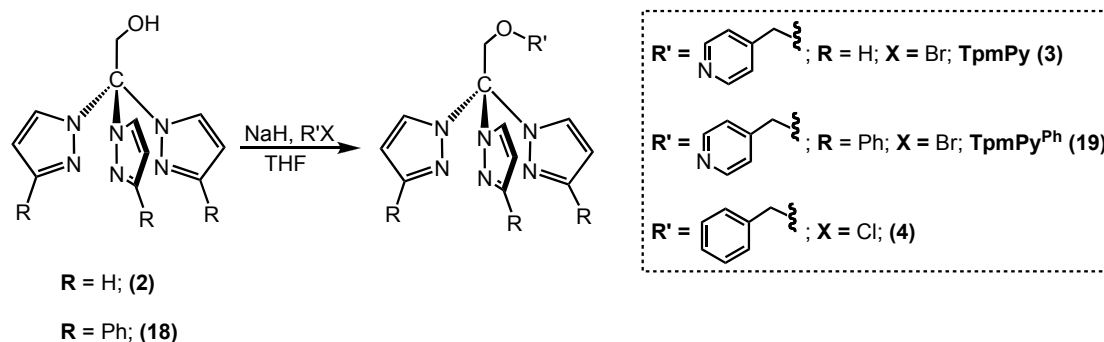
Thiosyl-protected aziridine has been prepared according to the known procedure:⁸³⁻⁸⁶ starting from the complete thiosylation of ethanolamine, with

subsequent cyclization upon deprotonation of sulfonamide with potassium hydroxide. The sodium salt of **(2)** is reacted to thiosylated aziridine to yield quantitatively the desired compound, TsNHCH₂CH₂OCH₂C(pz)₃ (Ts = thiosyl, pz = pyrazolyl) **(5)**. The latter is stable in air, but its crystallisation resulted more difficult due to the presence of the additional sulfonamido alkyl chain. Several attempts to obtain the primary amine, removing the thiosyl protection, led to decomposition of the tris(pyrazolyl) backbone. In fact, most methods⁸⁷ to remove the N-protection involve extremely acidic conditions that promote the degradation of the compound.

The coordination chemistry of the new N-thiosyl-2-(tris-2,2,2-(1-pyrazolyl)ethanol)ethaneamine **(5)** ligand has been studied (see Experimental Part).

1.3.2.1.3 Benzyl and 4-pyridyl derivative of tris-2,2,2-(1-pyrazolyl)ethanol

In addition to the previously reported functionalizations, the reactivity of sodium alkoxide of tris-2,2,2-(1-pyrazolyl)ethanol has been studied with benzyl chloride and 4-bromomethyl pyridine (Scheme 1.10). As expected, the nucleophilic substitution of the bromobenzyl species proceeds with higher purity than that of the chloro-derivative. The O-benzylated product has been isolated after chromatographic purification in reasonable yield.



Scheme 1.10 Synthesis of 4-((tris-2,2,2-(pyrazol-1-yl)ethoxy)methyl)pyridine, TpmPy **(3)**, 4-((tris-2,2,2-(3-phenylpyrazol-1-yl)ethoxy)methyl)pyridine, TpmPy^{Ph} **(19)** and its benzyl analogue **(4)**.

The synthesis of 4-pyridyl derivative of tris-2,2,2-(1-pyrazolyl)ethanol, **TpmPy**^(*) (**3**), proceeds readily yielding the product in good yield and purity. It is conveniently crystallized from diethyl ether (Figure 1.9).

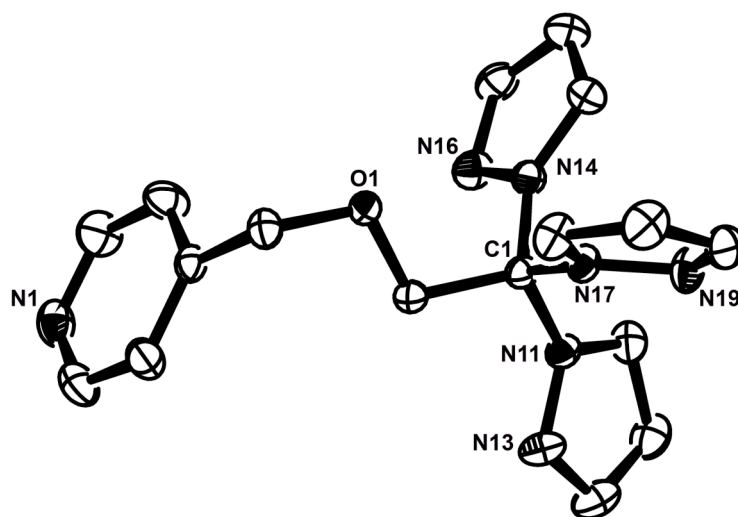


Figure 1.9 ORTEP plot of *TpmPy* (**3**) ellipsoids are shown at 50% of probability.

TpmPy (**3**) bearing the additional pyridyl moiety holds two new important features: first, the new group can modify the coordination chemistry of the ligand, being involved in complexation reactions toward metal centers with good affinity to pyridyl ligand. Moreover, the extra heterocycle could increase the hydrophilicity of the compound upon protonation of the nitrogen atom. In fact, **TpmPy**, while highly soluble in all common organic solvents (i.e., Et₂O, CH₂Cl₂, CH₃Cl, MeOH, EtOH or acetone) and moderately soluble in water ($S_{25^{\circ}\text{C}} \approx 10 \text{ mg}\cdot\text{mL}^{-1}$) as a free base, becomes, upon protonation of the pyridine, well water soluble as a salt.

A substantial investigation of the coordination chemistry of this new scorpionate has been carried out in this thesis and is described in Chapter 3.

* For this new derivative it has been used the Trofimenko's nomenclature that indicates the substituent(s) at the pyrazolyl rings by an upper index. In this case, the suffix "Py" -in **TpmPy**- refers to the pyridyl-pendant chain at the apical position.

1.4 Carbon functionalization via radical pathway

In the last decade, it is believed that further synthetic development toward the functionalization of the central methine carbon atom of the tris(pyrazolyl)methane derivatives would be greatly advantageous,⁷⁹ as such changes to the backbone can dramatically influence the properties of the complexes, as well as permitting their attachment on a solid support.⁸⁸

As previously discussed, substitution at the central methine carbon atom can be achieved by reacting a suitable electrophile (*e.g.* RBr, with R = benzyl; 4-pyridyl; -CH₂CH₂SO₃⁻Li⁺ for sulfonate derivatives; thiosylated aziridines for ammonium derivatives) with the carbanion ⁻C(pz)₃ formed by deprotonation of Tpm.^{22,52,79,88,89} However, this method resulted unsuccessful for sterically hindered tris(pyrazolyl)methanes, with general formula HC(pz^R)₃ (R ≠ H) and, in order to explore new routes toward the functionalization of the central methine carbon, the possibility of a radical pathway has been explored in this study.

In particular, tris(3,5-dimethylpyrazolyl)methane, HC(pz^{Me2})₃ (pz^{Me2} = 3,5-dimethylpyrazolyl), Tpm^{Me2} (Table 1.1, compound **(11)**), has currently attracted a great interest due to its specific electronic and steric properties which give transition metal complexes unique attributes.^{79,89,90} The corresponding red carbanion ⁻C(pz^{Me2})₃ has been recently reported to display an unusual stability at room temperature that has even allowed the structural characterisation of its lithium complex as [⁻C(pz^{Me2})₃Li⁺(thf)] (**(7)**) (Scheme 1.11, reaction **(a)**).⁹¹ This inertness of the carbanion has recently been further confirmed with the isolation and structural characterisation of several complexes containing the sp³ hybridised carbanion⁵⁰ which acts as a six electron N₃-donor face-capping ligand, *e.g.* in [Mg{C(pz^{Me2})₃}Cl], [Mg{C(pz^{Me2})₃}₂], [Zn{C(pz^{Me2})₃}Me],⁴⁹ [M{C(pz^{Me2})₃}₂] (with M = Fe(II), Co(II)),⁹² [M{C(pz^{Me2})₃}(PPh₃)] (M = Cu(I), Ag(I))⁴⁸ or in [Ti(NBut){C(pz^{Me2})₃}Cl(THF)].⁹³ Curiously, this carbanion appears to form stable carbon-metal bonds *e.g.* with gold(I) as in [Au{C(pz^{Me2})₃}(PPh₃)],⁴⁸ as well as its unsubstituted analogue in the W(Mo)/Au heterodimetallic compounds [M(CR)(CO)₂Au{C(pz)₃}(C₆F₅)].^{57,58}

However, the carbanion has been shown to be inert to electrophiles, thus preventing the incorporation of a substituent at the central carbon, what has been

accounted for by the steric hindrance associated to the three methyl groups in position 5 of the pyrazolyl rings. The latter, in fact, upon coordination toward the metal center move to the axial orientation and create a sort of cage around the carbanion (Figure 1.10, A); on the other hand, in absence of a metal ion the pyrazolyl rings are free to rotate and leave a ‘naked’ carbanion (Figure 1.10, B). Thus, during the deprotonation of Tpm^{Me_2} -via BuLi - the temporary formation of the lithium complex (**7**) has been recognized to be the reason of stability of the carbanion.

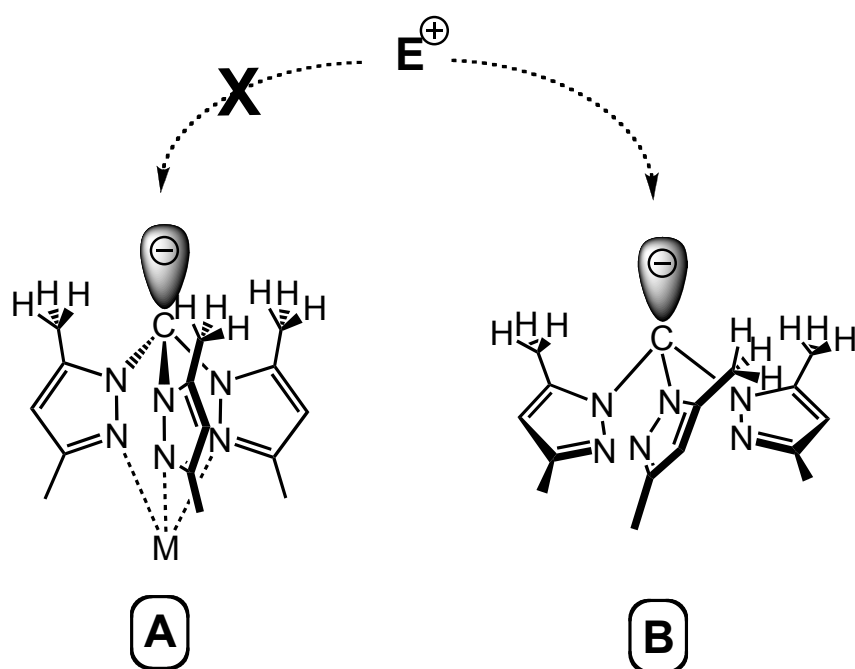
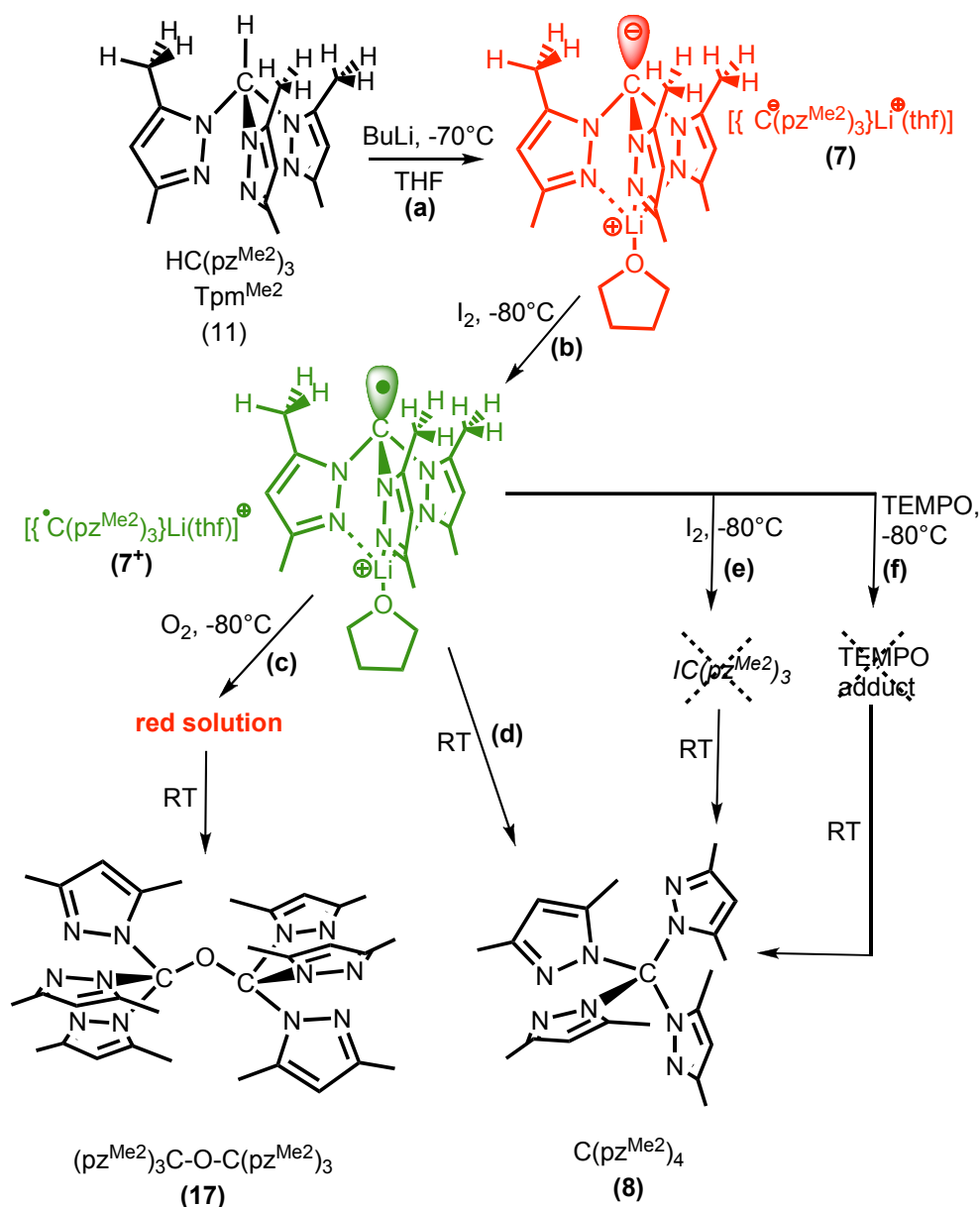


Figure 1.10 Influence of metal coordination on the orientation of the 5-methyl groups of ${}^{-}\text{C}(\text{pz}^{\text{Me}_2})_3$

The relative inertness of this carbanion led us to embark on the generation of its corresponding oxidised radical form ${}^{\bullet}\text{C}(\text{pz}^{\text{Me}_2})_3$ and the exploration of the reactivity of the latter. In the next Section it is discussed in detail the preparation of the anionic [$\{\text{C}(\text{pz}^{\text{Me}_2})_3\}\text{Li}^+(\text{thf})$] (**7**), the generation and identification of the C-centered radical ${}^{\bullet}\text{C}(\text{pz}^{\text{Me}_2})_3$ as its Li^+ salt, [$\{\text{C}(\text{pz}^{\text{Me}_2})_3\}\text{Li}(\text{thf})\}^+$ (**7**⁺) and its chemical behavior toward O_2 , TEMPO (2,2,6,6-tetramethyl-1-piperidinyloxy) and I_2 .

1.4.1 Identification of the radical $\cdot\text{C}(\text{pz}^{\text{Me}_2})_3$, (7^\cdot)

Upon reaction of tris(3,5-dimethylpyrazolyl)methane Tpm^{Me_2} (**11**) with an equivalent amount of butyllithium at -70°C in THF, a red solution of the complex $[\cdot\text{C}(\text{pz}^{\text{Me}_2})_3]\text{Li}^+(\text{thf})$ (**7**) was formed (Scheme 1.11, reaction (a)).



Scheme 1.11 Synthetic route to (7^\cdot) and its derived products (**17**) and (**8**).

As expected from a previous report,⁹¹ (**7**) was found to be stable upon warming to room temperature, and evaporation of the solvent gave a red-orange solid with ^1H NMR data (in $\text{THF-}d_8$) that are identical to those reported for (**7**) produced by

using MeLi as a base. Importantly, the $^1\text{H-NMR}$ of the crude solid (**7**) did not show any significant signals of either $\text{HC}(\text{pz}^{\text{Me}_2})_3$ (**11**) or other side products, indicating the clean quantitative formation of (**7**). Therefore, (**7**) was used without any further purification.

Careful oxidation of (**7**), at $-80\text{ }^\circ\text{C}$ using 0.5 eq of I_2 ,^(*) causes an instantaneous color change to deep dark green, the formed species (**7**⁺) being stable for several hours only below $-60\text{ }^\circ\text{C}$ under argon (Scheme 1.11, reaction (**b**)). The X-band EPR spectrum (Figure. 1.10) of a 1 mM THF frozen solution of (**7**⁺),^(**) recorded at 95 K, exhibits an intense single isotropic signal at $g = 2.0026$ (with a peak-to-peak line width of *ca.* 15 G and no resolved hyperfine splitting) that is characteristic of an organic radical. The lack of any hyperfine structure in the EPR spectrum precludes any analysis of the spin density distribution within this species. However, since the line width of the signal is relatively narrow (*ca.* 15 G), any hyperfine splitting should be relatively small; this may indicate that the unpaired electron is not (or only to a limited extent; *vide infra*) localised on the *N*-pyrazole atoms, mostly residing on the central methine carbon.

This is in accord with the (pseudo)tetrahedral conformation of the carbanion $\text{C}(\text{pz}^{\text{Me}_2})_3$ in (**7**) which lacks *p*-delocalization. Thus, the green species should be the C-based radical $\text{C}(\text{pz}^{\text{Me}_2})_3$, which presumably exists as the lithium complex $[\{\text{C}(\text{pz}^{\text{Me}_2})_3\}\text{Li}(\text{thf})]^+$ (**7**⁺), formulated in a comparable manner to the parent $[\{\text{C}(\text{pz}^{\text{Me}_2})_3\}\text{Li}^+(\text{thf})]$ (**7**).

In order to corroborate the above hypothesis, theoretical calculations of (**7**) and (**7**⁺) using the density functional theory (DFT) have been performed by Dr. M. L. Kuznetsov (see Experimental Part). As shown in Table 1.3, the calculated bond lengths in (**7**) are in reasonable agreement with the corresponding X-ray structural data.⁹¹ The maximum deviations of the theoretical and experimental parameters are 0.06 Å for the Li–O bond and 0.03 Å for the Li⋯C1 distance whereas the difference

* The use of a silver salt (e.g. $\text{Ag}[\text{BF}_4]$) as a one-electron oxidizing agent has proved to be unsuitable, as the only product identified, after purification, was the sandwich complex $[\text{Ag}\{\text{HC}(\text{pz}^{\text{Me}_2})_3\}_2][\text{BF}_4]$ (**48**) which was fully characterised including by X-ray crystallography (see Experimental, Chapter 6).

** In this experiment, the anion was generated in a 1mM concentration in THF; addition of 0.5 eq of I_2 produces the radical which is present in $\leq 1\text{mM}$ concentration (a suitable concentration for the detection of radical species by EPR spectroscopy) and the resulting solution was carefully transferred at $-80\text{ }^\circ\text{C}$ to an EPR tube (kept under argon at $-80\text{ }^\circ\text{C}$); the tube was then immediately cooled (and the solution frozen) in liquid nitrogen (77 K). No color change has been detected during or after the transfer, indicating that the bright green color characteristic of the radical remained (Chapter 6).

for the other bonds does not exceed 0.02 Å often falling within the 3σ interval of the X-ray data.

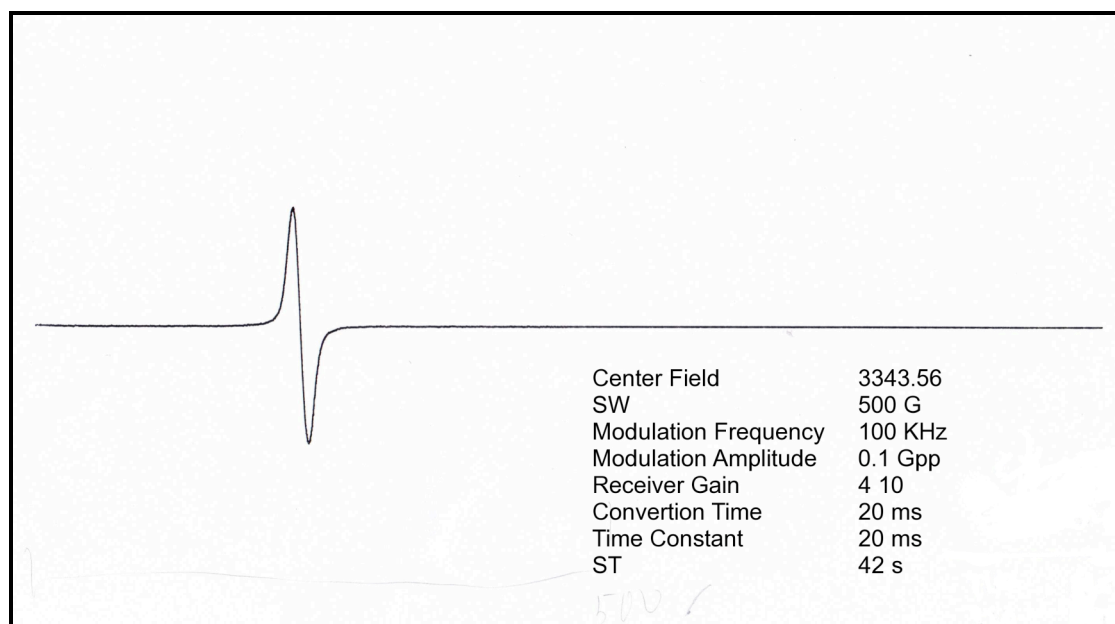


Figure 1.11 EPR spectrum of a 1 mM frozen THF solution of $[\{C(pz^{Me_2})_3\}Li(thf)]^+$ (7^+), recorded at 95 K in a Bruker ESP 300E spectrometer with an A-500 RF power amplifier.

The comparison of the equilibrium geometries of (**7**) and (7^+) (Table 1.3) reveals that the oxidation mostly affects the geometry at the C1 carbon atom, namely (i) the N–C1–N angles significantly increase, (ii) the C1–N bonds and the distance between C1 and the plane formed by the N1, N2, and N3 atoms (P_{NNN}) shorten, (iii) the angles between the pyrazolylic planes noticeably decrease, and (iv) the dihedral angles NN⋯NN characterizing the mutual orientation of the pyrazolyl rings increase from 5.29°–6.31° in (**7**) where all N–N bonds are almost parallel, to 28.70°–29.00° in (7^+) where the pyrazolyl rings appear to be twisted relative to each other. These findings indicate a flattening of the tetrahedral geometry (*i.e.* C_{3v} axes, see Section 1.2.3) of the C1N₃ moiety upon oxidation.

As a result, the C1⋯Li⁺ distance becomes shorter by 0.117 Å despite the elongation of the Li–N bonds. Such a flattening has been interpreted by the Natural Bond Orbital (NBO) analysis (Table 1.4), which allows the determination of the orbitals hybridization type. This analysis has demonstrated that the hybridization of the orbital of the C1 atom bearing the lone electron pair in (**7**) is $sp^{4.2}$ (where the superscript index indicates the p-character/s-character ratio of the hybrid orbital). The

oxidation results in a significant increase of the relative contribution of the p orbitals and the hybridization type in (7^+) becomes $sp^{8.2}$. By other words, the orbital of C1 bearing the unpaired electron in (7^+) has predominantly p character.

Table 1.3 Comparison of the experimental geometrical parameters reported⁶ for (**7**) with those obtained by DFT calculations for (**7**) and (7^+).

Bond Distances (Å)	[C(pz ^{Me2}) ₃ Li ⁺ (thf)] (7)			[C(pz ^{Me2}) ₃ Li(thf)] ⁺ (7^+)
	X-ray ^a	DFT _{calcd} ^a	DFT _{calcd} (this study)	DFT _{calcd} (this study)
Li...C1	2.890	2.852	2.857	2.740
avLi-N	2.023	2.040	2.048	2.190
Li-O	1.908	1.983	1.972	1.905
avC1-N	1.448	1.449	1.448	1.403
avN-N	1.371	1.382	1.379	1.387
avC-N	1.326	1.331	1.333	1.330
avC-C	1.388	1.414	1.411	1.422
avC-C	1.364	1.384	1.385	1.376
avN-C	1.353	1.363	1.363	1.375
Distance C1...P(NNN) (Å)	0.483	-	0.455	0.310
Angles between pz planes (°)	120.66		120.10	110.63
	120.18	-	117.55	112.70
	119.15		120.16	112.51
Angle N-C1-N	109.70		110.61	115.24
	109.47	-		115.33
	109.21			115.19
Dihedral angles pz₁NN- pz₂NN (°)	0.35		6.31	28.70
	1.56	-	5.29	29.00
	2.59		5.96	28.94

^a Reference.⁹¹

The calculated atomic spin densities in (7^+) (see Figure 1.12) reveal that the unpaired electron is mainly localized at the methine carbon atom C1 (spin density of 0.74). The remaining spin density is equally distributed onto the pyrazole rings (altogether ~0.09 for each ring). Thus, the low spin density on the pyrazole ring does not allow strong hyperfine coupling at N ($I = 1$) or Pz-H ($I = 1/2$), what justifies the

relatively narrow EPR signal obtained for (**7**⁺) (Figure 1.11) Though the band width of the latter signal of 15 G suggests a certain amount of coupling, a decrease of the modulation amplitude (during EPR measurements) as low as 0.1G did not allow to resolve these couplings. Since the three pyrazole rings are equivalent, the broadening of the signal may result from the hopping of the electron to pass from one ring to the other.

Table 1.4 Results of the NBO analysis of (**7**) and (**7**⁺); (the occupation, hybridization (η) and percent contribution of atomic orbitals to bond orbitals are indicated).

Bond orbital		(7)	(7 ⁺)
Lone pair or unpaired electron	Occ.	1.81	0.92
	η	s ^{19.19} p ^{80.78}	s ^{10.87} p ^{89.13}
C1-N1	Occ.	1.98	0.99
	C1(%; η)	34.06;s ^{26.90} p ^{72.93}	36.81;s ^{29.68} p ^{70.20}
	N1(%; η)	65.94;s ^{36.24} p ^{63.73}	63.19;s ^{34.52} p ^{65.45}
C1-N2	Occ.	1.98	0.99
	C1(%; η)	34.08;s ^{26.94} p ^{72.89}	36.85;s ^{29.76} p ^{70.13}
	N1(%; η)	65.92;s ^{36.26} p ^{63.72}	63.15;s ^{34.44} p ^{65.53}
C1-N3	Occ.	1.98	0.99
	C1(%; η)	34.05;s ^{26.94} p ^{72.89}	36.83;s ^{29.74} p ^{70.15}
	N1(%; η)	65.95;s ^{36.27} p ^{63.71}	63.17;s ^{34.44} p ^{65.52}

Thus, the results are convincing and consistent with the initial hypothesis based on the EPR study, both indicating that (**7**⁺) consists of the C-based radical $\cdot\text{C}(\text{pz}^{\text{Me}_2})_3$, presumably coordinated to the lithium ion via the pyrazole N-atoms, being formulated as [$\{\cdot\text{C}(\text{pz}^{\text{Me}_2})_3\}\text{Li}(\text{thf})$]⁺.

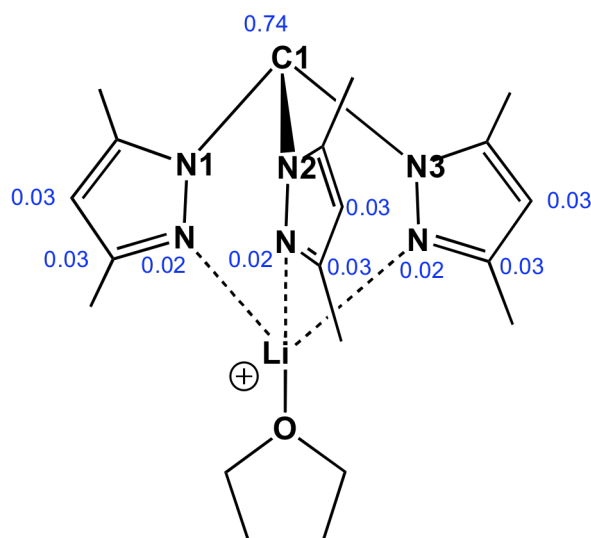


Figure 1.12. Calculated spin density distribution in the optimized geometry of (7^+).

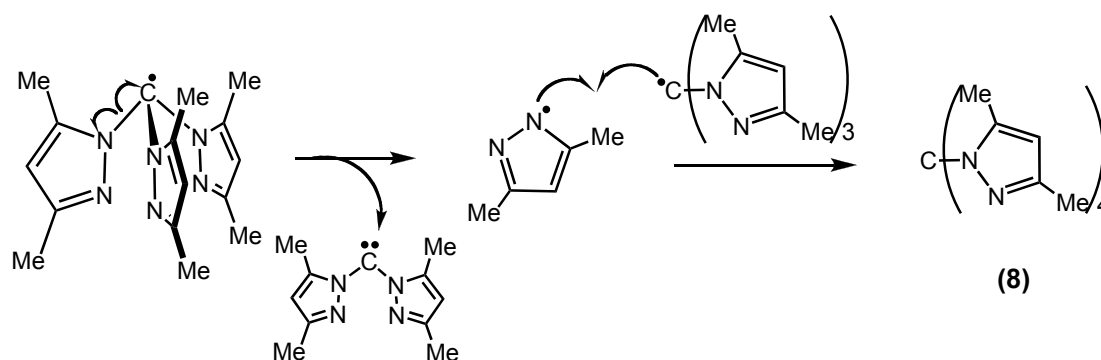
1.4.2 Reactivity of $\cdot\text{C}(\text{pz}^{\text{Me}_2})_3$

As a preliminary investigation of the reactivity of (7^+) and in order to prove that substitution at the central carbon can be achieved, freshly generated (7^+) was reacted with various reagents such as I_2 (0.5 eq.), O_2 (excess), and TEMPO (1eq.) aiming the production of the iodo-compound $\text{IC}(\text{pz}^{\text{Me}_2})_3$, a C-peroxo species, and a TEMPO adduct, respectively.

Upon bubbling O_2 through a THF solution of (7^+), at $-80\text{ }^\circ\text{C}$, the reaction mixture turned deep red within seconds (Scheme 1.11, reaction (c)). Subsequent work-up and purification led to the isolation of a single compound, (**17**). The ^1H NMR in CDCl_3 of (**17**) exhibits three singlets at δ 5.83, 2.41 and 2.26 with 3: 9: 9 integrating ratios, respectively, which are typically assigned to the 4-H pyrazolyl atom, and the methyl groups at the 3 and 5 positions, correspondingly. Furthermore, positive electrospray shows two main peaks at 611 and 305 which may be attributed to $[\text{O}\{\text{C}(\text{pz}^{\text{Me}_2})_3\}_2 + \text{H}]^+$ and $[\text{O}\{\text{C}(\text{pz}^{\text{Me}_2})_3\}_2]^{2+}$ respectively. Thus, in the absence of X-ray structural data, this new species was tentatively formulated as the bis(tris(3,5-dimethylpyrazolyl)methane)ether compound $(\text{pz}^{\text{Me}_2})_3\text{C}-\text{O}-\text{C}(\text{pz}^{\text{Me}_2})_3$.

In all the other attempted reactions (Scheme 1.11, reactions (e) and (f), with I_2 and TEMPO respectively), three compounds were identified after work-up, *i.e.* free 3,5-dimethylpyrazole, the starting material $\text{HC}(\text{pz}^{\text{Me}_2})_3$ and a new product, (**8**). The same was observed when (7^+) was warmed up to room temperature without addition

of any reagents (Scheme 1.12, reaction **(d)**), what indicates that **(8)** does not result from a radical condensation with the reagents but likely is a decomposition product of $\cdot\text{C}(\text{pz}^{\text{Me}2})_3$ in **(7⁺)**. The three products were separated by chromatography column over silica, and **(8)** was identified as the unprecedented tetrakis(3,5-dimethylpyrazolyl)methane, $\text{C}(\text{pz}^{\text{Me}2})_4$, as indicated by ^1H , ^{13}C NMR, IR, MS-EI and X-ray crystallography (see Section 1.4.4). It reasonable to propose that a N-centered pyrazolyl radical $\cdot\text{pz}^{\text{Me}2}$, formed by decomposition of $\cdot\text{C}(\text{pz}^{\text{Me}2})_3$, couples with the parent $\cdot\text{C}(\text{pz}^{\text{Me}2})_3$ to give $\text{C}(\text{pz}^{\text{Me}2})_4$ (Scheme 1.12).



Scheme 1.12 Proposed pathway for the formation of $\text{C}(\text{pz}^{\text{Me}2})_4$ (**8**).

1.4.3 Characterisation of $\text{C}(\text{pz}^{\text{Me}2})_4$ (**8**)

The X-ray crystal structural analysis of **(8)** confirms its formulation as $\text{C}(\text{pz}^{\text{Me}2})_4$ without ambiguity (see Figure 1.13) and thus demonstrates that substitution at the central methine carbon of $\text{HC}(\text{pz}^{\text{Me}2})_3$ can be achieved. Bond lengths (\AA) and angles ($^\circ$) in the structure of **(8)** are as expected for pyrazole compounds (see Table 1.5).

Table 1.5. Selected bond lengths (\AA) and angles ($^\circ$) for **(8)**.

(\AA)		$(^\circ)$	
C1 N31	1.455(3)	N21-C1-N31	110.92(18)
C1 N41	1.455(3)	N31-C1-N11	106.62(19)
C1 N11	1.458(3)	N11-C1-N41	110.66(18)
C1 N21	1.461(3)	N41-C1-N21	106.71(19)
		N31-C1-N41	110.73(19)
		N11-C1-N21	111.27(18)

However, a unique and striking feature of the structure is the presence of intramolecular C-H--- π interactions specifically between each 5-CH₃ group and an adjacent pyrazolyl π -ring, as indicated in Figure 1.13. The distance between the C-H hydrogen and the centroid of the pyrazolyl ring lies in the 2.50 – 2.66 Å range, indicating a relatively strong non-covalent interaction (Table 1.5).⁹⁴⁻⁹⁷

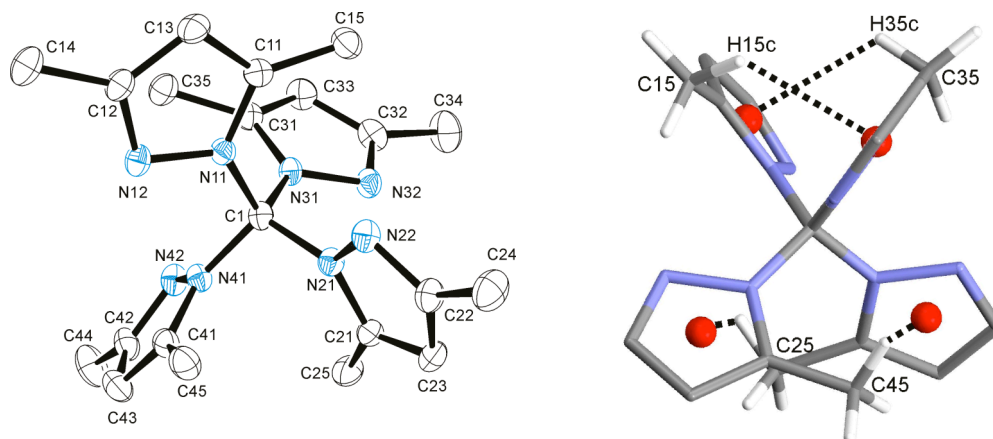


Figure 1.13. Representation of the molecular structure of $C(pz^{Me_2})_4$ (**8**): (left) ORTEP plot shown at 50% probability (H-atoms have been omitted for clarity) and (right) representation of the intramolecular C-H--- π interactions involving the 5-CH₃ group and an adjacent pyrazolyl π -ring (only the H-atoms of 5-CH₃ are shown and the 3-CH₃ groups have been omitted for clarity; the centroid of the pyrazole ring is represented as a red dot).

The ¹H-NMR spectrum (Figure 1.14) of (**8**) in CDCl₃ exhibits the 3-CH₃ resonance at a chemical shift (δ 2.1) that is close to that (δ 2.2) of HC(pz^{Me₂})₃, but the resonance of the 5-CH₃ (δ 1.6) is unusually shifted to a lower frequency relatively to the corresponding one (δ 2.0) of HC(pz^{Me₂})₃. These observations may be indicative⁹⁴⁻¹⁰⁰ of a significant magnetic effect exerted by the pyrazolyl rings (presumably *via* a ring current mechanism) on the 5-CH₃ protons, and may signify that the C-H--- π interactions are retained in solution. It is noteworthy that the 1.6 ppm signal appears to be independent of the dilution factor (1/10/100) in various solvents such as CDCl₃, CD₃OD and acetone-*d*₆. Moreover, lowering the temperature to -60 °C did not induce any significant change either in the resolution or in the position of this resonance (see experimental chapter).

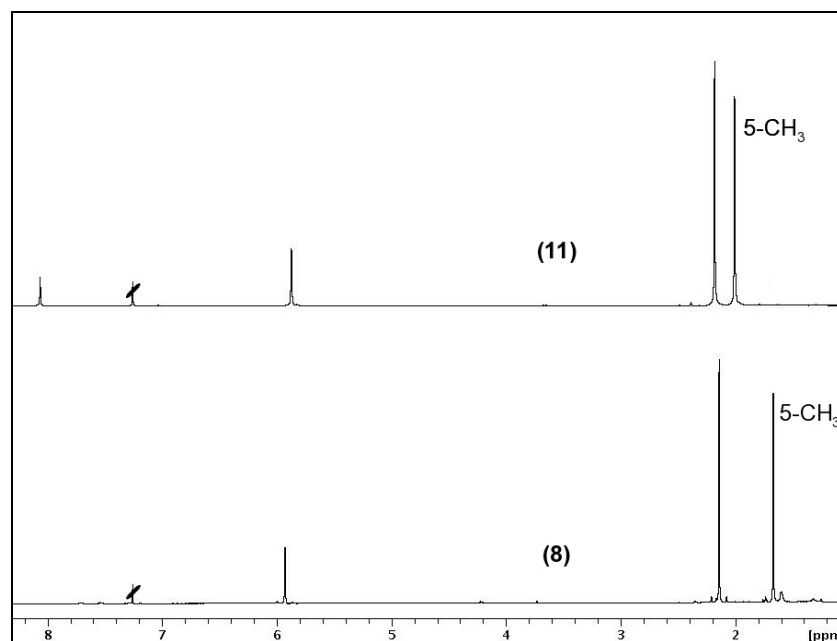


Figure 1.14. $^1\text{H-NMR}$ (CDCl_3) of compounds **(11)** (top) and **(8)** (bottom).

1.4.4 Future studies on the radical pathway

The above preliminary studies have demonstrated that substitution (functionalization) at the methine carbon of $\text{HC}(\text{pz}^{\text{Me}_2})_3$ is feasible, despite the steric hindrance imposed by the methyl groups, *via* a radical pathway involving the $\cdot\text{C}(\text{pz}^{\text{Me}_2})_3$ radical. However, in order to reach general applicability to different substituents, a careful control of the reaction will be required to compete favourably with the formation of $\text{C}(\text{pz}^{\text{Me}_2})_4$ (**8**).

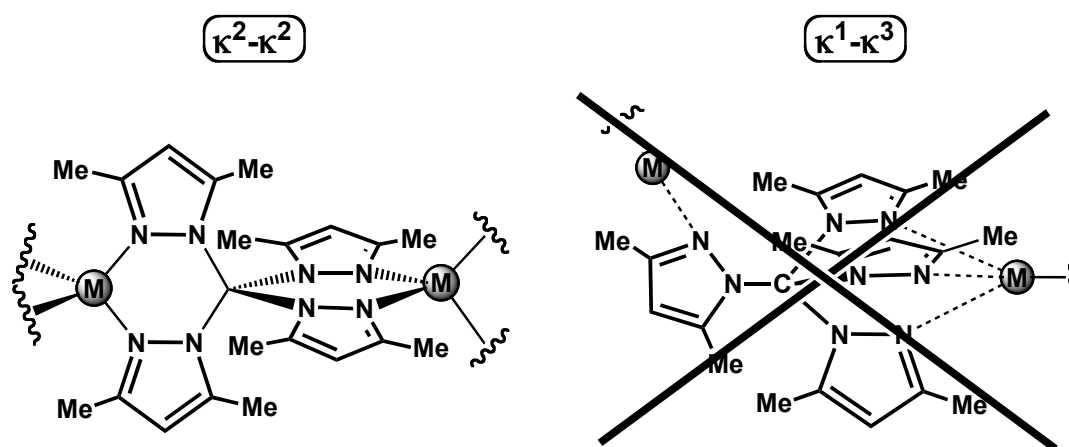


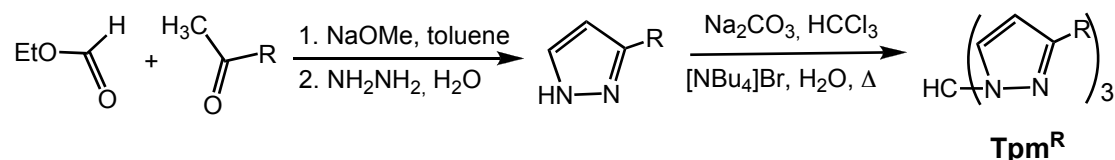
Figure 1.15 Proposed coordination of **(8)**.

Moreover, a possible study of the coordination chemistry of the new tetradentate ligand (**8**) could be an important topic to develop, taking into account its potential ability to act as ‘bridging ligand’ and that a reasonable research should be oriented to investigate a potential N_2/N_2 , double bidentated ability of the ligand (Figure 1.15, κ^2 - κ^2 type), being potentially the N_3/N sterically hindered.

1.5 Appendix 1.A: synthesis of other Tpm derivatives

1.5.1 Sterically hindered Tpm^{tBu} and Tpm^{iPr}

As briefly described in Table 1.1, the synthesis of non-common derivatives of Tpm such as Tpm^{tBu} and Tpm^{iPr} (namely those for which the corresponding pyrazole is not commercially available or not commercially convenient) proceeds with the complete synthesis of the substituted pyrazole (Scheme 1.13). The latter, in fact, is easily prepared from its precursor, via a condensation of β -diketone and hydrazine.^{17,18}



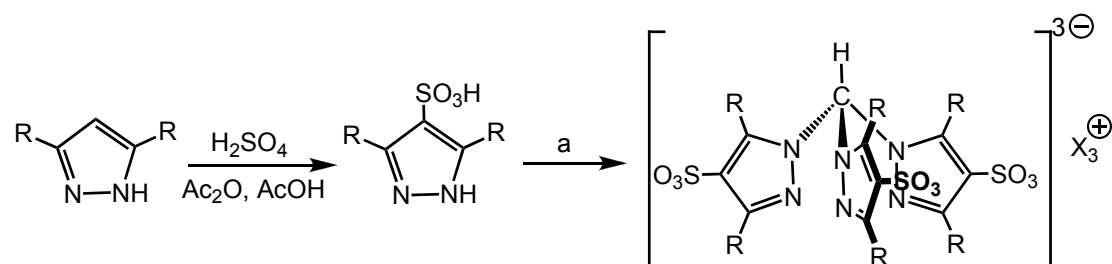
Scheme 1.13 Synthesis of Tpm^R (R = tBu, iPr)

In particular, for the synthesis of Tpm^{tBu} and Tpm^{iPr}, it has been necessary to start from the commercially available 3,3-dimethyl-2-butanone and 3-methyl-2-butanone, respectively. After the first step, the pyrazole itself has been directly used without any further purification for the next step, that has been carried out with the same conditions used for the Tpm^{Ph} (see Section 1.2.4, Table 1.1 and Experimental Chapter). These ‘bulky’ Tpm derivatives are, in fact, characterised by their high hydrophobic nature: it has been noticed that 3-phenyl and 3-*t*butyl pyrazoles need longer time and a vigorous stirring to be deprotonated to pyrazolate in the described conditions (Na₂CO₃ in water), with respect to the unsubstituted pyrazole.

1.5.2 Polysulfonated derivative of Tpm: toward water solubility

In addition to the possibility to prepare differently substituted pyrazoles starting from the condensation of various methyl ketones with ethyl formate and hydrazine,^{17,18} it has been explored, in this thesis, the direct functionalization of pyrazole, itself, *via* electrophilic attack¹⁰¹⁻¹⁰³. In particular, it has been prepared the

sulfonated derivative¹⁰⁴ and the corresponding 4-pyrazole sulfonic acid has been reacted to prepare the related Tpm bearing three sulfonate moieties (Scheme 1.14)



Scheme 1.14 Schematic procedure for the synthesis of tris(4-sulfonate-pyrazolyl)methane derivatives. Conditions (a) are fully described in the text.

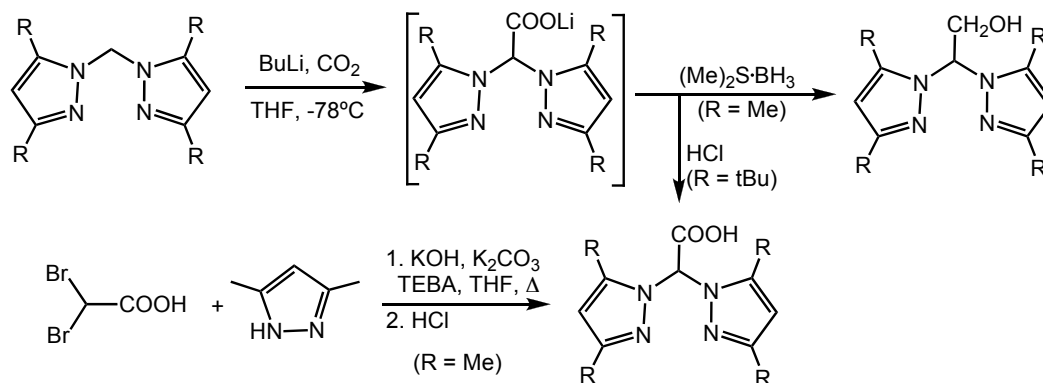
The starting 4-pyrazole sulfonic acid and its analogue 3,5-dimethylpyrazole incorporate unique properties and their high hydrophilicity alters the reactivity. The classical method for the synthesis of the scorpionate derivative has been attempted but was, in fact, unsuccessful. One reason of this low reactivity could be associated to the higher difficulty of the chloroform molecule to reach the proximity of the bis anionic 4-sulfonate pyrazolate, and this impediment could drastically decrease the yield, besides the presence of phase transfer, $[\text{NBu}_4]\text{Br}$. Different attempts, avoiding the use of water, have been carried out in this thesis: (i) the employment of methanolic solution of $[\text{NBu}_4]\text{OH}$ to deprotonate the pyrazole suspended in chloroform did not afford the desired product; unsuccessful results has been also obtained with (ii) an excess of sodium carbonate in DMF/ CHCl_3 mixture and (iii) a stoichiometric amount of NaH in THF.

The potential interest around this Tpm derivative should, in future, stimulate the development of alternative synthetic pathways that possibly proceed with the protection of the sulfonate functionality as an ester (*i.e.* neopentyl, isobutyl or isopropyl)¹⁰⁵⁻¹⁰⁸ to achieve a substrate more soluble in organic solvents for the preparation of the corresponding scorpionate.

1.5.3 Tpm derivatives incorporating new functional groups at the central carbon

Several reactions have been attempted in order to prepare Tpm derivatives that incorporate, by a direct route, some functional groups. Different works¹⁰⁹⁻¹¹³ report

interesting modifications of bis(pyrazolyl)methane analogue (Bpm) that encouraged to plan various reactions for the synthesis of unprecedented derivatives of Tpm (Scheme 1.15).



Scheme 1.15 Schematic synthetic routes for functionalization of bis(pyrazolyl)methane

The central carbon position of Bpm could be carboxylated –via BuLi deprotonation– and this example persuades to venture on this route for the synthesis of the carboxylated analogue of Tpm. Conscious that the tertiary carbon of Tpm could show an higher instability than its analogue of Bpm, different pathways to prepare the carboxylic acid derivative of Tpm (reactions **A**, **B** and **C**, Scheme 1.16) have been attempted in this work. The latter compound, in fact, could hold a great significance, as a pro-ligand, due to its unique properties of solubility (*i.e.* hydrophylicity) and coordination ability, taking into account the known¹¹⁴ coordination chemistry of its analogue bis(pyrazolyl)acetate. From the variably substituted Tpm, it has been successfully removed, in this work, the apical proton and the carbanion carboxylated to obtain the lithium carboxylate derivative, $\text{Li}[\text{OOC}-\text{C}(\text{pz})_3]$, characteristic for its ν_{CO_2} at 1704 and 1682 cm^{-1} (Figure 1.16). This derivative has also been achieved by oxidation of the terminal alcohol tris-2,2,2-(1-pyrazolyl)ethanol²² (reaction **C**) and by nucleophilic substitution of trichloroacetic acid (reaction **B**). The latter synthesis does not proceed easily and gives the mixture of mono- and bis- substituted and byproducts.

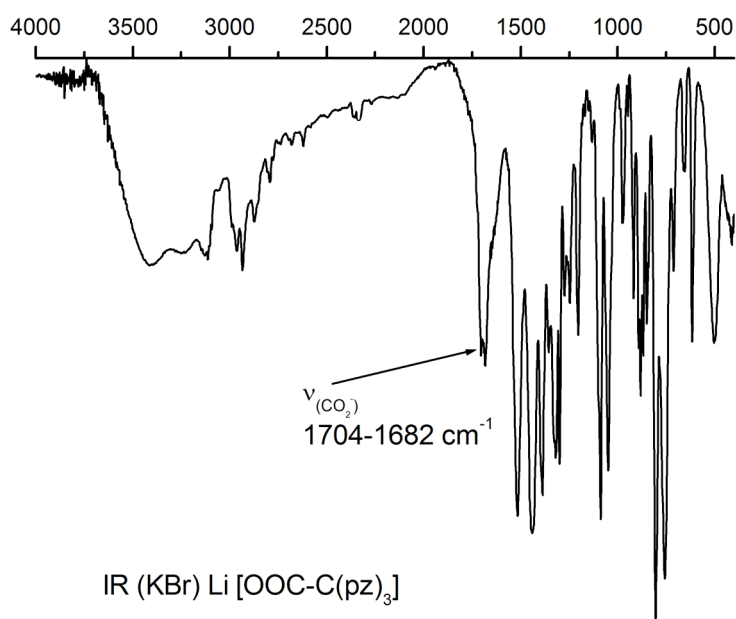
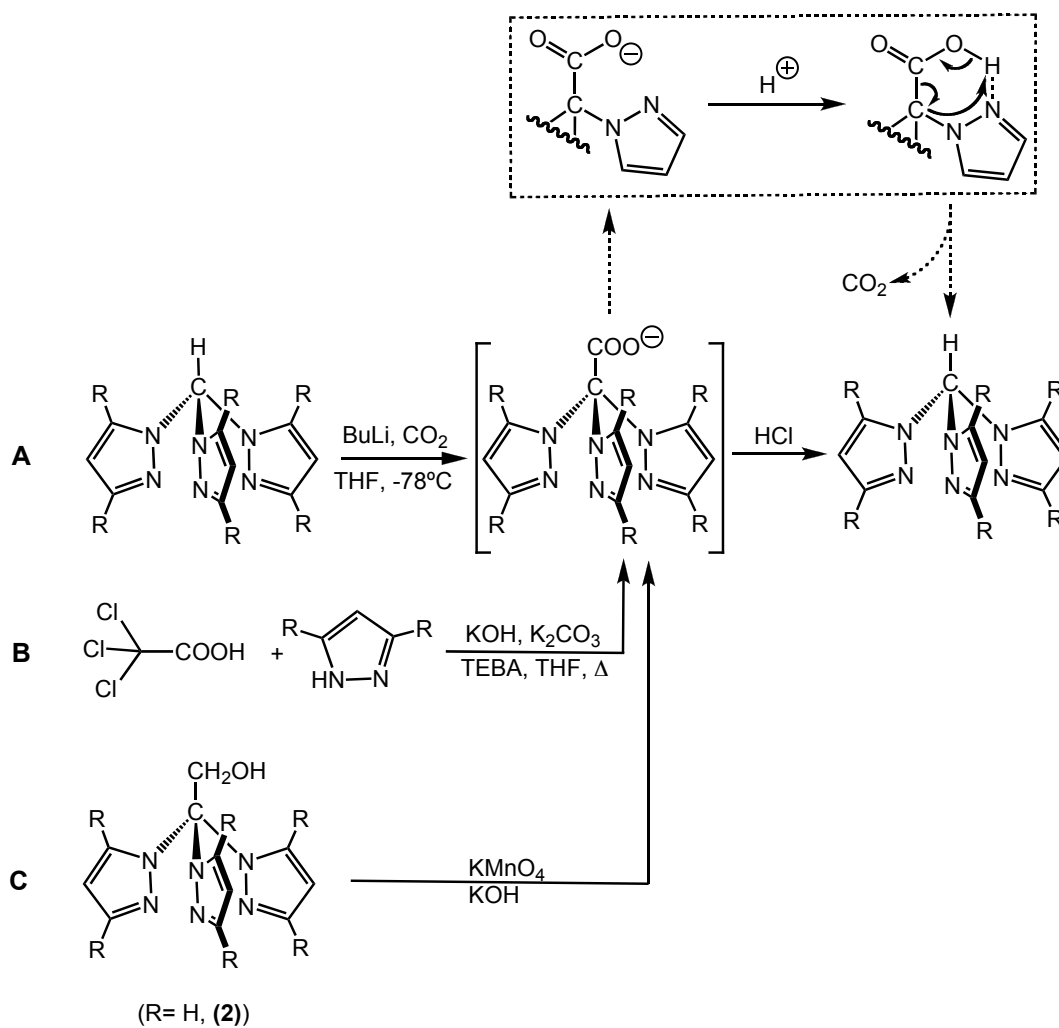


Figure 1.16 IR spectrum of carboxylated Tpm derivative, Li[OOC-C(pz)₃].

At the final stage, the addition of acid to the carboxylate solution produces the decarboxylation of the derivative and formation of the starting Tpm ligand. Steric and electronic effects could induce the high instability of the corresponding carboxylic acid. A proposed decarboxylation mechanism assisted from the nitrogen atom of an adjacent pyrazolyl ring is shown in Scheme 1.16: the weakly basic nitrogen could promote the activation of the carboxylic group and the decarboxylation process. This decomposition mechanism from the intermediate carboxylate is suggested by the detection of the quantitative formation of Tpm, HC(pz)₃, from reaction of **(2)** with KOH and KMnO₄ in water and subsequent acidification with HCl (Scheme 1.16, C).



Scheme 1.16 Three different reactions for the synthesis of Tpm carboxylic acid. The mechanism of decarboxylation process, proposed in this study, is highlighted.

In order to explore the synthetic strategies of functionalization of Tpm, a modification of a previous reaction **B** (Scheme 1.16) has been carried out: 3 eq of 3,5-dimethylpyrazole have been reacted with trichloro acetonitrile. The reaction does not proceed to completion but appears promising to further studies.

1.6 Appendix 1.B: Dendritic-Tpm ligands

In collaboration with the group of Prof. Anne-Marie Caminade of the University of Toulouse, the possibility to support the Tpm on a dendritic surface has been explored.

The class of dendrimers used for this purpose has been the N_3P_3 -type, better known as phosphorus dendrimer.¹¹⁵⁻¹²³ In general, this dendrimer started with a $PSCl_3$ core or better with $N_3P_3Cl_6$ (phosphonitrilic chloride trimer (Figure 1.17)), which, at small generation, gave a conical (or a cauliflower structure) dendrimer.

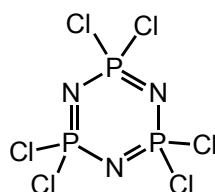


Figure 1.17 The core of phosphorus dendrimer.

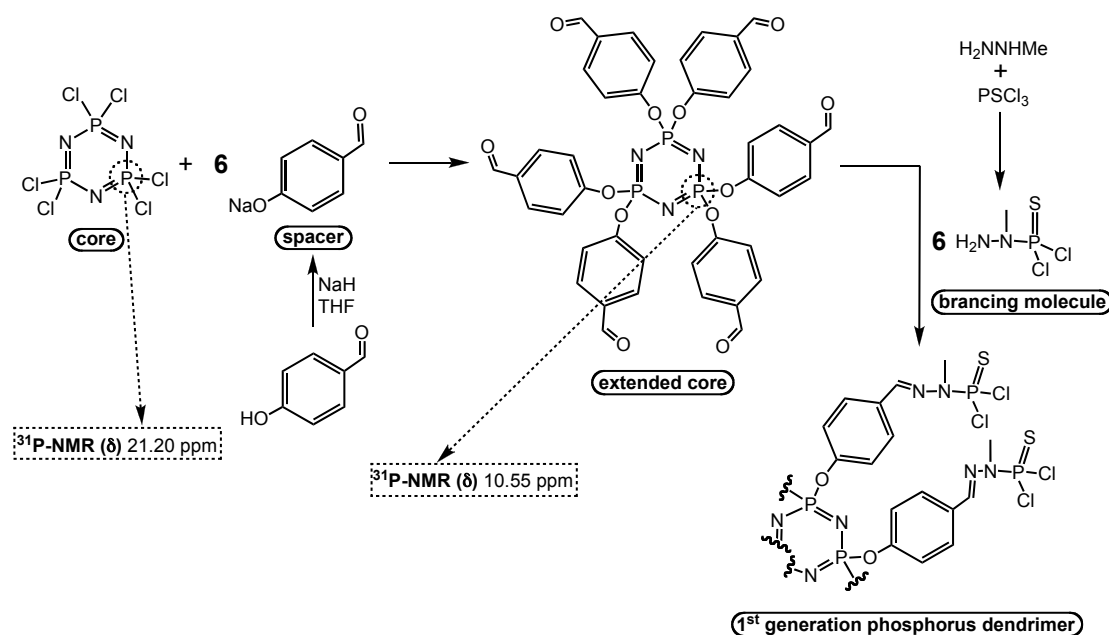
From the central core, using a ‘spacer’ and a ‘branching molecule’ a first generation dendrimer suitable for our studies has been prepared. In Scheme 1.17 it is represented the first step of growth of the phosphorus dendrimer:

-the nucleophilic substitution of the core $N_3P_3Cl_6$ with 6 equivalents of sodium salt of 4-hydroxybenzaldehyde, previously prepared, leads to a sort of ‘extended core’. This product is not yet a dendrimer, since the branching points have not multiplied but merely stayed the same, thus the 4-hydroxybenzaldehyde is, formally, considered as a *spacer*.

-the ‘branching molecule’ used for this study has been prepared from monomethylhydrazine with thiophosphorylchloride (solubilized in chloroform): six equivalents of N-methylhydrazido thiophosphoryldichloride (‘branching molecule’, Scheme 1.17) is condensed with the aldehydic terminations of the macromolecule to yield the first generation phosphorus dendrimer.

The multistep synthesis has been monitored by NMR: the first step, that leads to the macromolecule bearing six-aldehydic terminations, proceeded overnight in THF for completion: the complete disappearance of phosphorus signal at δ 21.20 ppm

in the ^{31}P - $\{^1\text{H}\}$ -NMR spectrum, corresponding to phosphorus atoms in the starting material, $\text{N}_3\text{P}_3\text{Cl}_6$, and the presence of higher shielded resonance, at δ 10.55 ppm, ascribed to the product (Scheme 1.17). Successively, the ^1H -NMR experiments allow to confirm the formation of the final product: the aldehyde and the hydrazone protons, of the intermediate and final product, could be detected at δ 9.89 and 7.63 ppm, respectively.

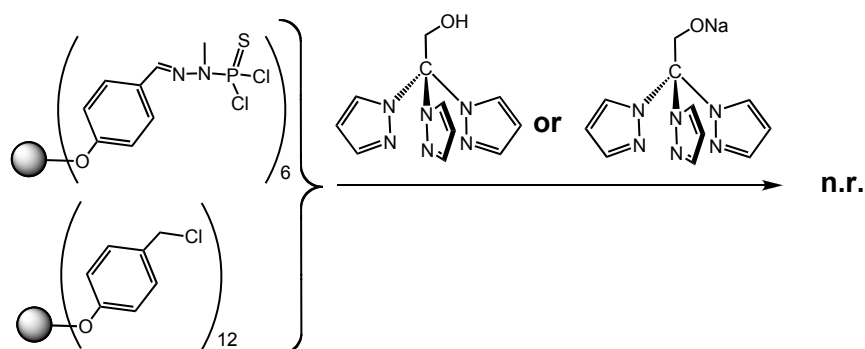


Scheme 1.17 Synthesis of the 1st generation of phosphorus dendrimer.

Based on the nature of the functional groups on the dendritic terminations, the tris-2,2,2-(1-pyrazolyl)ethanol (**2**) (Section 1.3.2) has been selected as the most promising candidate for the final step of condensation with the phosphorus dendrimer: the hydroxy moiety of the scorpionate holds, in principle, the nucleophilic character to react with the thiophosphonyldichloride (*i.e.* -PSCl₂) terminations. In addition to that, the group of Toulouse has provided two other phosphorus dendrimers, with benzylic-halide terminations on the surface, to attempt for the reaction: in fact, as reported in Section 1.3.2.1.3, (**2**) reacts readily –upon deprotonation with sodium hydride– with activated benzylic positions (*i.e.* chloro, bromo or iodo-benzyl groups).

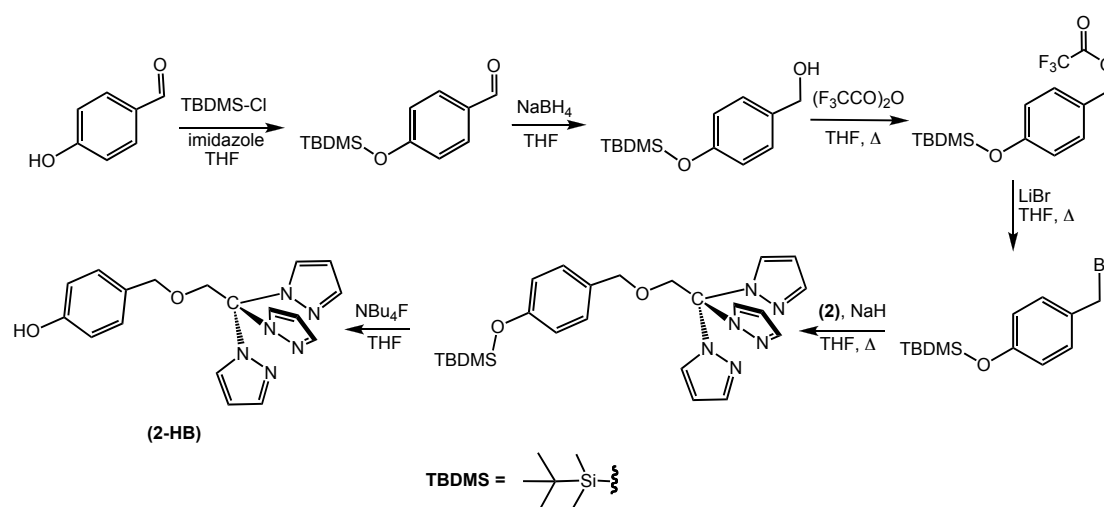
The preliminary attempts have failed: a partial substitution or decomposition of the dendrimer has been detected. In fact, as in the case of the preparation of

dendritic scaffold, all these reactions usually need peculiar conditions to achieve the complete substitution on the surface: long reaction time and mild conditions generally promote the total saturation of active terminations of the macromolecule. The hydroxy group of **(2)** was not enough active to saturate the thiophosphoryldichloride (*i.e.* -PSCl₂) and the sodium alkoxide derivative of **(2)** exhibits a too intense reactivity for the dendrimer molecule leading to a partial decomposition of the building block (Scheme 1.18).



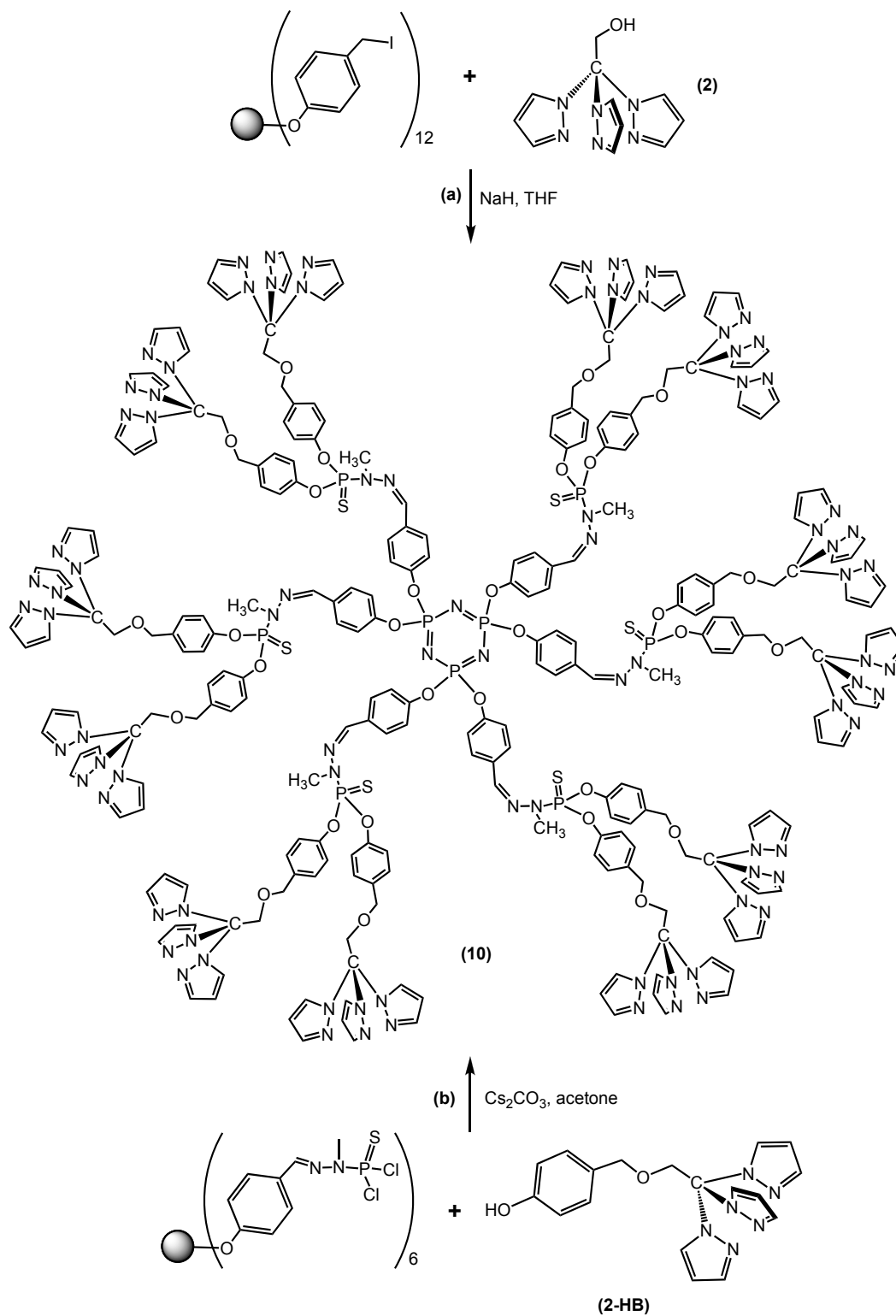
Scheme 1.18 Unsuccessful attempts for the final coupling.

The best result has been obtained for the iodo-benzyl derivative (*i.e.* N₃P₃-G₆₀-I₁₂) of the dendrimer molecule that provides the final product **(10)** in moderate yield (Scheme 1.20, **(a)**). An alternative pathway has been explored, passing through a modification of the tris-2,2,2-(1-pyrazolyl)ethanol **(2)**. A multistep synthesis of 4-hydroxybenzyl derivative of **(2)**, (*i.e.* HO-C₆H₄-OCH₂C(pz)₃ **(2-HB)**), has been successfully carried out in Toulouse (Scheme 1.19).



Scheme 1.19 Synthesis of 4-(2,2,2-tri(pyrazolyl)ethoxy)methylphenol.

The final condensation has been performed in the presence of a large excess (15 eq) of **(2-HB)** and 30 eq of cesium carbonate and provided the final product in good purity (Scheme 1.20).



Scheme 1.20 The new tris(pyrazolyl)methane-based phosphorus dendrimer **(10)**.

The two synthetic pathways (Scheme 1.20, **(a)** and **(b)**) lead to the final Tpm-based dendrimer (**10**). Both of them hold inconveniences and strong points:

Method **(a)** is more simple and practical, since the starting materials are more easily accessible. On the other hand, the final coupling should be carefully controlled and could lead to a lower yield compared to method **(b)**. The latter, in fact, has the good point to proceed with a cleaner final step, but the preparation of the 4-(tris-2,2,2-tris(pyrazolyl)ethoxymethyl)phenol (**2-HB**) compound results to be difficult and tedious. Moreover, the use of a large excess of the scorpionate derivative in method **(b)** is not convenient and produces a relevant waste of compound.

The study revealed that the anchorage of a tris(pyrazolyl)methane derivative on a dendritic surface is feasible and generates an important support for further studies in supramolecular and coordination chemistry and in catalysis; but these preliminary results show that the synthetic process requires further investigation to ease the preparation of intermediates, improve the partial and the total yields and the purity. To earn a reasonable amount of compound (**10**) to study the further connection to a metal center and a possible application in catalysis, it is necessary a too large “synthetic effort” that not allows to consider, at this stage, this work sufficiently convenient and attractive.

References

- [1] Trofimenko, S., *J. Am. Chem. Soc.* **1967**, *89*, 3170.
- [2] Schubert, D. M.; Knobler, C. B.; Trofimenko, S.; Hawthorne, M. F., *Inorg. Chem.* **1990**, *29*, 2364.
- [3] Calabrese, J. C.; Trofimenko, S., *Inorg. Chem.* **1992**, *31*, 4810.
- [4] Carmona, D.; Lahoz, F. J.; Atencio, R.; Edwards, A. J.; Oro, L. A.; Lamata, M. P.; Esteban, M.; Trofimenko, S., *Inorg. Chem.* **1996**, *35*, 2549.
- [5] Looney, A.; Han, R.; McNeill, K.; Parkin, G., *J. Am. Chem. Soc.* **1993**, *115*, 4690.
- [6] Kitajima, N.; Tolman, W. B., Coordination Chemistry with Sterically Hindered Hydrotris(pyrazolyl)borate ligands organometallic and bioinorganic perspectives. In *Progress in Inorganic Chemistry, Vol 43*, John Wiley & Sons Inc: New York, 1995; Vol. 43, pp 419.
- [7] Schneider, J. L.; Carrier, S. M.; Ruggiero, C. E.; Young, V. G.; Tolman, W. B., *J. Am. Chem. Soc.* **1998**, *120*, 11408.
- [8] Vahrenkamp, H., *Acc. Chem. Res.* **1999**, *32*, 589.
- [9] Hu, Z. B.; Williams, R. D.; Tran, D.; Spiro, T. G.; Gorun, S. M., *J. Am. Chem. Soc.* **2000**, *122*, 3556.
- [10] Thompson, J. S.; Harlow, R. L.; Whitney, J. F., *J. Am. Chem. Soc.* **1983**, *105*, 3522.
- [11] Dias, H. V. R.; Fianchini, M., *Angew. Chem., Int. Ed.* **2007**, *46*, 2188.
- [12] Trofimenko, S.; Calabrese, J. C.; Thompson, J. S., *Angew. Chem., Int. Ed.* **1989**, *28*, 205.
- [13] Rheingold, A. L.; Haggerty, B. S.; Trofimenko, S., *Angew. Chem., Int. Ed.* **1994**, *33*, 1983.
- [14] Macchioni, A.; Bellachioma, G.; Cardaci, G.; Gramlich, V.; Ruegger, H.; Terenzi, S.; Venanzi, L. M., *Organometallics* **1997**, *16*, 2139.
- [15] Trofimenko, S., *Chem. Rev.* **1993**, *93*, 943.
- [16] Pettinari, C., *Scorpionates II: Chelating Borate Ligands*. Imperial College Press London, 2008
- [17] Trofimenko, S.; Calabrese, J. C.; Thompson, J. S., *Inorg. Chem.* **1987**, *26*, 1507.

- [18] Trofimenko, S.; Calabrese, J. C.; Domaille, P. J.; Thompson, J. S., *Inorg. Chem.* **1989**, *28*, 1091.
- [19] Zhao, N.; Bullinger, J. C.; Van Stipdonk, M. J.; Stern, C. L.; Eichhorn, D. M., *Inorg. Chem.* **2008**, *47*, 5945.
- [20] Fujisawa, K.; Tada, N.; Ishikawa, Y.; Higashimura, H.; Miyashita, Y.; Okamoto, K. I., *Inorg. Chem. Commun.* **2004**, *7*, 209.
- [21] Hüchel, W.; Bretschneider, H., *Chem. Ber.* **1937**, *9*, 2024.
- [22] Reger, D. L.; Grattan, T. C.; Brown, K. J.; Little, C. A.; Lamba, J. J. S.; Rheingold, A. L.; Sommer, R. D., *J. Organomet. Chem.* **2000**, *607*, 120.
- [23] Humphrey, E. R.; Mann, K. L. V.; Reeves, Z. R.; Behrendt, A.; Jeffery, J. C.; Maher, J. P.; McCleverty, J. A.; Ward, M. D., *New J. Chem.* **1999**, *23*, 417.
- [24] Titze, C.; Hermann, J.; Vahrenkamp, H., *Chem. Ber.* **1995**, *128*, 1095.
- [25] Trofimenko, S., *Adv. Chem. Ser.* **1976**, 289.
- [26] Trofimenko, S., *Prog. Inorg. Chem.* **1986**, *34*, 115.
- [27] Brunker, T. J.; Cowley, A. R.; O'Hare, D., *Organometallics* **2002**, *21*, 3123.
- [28] Reger, D. L.; Collins, J. E.; Jameson, D. L.; Castellano, R. K.; Canty, A. J.; Jin, H., *Inorg. Synth.* **1998**, *32*, 63.
- [29] Benisvy, L.; Wanke, R.; Kuznetsov, M. L.; da Silva, M.; Pombeiro, A. J. L., *Tetrahedron* **2009**, *65*, 9218.
- [30] Trofimenko, S.; Calabrese, J. C.; Kochi, J. K.; Wolowiec, S.; Hulsbergen, F. B.; Reedijk, J., *Inorg. Chem.* **1992**, *31*, 3943.
- [31] Reger, D. L.; Little, C. A.; Young, V. G.; Maren, P., *Inorg. Chem.* **2001**, *40*, 2870.
- [32] Reger, D. L.; Gardinier, J. R.; Elgin, J. D.; Smith, M. D., *Inorg. Chem.* **2006**, *45*, 8862.
- [33] Frohnäpfel, D. S.; White, P. S.; Templeton, J. L.; Ruegger, H.; Pregosin, P. S., *Organometallics* **1997**, *16*, 3737.
- [34] Wanke, R.; Smolenski, P.; da Silva, M.; Martins, L.; Pombeiro, A. J. L., *Inorg. Chem.* **2008**, *47*, 10158.
- [35] Otting, G.; Messerle, B. A.; Soler, L. P., *J. Am. Chem. Soc.* **1996**, *118*, 5096.
- [36] Edwards, P. G.; Harrison, A.; Newman, P. D.; Zhang, W. J., *Inorg. Chim. Acta* **2006**, *359*, 3549.

- [37] Amoroso, A. J.; Jeffery, J. C.; Jones, P. L.; McCleverty, J. A.; Rees, L.; Rheingold, A. L.; Sun, Y. M.; Takats, J.; Trofimenko, S.; Ward, M. D.; Yap, G. P. A., *J. Chem. Soc., Chem.* **1995**, 1881.
- [38] Mehn, M. P.; Fujisawa, K.; Hegg, E. L.; Que, L., *J. Am. Chem. Soc.* **2003**, *125*, 7828.
- [39] Wang, L. Y.; Chambron, J. C., *Org. Lett.* **2004**, *6*, 747.
- [40] Kim, K.; Lippard, S. J., *J. Am. Chem. Soc.* **1996**, *118*, 4914.
- [41] Bergquist, C.; Parkin, G., *Inorg. Chem.* **1999**, *38*, 422.
- [42] Mirica, L. M.; Ottenwaelder, X.; Stack, T. D. P., *Chem. Rev.* **2004**, *104*, 1013.
- [43] Olson, M. D.; Rettig, S. J.; Storr, A.; Trotter, J.; Trofimenko, S., *Acta Crystallogr., Sect. C* **1991**, *47*, 1543.
- [44] Calabrese, J. C.; Domaille, P. J.; Thompson, J. S.; Trofimenko, S., *Inorg. Chem.* **1990**, *29*, 4429.
- [45] Nabika, M.; Kiuchi, S.; Miyatake, T.; Okamoto, K. I.; Fujisawa, K., *J. Mol. Catal.* **2007**, *269*, 163.
- [46] Kaim, W.; Titze, C.; Schurr, T.; Sieger, M.; Lawson, M.; Jordanov, J.; Rojas, D.; Garcia, A. M.; Manzur, J., *Z. Anorg. Allg. Chem.* **2005**, *631*, 2568.
- [47] Fujisawa, K.; Ono, T.; Aoki, H.; Ishikawa, Y.; Miyashita, Y.; Okamoto, K.; Nakazawa, H.; Higashimura, H., *Inorg. Chem. Commun.* **2004**, *7*, 330.
- [48] Krummenacher, I.; Ruegger, H.; Breher, F., *Dalton Trans.* **2006**, 1073.
- [49] Bigmore, H. R.; Meyer, J.; Krummenacher, I.; Rugger, H.; Clot, E.; Mountford, P.; Breher, F., *Chem. Eur. Jour.* **2008**, *14*, 5918.
- [50] Kuzu, I.; Krummenacher, I.; Meyer, J.; Armbruster, F.; Breher, F., *Dalton Trans.* **2008**, 5836.
- [51] Reger, D. L.; Grattan, T. C., *Synthesis-Stuttgart* **2003**, 350.
- [52] Klaui, W.; Berghahn, M.; Rheinwald, G.; Lang, H. R., *Angew. Chem., Int. Ed.* **2000**, *39*, 2464.
- [53] Esteruelas, M. A.; Oro, L. A.; Claramunt, R. M.; Lopez, C.; Lavandera, J. L.; Elguero, J., *Organomet. Chem.* **1989**, *366*, 254.
- [54] Byers, P. K.; Canty, A. J.; Honeyman, R. T.; Claremont, R. M.; Lopez, C.; Lavandera, J. L.; Elguero, J., *Gazz. Chim. Ital.* **1992**, *122*, 341.
- [55] Reger, D. L.; Watson, R. P.; Smith, M. D., *Inorg. Chem.* **2006**, *45*, 10077.
- [56] Reger, D. L.; Semeniuc, R. F.; Smith, M. D., *Dalton Trans.* **2008**, 2253.

- [57] Byers, P. K.; Carr, N.; Stone, F. G. A., *J. Chem. Soc., Dalton* **1990**, 3701.
- [58] Byers, P. K.; Stone, F. G. A., *J. Chem. Soc., Dalton* **1991**, 93.
- [59] Klaui, W.; Berghahn, M.; Frank, W.; Reiss, G. J.; Schonherr, T.; Rheinwald, G.; Lang, H., *Eur. J. Inorg. Chem.* **2003**, 2059.
- [60] Tisato, F.; Refosco, F.; Bandoli, G.; Pilloni, G.; Corain, B., *Inorg. Chem.* **2001**, *40*, 1394.
- [61] Papish, E. T.; Taylor, M. T.; Jernigan, F. E.; Shawhan, R. R.; Rodig, M. J.; Yap, G. P. A. In *Synthesis of water-soluble zinc and cobalt complexes using tris(pyrazolyl)methane sulfonate ligands*, 230th National Meeting of the American-Chemical-Society, Washington, DC, Aug 28-Sep 01, 2005; Washington, DC, 2005; pp 309.
- [62] Alegria, E. C. B.; Martins, L.; Haukka, M.; Pombeiro, A. J. L., *Dalton Trans.* **2006**, 4954.
- [63] Papish, E. T.; Taylor, M. T.; Jernigan, F. E.; Rodig, M. J.; Shawhan, R. R.; Yap, G. P. A.; Jove, F. A., *Inorg. Chem.* **2006**, *45*, 2242.
- [64] Chenskaya, T. B.; Berghahn, M.; Kunz, P. C.; Frank, W.; Klaui, W., *J. Mol. Struct.* **2007**, *829*, 135.
- [65] Smolenski, P.; Dinoi, C.; da Silva, M.; Pombeiro, A. J. L., *J. Organomet. Chem.* **2008**, *693*, 2338.
- [66] Reger, D. L.; Collins, J. E., *Organometallics* **1996**, *15*, 2029.
- [67] Conry, R. R.; Ji, G. Z.; Tipton, A. A., *Inorg. Chem.* **1999**, *38*, 906.
- [68] Lehnert, N.; Cornelissen, U.; Neese, F.; Ono, T.; Noguchi, Y.; Okamoto, K.; Fujisawa, K., *Inorg. Chem.* **2007**, *46*, 3916.
- [69] Fujisawa, K.; Ono, T.; Ishikawa, Y.; Amir, N.; Miyashita, Y.; Okamoto, K.; Lehnert, N., *Inorg. Chem.* **2006**, *45*, 1698.
- [70] Klaui, W.; Schramm, D.; Peters, W.; Rheinwald, G.; Lang, H., *Eur. J. Inorg. Chem.* **2001**, 1415.
- [71] Kunz, P.; Kurz, P.; Spingler, B.; Alberto, R., *Acta Crystallogr. Sect. E: Struct. Rep. Online* **2007**, *63*, M363.
- [72] Reger, D. L.; Wright, T. D.; Semeniuc, R. F.; Grattan, T. C.; Smith, M. D., *Inorg. Chem.* **2001**, *40*, 6212.
- [73] Reger, D. L.; Semeniuc, R. F.; Smith, M. D., *Inorg. Chem.* **2001**, *40*, 6545.
- [74] Reger, D. L.; Semeniuc, R. F.; Smith, M. D., *J. Chem. Soc., Dalton* **2002**, 476.

- [75] Reger, D. L.; Semeniuc, R. F.; Smith, M. D., *J. Organomet. Chem.* **2003**, *666*, 87.
- [76] Reger, D. L.; Semeniuc, R. F.; Smith, M. D., *Dalton Trans.* **2003**, 285.
- [77] Reger, D. L.; Gardinier, J. R.; Bakbak, S.; Semeniuc, R. F.; Bunz, U. H. F.; Smith, M. D., *New J. Chem.* **2005**, *29*, 1035.
- [78] Reger, D. L.; Semeniuc, R. F.; Captain, B.; Smith, M. D., *Inorg. Chem.* **2005**, *44*, 2995.
- [79] Reger, D. L.; Semeniuc, R. F.; Little, C. A.; Smith, M. D., *Inorg. Chem.* **2006**, *45*, 7758.
- [80] Silva, T. F. S.; Mishra, G. S.; da Silva, M. F. G.; Wanke, R.; Martins, L.; Pombeiro, A. J. L., *Dalton Trans.* **2009**, 9207.
- [81] Sen, S. E.; Roach, S. L., *Synthesis-Stuttgart* **1995**, 756.
- [82] Li, Z.; Zhou, Z.; Wang, L.; Zhou, Q.; Tang, C., *Tetrahedron: Asymmetry* **2002**, *13*, 145.
- [83] Hope, D. B.; Horncastle, K. C., *Journal of the Chemical Society* **1966**, 1098.
- [84] Martin, A. E.; Ford, T. M.; Bulkowski, J. E., *Journal Organic Chemistry* **1982**, *47*, 412.
- [85] Dietrich, B.; Hosseini, M. W.; J.-M. Lehn, J.-M.; Sessions, R. B., *Helv. Chim. Acta* **1985**, *68*, 289.
- [86] Pallavicini, P. S.; Perotti, A.; Poggi, A.; Seghi, B.; Fabbrizzi, L., *J. Am. Chem. Soc.* **1987**, *109*, 5139.
- [87] Greene, T. W.; Wuts, P. G. M., *Chemistry - Protective Groups In Organic Synthesis 3rd Edition*. Wiley-Interscience Publication: New York, 1999.
- [88] Sanchez-Mendez, A.; Ortiz, A. M.; de Jesus, E.; Flores, J. C.; Gomez-Sal, P., *Dalton Trans.* **2007**, 5658.
- [89] Bigmore, H. R.; Dubberley, S. R.; Kranenburg, M.; Lawrence, S. C.; Sealey, A. J.; Selby, J. D.; Zuideveld, M. A.; Cowley, A. R.; Mountford, P., *Chem. Commun.* **2006**, 436.
- [90] Reger, D. L.; Little, C. A.; Rheingold, A. L.; Lam, M.; Liable-Sands, L. M.; Rhagitan, B.; Concolino, T.; Mohan, A.; Long, G. J.; Briois, V.; Grandjean, F., *Inorg. Chem.* **2001**, *40*, 1508.
- [91] Breher, F.; Grunenberg, J.; Lawrence, S. C.; Mountford, P.; Ruegger, H., *Angew. Chem., Int. Ed.* **2004**, *43*, 2521.
- [92] Kuzu, I.; Krummenacher, I.; Hewitt, I. J.; Lan, Y.; Mereacre, V.; Powell, A. K.; Hoefler, P.; Harmer, J.; Breher, F., *Chem. Eur. Jour.* **2009**, *15*, 4350.

- [93] Lawrence, S. C.; Skinner, M. E. G.; Green, J. C.; Mountford, P., *Chem. Commun.* **2001**, 705.
- [94] Muller-Dethlefs, K.; Hobza, P., *Chem. Rev.* **2000**, *100*, 143.
- [95] Hobza, P.; Havlas, Z., *Chem. Rev.* **2000**, *100*, 4253.
- [96] Nishio, M., *Cryst. Eng. Comm.* **2004**, *6*, 130.
- [97] Janiak, C., *J. Chem. Soc., Dalton* **2000**, 3885.
- [98] Gamez, P.; Mooibroek, T. J.; Teat, S. J.; Reedijk, J., *Acc. Chem. Res.* **2007**, *40*, 435.
- [99] Joseph, J.; Jemmis, E. D., *J. Am. Chem. Soc.* **2007**, *129*, 4620.
- [100] Lu, Y. X.; Zou, J. W.; Wang, Y. H.; Yu, Q. S., *Chem. Phys.* **2007**, *334*, 1.
- [101] Knorr, L., *Justus Liebigs Annalen der Chemie* **1894**, 279, 188.
- [102] Huttel, R.; Biichele, F.; Jochum, P., *Chem. Ber.* **1955**, *88*, 1577.
- [103] Olah, G. A.; Narang, S. C.; Fung, A. P., *Journal Organic Chemistry* **1981** *46*, 2706.
- [104] Grandberg, I. I.; Nam, N. L.; Sorokin, V. I., *Chem. Heterocycl. Compd.* **1997**, *33*, 532.
- [105] Musicki, B.; Widlanski, T. S., *J. Org. Chem.* **1990**, *55*, 4231.
- [106] Musicki, B.; Widlanski, T. S., *Tetrahedron Lett.* **1991**, *32*, 1267.
- [107] Xie, M.; Widlanski, T. S., *Tetrahedron Lett.* **1996**, *37*, 4443.
- [108] Roberts, J. C.; Gao, H.; Gopasamy, A.; Kongsjahju, A.; Patch, R. J., *Tetrahedron Lett.* **1997**, *38*, 355.
- [109] Julia, S.; Sala, P.; Delmazo, J.; Sancho, M.; Ochoa, C.; Elguero, J.; Fayet, J. P.; Vertut, M. C., *J. Heterocycl. Chem.* **1982**, *19*, 1141.
- [110] Otero, A.; Fernandez-Baeza, J.; Tejeda, J. B.; Antinolo, A.; Carrillo-Hermosilla, F.; Diez-Barra, E.; Lara-Sanchez, A.; Fernandez-Lopez, M., *J. Chem. Soc., Dalton* **2000**, 2367.
- [111] Otero, A.; Fernandez-Baeza, J.; Tejeda, J.; Antinolo, A.; Carrillo-Hermosilla, F.; Diez-Barra, E.; Lara-Sanchez, A.; Fernandez-Lopez, M.; Lanfranchi, M.; Pellinghelli, M. A., *J. Chem. Soc., Dalton* **1999**, 3537.
- [112] Beck, A.; Weibert, B.; Burzlaff, N., *Eur. J. Inorg. Chem.* **2001**, 521.
- [113] Claramunt, R. M.; Hernandez, H.; Elguero, J.; Julia, S., *Bull. Soc. Chim. Fr.* **1983**, *2*, 5.

- [114] Marchetti, F.; Pettinari, C.; Cerquetella, A.; Cingolani, A.; Pettinari, R.; Monari, M.; Wanke, R.; Kuznetsov, M. L.; Pombeiro, A. J. L., *Inorg. Chem.* **2009**, *48*, 6096.
- [115] Launay, N.; Caminade, A. M.; Majoral, J. P., *J. Am. Chem. Soc.* **1995**, *117*, 3282.
- [116] Larre, C.; Donnadiou, B.; Caminade, A. M.; Majoral, J. P., *J. Am. Chem. Soc.* **1998**, *120*, 4029.
- [117] Maraval, V.; Laurent, R.; Donnadiou, B.; Mauzac, M.; Caminade, A. M.; Majoral, J. P., *J. Am. Chem. Soc.* **2000**, *122*, 2499.
- [118] Caminade, A. M.; Maraval, V.; Laurent, R.; Turrin, C. O.; Sutra, P.; Leclaire, J.; Griffe, L.; Marchand, P.; Baudoin-Dehoux, C.; Rebout, C.; Majoral, J. P., *Comptes Rendus Chimie* **2003**, *6*, 791.
- [119] Majoral, J. P.; Caminade, A. M., What to do with phosphorus in dendrimer chemistry. In *New Aspects in Phosphorus Chemistry II*, 2003; Vol. 223, pp 111.
- [120] Maraval, V.; Caminade, A. M.; Majoral, J. P.; Blais, J. C., *Angew. Chem., Int. Ed.* **2003**, *42*, 1822.
- [121] Maraval, V.; Pyzowski, J.; Caminade, A. M.; Majoral, J. P., *J. Org. Chem.* **2003**, *68*, 6043.
- [122] Servin, P.; Rebout, C.; Laurent, R.; Peruzzini, M.; Caminade, A. M.; Majoral, J. P., *Tetrahedron Lett.* **2007**, *48*, 579.
- [123] Caminade, A. M.; Servin, P.; Laurent, R.; Majoral, J. P., *Chem. Soc. Rev.* **2008**, *37*, 56.

2 Cu^I complexes of Li(Tpms^{Ph})

Table of contents

Abstract	76
2.1 Introduction	78
2.2 Syntheses of Tpm^{Ph} and Li(Tpms^{Ph}) and metal complexes	80
2.2.1 Syntheses of the sterically hindered scorpionates Tpm ^{Ph} and Li(Tpms ^{Ph})	80
2.2.2 Syntheses of the Cu ^I complexes [Cu(Tpms ^{Ph})L] [L = MeCN (20), PTA (21), HMT (22)] and [Cu(Tpms ^{Ph})(mPTA)][PF ₆] (23)	81
2.3 X-ray molecular structures of complexes [Cu(Tpms^{Ph})L] [L = MeCN (20), PTA (21), HMT (22)] and [Cu(Tpms^{Ph})(mPTA)][PF₆] (23)	84
2.4 NMR solution studies	91
2.5 Cu-Tpms^{Ph} complexes (20)-(23): overview	95
2.6 Appendix 2.A: study of the Cu^I-Tpms^{Ph} system on the activation of nitriles, isonitriles and carbon monoxide	98
2.6.1 Syntheses of [Cu(Tpms ^{Ph})(CyNC)] (24) and [Cu(Tpms ^{Ph})(XyNC)] (25) (CyNC = cyclohexyl isocyanide; XyNC = 2,6-dimethylphenyl isocyanide) and their reactivity toward nucleophiles: 3-iminoisoindolin-1-one and methylamine	98
2.6.2 Synthesis of [Cu(Tpms ^{Ph})(CO)] (27) and its unexpected instability	102
2.7 Appendix 2.B: dioxygen coordination at the ‘Cu^I-Tpms^{Ph}’ system	104
2.8 Appendix 2.C: catalytic studies of [Cu(Tpms^{Ph})(MeCN)] (20)	108
References	111

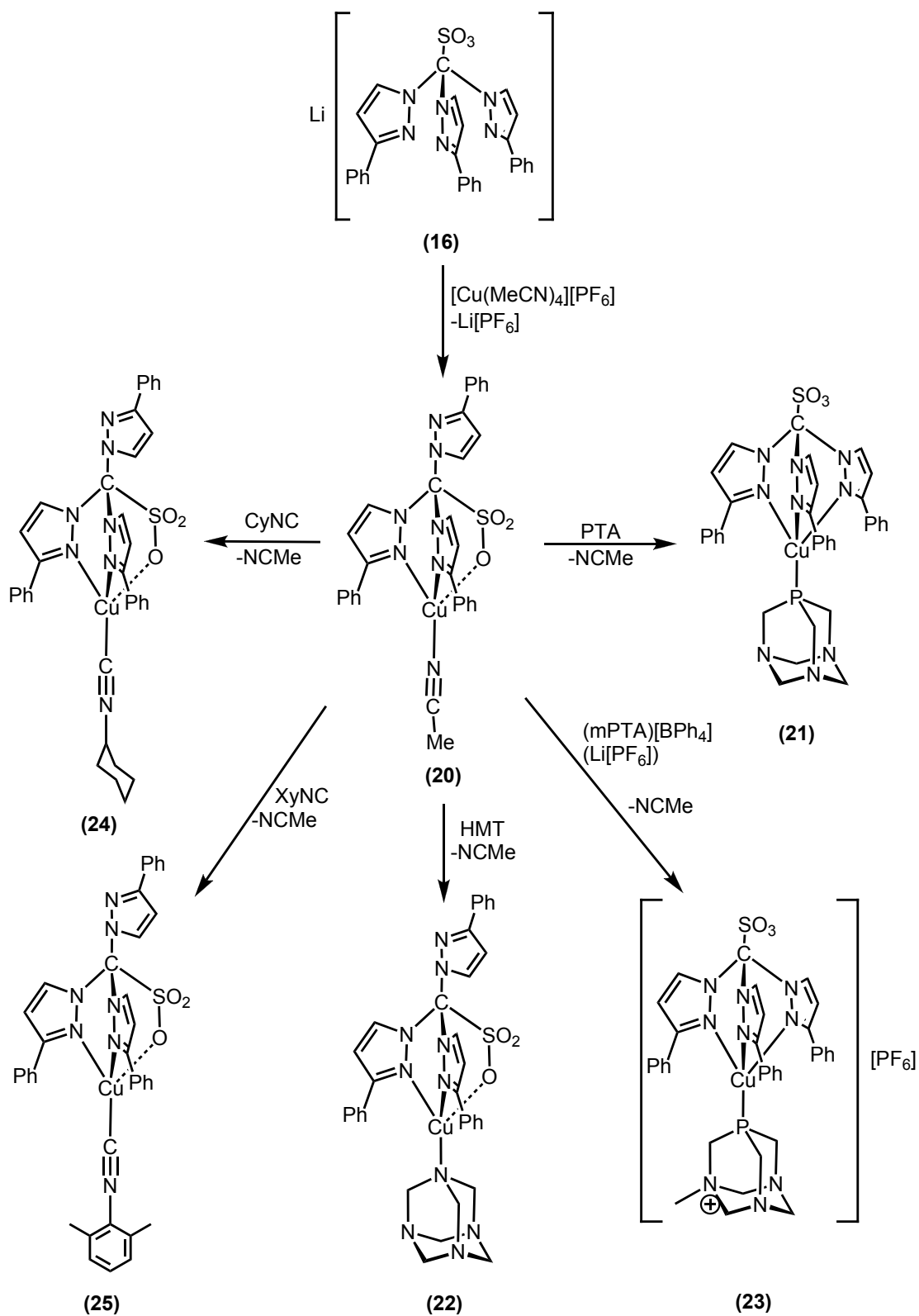
Abstract

The new sterically hindered scorpionate tris(3-phenylpyrazolyl)methanesulfonate lithium salt, Li(Tpms^{Ph}) (**16**), has been synthesized and its coordination behavior toward a Cu^I center has been studied.

The reaction between Li(Tpms^{Ph}) (**16**) and [Cu(MeCN)₄][PF₆] yields [Cu(Tpms^{Ph})(MeCN)] (**20**), which bears an acetonitrile molecule ligated to copper center and shows the scorpionate coordinated via the N,N,O chelating mode, involving the sulfonate moiety. Compound (**20**) has been studied to explore the versatility of the new “Cu-scorpionate” system upon ligand displacement reactions. This derivative, in fact, in the presence of 1,3,5-triaza-7-phosphaadamantane (PTA), hexamethylenetetramine (HMT) or *N*-methyl-1,3,5-triaza-7-phosphaadamantane tetraphenylborate ((mPTA)[BPh₄]) gives the corresponding complexes [Cu(Tpms^{Ph})(PTA)] (**21**), [Cu(Tpms^{Ph})(HMT)] (**22**) and [Cu(Tpms^{Ph})(mPTA)][PF₆] (**23**) (formed in the presence of Li[PF₆] liberated in the formation of (**20**)). In the complexes (**21**)-(**23**) the new scorpionate ligand adapts its coordination mode (*i.e.* N,N,N- or N,N,O-coordination modes) according to the steric and electronic properties of the extra ligand.

The high flexibility of the starting complex (**20**) favours the study of a possible metal-activation of nitriles and isocyanides. The replacement of acetonitrile molecule with cyclohexyl isocyanide (CyNC) and *m*-xylyl isocyanide (XyNC) gives the corresponding complexes [Cu(Tpms^{Ph})(CyNC)] (**24**) and [Cu(Tpms^{Ph})(XyNC)] (**25**) that were reacted with 3-iminoisoindolin-1-one (L) giving the substitution product [Cu(Tpms^{Ph})(L)], while a stronger nucleophile, such as monomethylamine, reacts with acetonitrile moiety of (**20**) leading to [Cu(Tpms^{Ph})(NH=C(Me)NHMe)] (**26**).

Moreover, the “Cu(Tpms^{Ph})” scaffold resulted to be a promising center for the coordination of small molecules: the identification of the carbonyl complex [Cu(Tpms^{Ph})(CO)] (**27**) and the isolation of the polinuclear [Cu(μ-O)(Tpms^{Ph})]₂ (**28**), [(μ-Cu^{II}){Cu^I(Tpms^{Ph})(μ-OH₂)(OMe)}₂] (**29**) and [(μ-Cu){Cu(μ-O)(Tpms^{Ph})}₂] (**50**) represent encouraging examples for further studies in this field.

Scheme 2.0 Cu^I complexes bearing Tpms^{Ph}.

2.1 Introduction

Copper species are widely present in Nature as mono- or multi-nuclear metal complexes and play a crucial role in different enzymes and catalytic systems, leading to a currently growing interest in the development of new copper models.¹⁻⁶ In bioinorganic and organometallic chemistry the systems involving this metal represent one of the most relevant areas of investigation.⁷⁻¹¹ In pursuit of recent investigations of the coordination chemistry of N-, P- and O-donor ligands,^{12,13} including the scorpionate-type tris(pyrazolyl)methane,¹⁴⁻¹⁶ toward copper(I) and (II) sites, we have now focused our attention on the synthesis of a new class of copper complexes bearing a sterically hindered chelating facially binding scorpionate that could modulate the coordination properties of the metal center.¹⁷⁻²⁰

As clarified in Chapter 1 (Section 1.2.4), for Tpm, the role of substituents at position 3 of the pyrazolyl rings is especially crucial for the additional steric hindrance that they introduce.^{19,21,22} The latter is, in fact, the main reason of the modulation of the coordination attitude of the resulting metal complex.

It has been described^{19,23} that the most common bulky substituents have an hydrophobic nature (*i.e.* *t*Bu, Ph, *i*Pr,...), therefore to increase the hydrophilic character of the final Cu-complex for further possible applications in catalysis or bioinorganic chemistry,²⁴⁻²⁶ an extra moiety should be inserted. As previously explained, apart from the pyrazolyl ring, the central methine carbon is an useful position for the functionalization of the ligand and the sulfonation^{27,28} at this point is an easy reaction to achieve a ‘more hydrosoluble’ scorpionate derivative (see also Li(Tpms) **(9)**, Section 1.3.1). Moreover, these ionic functionalized tris(pyrazolyl)methane derivatives exhibit a relevant coordination versatility,²⁸ acting as either a tripodal or a bipodal ligand (*i.e.* with N₃-, N₂O-, N₂- or NO-coordination modes) with the possibility of involving the sulfonate moiety in the coordination.²⁸⁻³¹ This flexibility allows exploring the behavior of the resulting complexes toward further ligand binding to the metal center. Many examples³²⁻³⁴ in these fields^{24,35} of hydrosoluble metal complexes of tris(pyrazolyl)borate (Tp) and derived ligands constitute an important precedent to embark in this study and motivate the investigation for possible further applications.³⁶⁻³⁹

The study aimed at the investigation of the coordination behavior of a new scorpionate that could combine the flexibility and water solubility of the sulfonato-functionalized class with the sterically demanding features of the 3-substituted tris(pyrazolyl) ligands. For these purposes, a new Tpms derivative bearing a phenyl ring at the 3-position of pyrazolyl rings has been designed. When ligating a metal center, such a bulky species would be expected to provide a ‘steric control’ on the other coordination position(s) of the complex, selecting the suitable ligands on the opposite side, namely preventing the formation of “sandwich” complexes (with two of such scorpionate ligands).^{17,19}

Hence, herein it is presented the synthesis of the new tris(3-phenylpyrazolyl)methanesulfonate (Tpms^{Ph})⁻ (**16**) and its coordination behavior toward copper(I).

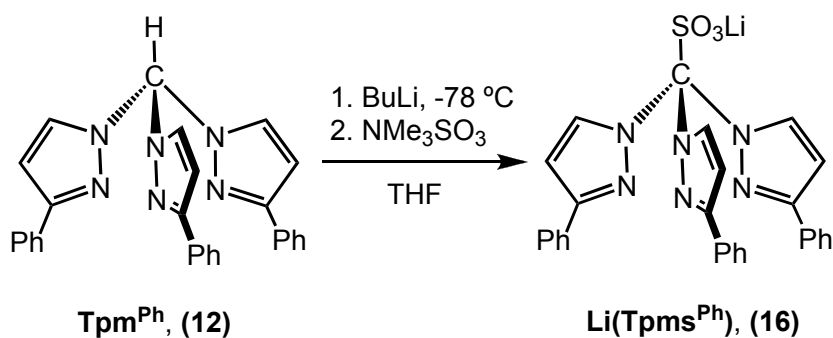
The isolation of a stable acetonitrile intermediate [Cu(Tpms^{Ph})(MeCN)] (**20**) opened to a carefully study of ligand displacement for the “Cu(I)-scorpionate” system. The use of two water soluble phosphines,^{40,41} 1,3,5-triaza-7-phosphaadamantane (PTA) and *N*-methyl-1,3,5-triaza-7-phosphaadamantane tetraphenyl borate ((mPTA)[BPh₄]), and of the related hexamethylenetetramine (HMT), has been considered for achieving an enhanced solubility in water of their complexes, a feature of interest for applications in biological systems⁴²⁻⁴⁷ and aqueous phase catalysis.⁴⁸⁻⁵⁰ The new water soluble complexes could represent a potentially active class of catalysts bearing a flexible labile ligand that would provide a convenient entry to further reactivity studies: *i.e.* coordination of small molecules (nitriles, isonitriles, CO, see Section 2.4), dioxygen activation (Section 2.5),^{1,51,52} catalytic studies (Section 2.6) and development of inorganic enzyme models.³⁶

2.2 Syntheses of Tpm^{Ph} and Li(Tpms^{Ph}) and metal complexes

2.2.1 Syntheses of the sterically hindered scorpionates Tpm^{Ph} and Li(Tpms^{Ph})

As fully described in Chapter 1, hydrotris(3-phenylpyrazolyl)methane, Tpm^{Ph} (**12**), was prepared by modifying Reger's procedure⁵³ in order to obtain the pure desired product without chromatographic purification. Hence, at the final stages, we have treated a toluene solution of the crude product with a catalytic amount of trifluoroacetic acid (in order to isomerise⁵⁴ the mixture of regioisomers to the desired 3-isomer compound, see also Section 1.2.2 Tpm: stability) and then crushed the final crude solid in diisopropyl ether to afford the pure Tpm^{Ph} compound.

Starting from Tpm^{Ph} we were able to prepare the tris(3-phenylpyrazolyl)methanesulfonate species as the lithium salt, Li(Tpms^{Ph}) (**16**), in good yield, following a process known²⁷ for the synthesis of unsubstituted Tpms, *i.e.*, by deprotonation of the methine carbon by BuLi, at low temperature, followed by sulfonation with the SO₃NMe₃ adduct (Scheme 2.1, see also Section 1.3.1)). As the Tpm^{Ph}, the sulfonate derivative shows a well resolved ¹H-NMR spectrum (acetone-*d*₆) with only one set of resonances for the three equivalent pyrazolyl rings: one pattern of signals for the phenyl protons and a pair of doublets (*J*_{HH}=2.7 Hz) at δ 8.22 and 6.83 ppm for the 5-H and 4-H pyrazolyl protons, respectively.

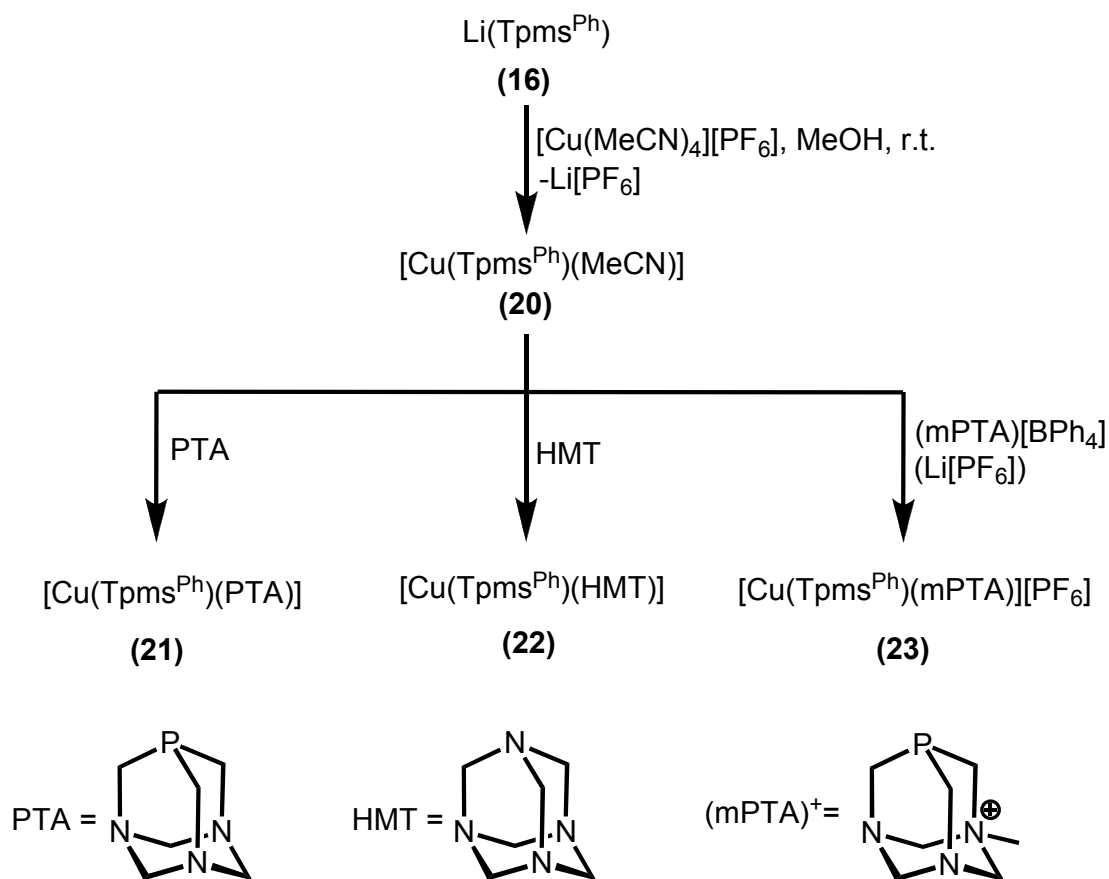


Scheme 2.1 Synthesis of Li(Tpms^{Ph}) (16)

Tpm^{Ph} (**12**) and its sulfonate Li(Tpms^{Ph}) (**16**) represent a highly sterically hindered class of scorpionates. Moreover, the sulfonate derivative shows interesting properties in terms of solubility. In fact, in spite of the presence of three phenyl rings, Li(Tpms^{Ph}) is well soluble in all common polar solvents, i.e., MeOH, EtOH, acetone and water ($S_{25^{\circ}\text{C}} \approx 90 \text{ mg}\cdot\text{mL}^{-1}$), and shows a decreasing solubility in medium polarity solvents and in non-polar ones.

2.2.2 Syntheses of the Cu^I complexes [Cu(Tpms^{Ph})L] [L = MeCN (**20**), PTA (**21**), HMT (**22**)] and [Cu(Tpms^{Ph})(mPTA)][PF₆] (**23**)

Reaction of Li(Tpms^{Ph}) (**16**) with [Cu(MeCN)₄][PF₆] in methanol proceeds readily at room temperature to give [Cu(Tpms^{Ph})(MeCN)] (**20**) bearing the anionic Tpms^{Ph} ligand and one bound molecule of acetonitrile, in good yield (Scheme 2.2). The neutral Cu^I complex (**20**) precipitates from the concentrated reaction mixture, as a white solid, which is sparingly soluble in water ($S_{25^{\circ}\text{C}} \approx 4 \text{ mg}\cdot\text{mL}^{-1}$), MeOH, EtOH or DMSO, and well soluble in Me₂CO, CHCl₃ or CH₂Cl₂. It is stable in air when dried, but is relatively unstable in solution (after 2-3 days the color changes to green, typical of a Cu^{II} oxidized product). It was characterized, as the compounds (**21**)-(**23**) described below, by NMR and IR spectroscopies, elemental analysis and X-ray diffraction. The ¹H and ¹³C NMR and IR spectra of (**20**) confirm the presence of its ligands: the NMR shifted resonances of Tpms^{Ph} and an IR weak and broad NC stretching band at 2316 cm⁻¹, well above that of the uncoordinated NCMe, i.e., 2253 cm⁻¹. This positive coordination shift [$\Delta\nu_{(\text{NC})} = 63 \text{ cm}^{-1}$] indicates that the acetonitrile is behaving as a very weak π -acceptor, acting mainly as an effective σ -donor ligand, in accord with related scorpionate complexes.^{55,56}



*Scheme 2.2 Syntheses of the complexes $[\text{Cu(Tpms}^{\text{Ph}})L]$ [$L = \text{MeCN}$ (**20**), PTA (**21**), HMT (**22**) and $[\text{Cu(Tpms}^{\text{Ph}})(\text{mPTA})][\text{PF}_6]$ (**23**).*

Treatment of a methanolic solution of **(20)**, formed *in situ*, with PTA (0.9 eq.) in methanol leads to the precipitation of $[\text{Cu(Tpms}^{\text{Ph}})(\text{PTA})]$ (**21**), as a white solid isolated in high yield (88%). This complex shows a good solubility in acetone and dichloromethane, and it is fairly soluble in water ($S_{25^\circ\text{C}} \approx 6 \text{ mg}\cdot\text{mL}^{-1}$). The addition of PTA to the reaction mixture should be slow to yield **(21)** in high purity. Traces of the by-product $[\text{Cu(PTA)}_4][\text{PF}_6]$ are formed when the addition is faster or the phosphine is used in a higher amount, indicating a stronger coordination ability of PTA to Cu(I) in comparison with Tpms^{Ph} . The formation of $[\text{Cu(PTA)}_4][\text{PF}_6]$ is evidenced by the quartet ($^1J_{\text{P-Cu}} = 760 \text{ Hz}$) resonance at $\delta -80$ observed by $^{31}\text{P}\{^1\text{H}\}$ NMR, which is analogous to that known⁵⁷ for $[\text{Cu(PTA)}_4][\text{NO}_3]$.

In the $^1\text{H-NMR}$ spectrum of **(21)** (acetone- d_6) the resonances for the PTA moiety confirm its coordination to copper and appear shifted to lower field relatively to those of the free PTA: the six equivalent protons close to the P-atoms give a broad

singlet at δ 2.97 and the other resonances for the protons near the N-atoms display the expected AB pattern at δ 3.96-4.16 ppm. The Tpms^{Ph} resonances are given below. The ³¹P{¹H} NMR spectrum shows a single broad signal at δ -93 ppm. Further NMR experiments at different temperatures reveal additional information on the behavior of compound **(21)** in solution that will be discussed in Section 2.2.4. The IR spectrum confirms the presence of Tpms^{Ph} (stretching bands at 1539 (C=N), 1048 (SO) and 643 (CS) cm⁻¹)³¹ and PTA (1015, 972 and 950 cm⁻¹) (full description in the Experimental part).

Similarly to the reaction with PTA, the acetonitrile complex **(20)** formed *in situ* (hence in the presence of the Li[PF₆] co-product) reacts with hexamethylenetetramine (HMT) or *N*-methyl-1,3,5-triaza-7-phosphaadamantane tetraphenyl borate ((mPTA)[BPh₄]) to yield the corresponding complexes [Cu(Tpms^{Ph})(HMT)] **(22)** or [Cu(Tpms^{Ph})(mPTA)][PF₆] **(23)** (Scheme 2.2). The ¹H-NMR spectrum of **(22)** at 188 K shows two types of methylene protons for the ligated HMT (*i.e.* an AB spin system and a broad singlet) confirming the coordination by one of nitrogen atoms. However, at room temperature, only a broad singlet is observed due to an average effect of a dynamic process (see below, NMR Section 2.2.4). The isolation, upon precipitation, of compound **(23)**, instead of the [BPh₄]⁻ analogue, indicates that the former is less soluble than the latter. As observed for **(20)**, compounds **(21)**-**(23)** are soluble in water ($S_{25^{\circ}\text{C}} \approx 6\text{-}7 \text{ mg}\cdot\text{mL}^{-1}$).

2.3 X-ray molecular structures of complexes [Cu(Tpms^{Ph})L] [L = MeCN (20), PTA (21), HMT (22)] and [Cu(Tpms^{Ph})(mPTA)][PF₆] (23)

The molecular structures of compounds (20)-(23) were determined by single crystal X-ray diffraction analyses performed by Dr. M. Fátima C. Guedes da Silva. The ORTEP plots are depicted in Figures. 2.1-2.4, the ellipsoids being shown at 50% probability and the hydrogen atoms being omitted for clarity. Crystallographic details are given in the Experimental Chapter, selected bond distances in Table 2.1, and selected angles in Table 2.2.

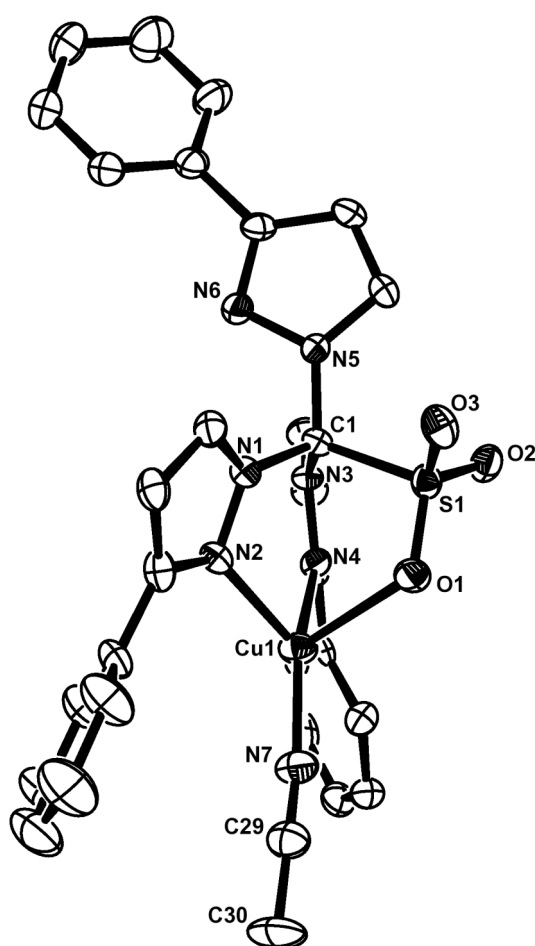


Figure 2.1 ORTEP plot of [Cu(Tpms^{Ph})(MeCN)] (20), with ellipsoids shown at 50% probability.

Single crystals of compounds **(20)** to **(22)** suitable for X-ray diffraction were obtained by slow evaporation in air of acetone solutions. In complexes **(20)** and **(22)** (Figures. 2.1 and 2.2), the anionic tris(3-phenylpyrazolyl)methanesulfonate group acts as a tridentate ligand with the N,N,O coordination mode to the Cu ion through the two pyrazolyl nitrogens N(2) and N(4) and the oxygen O(1) of the sulfonate moiety. The coordination around each copper is highly distorted tetrahedral with the N2-Cu1-N7 and N4-Cu1-N7 angles of 121.02(12)° and 146.62(12)° for **(20)** or 147.73(14)° and 124.27(14)° for **(22)**, and the O1-Cu1-N7 angle of a much lower value (109.82(11)° for **(20)** or 92.38(12)° for **(22)**). Moreover, the Cu(1)-O(1) bond length (2.326(2) Å for **(20)** or 2.412(2) Å for **(22)**) is significantly longer than the Cu-O bond in Cu-OSO₂ (2.136(6) Å) and Cu-ONO₂ (2.110(6) Å) in Na₅[Cu(TPPTS)]·5H₂O (TPPTS = tris(*m*-sulfonatophenyl)phosphate) and [Cu(NO₃)(AsPh₃)₃], respectively.^{58,59} However, it is within the sum of their van der Waals radii and is in accord with other Cu-Tpms complexes.⁶⁰ In **(20)** the Cu(1)-N(7) distance of 1.858 Å is comparable to that observed in a analogue acetonitrile copper(I) complexes,⁵³⁻⁵⁶ although *ca.* 0.1 Å shorter than that found in **(22)**.

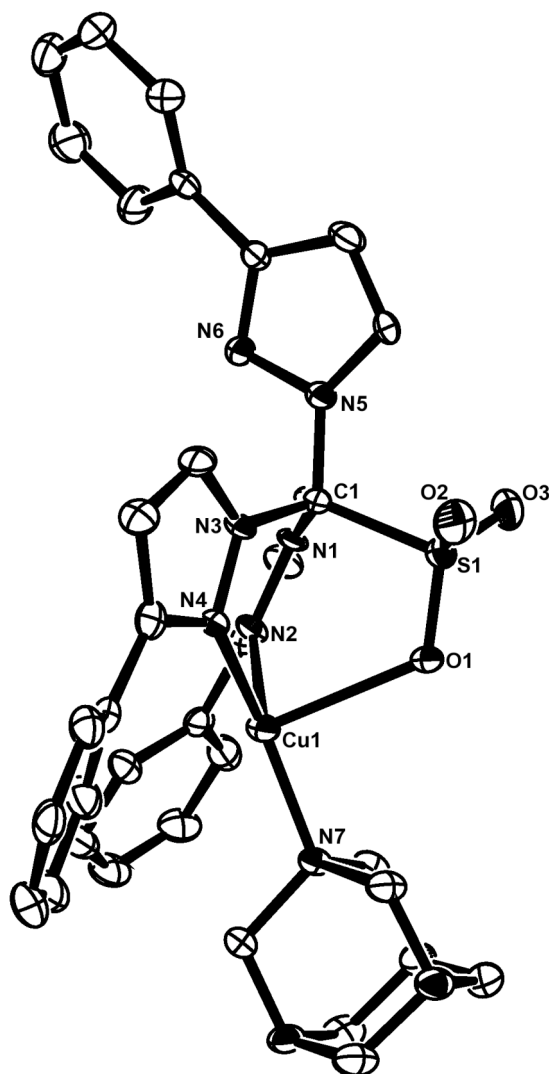


Figure 2.2 ORTEP plot of $[\text{Cu}(\text{Tpms}^{\text{Ph}})(\text{HMT})]$ (**22**), with ellipsoids shown at 50% probability.

The Cu-N-N-C (where C is at pyrazolyl) torsion angles of the pyrazolyl rings present values from $150.1(2)^\circ$ (in **(20)**) to $179.0(3)^\circ$ (in **(22)**), whereas the Cu-N-N-C(1) torsion angles (defining⁶¹ the degree of tilting of the rings with respect to the C_s axis of the molecule) are in the range of $12.3(5)^\circ$ (in **(22)**) to $22.5(3)^\circ$ (in **(20)**) (Table 2.3).

In compounds **(21)** and **(23)**, the anionic TpmsPh acts as a tridentate N,N,N-ligand (Figures 2.3 and 2.4). The N-Cu-N angles are restrained by the chelate rings to $84.5(3)^\circ$ – $89.06(16)^\circ$, while the wider N-Cu-P angles are within the range of $125.24(12)^\circ$ – $129.9(2)^\circ$. In both structures there is a high degree of tilting of the pyrazolyl rings with the Cu-N-N-C(1) torsion angles from $29.6(10)^\circ$ in **(23)** to

42.2(5)° in (**21**) being drastically higher than those for other scorpionate analogues.⁶² Similarly, we can compare the Cu-N-N-C (where C is at pyrazolyl) torsion angles, averaging 133° for (**21**) and 139° for (**23**), with their analogues in the related Cu(I) complexes [Cu(Tpm^{tBu})L][PF₆] (Tpm^{tBu} = tris(3-*tert*butylpyrazolyl)methane; L = CO or NCMe)⁵⁶ with a maximum torsion angle of 171° (L = NCMe). In the present structures, the distortion can tentatively be attributed to steric effects associated to the phenyl substituent in the pyrazolyl rings and to the PTA or (mPTA)⁺ ligands.

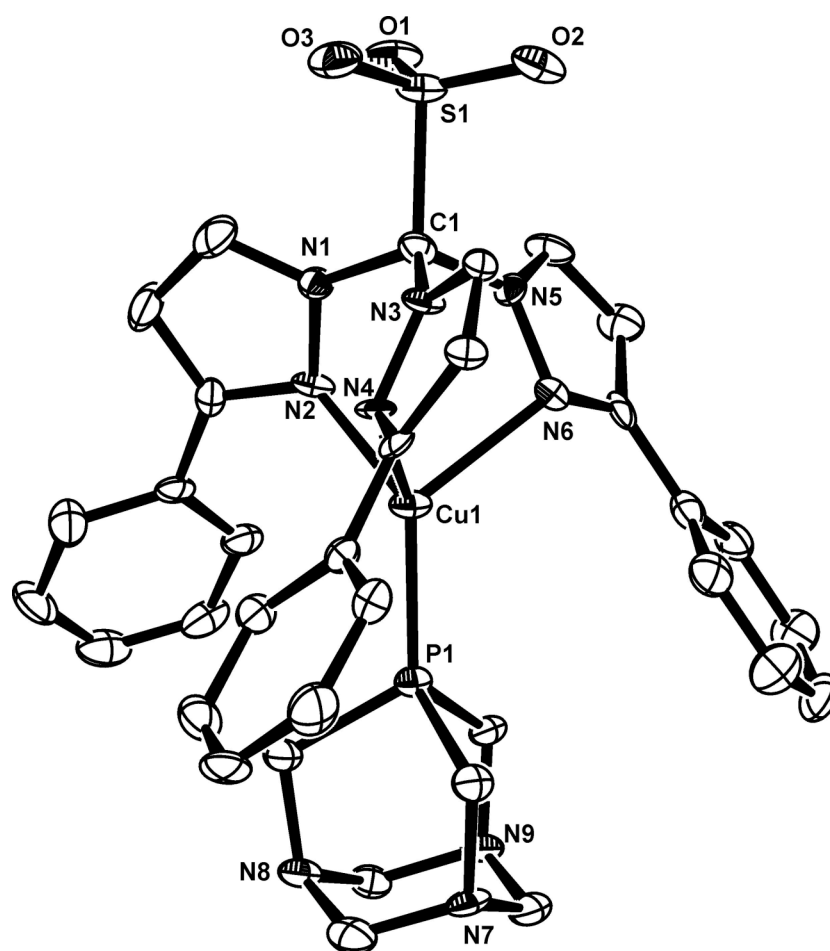


Figure 2.3 ORTEP plot of [Cu(Tpms^{Ph})(PTA)] (**21**), with ellipsoids shown at 50% probability; one molecule of acetone is omitted for clarity.

Table 2.1 Selected bond distances [\AA] for compounds $[\text{Cu}(\text{Tpms}^{\text{Ph}})(\text{MeCN})]$ (**20**), $[\text{Cu}(\text{Tpms}^{\text{Ph}})(\text{PTA})]$ (**21**), $[\text{Cu}(\text{Tpms}^{\text{Ph}})(\text{HMT})]$ (**22**) and $[\text{Cu}(\text{Tpms}^{\text{Ph}})(\text{mPTA})][\text{PF}_6]$ (**23**).

	(20)	(22)		(21) · C ₃ H ₆ O	(23) · C ₃ H ₆ O
Cu(1)-N(2)	2.065(3)	1.968(4)	Cu(1)-N(2)	2.170(4)	2.112(8)
Cu(1)-N(4)	1.996(3)	2.052(3)	Cu(1)-N(4)	2.138(4)	2.099(8)
Cu(1)-O(1)	2.326(2)	2.412(2)	Cu(1)-N(6)	2.099(4)	2.104(8)
C(1)-N(1)	1.458(4)	1.471(5)	C(1)-N(1)	1.446(7)	1.463(13)
C(1)-N(3)	1.465(4)	1.459(5)	C(1)-N(3)	1.465(7)	1.464(13)
C(1)-N(5)	1.429(5)	1.434(5)	C(1)-N(5)	1.446(7)	1.419(13)
Cu(1)-N(7)	1.858(4)	1.956(3)	Cu(1)-P(1)	2.1492(15)	2.139(3)
S(1)-O(1)	1.453(3)	1.452(3)	C(1)-S(1)	1.883(6)	1.893(10)
S(1)-O(2)	1.438(2)	1.441(3)			
S(1)-O(3)	1.446(2)	1.442(3)			
N(7)-C(29)	1.145(6)	-			

Table 2.2 Selected angles [$^{\circ}$] for compounds $[\text{Cu}(\text{Tpms}^{\text{Ph}})(\text{MeCN})]$ (**20**), $[\text{Cu}(\text{Tpms}^{\text{Ph}})(\text{PTA})]$ (**21**), $[\text{Cu}(\text{Tpms}^{\text{Ph}})(\text{HMT})]$ (**22**) and $[\text{Cu}(\text{Tpms}^{\text{Ph}})(\text{mPTA})][\text{PF}_6]$ (**23**).

	(20)	(22)		(21) · C ₃ H ₆ O	(23) · C ₃ H ₆ O
N2-Cu1-N7	121.02(12)	147.73(14)	N2-Cu1-P1	125.24(12)	127.1(2)
N4-Cu1-N7	146.62(12)	124.27(14)	N4-Cu1-P1	129.05(12)	127.8(2)
O1-Cu1-N7	109.82(11)	92.38(12)	N6-Cu1-P1	128.95(13)	129.9(2)
N2-Cu1-N4	88.65(11)	87.80(14)	N2-Cu1-N4	85.14(16)	86.9(3)
O1-Cu1-N4	86.34(10)	86.63(12)	N4-Cu1-N6	85.06(16)	85.5(3)
O1-Cu1-N2	84.26(9)	84.99(12)	N2-Cu1-N6	89.06(16)	84.5(3)
C1-S1-O1	104.38(16)	103.07(16)			
C1-S1-O3	103.15(15)	104.56(19)	Cu1N2-N1C2	138.2(4)	137.1(7)
C1-S1-O2	103.51(14)	103.32(19)	Cu1N4-N3C11	136.1(4)	141.8(7)
O2-S1-O1	114.81(15)	114.1(2)	Cu1N6-N5C20	126.0(4)	137.3(7)
O2-S1-O3	115.02(14)	115.7(2)	Cu1N2-N1C1	32.9(5)	36.0(9)
O3-S1-O1	113.95(15)	114.04(18)	Cu1N4-N3C1	39.1(5)	29.6(10)
			Cu1N6-N5C1	42.4(5)	33.2(10)
Cu1N4-N3C11	167.9(2)	179.0(3)			
Cu1N2-N1C2	150.1(2)	156.0(3)			
Cu1N4-N3C1	22.5(3)	12.3(5)			
Cu1N2-N1C1	18.0(3)	18.5(5)			

Moreover, the solid state structure of compound (**23**) (Figure 2.4) exhibits the presence of intramolecular C-H--- π interactions specifically between the C(29)-H(22) moiety and the closest phenyl ring (*i.e.* C(5-10)). The distance between the C-H hydrogen and the centroid of this ring is 2.489 Å, indicating a relatively strong non-covalent interaction.⁶³⁻⁶⁶ Similarly, each of the other two phenyl rings interacts with the corresponding H atom of a methylene group of (mPTA)⁺ (although at longer 2.520 and 2.594 Å distances), constituting a sort of symmetrical intramolecular interaction that probably helps to stabilise the N,N,N-coordination mode, in the solid state.

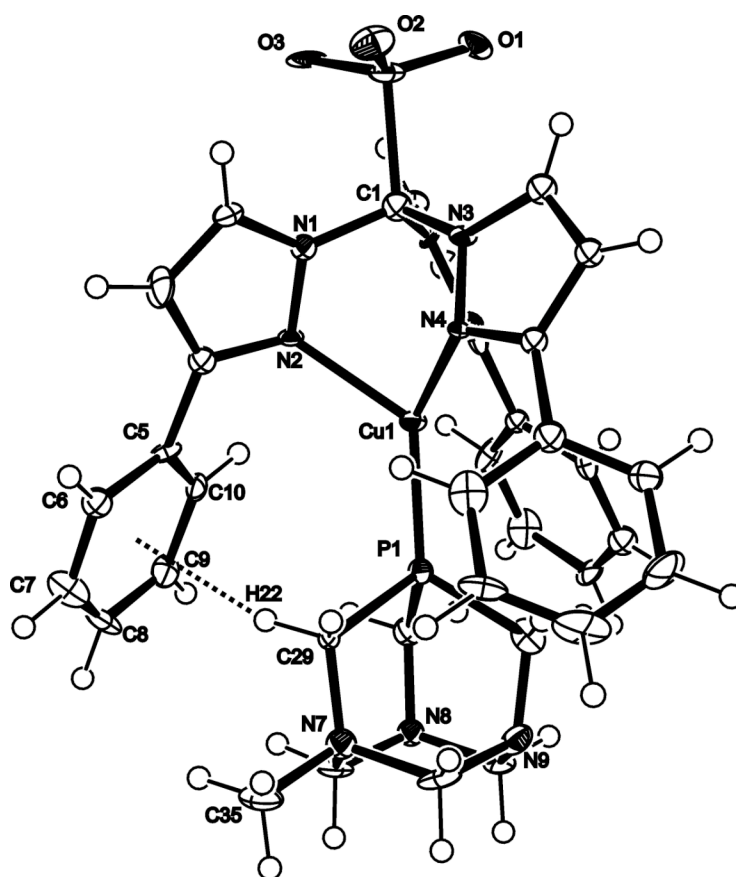


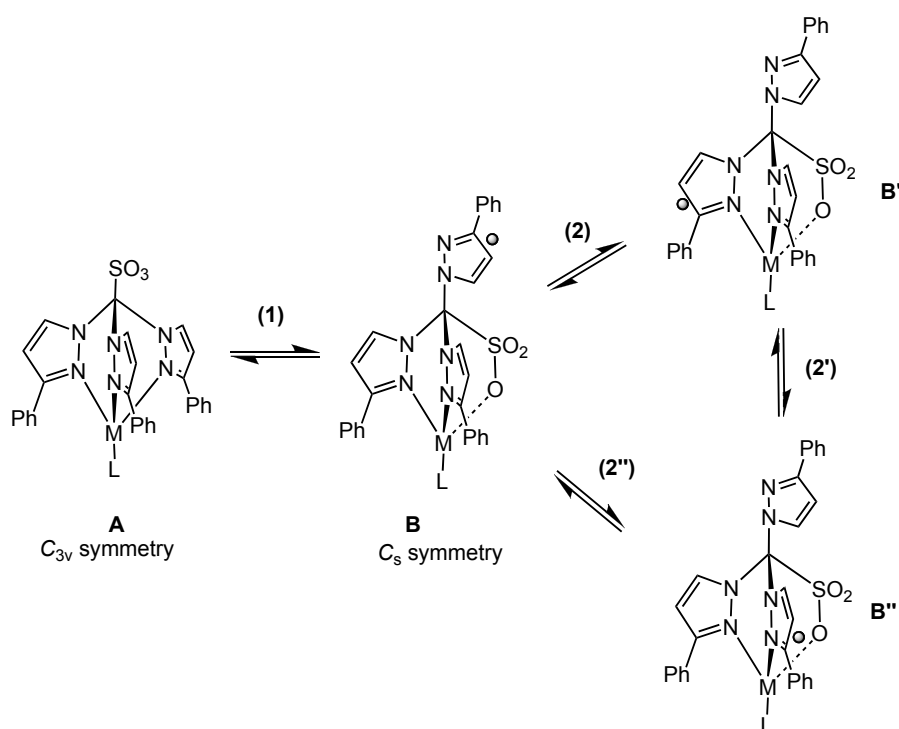
Figure 2.4 ORTEP plot of $[\text{Cu}(\text{Tpms}^{\text{Ph}})(\text{mPTA})][\text{PF}_6]$ (**23**), with ellipsoids shown at 50% probability; hydrogen atoms are shown but the $[\text{PF}_6]^-$ counter-ion and one molecule of crystallization acetone are omitted for clarity. The dashed line indicates the C-H--- π intramolecular (2.489 Å) interaction between C(29)-H(22) and the π -phenyl ring (C(5) to C(10)).

In the case of complexes **(20)** and **(22)**, bearing N-donor ligands (MeCN and HMT, respectively) that are effective σ -electron donors and not appreciable π -acceptors, the metal tends to prefer the weaker electron-donating N₂O-coordination mode of Tpms^{Ph}. The stronger electron-releasing N₃-coordination of the latter ligand appears to be the preferable one for complexes **(21)** and **(23)** with π -acceptor phosphine ligands, in spite of the stronger steric hindrance associated to this type of coordination in comparison with the N₂O-mode.

2.4 NMR solution studies

The complexes exhibit fluxional behavior in solution, as shown by variable temperature NMR studies (Table 2.3) which have allowed to check if the coordination modes of the Tpms^{Ph} ligand observed in the solid state are retained in solution.

Hence, compound (**21**), with the N₃-type coordination in the solid state, as established by X-ray diffraction (see above), in solution (acetone-*d*₆) at room temperature shows, in the ¹H-NMR spectrum, the expected resonances for the 4-H and 5-H protons of the three equivalent pyrazolyl rings. This pattern essentially remains upon cooling until 200 K, indicating the preservation of the N₃-coordination at low temperature. Only traces of the pattern associated to the N₂O-coordination were then detected (Figure. 2.5b), as a result of the shift at low temperature, toward this mode, of the equilibrium (**1**, Scheme 2.3) between the two coordination forms. In accord, such a type of Tpms coordination equilibrium is known^{29,30} to be temperature dependent.



Scheme 2.3 Equilibria between the two different Tpms^{Ph} coordination modes for complexes of general formula [M(Tpms^{Ph})L]: type **A**, N₃-coordination, C_{3v}-symmetry; type **B**, N₂O-coordination, C_s-symmetry, where is also shown the dynamic process among different N₂O-coordination modes.

In contrast, the other complexes ((**20**), (**22**) and (**23**)) display low temperature ¹H-NMR limit spectra that are consistent with the N₂O-coordination (two equivalent and one non-equivalent pyrazolyl rings, Fig. 2.5a),²⁸ which is also the observed one for (**20**) and (**22**) in the solid state. In the case of (**23**), linkage isomerisation (**1**, Scheme 2.3) of the N₃-mode exhibited in the solid state has occurred in solution (only traces of the N₃-coordination are detected).

Table 2.3 Selected ¹H-NMR (acetone-d₆) chemical shifts (δ) for compounds [Cu(Tpms^{Ph})(MeCN)] (**20**), [Cu(Tpms^{Ph})(PTA)] (**21**), [Cu(Tpms^{Ph})(HMT)] (**22**) and [Cu(Tpms^{Ph})(mPTA)][PF₆] (**23**).

Compound		Room temperature (δ)	Low temperature limit (δ)
(20)	4-H	6.94 (3H)	7.35 (1H), 7.00 (2H)
	5-H	8.07 (3H)	8.87 (1H), 7.27 (2H)
(21)	4-H	6.92 (3H)	7.12 (3H) ^a
	5-H	8.50 (3H)	8.85 (3H) ^a
(22)	4-H	6.92 (3H)	7.35 (1H), 6.90 (2H)
	5-H	7.84 (3H)	8.91 (1H), 7.22 (2H)
(23)	4-H	6.96 (3H)	7.35 (1H), 6.96 (2H) ^b
	5-H	^c	8.94 (1H), 7.28 (2H) ^b

^a With a small amount of N₂O-coordination ($K_{eq} = [\text{N}_3\text{-coordinated species}]/[\text{N}_2\text{O-coordinated species}] = 3.2$) at 8.92, 7.35 (for 5-H) and 7.41, 6.97 (for 4-H). ^b With traces of N₃-coordination ($K_{eq} = [\text{N}_3\text{-coordinated species}]/[\text{N}_2\text{O-coordinated species}] = 0.12$) at 8.87 (for 5-H) and 7.08 (for 4-H). ^c Very broad resonance under the phenyl rings resonances at δ ca. 8.05-7.90, detected by HMQC ¹³C-¹H NMR.

However, at room temperature, all complexes (**20**)-(**23**) display ¹H-NMR spectra that are indicative of the equivalence of the three pyrazolyl rings (Table 2.3). In the case of (**21**) (see above), this is conceivably due to the N₃-type coordination (form **A**, Scheme 2.3) that is retained from the solid state, whereas for the other complexes ((**20**), (**22**) and (**23**)), it can be ascribed to the fast equilibria (**2**, **2'** and **2''**, Scheme 2.3) among the three forms (**B**, **B'** and **B''**) with N₂O-coordination. Decreasing the temperature leads to a split to a double pattern with two distinct sets of resonances in the 2:1 ratio (Fig. 2.5a, at 213K).

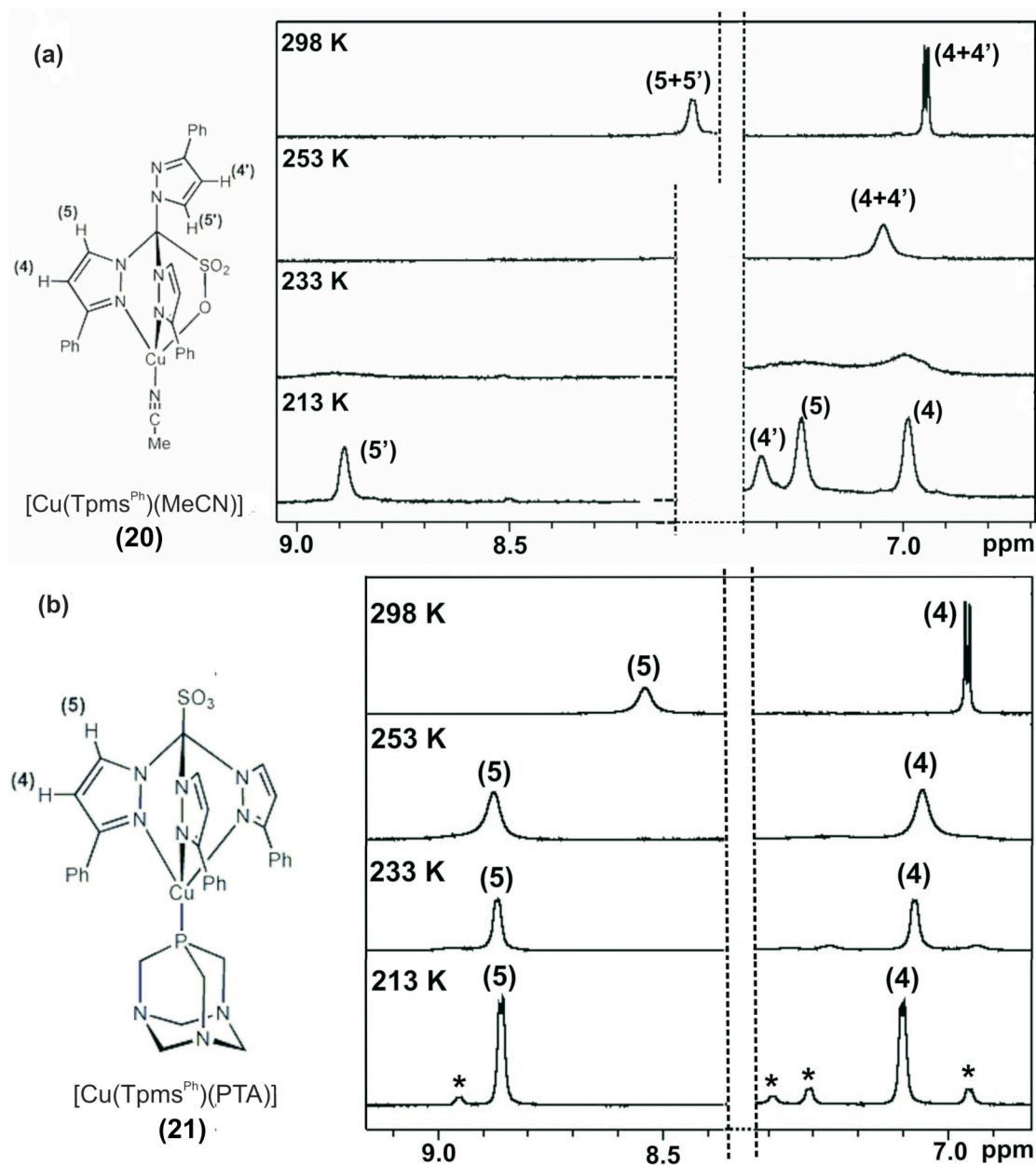


Figure 2.5. Variable temperature (298 – 213 K) ¹H NMR spectra (selected δ ppm ranges) for (20) (a) and (21) (b) in acetone-d₆. (*) indicates traces of the N₂O-coordination isomer.

The Tpms^{Ph} complexes (20) and (22), bearing a N-donor ligand (MeCN or HMT, respectively), preserve, in solution, the N₂O-coordination observed in solid state, while for compounds (21) and (23), with a π-acceptor phosphine ligand (PTA or (MePTA)⁺, correspondingly), the metal prefers the stronger electron-releasing N₃-coordination mode of Tpms^{Ph}. This argument holds specially for (23), with the cationic alkylated (mPTA)⁺ ligand, expected to be, like the protonated PTA,⁶⁷⁻⁶⁹ a

more effective π -acceptor than PTA in **(21)**. In fact, the $^{31}\text{P}\{^1\text{H}\}$ -NMR signal (δ -70.9 ppm) of compound **(23)** is shifted to lower field relatively to that (δ -93.3 ppm) of complex **(21)**. Nevertheless, in solution, the less effective electron-donor N₂O-coordination appears to become dominant, what conceivably results from both steric and electronic effects. The (mPTA)⁺ ligand would prefer to avoid the more sterically demanding Tpms^{Ph} N₃-binding in accord with the fact that the molecular structure of **(23)** (Fig. 5), in the solid state, shows a tilted N₃-bound Tpms^{Ph} ligand to minimize the steric interaction between its phenyl rings and (mPTA)⁺. Moreover, the cationic phosphine could influence the electrostatic metal interaction with the sulfonate moiety, hampering the charge separation between the positive metal and the negative SO₃⁻ group, thus favoring the N₂O-mode.

2.5 Cu-Tpms^{Ph} complexes (20)-(23): overview

The collected results clarify the behavior of the flexible scorpionate that could be involved in coordination to the metal. A possible effect of the sulfonate moiety in the reactivity of the resulting complexes has been object of these studies. For instance, the acetonitrile substitution of compound (20) is easily accomplished with phosphines or amines. On the other hand, the carbonylation reaction of (20) (see Section 2.6.2) manifests unexpected difficulties probably due to the presence of the additional sulfonate group and should be further investigated.

In general, several considerations of these results could be done and open to further studies on this Cu-scorpionate system. In fact, the ¹H-NMR chemical shifts of 5-H pyrazolyl protons of N₃- and N₂O-scorpionates show interesting details.

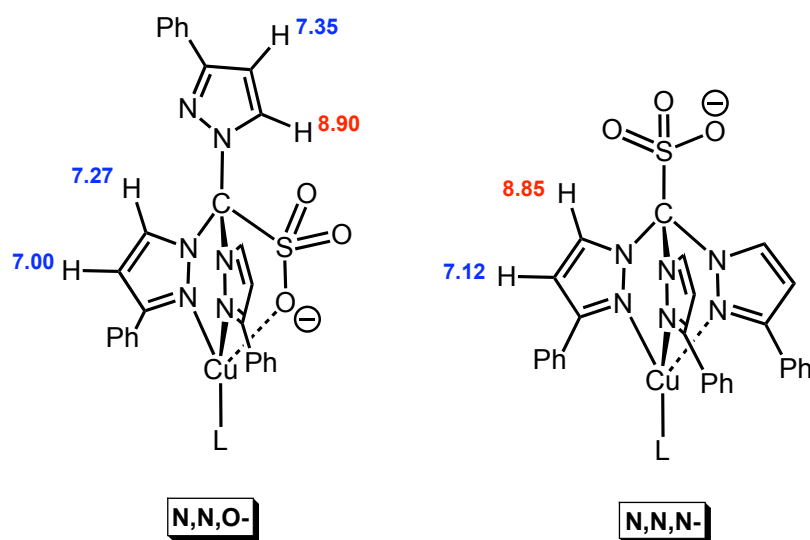


Figure 2.6 Schematic representation of the average chemical shifts for 4(H) and 5(H) of pyrazolyl ring for N₂O- and N₃- coordination modes of compounds (20)-(23).

Compounds (20)-(23) show, in their corresponding low temperature limit ¹H-NMR spectra, a consistent pattern: the pyrazolyl proton at 5 position of the N₃-scorpionate of (21) is visible at δ 8.85 while the analogous resonance for the N₂O-compounds (20), (22) and (23) of the two ligated pyrazolyl rings is observed at a higher field (*i.e.* δ 7.27, 7.22, 7.28 for (20), (22) and (23), respectively) and that of the free pyrazolyl ring appears in the δ 8.87-8.94 range (Figure 2.6). It is worthwhile to

try justify this great shifts of the resonances: as intentionally drawn in the Figure 2.6 a possible role of the sulfonate moiety could be considered. Although an H-bond interaction that includes the aromatic pyrazolyl proton at position 5 is difficult to visualize, since this type of interactions demand non-aromatic, more labile and detached hydrogen atoms (*i.e.* alcohols, amines), the difference between the 5-H of coordinated pyrazolyl rings in the N₃ and N₂O compounds is remarkable ($\Delta\delta$ 1.58 ppm). Moreover, it is unusual that the free pyrazolyl ring (in the N₂O-compounds, **(20)**, **(22)** and **(23)**) displays similar ¹H-NMR resonances to those of ligated rings in **(21)** (*i.e.* δ 8.87/7.35 and 8.85/7.12 of 4(H) and 5(H) for **(20)** and **(21)** respectively). The X-ray structure of **(21)** (Figure 2.3) shows the oxygen atoms of sulfonate moiety not aligned to the 5-(H) of pyrazolyl rings (Figure 2.7), and the minimum S-O \cdots H-pz distance is in the range of 2.484-2.565 Å (O(2)-H(11), O(1)-H(20) and O(3)-H(2), Figure 2.7). Thus a -SO \cdots H(pz) interaction between the sulfonate group and pyrazolylic protons has to be excluded in the solid state.

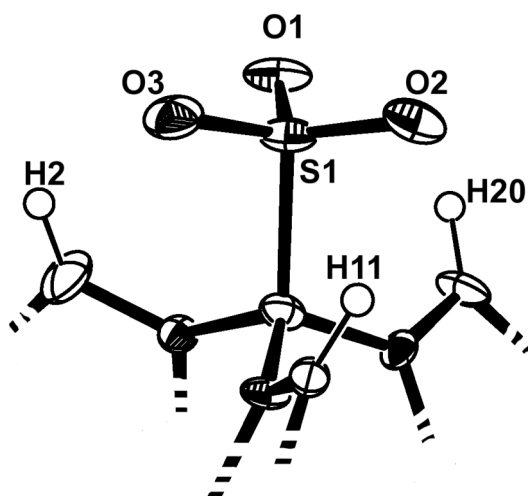


Figure 2.7 Expanded image of ORTEP plot of **(21)**.

Nevertheless, the above NMR shift does not depend exclusively on the metal coordination: the free ligand^(*) **(16)** shows its proton resonances at δ 8.22 and 6.83 which upon coordination move to δ 7.27 and 7.00 for **(20)** and δ 8.85 and 7.12 for **(21)**.

* It is appropriate to consider **(16)** as lithium complex, and consequently its ¹H-NMR resonances concern [Li(Tpms^{Ph})] (see also Sections 1.3.1 and 1.4).

It is reasonable to assume that the scorpionate (**16**) in these Cu^I-complexes is involved in inter- or intramolecular interactions that are retained in solution and determine the unpredicted ¹H-NMR shift of the 5-(H) of pyridyl rings.

In general, all these experimental results reflect the tripodal coordination flexibility of (**16**). From solution NMR and X-ray diffraction experiments it is possible to conclude that Tpms^{Ph} tends to adapt its coordination mode to the electronic and steric preferences of the metal center. In fact, compounds (**20**) and (**22**), bearing N-donor ligands (acetonitrile and HMT, respectively) with an expected stronger electron-donor ability display the N₂O coordination, involving the weak electron-donor sulfonate moiety; whereas those containing phosphines with a π-acceptor character (*i.e.* compounds (**21**) and (**23**)) tend to exhibit the N₃ capping coordination that provides a more effective electron-release to the metal. Moreover, compound (**23**), bearing the cationic methylated PTA, shows in solution a good affinity for the N₂O coordination mode, with the bound anionic sulfonate moiety, lowering the steric interaction between the Tpms^{Ph} and the phosphine.

The complexes described here are soluble in water and the flexibility of the new scorpionate ligand, bearing the labile sulfonate group, provides a good example of a versatile ligand able to be employed in further reactivity studies, namely of metalloenzyme models.

2.6 Appendix 2.A: study of the Cu^I-Tpms^{Ph} system on the activation of nitriles, isonitriles and carbon monoxide

It has been achieved, in this thesis, an easy and powerful synthetic procedure to afford a new class of Cu^I complexes bearing a bulky tris(pyrazolyl)methane ligand. In particular, the preparation of the stable intermediate acetonitrile complex **(20)** encourages the study of the stability of the coordinated nitrile molecule and its derivatives.⁷⁰ The Cu^I center has been the object of an underdeveloped study in this field, since its low oxidation state is not expected to favour the activation of nitriles and isonitriles toward nucleophiles. In spite of that, the promising stability of compound **(20)** prompts the study of the Cu^I-nitrile and -isonitrile systems. In fact, starting from our experience on the metal-mediated activation of a CN triple bond (*i.e.* nitriles⁷¹⁻⁷⁶ and isonitriles⁷⁷⁻⁸⁰) a preliminary investigation of the Cu^I-scorpionate system has been planned.

Despite the presence of sterically hindered phenyl substituents on the ligand, it is evident from Figure 2.1 that the N,N,O-coordination mode of the (Tpms^{Ph})⁻ in compound **(20)** allows a further chemical reaction at the nitrile molecule and we have demonstrated that substitution of this ligand can be easily achieved. Furthermore, one can imagine that in the presence of a non-coordinating nucleophile, it would be possible to drive the nucleophilic attack onto the C-carbon atom of the nitrile group. Moreover, the substitution of the nitrile moiety with different isonitriles has been successfully studied in order to verify the stability and the flexibility of this system.

2.6.1 Syntheses of [Cu(Tpms^{Ph})(CyNC)] **(24)** and [Cu(Tpms^{Ph})(XyNC)] **(25)** (CyNC = cyclohexyl isocyanide; XyNC = 2,6-dimethylphenyl isocyanide) and their reactivity toward nucleophiles: 3-iminoisoindolin-1-one and methylamine

Reactions of **(20)** with cyclohexyl isocyanide (CyNC) and 2,6-xylyl isocyanide (XyNC) in dry methanol lead to the formation of the corresponding isocyanide complexes [Cu(Tpms^{Ph})(CyNC)] **(24)** and [Cu(Tpms^{Ph})(XyNC)] **(25)**

(Scheme 2.0). They are moderately soluble in MeOH, EtOH, soluble in CH₂Cl₂, CHCl₃ and sparingly soluble in water ($S_{25^{\circ}\text{C}} \approx 3 \text{ mg}\cdot\text{mL}^{-1}$). Their variable temperature ¹H-NMR spectra indicate that the scorpionate assumes the N,N,O-coordination mode (see also Section 2.4 and Experimental part) and this coordination is retained in the solid state for compound **(24)** that exhibits an X-ray crystal structure with a highly distorted tetrahedral coordination geometry of the copper center (Figure 2.8) similarly to its analogue **(20)** and **(22)**. In fact, analogously, the Cu(1)-O(1) bond length is 2.377(2) Å within the sum of the corresponding van der Waals radii.

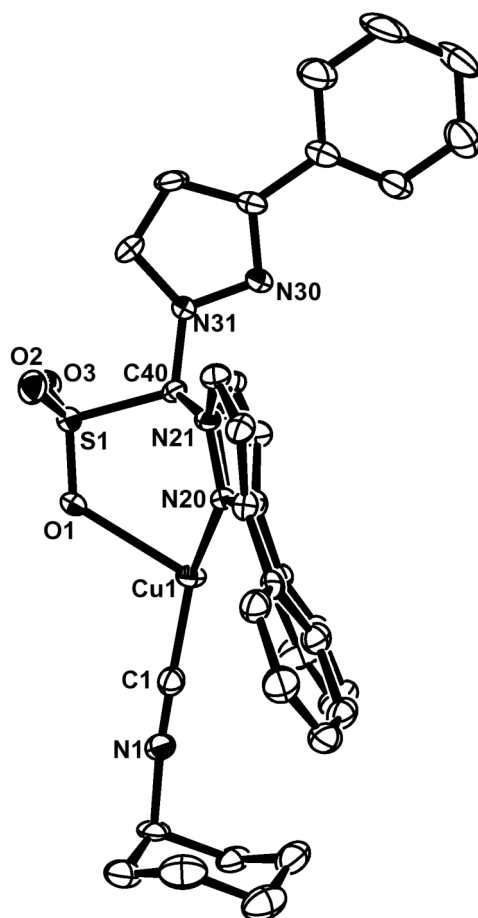


Figure 2.8 ORTEP plot of $[\text{Cu}(\text{Tpms}^{\text{Ph}})(\text{CyNC})]$ (**24**), with ellipsoids shown at 50% probability.

The IR spectra of compounds **(24)** and **(25)** show an intense ν_{CN} stretching band at 2191 and 2153 cm^{-1} , respectively (Figure 2.9). The minimal shifts from the corresponding frequencies of the uncoordinated isocyanides indicate that the activation of the isonitrile by the Cu center in **(24)** and **(25)** is negligible.

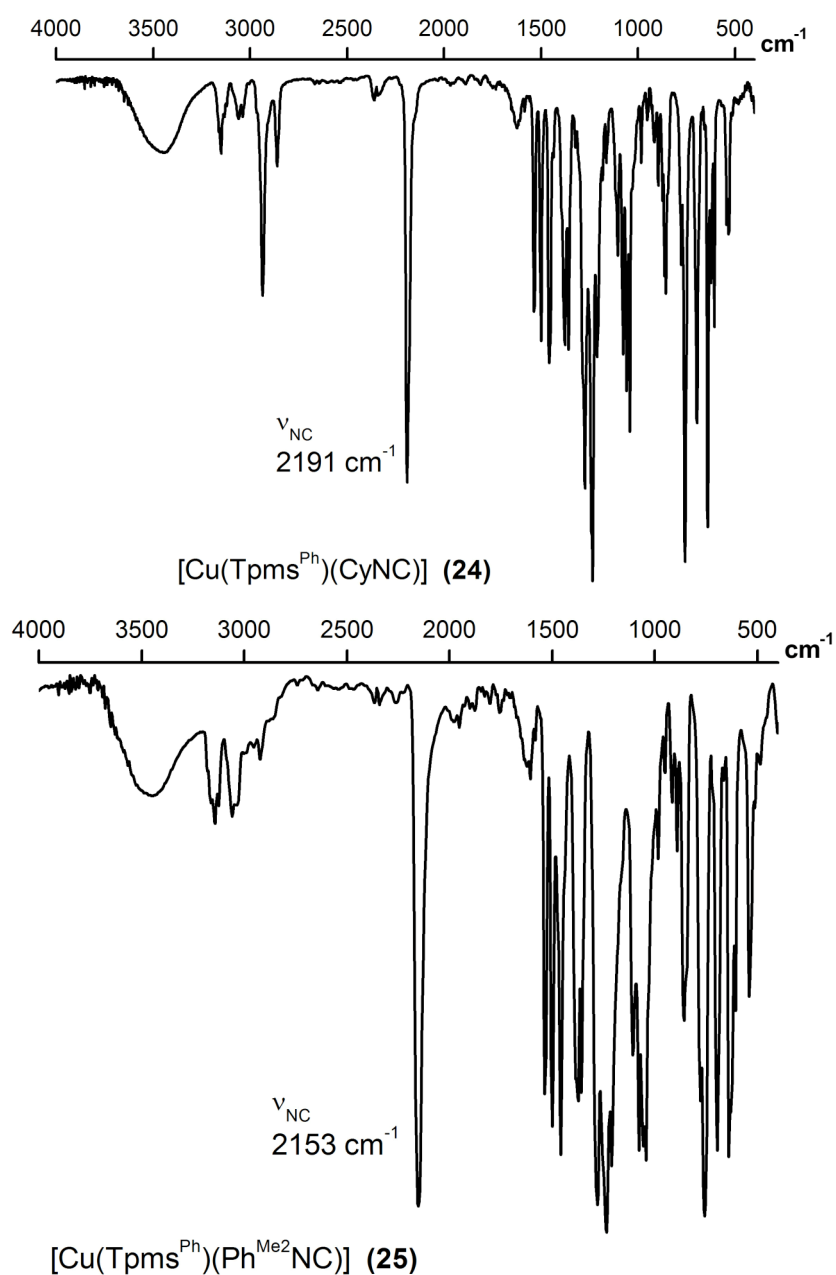
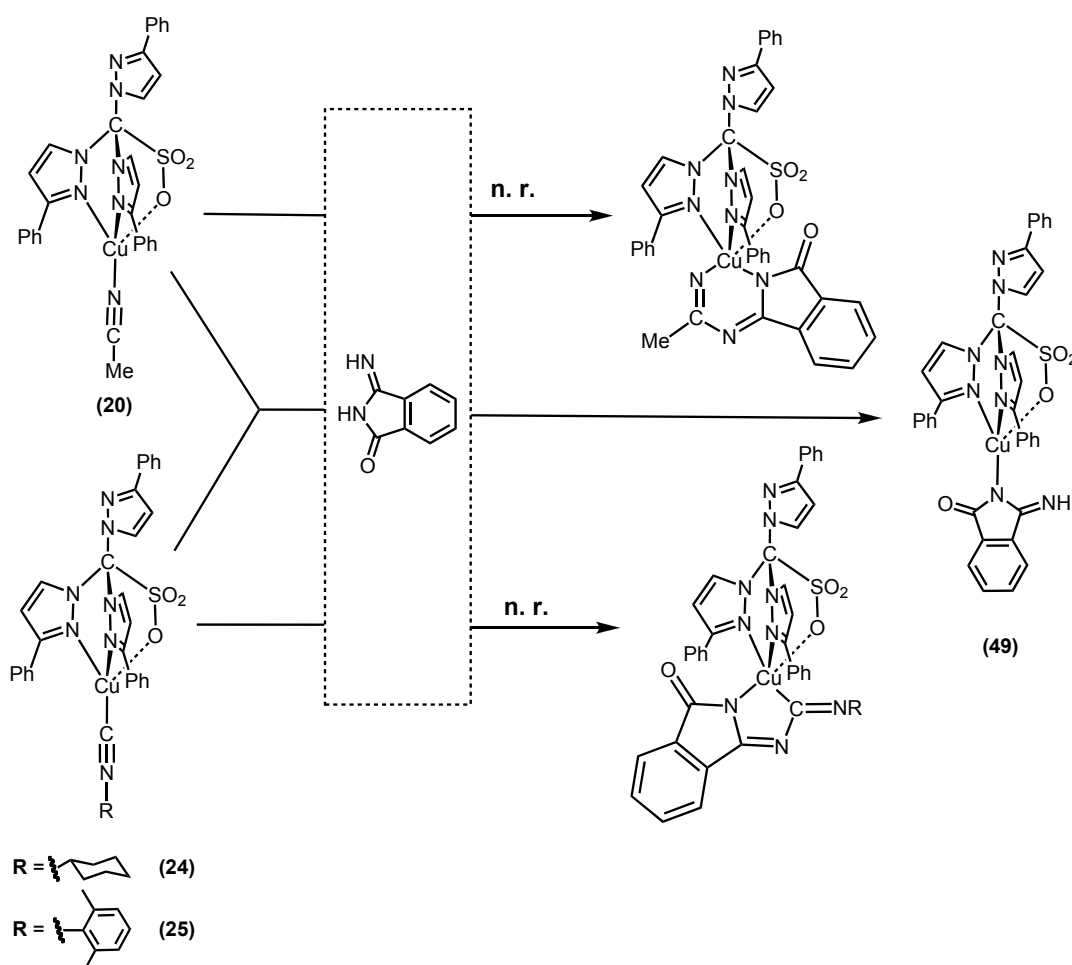


Figure 2.9 IR spectra of isonitrile complexes [Cu(Tpms^{Ph})(CyNC)] (**24**) and [Cu(Tpms^{Ph})(Ph^{Me2}NC)] (**25**).

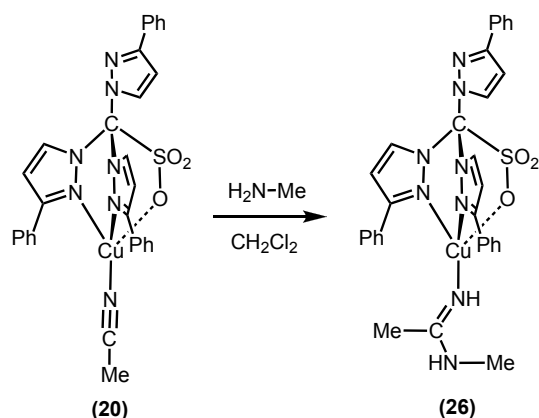
On the other hand, the IR frequency ν_{NC} of (**20**) (*i.e.* 2316 cm^{-1}) appears affected by the metal coordination, acting mainly as a σ -donor ligand and a very weak π -acceptor. However, the activation of the carbon position was shown, in this study, to be insufficient by preliminary attempted reactions of (**20**), (**24**) and (**25**) with specific nucleophiles^{81,82} (*i.e.* 3-iminoisindolin-1-ones derivatives); that result in a

ligand displacement leading to the formation of compound [Cu(Tpms^{Ph})(L)] (**49**) (L = 3-iminoisoindol-1-one) (Scheme 2.4).



Scheme 2.4 Schematic representation of the study of the nitrile and isonitrile Cu^I-activation.

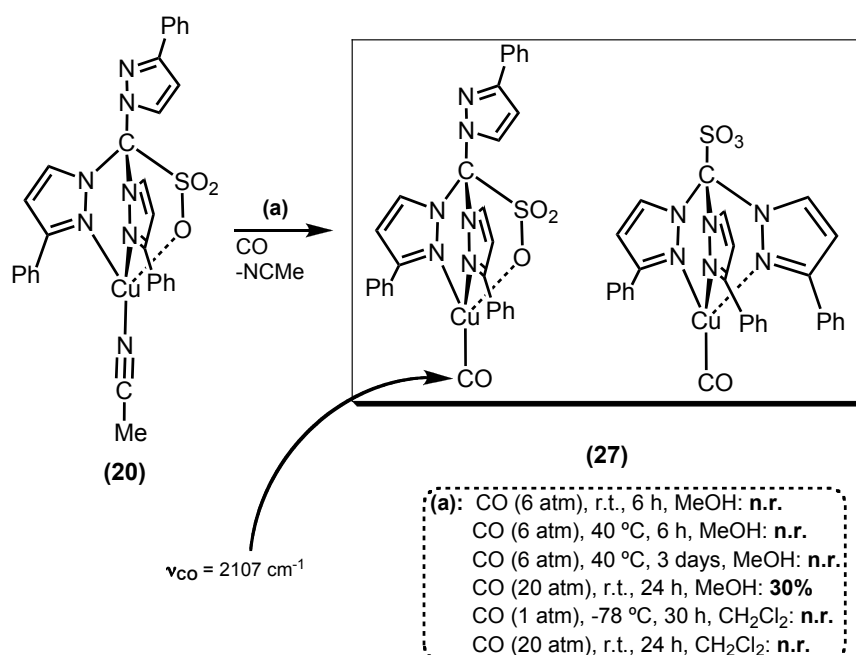
It is noteworthy to report that the 3-iminoisoindolinone is a bulky moderate nucleophile and the ligand displacement observed in these reactions could be due not exclusively to an insufficient activation of the CN bond. In fact, reaction of (**20**) with the more nucleophilic methylamine leads to the formation of the activation product (**26**) (Scheme 2.5). The latter has not successfully crystallized, but the ¹H-NMR spectrum shows the characteristic resonances for the N₂O-coordination mode that appears to be retained in solution from the starting material (**20**). Nevertheless, this preliminary result could be developed further toward the activation of the isonitrile derivatives (**24**) and (**25**).



Scheme 2.5 Synthesis of compound (26).

2.6.2 Synthesis of [Cu(Tpms^{Ph})(CO)] (27) and its unexpected instability

Carbon monoxide displacement of the ligated acetonitrile molecule in (20) has been investigated. Many examples^{56,83} of sterically hindered Tp and Tpm complexes of Cu^I report the easy preparation of carbon monoxide derivatives from the acetonitrile adducts. Many attempts have been carried out in this thesis (Scheme 2.6), showing an unexpected instability of the carbonyl analogue (27).

Scheme 2.6 Synthesis of [Cu(Tpms^{Ph})(CO)] (27).

Exclusively by using a high pressure of CO (20 atm) in a closed vessel, it was possible to isolate the expected carbonyl complex. Compound [Cu(Tpms^{Ph})(CO)] (**27**) shows a typical ν_{CO} at 2107 cm⁻¹ that is consistent with the analogous (Tpm)Cu-carbonyl complex (*i.e.* 2104 cm⁻¹ for [Cu(Tpm^{Ph})(CO)][PF₆])⁵⁶. However, it is important to remark that using the same reaction conditions described for the synthesis of similar compounds, the formation of (**27**) was not detected: a surprising instability leads to decomposition. There are no examples of carbonyl Cu-complexes bearing the sulfonate derivatives of Tpm: in fact, while the analogue [Cu(Tpm^{Ph})(CO)][PF₆] is readily prepared⁵⁶, the sulfonate [Cu(Tpms^{Ph})(CO)] (**27**) shows a high instability and an increased difficulty to be isolated. A possible role of the sulfonate moiety on the unpredictable instability of the carbonyl derivative should be further investigated.

2.7 Appendix 2.B: dioxygen coordination at the ‘Cu^I-Tpms^{Ph}’ system

In the introduction of this chapter it was recalled the known applications of copper(I) and (II) complexes in bioinorganic chemistry and biomimetic studies. In particular, many examples^{7,37,84-86} of poly(pyrazolyl) ligands indicate how this molecular scaffold is appropriate to mimic the environment of the metal center in the enzymatic active site.

Different reactions of **(16)** with [Cu(MeCN)₄][PF₆] have been attempted and in particular the formation of the intermediate [Cu(Tpms^{Ph})(MeCN)] **(20)** has evidenced that this half-capped complex is a highly reactive compound that in the presence of small coordinating molecules (*i.e.* phosphines, amines, nitriles, isonitriles,...) leads to the corresponding κ³-Tpms^{Ph}-Cu complexes.

The isolation (as deep dark blue/green crystals) and the identification of the dimer dicopper complex [Cu(μ-O)(Tpms^{Ph})₂] **(28)** from a methanolic solution of **(20)** left in air in the presence of a base suggests that this Cu-scorpionate system is able to activate the oxygen molecule (Figure 2.10) as similarly reported for different Tp⁸⁷⁻⁹⁰ and Tpm⁹¹ derivatives.

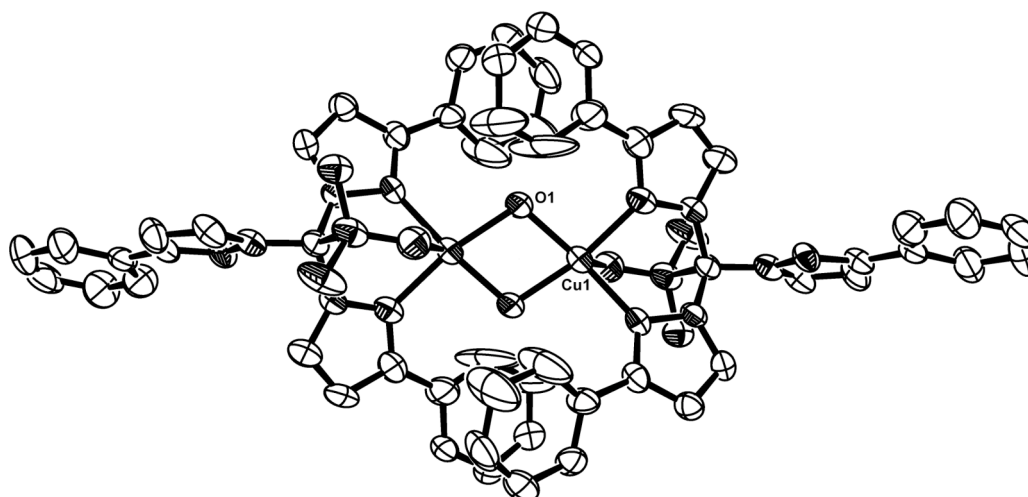


Figure 2.10 ORTEP plot of [Cu(μ-O)(Tpms^{Ph})₂] **(28)**, with ellipsoids shown at 50% probability. (hydrogen atoms are omitted for clarity, but no hydrogen atom was found for O(1))

In our case, the X-ray diffraction analysis of compound (**28**), performed by Dr. M. Fátima C. Guedes da Silva, reveals the absence of the hydrogen atom for the bridging oxygen O(1), even if the ellipsoid of the latter shows an unusual extension (Figure 2.11). The bond distances (Table 2.5) are consistent with the bis(μ -oxo)dicopper(III) system⁸⁴ that for compound [Cu(μ -O)(Tpms^{Ph})]₂ (**28**) results in a neutral dicopper(III) complex.

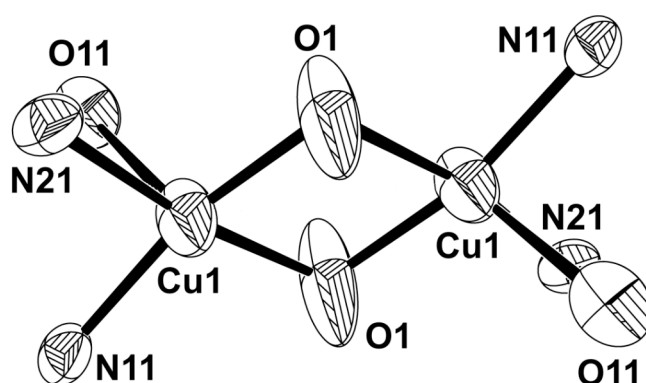


Figure 2.11 ORTEP plot of metal ion coordination spheres in the cation of (**28**). Ellipsoids are given with 50% of probability.

Table 2.5 Comparative selected bond distances [\AA]

	$[\mu\text{-OH-Cu}^{\text{II}}]_2$ ^(a)	$[\mu\text{-O-Cu}^{\text{III}}]_2$ ^(b)	$[\mu\text{-}\eta^2\text{-O-Cu}^{\text{II}}]_2$ ^(c)	(28)
Cu(1)-O(1)	1.942-1.949	1.82 (avg.)	1.92 (avg.)	1.857(7)
Cu(1)-O(1)				1.886(7)
Cu(1)-Cu(1)	3.0554(12)	2.80 (avg)	3.51 (avg.)	2.961(2)
O(1)-O(1)	-	2.32 (avg.)	1.42 (avg.)	2.291(2)

^(a) bis(μ -hydroxo)dicopper(II)⁹²; ^(b) bis(μ -oxo)dicopper(III)⁸⁴; ^(c) bis(μ -peroxo)dicopper(II).⁸⁴

At the same time the methanolic mixture of [Cu(MeCN)₄][PF₆] and Li(Tpms^{Ph}) (**16**) left in air, led to formation of the crystalline copper-bridged trimer $[(\mu\text{-Cu}^{\text{II}})\{\text{Cu}^{\text{I}}(\text{Tpms}^{\text{Ph}})(\mu\text{-OH}_2)(\mu\text{-OMe})\}_2]$ (**29**) (Figure 2.12).

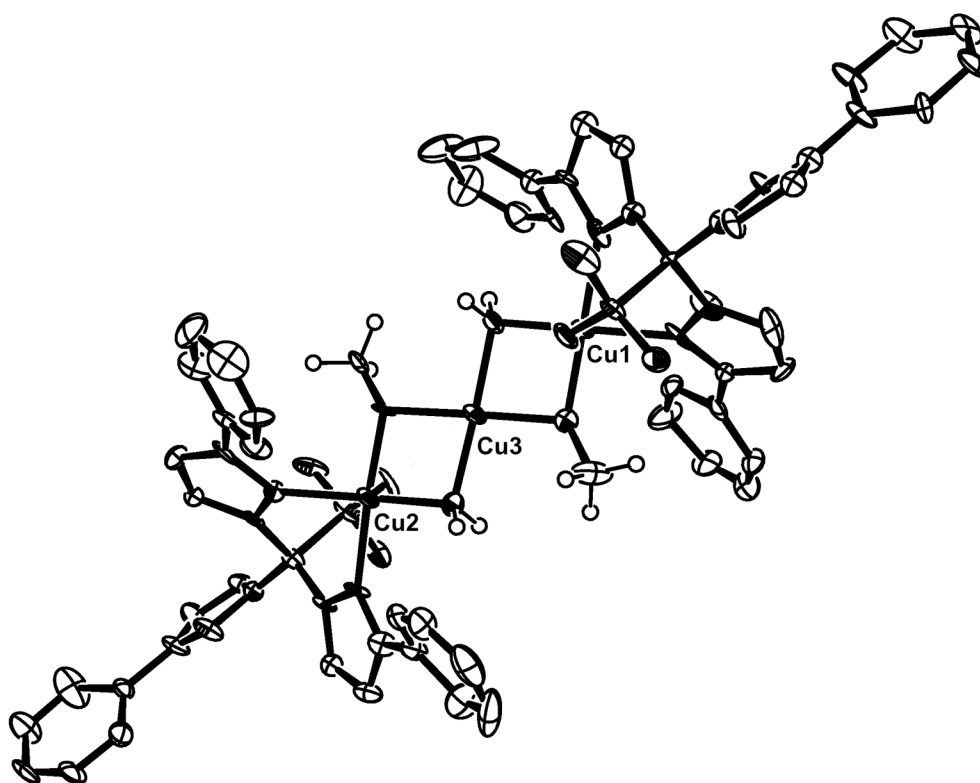


Figure 2.12 ORTEP plot of $[(\mu\text{-Cu}^{\text{II}})\{\text{Cu}^{\text{I}}(\text{Tpms}^{\text{Ph}})(\mu\text{-OH}_2)(\mu\text{-OMe})\}_2]$ (**29**), with ellipsoids shown at 50% probability (hydrogen atoms are omitted for clarity, except at the bridging ligands).

Compound (**29**) apparently exhibits a mixed valence tri-copper system: with the Cu^I-Cu^{II}-Cu^I backbone and the bridging water and methoxide stabilizing this system. Further study for the full characterisation should be accomplished, together with a tentative to investigate the electronic structure of compounds (**28**) and (**29**) that should display peculiar and interesting features in the corresponding EPR and UV/vis spectra.

Recently, another result have confirmed the behavior of this “Cu(Tpms^{Ph})” system: a methanolic solution of (**26**) (Scheme 2.5) in air formed compound $[(\mu\text{-Cu})\{\text{Cu}(\mu\text{-O})(\text{Tpms}^{\text{Ph}})\}_2]$ (**50**) (Figure 2.13) that appears to exhibit analogous characteristics to (**28**) incorporating the bridging oxygen O(1) and O(2). Additional study should be carried out for this new derivative to verify its features.

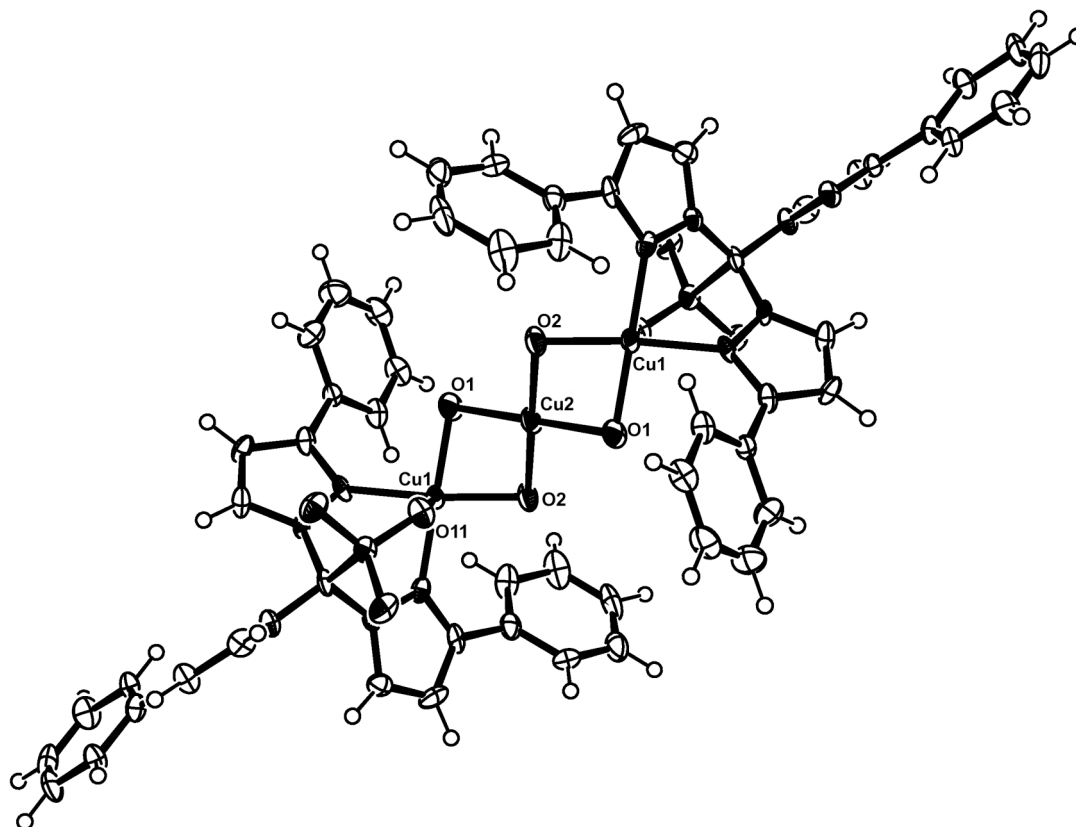


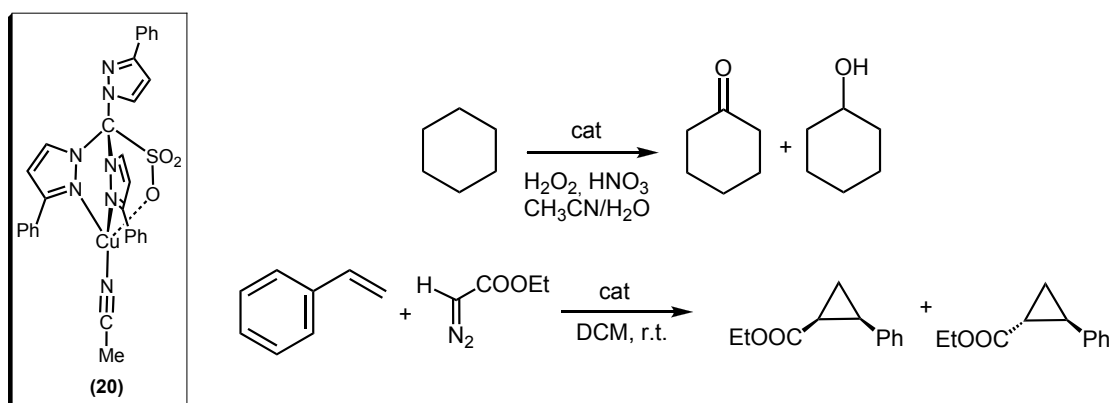
Figure 2.13 ORTEP plot of $[(\mu\text{-Cu})\{\text{Cu}(\mu\text{-O})(\text{Tpms}^{\text{Ph}})\}_2]$ (**50**), with ellipsoids shown at 50% probability. (no hydrogen atom was found for O(1) and O(2))

Nonetheless, these preliminary examples emphasize the function of this bulky scorpionate (**16**) that acts as a steric shield modulating the coordination chemistry of the Cu center and, at the same time, adapts its coordination mode to favour the access of a small molecule, such as dioxygen, water or solvent molecules.

2.8 Appendix 2.C: catalytic studies of [Cu(Tpms^{Ph})(MeCN)] (20)

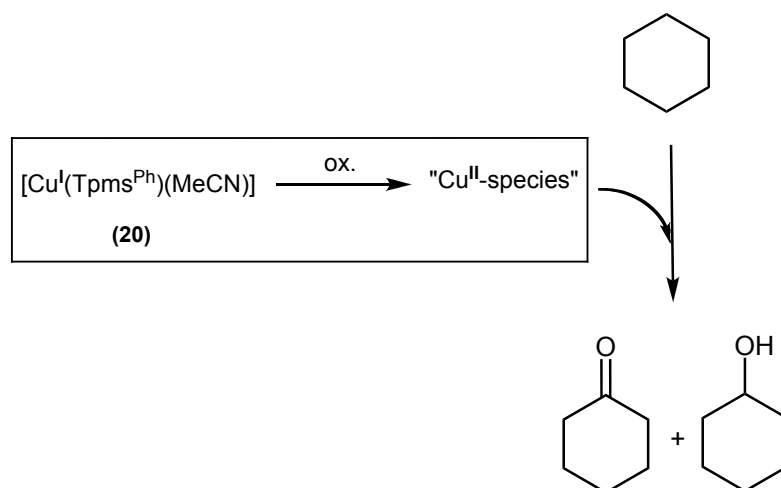
The acetonitrile scorpionate complex **(20)** represents itself an excellent scaffold for potential applications in catalysis. In fact, its resistant and flexible tripodal capping (*i.e.* Tpms^{Ph}) and the presence of the labile acetonitrile ligand are two peculiar features of a promising candidate for a possible catalytic use.

Hence, compound **(20)** has been tested, in this thesis, as a catalyst in different organic reactions (Scheme 2.7).



Scheme 2.7 Schematic representation of the attempted catalytic study of compound **(20)**.

In the pursuit of our experience^{12,93} in metal-catalyzed alkane oxidations, the Cu^I-complex **(20)** has been tested for the cyclohexane oxidation to form the corresponding ketone and alcohol derivatives.^{94,95} Since this reaction has been successfully achieved via Cu^{II}-catalysis, the Cu^I-complex **(20)** is expected to be oxidized to a copper(II) active species, in the presence of air or hydrogen peroxide (Scheme 2.8).



Scheme 2.8 Proposed transformation of the Cu(I)-complex (20) into an active Cu(II)-scorpionate intermediate.

In fact, the new scorpionate Tpms^{Ph} (**16**) is able to stabilize both the oxidation states of copper (*i.e.* +1 and +2): several preliminary studies,⁹⁶ performed in our group, of coordination chemistry of (**16**) toward the Cu^{II} chloride center indicate that the scorpionate is capable to face-cap the metal center in a N₂O-mode in [Cu^{II}(Tpms^{Ph})(Cl)(H₂O)].

Disappointingly, the results of these initial tests indicate that compound (**20**) does not display an appreciable catalytic effect and the yield (< 1 %) and TON (0.9-1.5) data are negligible in comparison with more simple and cheap Cu-catalysts (see Experimental Chapter).^{12,93}

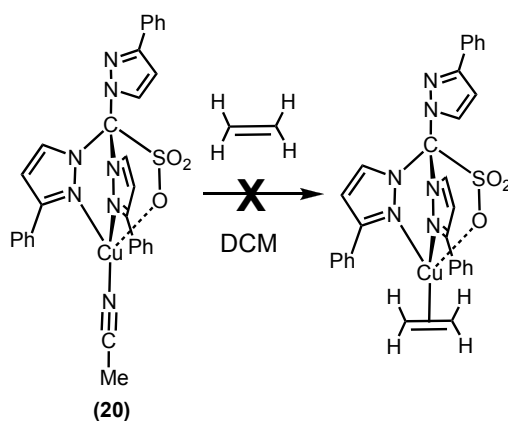
Moreover, a number of reactions to study the potential activity in cyclopropanation of alkenes has been studied in this thesis (Scheme 2.7). It was reported,⁹⁷ indeed, that sterically hindered tris(pyrazolyl)borate Cu^I-complexes are efficient catalysts for the activation of a diazocompound and analogous derivatives for cyclisation reactions (*i.e.* aziridination and cyclopropanation). The past experience⁹⁸ on this field prompted to investigate the possible activity of "scorpionate-Cu^I" systems toward this type of reactions.

The no-promising catalytic results^(*) suggest that compound (**20**) has low activity and selectivity toward the cyclopropanation. The formation, in high yield, of

* For 500/10/1 molar ratios of styrene/EDA/cat (EDA = ethyl diazoacetate), only a small amount of cyclopropane (ca 6% by ¹H-NMR) was obtained, the main by-product being diethylfumarate/maleate (see Experimental Chapter).

diethyl fumarate and maleate, as by-products, from carbene dimerization, is indicative of its poor activity.

Additionally, since it has been reported⁹⁷ that the ethylene adduct of the copper(II)-scorpionate [Cu(Tp^{Me2})(C₂H₄)] (Tp = tris(3,5-dimethylpyrazolyl)borate) is an active species for this type of catalysis, different attempts to prepare the ethylene derivative of **(20)** have been carried out but unfortunately were unsuccessful (Scheme 2.9).



Scheme 2.9 Attempted preparation of ethylene derivative of (20).

References

- [1] Solomon, E. I.; Sundaram, U. M.; Machonkin, T. E., *Chem. Rev.* **1996**, *96*, 2563.
- [2] Klinman, J. P., *Chem. Rev.* **1996**, *96*, 2541.
- [3] Koval, I. A.; Gamez, P.; Belle, C.; Selmeczi, K.; Reedijk, J., *Chem. Soc. Rev.* **2006**, *35*, 814.
- [4] Maheswari, P. U.; Roy, S.; den Dulk, H.; Barends, S.; van Wezel, G.; Kozlevcar, B.; Gamez, P.; Reedijk, J., *J. Am. Chem. Soc.* **2006**, *128*, 710.
- [5] Elsevier, C. J.; Reedijk, J.; Walton, P. H.; Ward, M. D., *Eur. J. Inorg. Chem.* **2003**, *9*, 1669.
- [6] Elsevier, C. J.; Reedijk, J.; Walton, P. H.; Ward, M. D., *Dalton Trans.* **2003**, 1869.
- [7] Kim, E.; Chufan, E. E.; Kamaraj, K.; Karlin, K. D., *Chem. Rev.* **2004**, *104*, 1077.
- [8] Chen, P.; Gorelsky, S. I.; Ghosh, S.; Solomon, E. I., *Angew. Chem., Int. Ed.* **2004**, *43*, 4132.
- [9] Koval, I. A.; Belle, C.; Selmeczi, K.; Philouze, C.; Saint-Aman, E.; Schuitema, A. M.; Gamez, P.; Pierre, J. L.; Reedijk, J., *J. Biol. Inorg. Chem.* **2005**, *10*, 739.
- [10] Koval, I. A.; Pursche, D.; Stassen, A. F.; Gamez, P.; Krebs, B.; Reedijk, J., *Eur. J. Inorg. Chem.* **2003**, 1669.
- [11] Uber, J. S.; Vogels, Y.; Van Den Helder, D.; Multikainen, I.; Turpeinen, U.; Fu, W. T.; Roubeau, O.; Gamez, P.; Reedijk, J., *Eur. J. Inorg. Chem.* **2007**, *26*, 4197.
- [12] Kirillov, A. M.; Kopylovich, M. N.; Kirillova, M. V.; Haukka, M.; da Silva, M.; Pombeiro, A. J. L., *Angew. Chem., Int. Ed.* **2005**, *44*, 4345.
- [13] Di Nicola, C.; Karabach, Y. Y.; Kirillov, A. M.; Monari, M.; Pandolfo, L.; Pettinari, C.; Pombeiro, A. J. L., *Inorg. Chem.* **2007**, *46*, 221.
- [14] Alegria, E. C. B.; Martins, L.; Haukka, M.; Pombeiro, A. J. L., *Dalton Trans.* **2006**, 4954.
- [15] Silva, T. E. S.; Alegria, E.; Martins, L.; Pombeiro, A. J. L., *Adv. Synth. Catal.* **2008**, *350*, 706.

- [16] Alegria, E. C. B.; Martins, L.; da Silva, M.; Pombeiro, A. J. L., *J. Organomet. Chem.* **2005**, *690*, 1947.
- [17] Trofimenko, S.; Calabrese, J. C.; Domaille, P. J.; Thompson, J. S., *Inorg. Chem.* **1989**, *28*, 1091.
- [18] Calabrese, J. C.; Domaille, P. J.; Thompson, J. S.; Trofimenko, S., *Inorg. Chem.* **1990**, *29*, 4429.
- [19] Edwards, P. G.; Harrison, A.; Newman, P. D.; Zhang, W. J., *Inorg. Chim. Acta* **2006**, *359*, 3549.
- [20] Amoroso, A. J.; Jeffery, J. C.; Jones, P. L.; McCleverty, J. A.; Rees, L.; Rheingold, A. L.; Sun, Y. M.; Takats, J.; Trofimenko, S.; Ward, M. D.; Yap, G. P. A., *J. Chem. Soc., Chem.* **1995**, 1881.
- [21] Kealey, S.; Long, N. J.; Miller, P. W.; White, A. J. P.; Gee, A. D., *Dalton Trans.* **2008**, 2677.
- [22] Katajima, N.; Tolman, W. B., *Prog. Inorg. Chem.* **1995**, *43*, 419.
- [23] Trofimenko, S., *Chem. Rev.* **1993**, *93*, 943.
- [24] Looney, A.; Han, R.; McNeill, K.; Parkin, G., *J. Am. Chem. Soc.* **1993**, *115*, 4690.
- [25] Katajima, N., *Advanced Inorganic Chemistry* **1992**, *39*, 1.
- [26] McCleverty, J. A.; Meyer, T. J., *Comprehensive Coordination Chemistry II: From Biology to Nanotechnology, vol. 1*. Elsevier Amsterdam: 2003.
- [27] Klaui, W.; Berghahn, M.; Rheinwald, G.; Lang, H. R., *Angew. Chem., Int. Ed.* **2000**, *39*, 2464.
- [28] Papish, E. T.; Taylor, M. T.; Jernigan, F. E.; Rodig, M. J.; Shawhan, R. R.; Yap, G. P. A.; Jove, F. A., *Inorg. Chem.* **2006**, *45*, 2242.
- [29] Klaui, W.; Schramm, D.; Peters, W.; Rheinwald, G.; Lang, H., *Eur. J. Inorg. Chem.* **2001**, 1415.
- [30] Klaui, W.; Berghahn, M.; Frank, W.; Reiss, G. J.; Schonherr, T.; Rheinwald, G.; Lang, H., *Eur. J. Inorg. Chem.* **2003**, 2059.
- [31] Chenskaya, T. B.; Berghahn, M.; Kunz, P. C.; Frank, W.; Klaui, W., *J. Mol. Struct.* **2007**, *829*, 135.
- [32] Parkin, G., *Chem. Commun.* **2000**, 1971.
- [33] Trofimenko, S., *Scorpionates: The Coordination Chemistry of Polypyrazolylborates Ligands*. Imperial College Press: London, 1999.
- [34] Trofimenko, S., *J. Am. Chem. Soc.* **1966**, *88*, 1842.

- [35] Byers, P. K.; Canty, A. J.; Skelton, B. W.; White, A. H., *Organometallics* **1990**, *9*, 826.
- [36] Beck, A.; Weibert, B.; Burzlaff, N., *Eur. J. Inorg. Chem.* **2001**, 521.
- [37] Hu, Z. B.; Williams, R. D.; Tran, D.; Spiro, T. G.; Gorun, S. M., *J. Am. Chem. Soc.* **2000**, *122*, 3556.
- [38] Schneider, J. L.; Carrier, S. M.; Ruggiero, C. E.; Young, V. G.; Tolman, W. B., *J. Am. Chem. Soc.* **1998**, *120*, 11408.
- [39] Vahrenkamp, H., *Acc. Chem. Res.* **1999**, *32*, 589.
- [40] Pruchnik, F. P.; Smolenski, P., *Appl. Organomet. Chem.* **1999**, *13*, 829.
- [41] Phillips, A. D.; Gonsalvi, L.; Romerosa, A.; Vizza, F.; Peruzzini, M., *Coord. Chem. Rev.* **2004**, *248*, 955.
- [42] Romerosa, A.; Bergamini, P.; Bertolasi, V.; Canella, A.; Cattabriga, M.; Gavioli, R.; Manas, S.; Mantovani, N.; Pellacani, L., *Inorg. Chem.* **2004**, *43*, 905.
- [43] Romerosa, A.; Saoud, M.; Campos-Malpartida, T.; Lidrissi, C.; Serrano-Ruiz, M.; Peruzzini, M.; Garrido, J. A.; Garcia-Maroto, F., *Eur. J. Inorg. Chem.* **2007**, 2803.
- [44] Bergamini, P.; Bertolasi, V.; Marvelli, L.; Canella, A.; Gavioli, R.; Mantovani, N.; Manas, S.; Romerosa, A., *Inorg. Chem.* **2007**, *46*, 4267.
- [45] Romerosa, A.; Campos-Malpartida, T.; Lidrissi, C.; Saoud, M.; Serrano-Ruiz, M.; Peruzzini, M.; Garrido-Cardenas, J. A.; Garcia-Maroto, F., *Inorg. Chem.* **2006**, *45*, 1289.
- [46] Scolaro, C.; Bergamo, A.; Brescacin, L.; Delfino, R.; Cocchietto, M.; Laurency, G.; Geldbach, T. J.; Sava, G.; Dyson, P. J., *J. Med. Chem.* **2005**, *48*, 4161.
- [47] Scolaro, C.; Geldbach, T. J.; Rochat, S.; Dorcier, A.; Gossens, C.; Bergamo, A.; Cocchietto, M.; Tavernelli, I.; Sava, G.; Rothlisberger, U.; Dyson, P. J., *Organometallics* **2006**, *25*, 756.
- [48] Horvath, I. T.; Joó, F., *Aqueous Phase Organometallic Catalysis*. Wiley-VCH: Weinheim, 1998.
- [49] Pruchnik, F. P.; Smolenski, P.; Wajda-Hermanowicz, K., *J. Organomet. Chem.* **1998**, *570*, 63.
- [50] Smolenski, P.; Pruchnik, F. P.; Ciunik, Z.; Lis, T., *Inorg. Chem.* **2003**, *42*, 3318.
- [51] Solomon, E. I.; Chen, P.; Metz, M.; Lee, S. K.; Palmer, A. E., *Angew. Chem., Int. Ed.* **2001**, *40*, 4570.

- [52] Magnus, K. A.; Hazes, B.; Ton-That, H.; Bonaventura, C.; Bonaventura, J.; Hol, W. G. J., *Proteins: Structure, Function and Genetics* **1994**, *19*, 302.
- [53] Reger, D. L.; Grattan, T. C.; Brown, K. J.; Little, C. A.; Lamba, J. J. S.; Rheingold, A. L.; Sommer, R. D., *J. Organomet. Chem.* **2000**, *607*, 120.
- [54] Reger, D. L.; Collins, J. E.; Jameson, D. L.; Castellano, R. K.; Canty, A. J.; Jin, H., *Inorg. Synth.* **1998**, *32*, 63.
- [55] Conry, R. R.; Ji, G. Z.; Tipton, A. A., *Inorg. Chem.* **1999**, *38*, 906.
- [56] Reger, D. L.; Collins, J. E., *Organometallics* **1996**, *15*, 2029.
- [57] Kirillov, A. M.; Smolenski, P.; da Silva, M.; Pombeiro, A. J. L., *Eur. J. Inorg. Chem.* **2007**, 2686.
- [58] Bowmaker, G. A.; Hart, R. D.; deSilva, E. N.; Skelton, B. W.; White, A. H., *Aust. J. Chem.* **1997**, *50*, 553.
- [59] Tisato, F.; Refosco, F.; Bandoli, G.; Pilloni, G.; Corain, B., *Inorg. Chem.* **2001**, *40*, 1394.
- [60] Santini, C.; Pellei, M.; Lobbia, G. G.; Cingolani, A.; Spagna, R.; Camalli, M., *Inorg. Chem. Commun.* **2002**, *5*, 430.
- [61] Frohnepfel, D. S.; White, P. S.; Templeton, J. L.; Ruegger, H.; Pregosin, P. S., *Organometallics* **1997**, *16*, 3737.
- [62] Reger, D. L.; Gardinier, J. R.; Elgin, J. D.; Smith, M. D., *Inorg. Chem.* **2006**, *45*, 8862.
- [63] Muller-Dethlefs, K.; Hobza, P., *Chem. Rev.* **2000**, *100*, 143.
- [64] Hobza, P.; Havlas, Z., *Chem. Rev.* **2000**, *100*, 4253.
- [65] Janiak, C., *J. Chem. Soc., Dalton* **2000**, 3885.
- [66] Nishio, M., *Cryst. Eng. Comm.* **2004**, *6*, 130.
- [67] Meij, A. M. M.; Otto, S.; Roodt, A., *Inorg. Chim. Acta* **2005**, *358*, 1005.
- [68] Mebi, C. A.; Frost, B. J., *Organometallics* **2005**, *24*, 2339.
- [69] Smolenski, P.; Pombeiro, A. J. L., *Dalton Trans.* **2008**, 87.
- [70] Rasika Dias, H. V.; Jin, W., *J. Am. Chem. Soc.* **1995**, *117*, 11381.
- [71] Gushchin, P. V.; Luzyanin, K. V.; Kopylovich, M. N.; Haukka, M.; Pombeiro, A. J. L.; Kukushkin, V. Y., *Inorg. Chem.* **2008**, *47*, 3088.
- [72] Luzyanin, K. V.; Kukushkin, V. Y.; Ryabov, A. D.; Haukka, M.; Pombeiro, A. J. L., *Inorg. Chem.* **2005**, *44*, 2944.

- [73] Kopylovich, M. N.; Kukushkin, V. Y.; Haukka, M.; Luzyanin, K. V.; Pombeiro, A. J. L., *J. Am. Chem. Soc.* **2004**, *126*, 15040.
- [74] Wagner, G.; Pombeiro, A. J. L.; Kukushkin, V. Y., *J. Am. Chem. Soc.* **2000**, *122*, 3106.
- [75] Pombeiro, A. J. L., *New J. Chem.* **1994**, *18*, 163.
- [76] Kukushkin, V. Y.; Pombeiro, A. J. L., *Chem. Rev.* **2002**, *102*, 1771.
- [77] Guedes da Silva, M. F. C.; Lemos, M. A. N. D. A.; Frausto da Silva, J. J. R.; Pombeiro, A. J. L.; Pellinghelli, M. A.; Tiripicchio, A., *J. Chem. Soc., Dalton* **2000**, 373.
- [78] Pombeiro, A. J. L., *Inorganic Chemistry Communications* **2001**, *4*, 585.
- [79] Pombeiro, A. J. L.; Guedes da Silva, M. F. C.; Michelin, R. A., *Coord. Chem. Rev.* **2001**, *218*, 43.
- [80] Michelin, R.; Pombeiro, A. J. L.; Guedes da Silva, M. F. C., *Coord. Chem. Rev.* **2001**, *218*, 75.
- [81] Kopylovich, M. N.; Luzyanin, K. V.; Haukka, M.; Pombeiro, A. J. L.; Kukushkin, V. Y., *Dalton Trans.* **2008**, 5220.
- [82] Luzyanin, K. V.; Pombeiro, A. J. L.; Haukka, M.; Kukushkin, V. Y., *Organometallics* **2008**, *27*, 5379.
- [83] Fujisawa, K.; Ono, T.; Ishikawa, Y.; Amir, N.; Miyashita, Y.; Okamoto, K.; Lehnert, N., *Inorg. Chem.* **2006**, *45*, 1698.
- [84] Mirica, L. M.; Ottenwaelder, X.; Stack, T. D. P., *Chem. Rev.* **2004**, *104*, 1013.
- [85] Hatcher, L. Q.; Karlin, K. D., *J. Biol. Inorg. Chem.* **2004**, *9*, 669.
- [86] Lewis, E. A.; Tolman, W. B., *Chem. Rev.* **2004**, *104*, 1047.
- [87] Baldwin, M. J.; Root, D. E.; Pate, J. E.; Fujisawa, K.; Kitajima, N.; Solomon, E. I., *J. Am. Chem. Soc.* **1992**, *114*, 10421.
- [88] Kitajima, N.; Fujisawa, K.; Fujimoto, C.; Moro-Oka, Y.; Hashimoto, S.; Kitagawa, T.; Toriumi, K.; Tatsumi, K.; Nakamura, A., *J. Am. Chem. Soc.* **1992**, *114*, 1277.
- [89] Kitajima, N.; Koda, T.; Hashimoto, S.; Kitagawa, T.; Moro-Oka, Y., *J. Am. Chem. Soc.* **1991**, *113*, 5664.
- [90] Kitajima, N.; Koda, T.; Hashimoto, S.; Kitagawa, T.; Moro-Oka, Y., *J. Chem. Soc., Chem.* **1988**, 151.
- [91] Cvetkovic, M.; Batten, S. R.; Moubaraki, B.; Murray, K. S.; Spiccia, L., *Inorg. Chim. Acta* **2001**, *324*, 131.

- [92] Kaim, W.; Titze, C.; Schurr, T.; Sieger, M.; Lawson, M.; Jordanov, J.; Rojas, D.; Garcia, A. M.; Manzur, J., *Z. Anorg. Allg. Chem.* **2005**, *631*, 2568.
- [93] Alegria, E. C. B.; Kirillova, M. V.; Martins, L.; Pombeiro, A. J. L., *Applied Catalysis a-General* **2007**, *317*, 43.
- [94] Ohta, T.; Tachiyama, T.; Yoshizawa, K.; Yamabe, T.; Uchida, T.; Kitagawa, T., *Inorg. Chem.* **2000**, *39*, 4358.
- [95] Shul'pin, G. B.; Gradinaru, J.; Kozlov, Y. N., *Organic & Biomolecular Chemistry* **2003**, *1*, 3611.
- [96] Rocha, B. G. M.; Wanke, R.; Guedes da Silva, M. F. C.; Pombeiro, A. J. L., Synthesis and coordination chemistry of sterically hindered scorpionates ligand Li[TpmsPh] toward NiII, ZnII and CuII metal centres. In 2PYCheM, P. Y. C. M., Ed. Aveiro, PT, 2010.
- [97] Perez, P. J.; Brookhart, M.; Templeton, J. L., *Organometallics* **1993**, *12*, 261.
- [98] Penoni, A.; Wanke, R.; Tollari, S.; Gallo, E.; Musella, D.; Ragaini, F.; DeMartin, F.; Cenini, S., *Eur. J. Inorg. Chem.* **2003**, 1454.

3 Toward an extra coordinating site: TpmPy and TpmPy^{Ph}

Table of contents

Abstract	118
3.1 Introduction	119
3.2 TpmPy (3) and TpmPy^{Ph} (19)	121
3.3 Coordination chemistry of (3) and (19)	123
3.3.1 Reaction of (3) with Fe ^{II}	123
3.3.2 Reactions of (3) and (19) with Ni ^{II} , Zn ^{II} and V ^{III}	128
3.3.3 Reactions of (3) and (19) with Pd ^{II}	133
3.4 Applications of (3) and (19) to the synthesis of bimetallic complexes	138
3.5 Pyridyl-functionalized scorpionates: overview	141
References	143

Abstract

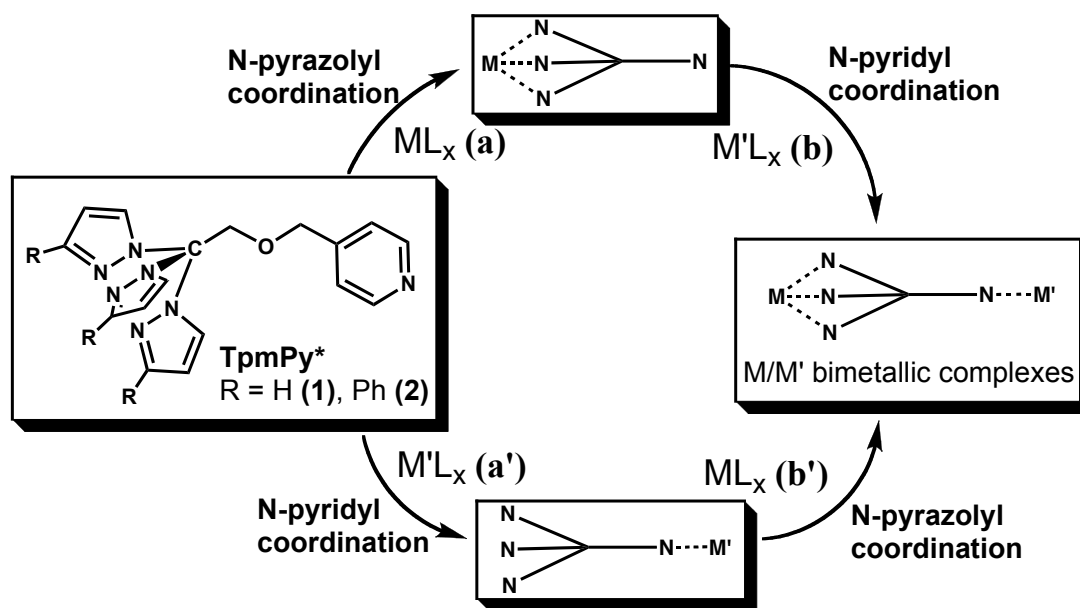
The new potentially N₄-multidentate pyridyl-functionalized scorpionates 4-((tris-2,2,2-(pyrazol-1-yl)ethoxy)methyl)pyridine (TpmPy, **(3)**) and 4-((tris-2,2,2-(3-phenylpyrazol-1-yl)ethoxy)methyl)pyridine (TpmPy^{Ph}, **(19)**) have been synthesized and their coordination behaviors toward Fe^{II}, Ni^{II}, Zn^{II}, Cu^{II}, Pd^{II} and V^{III} centers have been studied. Reaction of **(3)** with Fe(BF₄)₂ yields [Fe(TpmPy)₂](BF₄)₂ (**(30)**), that, in the solid state, shows the sandwich structure with trihapto ligands and coordination via the pyrazolyl arms, and is completely low spin (LS) until 400 K. Reactions of 2 eq of **(3)** or **(19)** with Zn^{II} or Ni^{II} chlorides give the corresponding metal complexes with general formula [MCl₂(TpmPy*)₂] (M = Zn, Ni; Tpm* = TpmPy, TpmPy^{Ph}) (**(31-33)**) where the ligand is able to coordinate through either the pyrazolyl rings (in case of [Ni(TpmPy)₂]Cl₂ (**(32)**)) or the pyridyl-side (for [ZnCl₂(TpmPy)₂] (**(31)**), [ZnCl₂(TpmPy^{Ph})₂] (**(33)**) and [NiCl₂(TpmPy^{Ph})₂] (**(34)**)). The reaction of **(3)** with VCl₃ gives the corresponding [VOCl₂(TpmPy)] (**(35)**) that shows the N₃-pyrazolyl coordination-mode. Moreover, **(3)** and **(19)** react with *cis*-[PdCl₂(CH₃CN)₂] to give the di-substituted complexes [PdCl₂(TpmPy)₂] (**(36)**) and [PdCl₂(TpmPy^{Ph})₂] (**(37)**), respectively, bearing the scorpionate coordinated *via* the pyridyl group. Compounds **(36)** and **(37)** react with Fe(BF₄)₂ to give the heterobimetallic Pd/Fe systems [PdCl₂(μ-TpmPy)₂Fe](BF₄)₂ (**(38)**) and [PdCl₂(μ-TpmPy^{Ph})₂Fe₂(H₂O)₆](BF₄)₄ (**(40)**), respectively. The former **(38)** can be also formed from reaction of **(30)** with *cis*-[PdCl₂(CH₃CN)₂]. On the other hand, reaction of **(30)** with Cu(NO₃)₂ generates [Fe(μ-TpmPy)₂Cu(NO₃)₂](BF₄)₂ (**(39)**), confirming the multidentate ability of the new chelating ligands.

3.1 Introduction

As illustrated on these pages, within the Tpm coordination chemistry there is a continuous growing interest to develop multiple coordination modes of this scorpionate ligand.¹⁻⁹ In fact, in Chapter 1 it has been shown how the functionalization of the central methine carbon atom with groups other than the hydrogen atom is of a crucial interest to extend the coordination properties of the ligand and opening to a variety of applications,^{7,10-14} in particular in supramolecular chemistry and multi-metallic systems. The polidentate character of such a type of ligands has also been investigated.¹⁵⁻¹⁷

The study¹⁸⁻²⁰ of this topic prompted us to design new multidentate tris(pyrazolyl)methane ligands bearing an additional N-donor group pending from the central methine carbon, and to study the role of this extra-unit on their coordination behavior, namely focusing on their potential to form heteronuclear species. Hence, the synthesis of the class of potential tetradentate scorpionates 4-((tris-2,2,2-(pyrazol-1-yl)ethoxy)methyl)pyridine (TpmPy) (**3**) and 4-((tris-2,2,2-(3-phenylpyrazol-1-yl)ethoxy)methyl)pyridine (TpmPy^{Ph}) (**19**) with an additional pyridyl moiety also able to coordinate has been carried out (Chapter 1).

In the current Chapter, it has been investigated the possible coordination pathways of these new ligands to explore their versatility (Scheme 3.1): (i) the coordination chemistry of the tripodal ‘scorpionate’ face of the ligands (step **(a)**); (ii) and the reactivity of the pyridyl moiety of the new ligands toward metal centers known to have a good affinity for pyridine (step **(a')**). The following steps (**(b)** and **(b')**) would consider the further coordination ability of the ligands toward the synthesis of hetero-bimetallic systems.

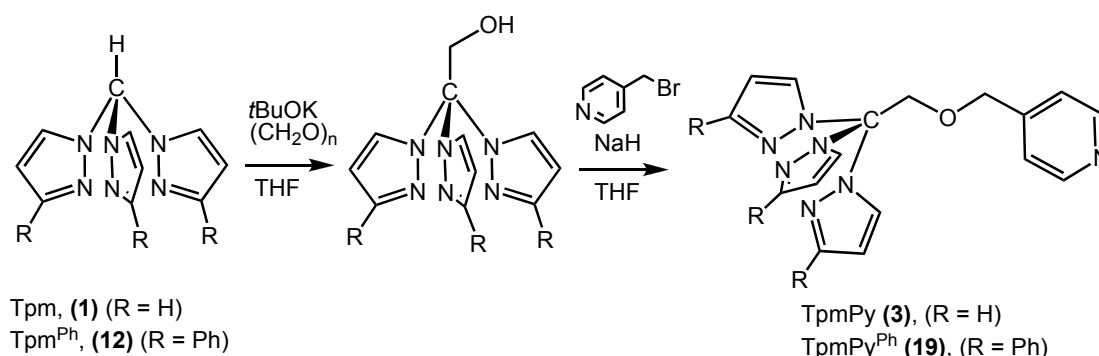


Scheme 3.1 Possible coordination pathways of TpmPy* (TpmPy (3) for R = H; TpmPy^{Ph} (19) for R = Ph).

The next sections, indeed, will report the coordination chemistry of these new ligands toward Fe^{II}, Zn^{II}, Ni^{II}, Pd^{II} and V^{III} centers, and their first application as doubly functionalized ligands to the preparation of hetero-bimetallic complexes, *i.e.* of Fe^{II}/Pd^{II} and Fe^{II}/Cu^{II} centers.

3.2 TpmPy (**3**) and TpmPy^{Ph} (**19**)

As mentioned in Chapter 1, starting from Tpm, it has been possible to prepare 4-(((tris-2,2,2-(pyrazol-1-yl)ethoxy)methyl)pyridine (TpmPy (**3**); Scheme 3.2, R = H) in good yield, following a two-steps synthetic process: the known²¹ tris-2,2,2-(pyrazol-1-yl)ethanol (**2**) reacts, upon deprotonation with sodium hydride, with 4-bromomethyl-pyridine to lead to the desired compound.



Scheme 3.2 Synthesis of the *N*₄-scorpionates TpmPy (**3**) and TpmPy^{Ph} (**19**).

Similarly, the ‘bulky’ analogue bearing phenyl groups as substituents at the 3-position of the pyrazolyl rings (TpmPy^{Ph} (**19**); Scheme 3.2, R = Ph) has been synthesized: starting from the hydrotris(3-phenylpyrazolyl)methane (**12**) the first step proceeded regularly to afford the hydroxy intermediate (**18**) that has been converted to the final compound (**19**). The latter can be easily purified by column chromatography at the final stage.

These products have been characterized by ¹H, ¹³C-NMR and IR spectroscopies, elemental analyses and, in the case of (**3**), also by X-ray diffraction analysis, its molecular structure being depicted in Figure 3.1. Both of them exhibit well resolved ¹H-NMR spectra (CDCl₃) with only one set of resonances for the three equivalent pyrazolyl rings and, in the case of (**19**), one pattern of signals for the phenyl protons. The resonances of the pyridyl ring protons appear as a pair of doublets at δ 8.53 and 7.06 (J_{HH}=6.2 Hz) for (**3**) and at δ 8.47 and 7.10 (J_{HH}=6.0 Hz) for (**19**) (see Experimental Chapter).

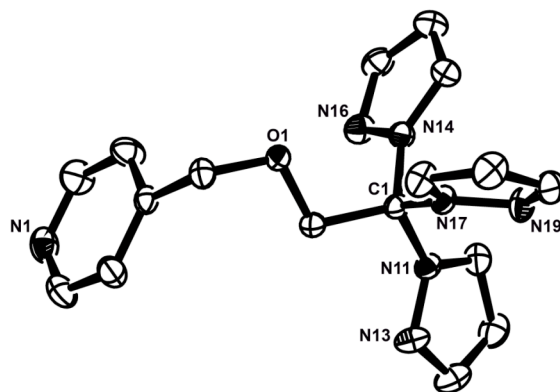


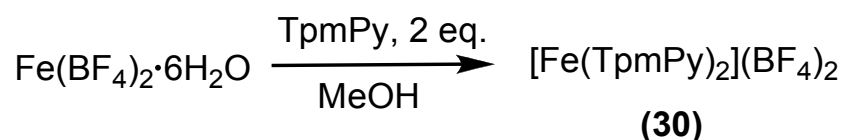
Figure 3.1 ORTEP plot of TpmPy (**3**), ellipsoids are shown at 50% of probability.

Compound (**3**) is well soluble in all common organic solvents (i.e., Et₂O, CH₂Cl₂, CH₃Cl, MeOH, EtOH and acetone) and moderately soluble in water ($S_{25^{\circ}\text{C}} \approx 10 \text{ mg}\cdot\text{mL}^{-1}$) as a free base, while upon protonation of the pyridine nitrogen becomes well water soluble as a salt. Compound (**19**) is not soluble in water, but is soluble in the usual organic solvents. Compounds (**3**) and (**19**) represent a new type of N₄-scorpionate derivatives, bearing not only the common three pyrazolyl rings but also one pyridyl group, thus possibly being able to bind different metal centers, with distinct affinities to the N-pyrazolyl and the N-pyridyl donor sites, allowing also to investigate their competition for such N-ligating functions. TpmPy^{ph} (**19**), being sterically hindered on the pyrazolyl-side, should be an important candidate to the synthesis of half-sandwich complexes with metals that normally would form the full sandwich complex with two tridentate scorpionate ligands.^{22,23}

3.3 Coordination chemistry of (3) and (19)

3.3.1 Reaction of (3) with Fe^{II}

Fe^{II} is a metal ion with one of the highest affinities for scorpionates and tends to form full sandwich complexes with two of such a type of ligands.²⁴⁻³³ Accordingly, reaction of 2 eq of TpmPy (3) with Fe(BF₄)₂·6H₂O in methanol proceeds readily at room temperature to give [Fe(TpmPy)₂](BF₄)₂ (30) bearing two ligated TpmPy (Scheme 3.3).



Scheme 3.3 Synthesis of [Fe(TpmPy)₂](BF₄)₂ (30).

Compound (30) is moderately soluble in CH₂Cl₂, MeOH, DMSO and DMF, and is well soluble in acetonitrile. It forms a pink powder and purple single crystals, as usual for a low spin (LS) Fe^{II} scorpionates at room temperature.²⁴⁻³³ Studies of the spin transition properties of related Fe^{II}-Tpm complexes, such as [Fe(Tpm)₂](BF₄)₂, [Fe(Tpm^{Me2})₃]₂(BF₄)₂ (Tpm^{Me2} = tris(3,5-dimethylpyrazolyl)methane) and their borate analogues [Fe(Tp)₃]₂(BF₄)₂ (Tp = tris(pyrazolyl)borate), [Fe(Tp^{Me2})₃]₂(BF₄)₂, (Tp^{Me2} = tris(3,5-dimethylpyrazolyl)borate), have been reported, indicating that complexes of this type show a temperature dependence spin crossover.²⁸⁻³⁰ Compound (30) is LS in the solid state and in solution at room temperature and keeps this spin state upon heating (to 400 K or 325 K, respectively); its solution ¹H-NMR spectrum (CD₃CN) at room temperature (298 K) appears as a typical one for a diamagnetic complex, and increasing the temperature until 325 K does not lead to any relevant modification, in contrast with what is observed for the tris(pyrazolyl)methane analogue [Fe(Tpm)₂](BF₄)₂ which shows an electronic spin transition from LS (S=0) to HS (S=2), in solution, above 223 K.²⁷ For the latter compound, the LS state in the solid state at room temperature starts to change to the HS state upon heating above

295 K, whereas in solution at room temperature it shows the contemporary presence of LS and HS.

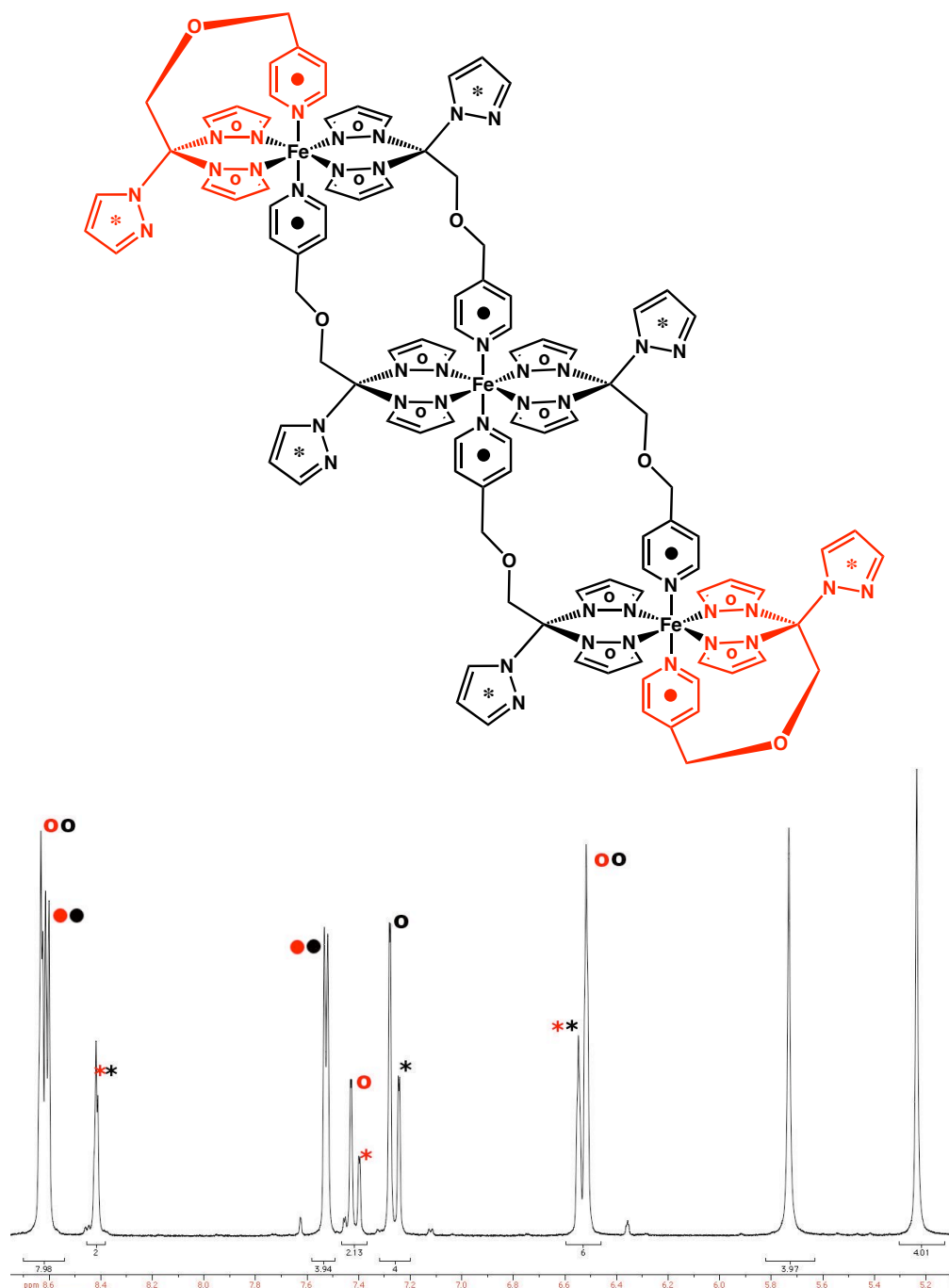


Figure 3.2 Proposed trimeric structure of $[Fe(TpmPy)_2](BF_4)_2$ (30) in acetonitrile solution based on the 1H -NMR (CD₃CN) spectrum assignment at -40°C of $[Fe(TpmPy)_2](BF_4)_2$ (3).

These different behaviors should be accounted for the differences between the ligands (i.e., Tpm and TpmPy). The pyridyl moiety, as possible competing

coordination site, could influence the electronic state of the metal. In fact, variable temperature ¹H-NMR experiments (CD₃CN) of **(30)** allow to distinguish all the resonances. The analysis of the resulting complex pattern of resonances (Figure 3.2), through two-dimensional NMR experiments (*i.e.* ¹H-COSY, ¹H/¹³C-HSQC and HMBC), indicates the unequivalence of the three pyrazolyl rings and suggests the competition of the pyridyl ring, in solution, for the iron center. However, this unexpected behavior in solution was not fully confirmed. The consistency of NMR observations (*i.e.* different batches, dilutions, temperatures) supports the possibility of the formation of a trimeric structure of **(30)** in solution: the lowshifted resonances assigned to pyridyl moieties (red and black dots, Figure 3.2) compared to the free ligand suggest their coordination, and the splitting that occurs for pyrazolyl protons should confirm their unequivalence (*i.e.* coordinated and free).

The possible equilibrium between N₂,N'-pz₂py and N₃-pz coordination modes could not be excluded, although the variable temperature ¹H-NMR experiment do not display any relevant shifts of the resonances that exclusively gains in resolutions (Figure 3.3).

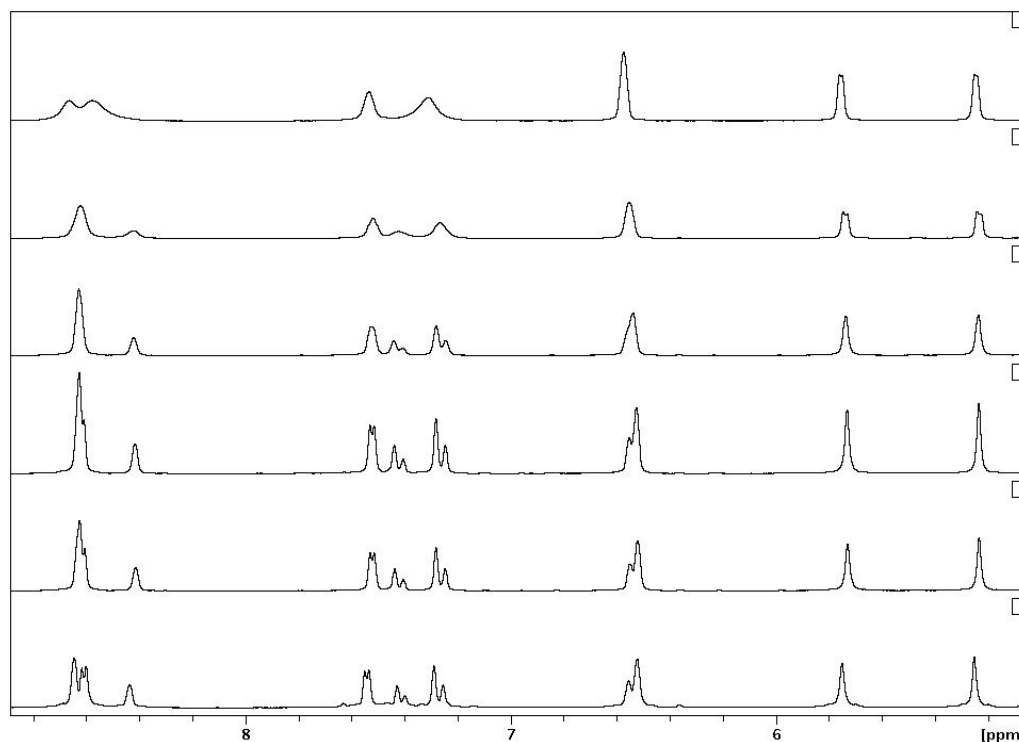


Figure 3.3 Variable temperature (298 – 233 K) ¹H-NMR (CD₃CN) experiments for **(30)**.

The solid-state structure of **(30)** has been determined by single crystal X-ray diffraction analysis and shows the TpmPy coordinated through the three pyrazolyl rings, leaving uncoordinated the pyridyl moiety (Figure 3.4, and Table 3.1). An intermolecular π - π interaction is observed between one pyridyl ring of a molecule and one pyrazolyl ring of another molecule (centroid/centroid distance of 3.4 Å), the angle between the planes being of ca. 5°. This interaction could stabilise the packing and the coordination mode through the three pyrazolyl rings.

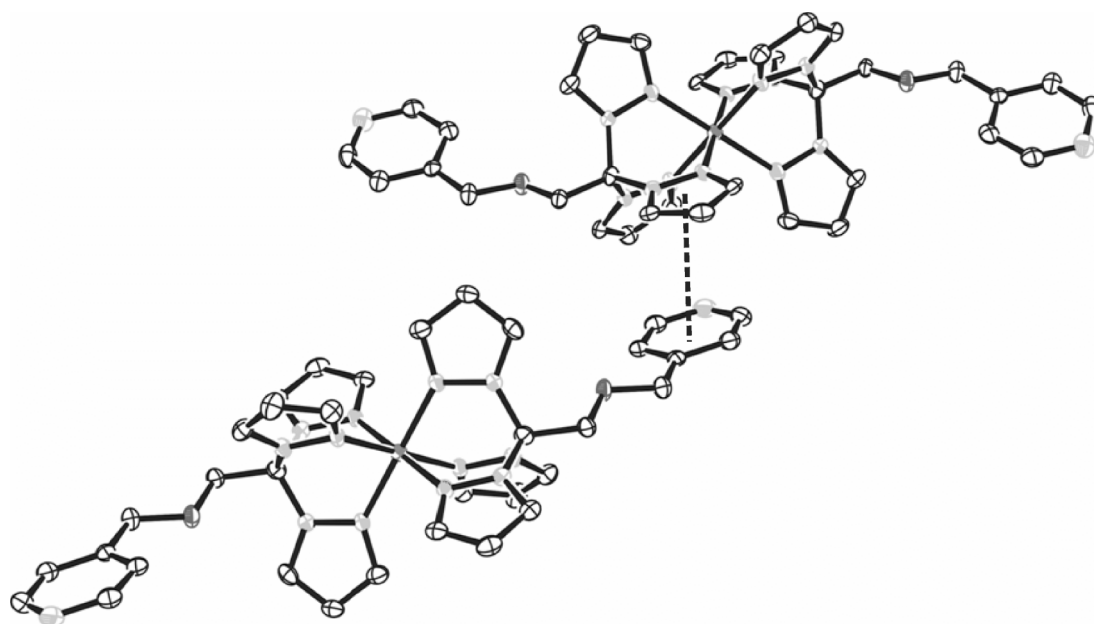


Figure 3.4 ORTEP plot of $[Fe(TpmPy)_2](BF_4)_2$ (**30**), where the ellipsoids are shown at 50% of probability and the tetrafluoroborate counter-ions are omitted for clarity. The dashed line indicates the π - π interaction (3.4 Å).

Moreover, as reported for other systems,²⁹ the minimum degree of tilting of the pyrazolyl rings from an ideal C_{3V} axis is typical for Fe^{II}-Tpm, LS, sandwich complexes: the Fe-N-N-C torsion angles, where n denotes the ring number, in an ideal case would be 180° and the metal atom would reside in the planes defined by the pyrazolyl rings. For compound **(30)** these angles are within the range of 174.31°-177.10°, confirming the pure low spin electronic state of the Fe^{II} center (Figure 3.5).

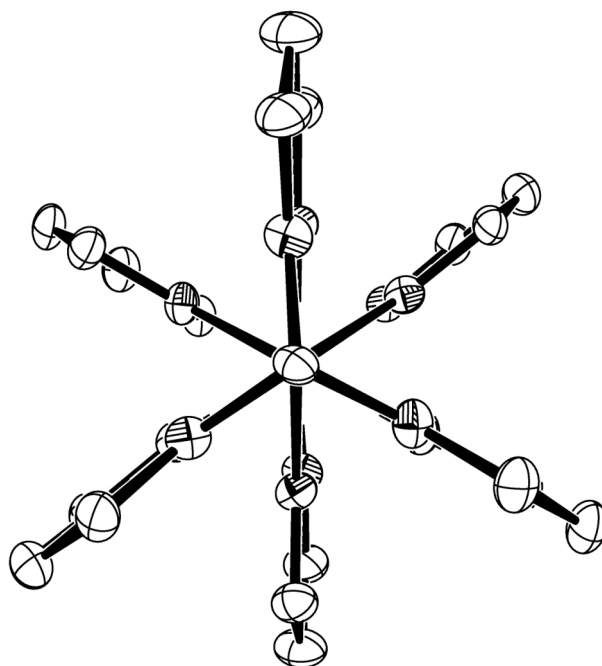


Figure 3.5 ORTEP plot of $[Fe(TpmPy)_2](BF_4)_2$ (**30**) (view down of the pseudo-three-fold axis), where the tetrafluoroborate counter-ions and pyridil pendants are omitted for clarity.

Electrochemical cyclic voltammetry in acetonitrile solution reveals a one electron reversible process (Figure 3.6) assigned to the $Fe^{II} \rightarrow Fe^{III}$ oxidation at $E_{1/2}^{ox} = +0.64$ V vs. Fc ($E_{1/2}^{ox} = +1.10$ V vs. SCE), typical for these type of compound (see Experimental Chapter).³³

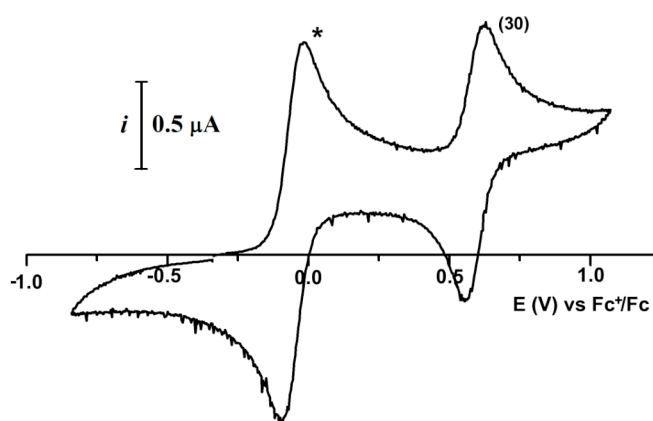
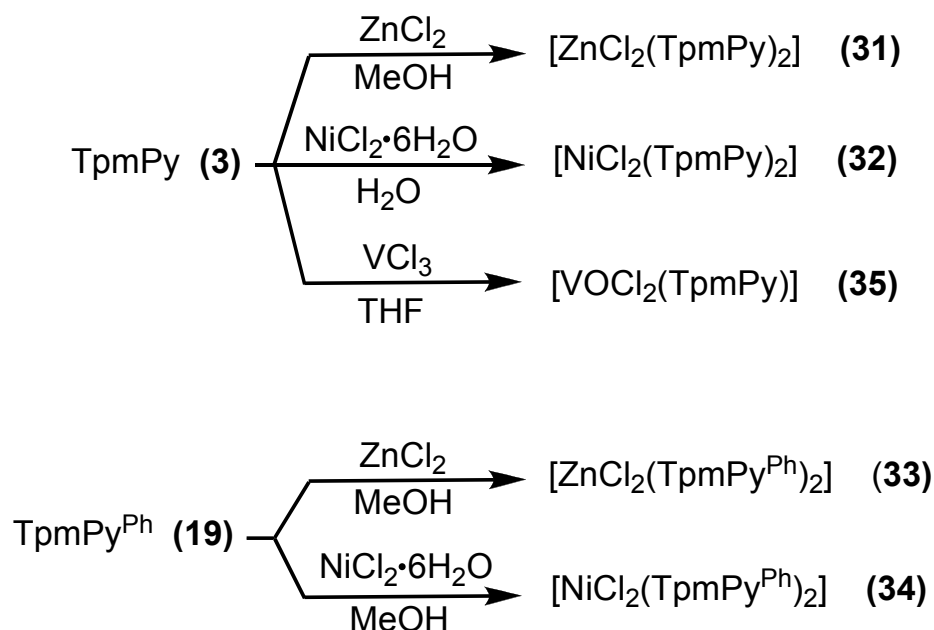


Figure 3.6 Cyclic voltammogram ($v = 120$ mV s⁻¹) of a ca. 1mM solution of (**30**) in CH_3CN with 0.2 M $[NBu_4][BF_4]$, at a platinum disc electrode ($d = 0.5$ mm).

3.3.2 Reactions of (3) and (19) with Ni^{II}, Zn^{II} and V^{III}

Reactions of (3) and (19) with Zn^{II} or Ni^{II} metal salts can, in principle, give full or half-sandwich complexes³⁴⁻⁴⁰ through the tripodal coordination of one or two scorpionates via the pyrazolyl rings, but the competition of the pyridyl arm for the metal can also occur in view of the known⁴¹⁻⁴⁶ metal affinity for this group.



Scheme 3.4 Syntheses of $[\text{MCl}_2(\text{TpmPy}^*)_2]$ ($M = \text{Ni}^{\text{II}}, \text{Zn}^{\text{II}}$; $\text{Tpm}^* = \text{TpmPy}, \text{TpmPy}^{\text{Ph}}$) (4-7) and $[\text{VOCl}_2(\text{TpmPy})]$ (35). Pyridyl-coordination: (31), (33), (34); pyrazolyl-coordination: (32), (35).

Reaction of two equivalents of TpmPy (3) with ZnCl₂ in methanol affords $[\text{ZnCl}_2(\text{TpmPy})_2]$ (31) (Scheme 3.4). The compound is well soluble in CH₂Cl₂ and sparingly soluble in MeOH and EtOH. The ESI-MS spectrum shows ionic fragments corresponding to $[\text{ZnCl}(\text{TpmPy})]^+$ and $[\text{Zn}(\text{TpmPy})_2]^{2+}$

The X-ray diffraction analysis of the solid-state structure of (31) shows a metal tetrahedral-type coordination with the two TpmPy ligands binding through the pyridyl rings, whereas the pyrazolyl groups remain uncoordinated (Figure 3.7, Table 3.1). This mode of TpmPy coordination is preserved in solution. In fact, in the ¹H-NMR spectrum, the pyridyl resonances are shifted to lower field (by *ca.* 0.1 ppm) relatively to those of the free ligand (*i.e.*, 8.51, 7.30 for (31) and 8.43, 7.20 for (3), in methanol-*d*₄, corresponding to 2,6-H and 3,5-H of the pyridyl ring, respectively),

whereas the pyrazolyl resonances remain almost unchanged. Moreover, NMR experiments at variable temperature confirm the equivalence²⁰ of the three uncoordinated pyrazolyl rings. In accord, the IR spectrum displays a shift of $\nu_{C=N}$ assigned to the pyridyl rings to higher wavenumbers compared to free **(3)** (*i.e.*, 1601 or 1621 cm^{-1} for **(3)** or **(31)**, respectively, Table 3.2).

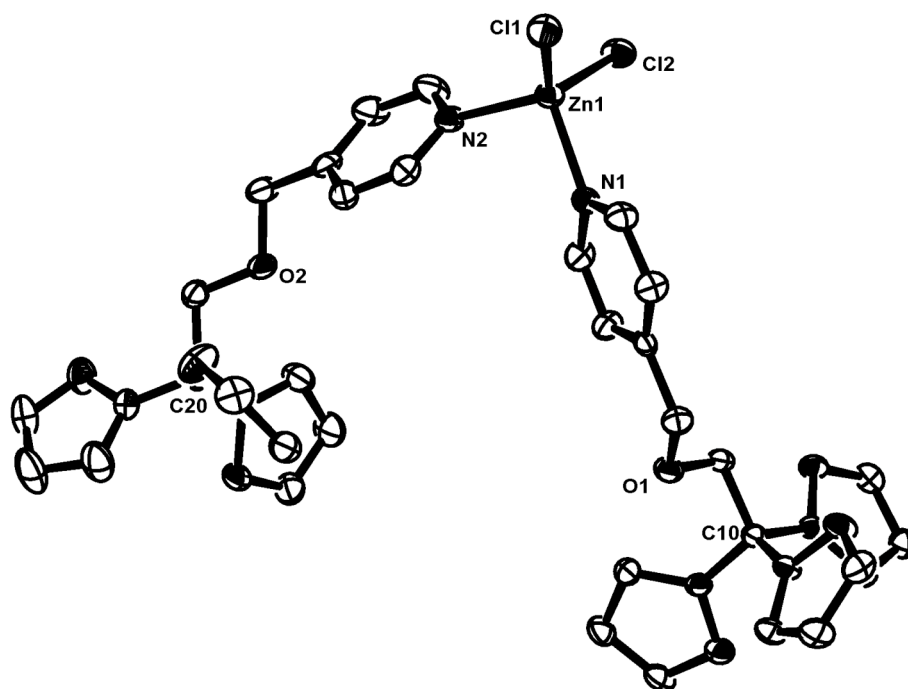


Figure 3.7 ORTEP plot of $[\text{ZnCl}_2(\text{TpmPy})_2]$ (**31**), with ellipsoids shown at 50% of probability.

The tetrahedral coordination around the zinc is slightly distorted with the internal angles of $100.69(8)^\circ$ for N1-Zn1-N2 and $119.77(3)^\circ$ for Cl1-Zn1-Cl2, *i.e.*, the larger angles concerns the chloride ligands. The Zn-N bond lengths are identical ($2.058(2)$ Å and $2.053(2)$ Å), like the Zn-Cl distances, thus showing a symmetrical elongation of the ideal tetrahedral geometry.

In contrast to the case of Zn^{II} , Ni^{II} chloride reacts with 2 eq of **(3)** to give (Scheme 3.4) the corresponding sandwich complex $[\text{Ni}(\text{TpmPy})_2]\text{Cl}_2$ (**32**) bearing two tri-hapto TpmPy ligands coordinated via the pyrazolyl rings, as shown by X-ray diffraction analysis (Figure 3.8, Tables 3.1).

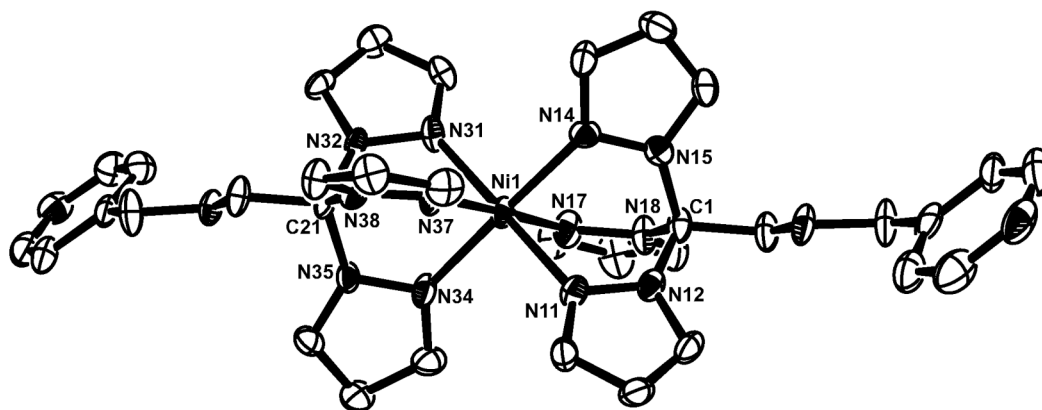


Figure 3.8 ORTEP plot of $[Ni(TpmPy)_2]Cl_2$ (**32**), with ellipsoids shown at 50% of probability and the two chlorides omitted for clarity.

The octahedral N_6 -coordination of nickel(II) is consistent with the 1H -NMR spectrum that shows its typical paramagnetic nature (octahedral Ni^{II} , $S=1$). Compound (**32**) is well soluble in water ($S_{25^\circ C} \approx 50 \text{ mg}\cdot\text{mL}^{-1}$), MeOH and EtOH, and sparingly soluble in $CHCl_3$, CH_2Cl_2 and acetonitrile. As for compound (**30**), the X-ray diffraction analysis of (**32**) confirms the scorpionate sandwich structure. The Ni-N distances are very close (2.038-2.068 Å range) and the degree of tilting of the pyrazolyl rings is very low (*i.e.*, Ni-N-N-C torsion angles, where n denotes the ring number, are within the range of 165.90° - 178.04°).

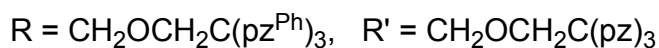
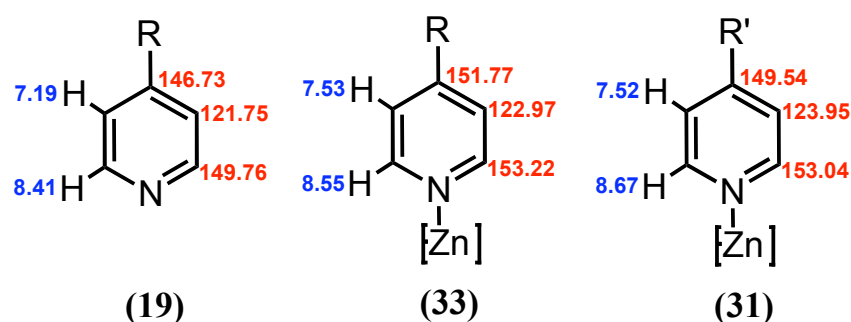


Figure 3.9 Selected 1H -NMR (blue) and ^{13}C -NMR (red) resonances (acetone- d_6) for free and coordinated pyridyl moiety, for compounds (**19**), (**33**) and (**31**).

Similarly to the previous synthetic procedures, we studied the reactions of Zn^{II} and Ni^{II} chlorides with TpmPy^{Ph} (**19**). The latter being sterically hindered at the

pyrazolyl-side, is expected to coordinate preferably through the pyridyl moiety. In fact, reaction of **(19)** with ZnCl₂ in methanol leads readily to the quantitative precipitation of [ZnCl₂(TpmPy^{Ph})₂] (**33**) which, has been characterised by IR, *far*-IR, NMR, MS and elemental analysis. Like its TpmPy analogue **(31)**, complex **(33)** bears the scorpionate ligands bound via the pyridyl groups. Its ¹H-NMR spectrum shows, in fact, the equivalence of its three pyrazolyl rings (without a significant shift relative to the free ligand) and a lower field coordination shift (of 0.14 and 0.33 ppm) for the pyridyl protons. The 2-, 6- and 4- pyridyl carbons appear low field shifted in the ¹³C-NMR spectrum, as for the analogue **(31)** (Figure 3.9); this feature appears to be common to all the complexes that exhibit pyridyl-coordination, as will be discussed below. Compound **(33)** is very soluble in CHCl₃, CH₂Cl₂, acetone, and moderately soluble in MeOH, while is insoluble in water.

Table 3.1 List of selected bond distances [\AA] and angles [$^\circ$] for compound TpmPy (**3**), [Fe(TpmPy)₂](BF₄)₂ (**30**), [ZnCl₂(TpmPy)₂] (**31**), [Ni(TpmPy)₂]Cl₂ (**32**) and [PdCl₂(TpmPy)₂] (**36**).

(3)		(30)		(31)	
C1-N11	1.4543(13)	C1-N13	1.468(6)	Zn1-N1	2.058(2)
C1-N14	1.4573(13)	C1-N16	1.466(7)	Zn1-N2	2.053(2)
C1-N17	1.4541(13)	C1-N19	1.466(7)	Zn1-Cl1	2.2103(7)
C1-C2	1.5315(15)	C1-C101	1.518(7)	Zn1-Cl2	2.2401(7)
O1C3-C4C8 ^a	118.31	Fe1-N11	1.965(4)	Cl1-Zn1-Cl2	119.77(3)
(32)		Fe1-N14	1.954(4)	Cl2-Zn1-N1	108.33(6)
Ni1-N14	2.050	Fe1-N17	1.949(4)	N1-Zn1-N2	100.69(8)
Ni1-N17	2.037	N17-Fe1-N14	87.71(17)	N2-Zn1-Cl1	115.51(6)
Ni1-N11	2.063	N17-Fe1-N11	87.98(17)	Cl2-Zn1-N2	104.80(6)
O1C4-C5C6 ^a	137.03	N14-Fe1-N11	86.67(17)	Cl1-Zn1-N1	105.94(6)
O2C23-C24C28 ^a	143.53	N24-Fe2-N21	85.72(18)	O1C6-C3C2 ^a	177.97
(36)		N24-Fe2-N27	87.93(17)	O2C26-C23C24 ^a	135.26
Pd1-N1	2.037(10)	N21-Fe2-N27	86.34(17)		
Pd1-Cl1	2.315(3)	O1C202-C203C204 ^a	176.76		
N1-Pd1-Cl1	89.6(3)	O1C102-C103C104 ^a	166.62		
O1C6-C3C2 ^a	137.91				

^a Refers to the O-C_{methylene}-C_{ipso}-C_{ortho} torsion angle.

Reaction of 2 eq of TpmPy^{Ph} (**19**) with NiCl₂ in methanol proceeds readily leading to the precipitation of [NiCl₂(TpmPy^{Ph})₂] (**34**) that also bears the scorpionate ligands coordinated through the pyridyl moieties. Hence, the pyrazolyl N₆-coordination mode observed for **(32)** with unsubstituted tris(pyrazolyl)methane ligands, is sterically hindered for **(34)**. The mass spectrum (EI) of **(34)** shows an equivalent pattern of fragmentation to that of its zinc analogue **(33)** (*e.g.*, peaks at *m/z*

656 and 662 for [Ni(TpmPy^{Ph})Cl]⁺ and [Zn(TpmPy^{Ph})Cl]⁺, respectively). The IR spectra of **(33)** and **(34)** show almost identical profiles for the 1800-400 cm⁻¹ region, in particular the shifted band at 1617 cm⁻¹ ascribed to $\nu_{C=N}$ of the coordinated pyridyl moiety (Figure 3.10 and Table 3.2). The ¹H-NMR spectrum of **(34)** shows broad resonances, where it is possible to distinguish those assigned to the pyrazolyl rings, while those of the pyridyl moiety collapse due to the proximity of the metal center.

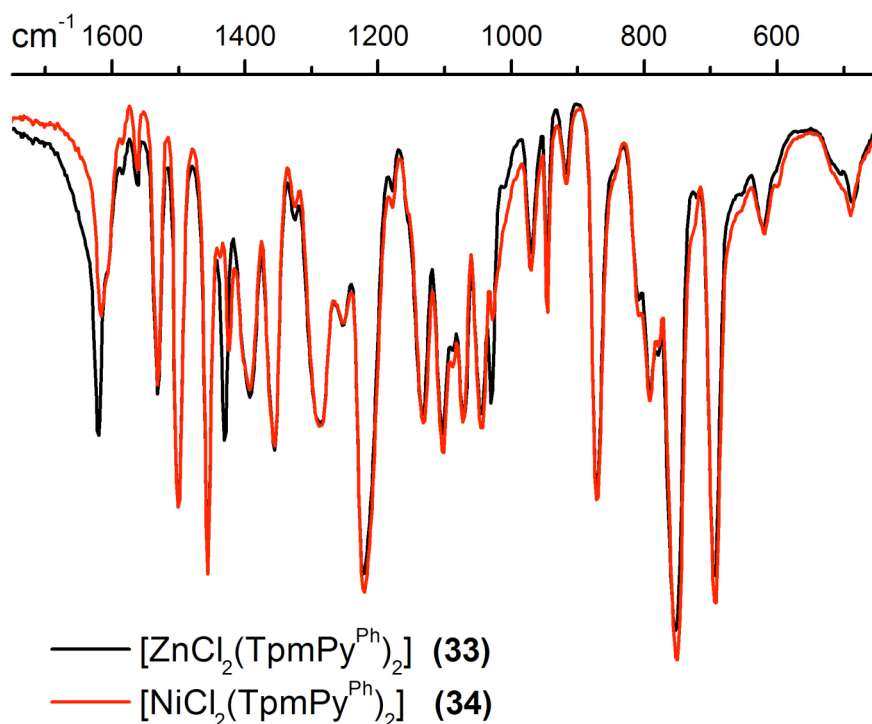
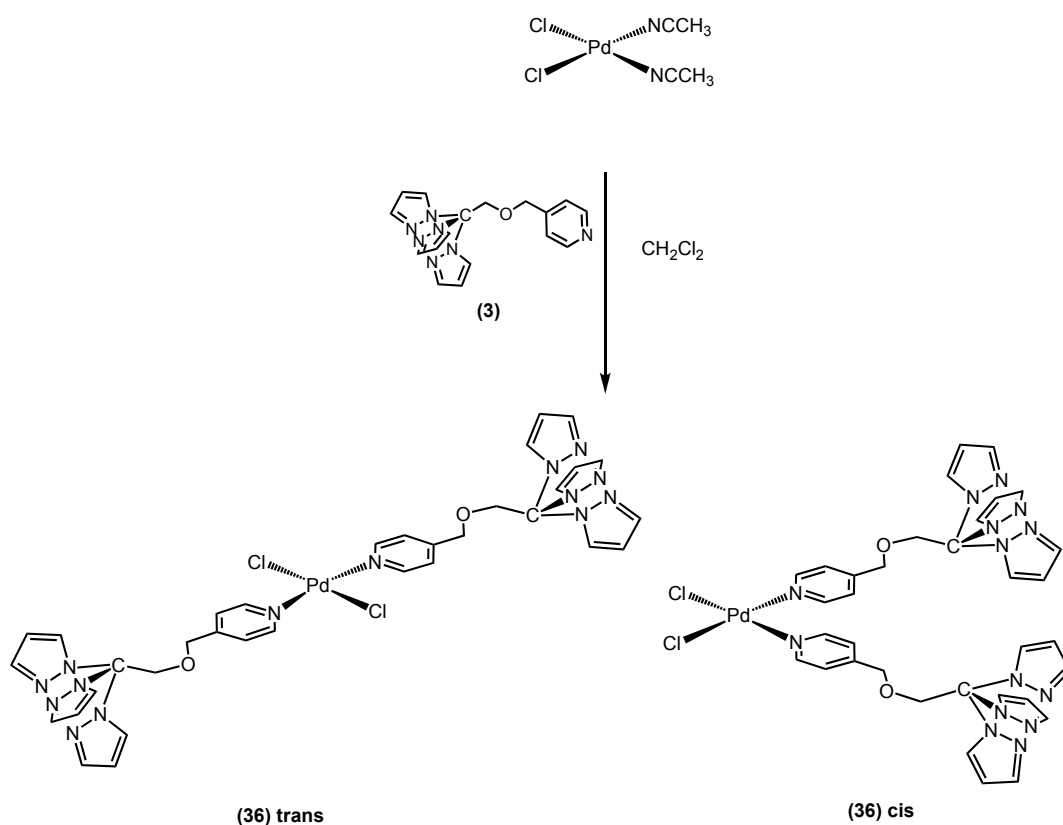


Figure 3.10 IR spectra of **(33)** and **(34)**.

The reaction of TpmPy **(3)** with V^{III} chloride (Scheme 3.4) also proceeds readily with the precipitation, as a pale blue powder, of [VOCl₂(TpmPy)] **(35)** with the N₃-pyrazolyl coordination. The compound has been characterised by MS, IR, *far*-IR and EPR spectroscopies, and elemental analysis. The EPR spectrum shows the expected signal (*i.e.*, with a eight-line pattern, $g = 1.9989$) for a vanadium(IV) (d^1 , $I=7/2$, $S=1/2$).⁴⁷

3.3.3 Reactions of (3) and (19) with Pd^{II}

Palladium(II) complexes bearing heterocyclic N-donor ligands are well known and the coordination chemistry of Pd-based complexes with pyrazoles, imidazoles and pyridines ligands has been deeply developed.⁴⁸⁻⁵⁰ Pd^{II} reacts^{37,51,52} easily with bis(pyrazolyl)methane (Bpm) and tris(pyrazolyl)methane (Tpm) to give typical square planar N,N-coordination compounds (involving two ligated pyrazolyl rings, and leaving one free in the case of Tpm). Moreover, the recognized affinity^{53,54} of this metal with the pyridyl N-donor group encouraged us to investigate its coordination chemistry toward these new “pyridyl-based” scorpionates.

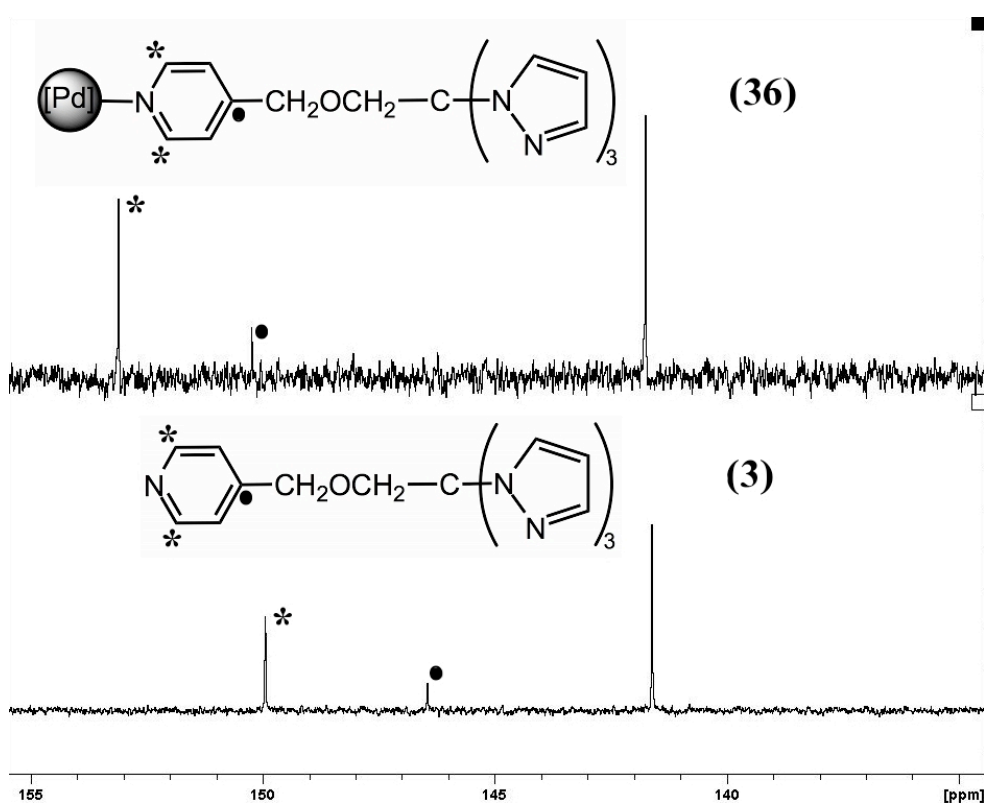


Scheme 3.5 Synthesis of [PdCl₂(TpmPy)₂] (36).

Reaction of *cis*-[PdCl₂(CH₃CN)₂] with 2 eq of (3) in dichloromethane gives the di-substituted product [PdCl₂(TpmPy)₂] (36) in quantitative yield (Scheme 3.5). The compound is stable and soluble in organic solvents such as CH₂Cl₂ and CHCl₃, but in DMSO undergoes a partial decomposition. In the ¹H-NMR spectrum the remarkable shift to lower field (by *ca.* 0.15 ppm) of the pyridyl resonances relatively

to those of the free ligand confirms the coordination through the pyridyl moiety, whereas the pyrazolyl groups remain equivalent.

The phenyl substituted analogue, [PdCl₂(TpmPy^{Ph})₂] (**37**), was prepared similarly, upon reaction of *cis*-[PdCl₂(CH₃CN)₂] with (**19**). In this case, the coordination through the pyridyl moiety is expected to be even more favorable than for the unsubstituted (**36**), since the pyrazolyl-side is highly hindered by the phenyl substituents. Compound (**37**) shows NMR coordination shifts comparable to those of (**36**). For instance, similarly to (**36**), the ¹³C-NMR (400 MHz) spectrum of (**37**) shows the 2,6- and 4- pyridyl carbons resonances (at δ 152.9 and 150.4, respectively) shifted to lower field (by 3.1 and 3.7 ppm, correspondingly) relatively to the free ligand. This behavior supports the expected deshielding upon pyridyl coordination, confirming that the *ortho* and the *para* positions are more influenced than the *meta* (Figure 3.11).



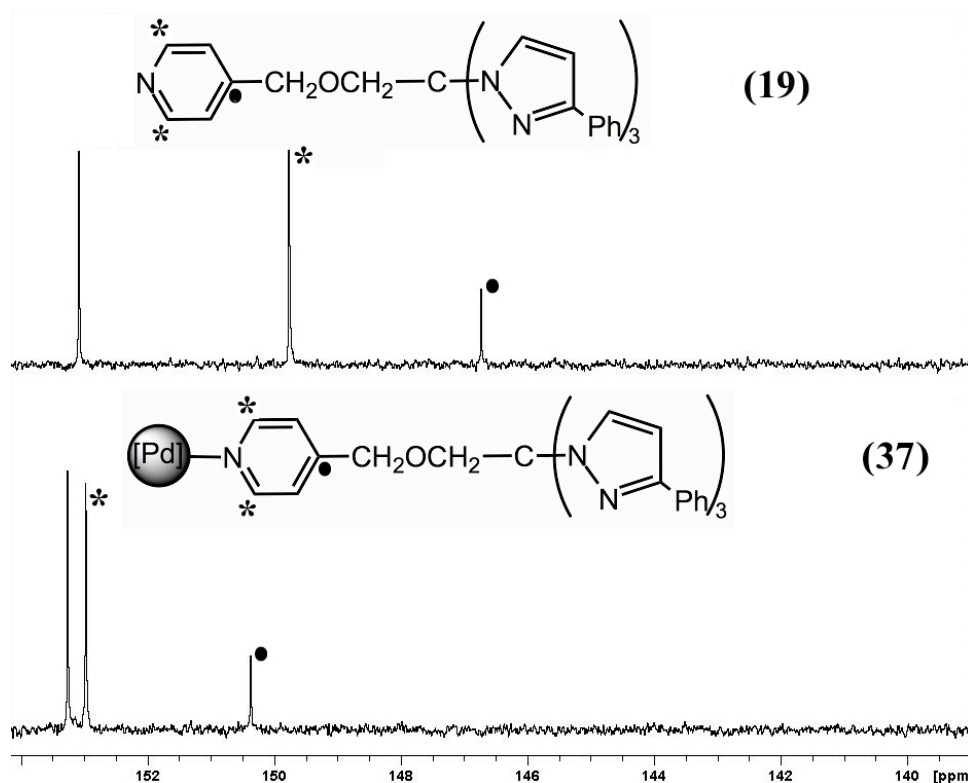


Figure 3.11 Shifting of 2,6-C (*) and 4-C (•) pyridyl carbons resonances in ^{13}C -NMR (400 MHz) spectra (CDCl_3) upon coordination of free **(3)** to Pd^{II} in $[\text{PdCl}_2(\text{TpmPy})_2]$ **(36)**, (top), and upon coordination of free **(19)** to Pd^{II} in $[\text{PdCl}_2(\text{TpmPy}^{\text{Ph}})_2]$ **(37)** (bottom).

Similarly, the IR spectra of **(36)** and **(37)** show a displacement to higher wavenumbers of the $\nu_{\text{C}=\text{N}}$ frequency compared to that of the corresponding free ligands **(3)** and **(19)** (from 1601 to 1619 and from 1603 to 1621, for the **(3)**/**(36)** and **(19)**/**(37)** pairs, respectively; Table 3 and Figure 3.12(a)). The mass spectra of **(36)** and **(37)** confirm the presence of two scorpionate ligands and the far-IR spectra reveals the bands ascribed to Pd-Cl stretching (Figure 3.13(b)).⁵⁵⁻⁶⁰ For **(36)**, the $\nu_{\text{Pd-Cl}}$ at 308 and 296 cm^{-1} , typical for a *cis*-isomer, appear shifted to higher wavenumbers in comparison to those of the starting compound *cis*- $[\text{PdCl}_2(\text{CH}_3\text{CN})_2]$ (255 and 242 cm^{-1}) suggesting a higher π -electron-acceptor character for the coordinated pyridyl species than that of the acetonitrile ligand. Moreover, another band is detected at 361 cm^{-1} being ascribed to the *trans* isomer, also present in the solid state in a lower amount. On the other hand, the analogue **(37)** shows just a single strong band at 365 cm^{-1} , corresponding to the *trans* isomer, which is preferably formed due to the steric hindrance of TpmPy^{Ph}. Attempted chromatographic separation of the two isomers of **(36)** resulted in decomposition of the compound.

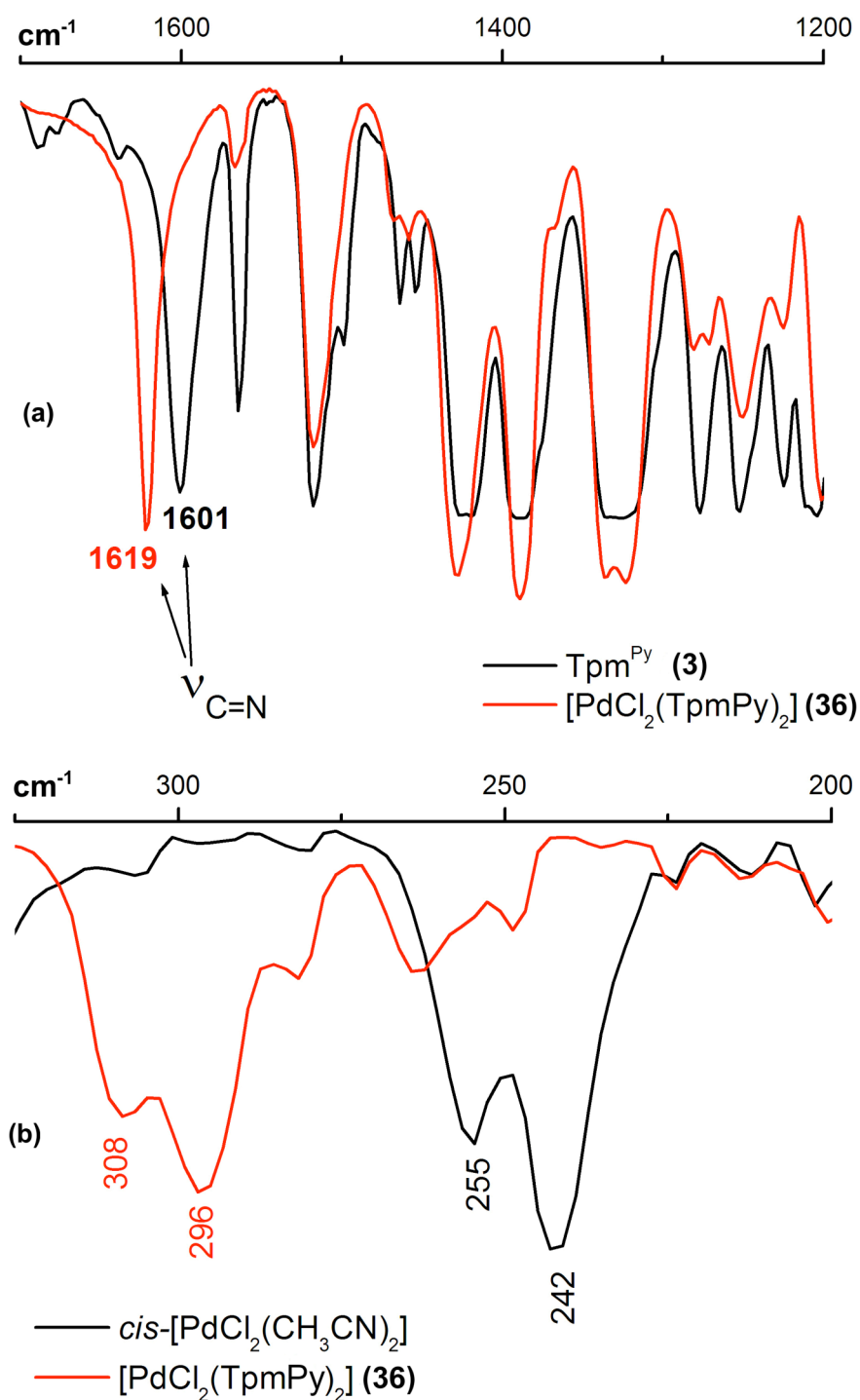


Figure 3.12 IR spectra of (**3**) and (**36**) (a), and far-IR spectra of the starting material *cis*-[PdCl₂(CH₃CN)₂] and (**36**) (b).

Furthermore, the *trans* isomer of (**36**) was identified in the X-ray diffraction analysis (from very poor quality crystals) that displays an almost perfect square-

planar geometry around the Pd(II) ion, with the two scorpionates in *trans* position (Figure 3.13) and the N(1)-Pd(1)-Cl(1) angles of 89.6(3)° (Table 3.1).

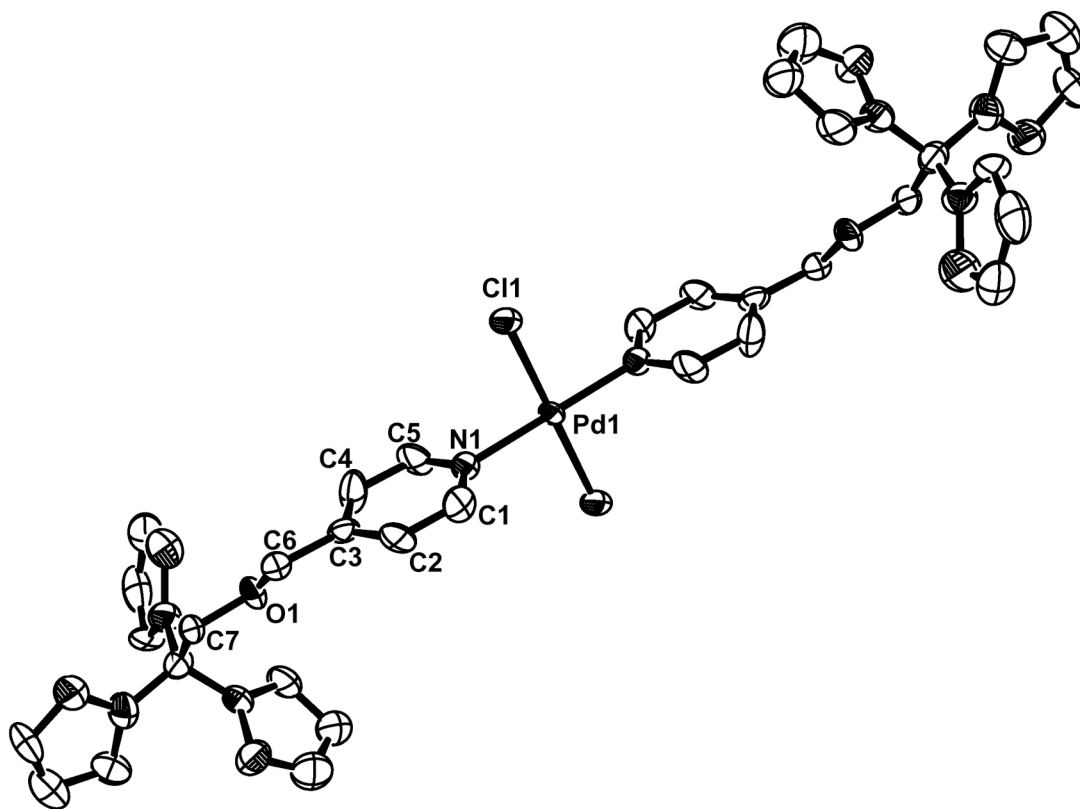
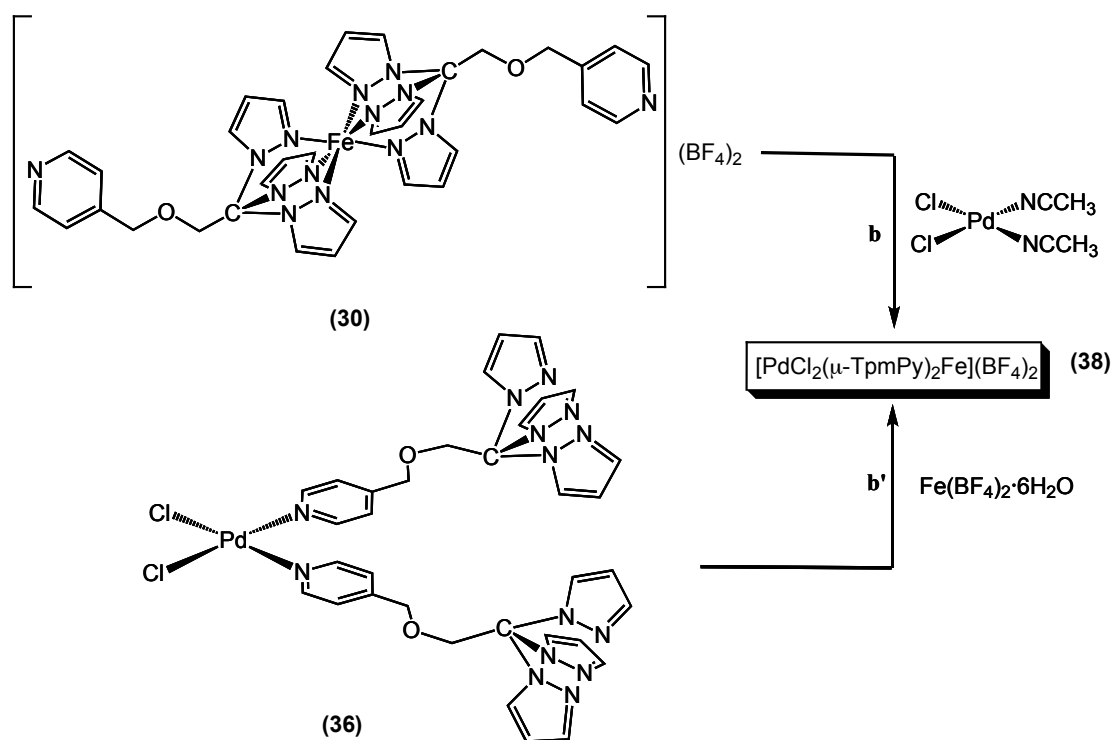


Figure 3.13. ORTEP plot of $[PdCl_2(TpmPy)_2]$ (**36**), with ellipsoids shown at 50% of probability. Hydrogen atoms are omitted for clarity.

3.4 Applications of (3) and (19) to the synthesis of bimetallic complexes

In order to investigate the multidentate ability of the new scorpionates of this work and the versatility of the new complexes prepared, we explored the “second” coordination step (**b** and **b'**, Scheme 1) of the latter compounds.

Reaction of equimolar amounts of $[\text{Fe}(\text{TpmPy})_2](\text{BF}_4)_2$ (**30**) and *cis*- $[\text{PdCl}_2(\text{CH}_3\text{CN})_2]$ gives $[\text{PdCl}_2(\mu\text{-TpmPy})_2\text{Fe}](\text{BF}_4)_2$ (**38**) (Scheme 3.6(b)), which alternatively can be obtained upon an equimolar reaction of $[\text{PdCl}_2(\text{TpmPy})_2]\text{I}$ (**36**) with $\text{Fe}(\text{BF}_4)_2 \cdot 6\text{H}_2\text{O}$ (Scheme 3.6(b')).



Scheme 3.6 Synthetic pathways for $[\text{PdCl}_2(\mu\text{-TpmPy})_2\text{Fe}](\text{BF}_4)_2$ (**38**).

Compound (**38**) has been characterized by IR and NMR spectroscopies, MS and elemental analysis. Besides, its ^1H -NMR spectrum at low temperature (253 K) indicates a fluxional behavior, in solution, suggesting a conceivable dynamic equilibrium between different structures (such as **A** and **B**, Figure 3.14).

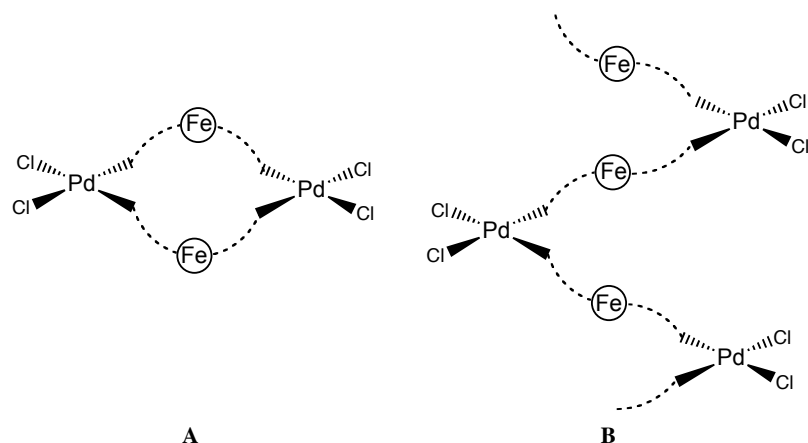
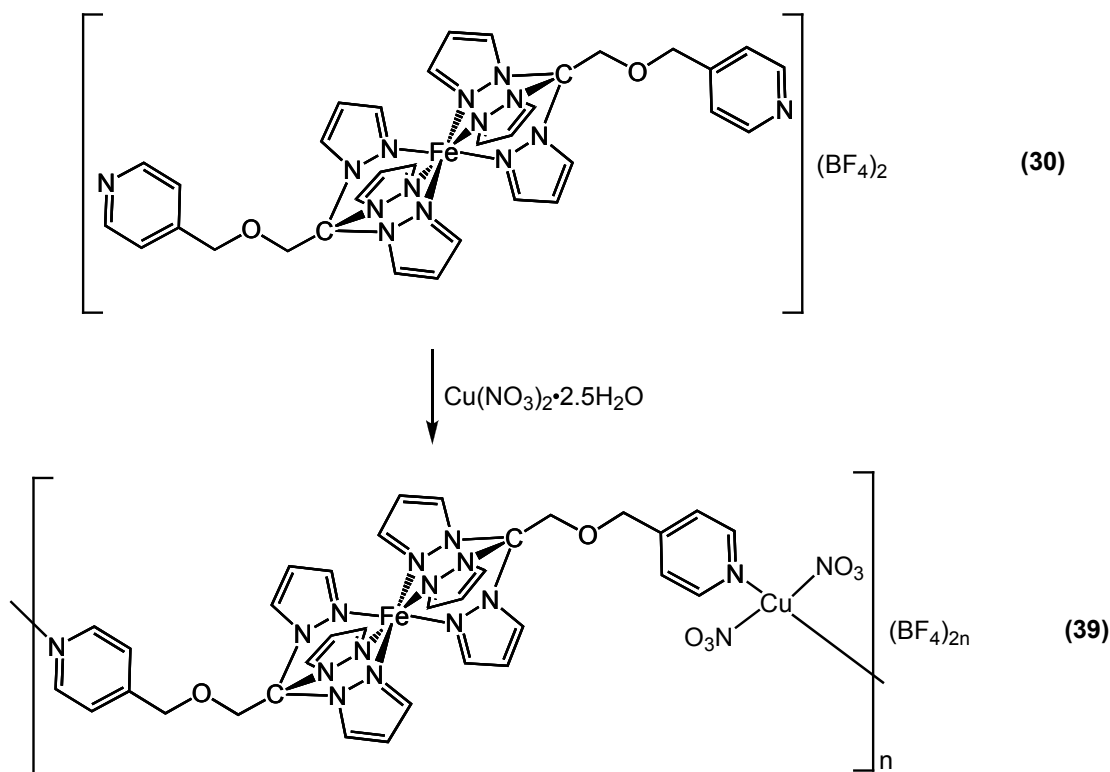


Figure 3.14. Conceivable structures of $[PdCl_2(\mu\text{-TpmPy})_2Fe](BF_4)_2$ (**38**).

Similarly, reaction of $[Fe(\text{TpmPy})_2](BF_4)_2$ (**30**) with $Cu(NO_3)_2 \cdot 2.5H_2O$ leads to the immediate precipitation of a pale violet solid of $[Fe(\mu\text{-TpmPy})_2Cu(NO_3)_2](BF_4)_2$ (**39**), where each pyridyl moiety is coordinated to Cu^{II} . This compound is well soluble in MeOH and sparingly soluble in CH_3CN , while it decomposes in H_2O after a few hours. The $^1H\text{-NMR}$ spectrum confirms the presence of paramagnetic Cu^{II} , where the pyridyl resonances appearing more affected by the metal electronic state. In the mass spectrum (EI) of (**40**), the peak at m/z 713 assigned to the double charged $[\{Fe(\mu\text{-TpmPy})_2Cu_2(\text{TpmPy})(NO_3)_3\}(BF_4)]^{++}$ fragment suggests a conceivable polymeric structure of the hetero-bimetallic system. Elemental analysis confirms the 1:1 Cu/Fe ratio (Scheme 3.7).



Scheme 3.7. Synthesis and proposed molecular structure (polymeric chain) of (39).

An interesting comparison with the synthesis of compound (38) emerges from the reaction of $[\text{PdCl}_2(\text{TpmPy}^{\text{Ph}})]$ (37) with $\text{Fe}(\text{BF}_4)_2 \cdot 6\text{H}_2\text{O}$ that gives the hydrated Fe-Pd-Fe complex $[\text{PdCl}_2(\mu\text{-TpmPy}^{\text{Ph}})_2\text{Fe}_2(\text{H}_2\text{O})_6](\text{BF}_4)_4$ (40) bearing each iron coordinated by the three pyrazolyl rings of one bridging TpmPy^{Ph}. Steric hindrance of the bulky Tpm^{PyPh} prevents the formation of the N₆-sandwich coordination at Fe^{II} (which, in contrast, occurs for compound (38)) leaving three coordination positions available for small ligands, such as water.^{7a} The ¹H-NMR spectrum of (40) is consistent with that of its precursor (37), and shows a modest shift of the pyrazolyl resonances on account of coordination to iron(II).

Polymeric structures can also be envisaged for these compounds, and eventually thwarted the crystallisation attempts and prevented their complete characterization.

3.5 Pyridyl-functionalized scorpionates: overview

As expected, this new multifunctional class of scorpionates bearing a pyridyl group pending from the methine carbon shows its double face coordination ability.

In the case of Fe^{II}, NMR and X-ray analyses of compound **(30)** reveal, by comparison with the Tpm analogous complex, that the pyridyl moiety promotes the stabilization of the low-spin (LS) state of Fe^{II} center, and is involved in coordination to iron center. In the cases of Ni^{II}, Zn^{II} and Pd^{II}, the extra N-donor pyridyl group shows a good affinity to the metal centers: the new pyridyl-based complexes of Ni, Zn and Pd (*i.e.* compounds **(31)**, **(33)**, **(34)**, **(36)** and **(37)**, respectively) provide relevant examples in this field. Moreover, by increasing the bulkiness of the pyrazolyl groups by introducing a phenyl substituent (as in **(19)**), the coordination through the pyridyl-side is forced: the two nickel complexes **(32)** and **(34)** (*i.e.* bearing the ligating scorpionates in the N₃-pyrazolyl and N-pyridyl coordination modes, respectively) provide a good model of steric inducement.

In general, the ¹H and ¹³C NMR, IR and far-IR spectroscopies allowed to confirm the coordination modes of the new scorpionate ligands in their metal complexes.

Table 3.2 Selected IR frequencies (KBr) for **(3)**, **(19)** and **(30)**-**(40)**.

Compound	$\nu_{C=N} / \text{cm}^{-1}$	$\nu_{C=C} / \text{cm}^{-1}$	
(3)	1601, 1564	1517	free ligand
(19)	1603, 1561	1530	free ligand
(30)	1562	1518	pz-coordination
(31)	1621, 1563	1518	py-coordination
(32)	1568	1522	pz-coordination
(33)	1620, 1531	1500	py-coordination
(34)	1617, 1531	1500	py-coordination
(35)	1519	1517	pz-coordination
(36)	1619, 1561	1517	py-coordination
(37)	1621, 1531	1500	py-coordination

(38)	1621, 1519	1513	py/pz-coordination
(39)	1620, 1517	1515	py/pz-coordination
(40)	1620, 1531	1499	py/pz-coordination

In particular ¹³C-NMR and IR spectra are of diagnostic value to distinguish between pyrazolyl- and pyridyl-coordination (Figures 6, S.1, S.2 and Table 3). Hence, a significant low field shift (*ca.* $\Delta\delta$ 2-3 ppm) for 2, 6- and 4-pyridyl carbons in the ¹³C-NMR spectra is peculiar of py-coordination. Furthermore, the latter coordination affects the IR $\nu_{C=N}$ corresponding to the pyridyl moiety that shifts to higher wavenumbers (*i.e.* within the range of 1617-1621 cm^{-1} , Table 3). The consistency of these behaviors illustrates an easy pattern for the characterization of these new complexes and generates a criterion for further studies in this field.

The multifunctional ligands are particularly adequate to the easy synthesis of heterobimetallic units, such as those of the current study. This represents a first application of this class of multidentate ligands that are expected to be able to coordinate to a wide variety of metal centers and to generate polymetallic species for further studies, *e.g.* in supramolecular and solid-supported chemistries, besides the various fields of common applications of scorpionate compounds.

References

- [1] Trofimenko, S., *J. Am. Chem. Soc.* **1966**, *88*, 1842.
- [2] Reger, D. L.; Grattan, T. C., *Synthesis-Stuttgart* **2003**, 350.
- [3] Trofimenko, S., *Scorpionates: The Coordination Chemistry of Polypyrazolylborates Ligands*. Imperial College Press: London, 1999.
- [4] Trofimenko, S., *Chem. Rev.* **1993**, *93*, 943.
- [5] Reger, D. L.; Watson, R. P.; Gardinier, J. R.; Smith, M. D.; Pellechia, P. J., *Inorg. Chem.* **2006**, *45*, 10088.
- [6] Reger, D. L.; Semeniuc, R. F.; Gardinier, J. R.; O'Neal, J.; Reinecke, B.; Smith, M. D., *Inorg. Chem.* **2006**, *45*, 4337.
- [7] Reger, D. L.; Semeniuc, R. F.; Little, C. A.; Smith, M. D., *Inorg. Chem.* **2006**, *45*, 7758.
- [8] Reger, D. L.; Gardinier, J. R.; Bakbak, S.; Semeniuc, R. F.; Bunz, U. H. F.; Smith, M. D., *New J. Chem.* **2005**, *29*, 1035.
- [9] Reger, D. L.; Semeniuc, R. F.; Smith, M. D., *J. Organomet. Chem.* **2003**, *666*, 87.
- [10] Klaui, W.; Berghahn, M.; Rheinwald, G.; Lang, H. R., *Angew. Chem., Int. Ed.* **2000**, *39*, 2464.
- [11] Reger, D. L.; Semeniuc, R. F.; Smith, M. D., *Inorg. Chem.* **2001**, *40*, 6545.
- [12] Reger, D. L.; Wright, T. D.; Semeniuc, R. F.; Grattan, T. C.; Smith, M. D., *Inorg. Chem.* **2001**, *40*, 6212.
- [13] Braga, D.; Polito, M.; Braccacini, M.; D'addario, D.; Tagliavini, E.; Prosepio, D. M.; Grepioni, F., *Chem. Commun.* **2002**, *10*, 1080.
- [14] Cotton, F. A.; Jin, J.-Y.; Li, Z.; Liu, C. Y.; Murillo, C. A., *Dalton Trans.* **2007**, *22*, 2328.
- [15] Rajadurai, C.; Schramm, F.; Brink, S.; Fuhr, O.; Ghafari, M.; Kruk, R.; Ruben, M., *Inorg. Chem.* **2006**, *45*, 10019.
- [16] Reger, D. L.; Gardinier, J. R.; Grattan, T. C.; Smith, M. D., *J. Organomet. Chem.* **2005**, *690*, 1947.
- [17] Astley, T.; Canty, A. J.; Hitchman, M. A.; Rowbott, G. L.; Skelton, B. W.; White, A. H., *J. Chem. Soc., Dalton* **1991**, 1981.

- [18] Alegria, E. C. B.; Martins, L.; Haukka, M.; Pombeiro, A. J. L., *Dalton Trans.* **2006**, 4954.
- [19] Alegria, E. C. B.; Martins, L.; da Silva, M.; Pombeiro, A. J. L., *J. Organomet. Chem.* **2005**, *690*, 1947.
- [20] Wanke, R.; Smolenski, P.; da Silva, M.; Martins, L.; Pombeiro, A. J. L., *Inorg. Chem.* **2008**, *47*, 10158.
- [21] Reger, D. L.; Grattan, T. C.; Brown, K. J.; Little, C. A.; Lamba, J. J. S.; Rheingold, A. L.; Sommer, R. D., *J. Organomet. Chem.* **2000**, *607*, 120.
- [22] Edwards, P. G.; Harrison, A.; Newman, P. D.; Zhang, W. J., *Inorg. Chim. Acta* **2006**, *359*, 3549.
- [23] Trofimenko, S.; Calabrese, J. C.; Domaille, P. J.; Thompson, J. S., *Inorg. Chem.* **1989**, *28*, 1091.
- [24] Gutlich, P.; Hauser, A.; Spiering, H., *Angew. Chem., Int. Ed.* **1994**, *33*, 2024.
- [25] Gutlich, P., Mossbauer Spectroscopy Applied to Inorganic Chemistry. In Long, G. J., Ed. New York, 1984; Vol. 1, p 207.
- [26] Kahn, O.; Martinez, C. J., *Science* **1998**, *44*, 279.
- [27] Muller, R. N.; Van der Elst, L.; Laurent, S., *J. Am. Chem. Soc.* **2003**, *125*, 8405.
- [28] Reger, D. L.; Little, C. A.; Rheingold, A. L.; Lam, M.; Liable-Sands, L. M.; Rhagitan, B.; Concolino, T.; Mohan, A.; Long, G. J.; Briois, V.; Grandjean, F., *Inorg. Chem.* **2001**, *40*, 1508.
- [29] Reger, D. L.; Little, C. A.; Young, V. G.; Maren, P., *Inorg. Chem.* **2001**, *40*, 2870.
- [30] Reger, D. L.; Gardinier, J. R.; Elgin, J. D.; Smith, M. D., *Inorg. Chem.* **2006**, *45*, 8862.
- [31] Batten, S. R.; Bjernemose, J.; Jensen, P.; Leita, B. A.; Murray, K. S.; Moubaraki, B.; Smitha, J. P.; Toftlund, H., *Dalton Trans.* **2004**, 3370.
- [32] Reger, D. L.; Elgin, J. D.; Foley, E. A.; Smith, M. D.; Grandjean, F.; Long, G. J., *Inorg. Chem.* **2009**, *48*, 9393.
- [33] Sheets, J. R.; Schultz, F. A., *Polyhedron* **2004**, *23*, 1037.
- [34] Zvargulis, E. S.; Buys, I. E.; Hambley, T. W., *Polyhedron* **1995**, *14*, 2267.
- [35] Supuran, C. Z.; Claramunt, R. M.; Lavandera, J. L.; Elguero, J., *Biol. Pharm. Bull.* **1996**, *19*, 1417.
- [36] Titze, C.; Hermann, J.; Vahrenkamp, H., *Chem. Ber.* **1995**, *128*, 1095.

- [37] Trofimenko, S., *J. Am. Chem. Soc.* **1970**, *92*, 5118.
- [38] Reger, D. L.; Little, C. A.; Smith, M. D., *Inorg. Chem.* **2002**, *41*, 4453.
- [39] Astley, T.; Gubis, J. M.; Hitchman, M. A.; Tiekink, E. R. T., *J. Chem. Soc., Dalton* **1993**, 509.
- [40] Hammes, B. S.; Carrano, C. J., *Inorg. Chem.* **1999**, *38*, 4593.
- [41] Steffen, W. L.; Palenik, G. J., *Inorg. Chem.* **1977**, *16*, 1119.
- [42] Blackmore, I. J.; Gibson, V. C.; Hitchcock, P. B.; Rees, C. W.; Williams, D. J.; White, A. J. P., *J. Am. Chem. Soc.* **2005**, *127*, 6012.
- [43] Westerhausen, M.; Kneifel, A. N.; Kalish, A., *Angew. Chem., Int. Ed.* **2005**, *44*, 96.
- [44] Bacchi, A.; Bosetti, E.; Carcelli, M., *Cryst. Eng. Comm.* **2007**, *9*, 313.
- [45] Long, G. J.; Clarke, P. J., *Inorg. Chem.* **1978**, *17*, 1394.
- [46] Wu, C. D.; Zhang, L.; Lin, W., *Inorg. Chem.* **2006**, *45*, 7278.
- [47] Silva, T. E. S.; Alegria, E.; Martins, L.; Pombeiro, A. J. L., *Adv. Synth. Catal.* **2008**, *350*, 706.
- [48] Qin, Z.; Jennings, M. C.; Puddephatt, R. J.; Muir, K. W., *Inorg. Chem.* **2002**, *41*, 5174.
- [49] Lee, C. K.; Ling, M. J.; Lin, I. J. B., *Dalton Trans.* **2003**, 4731.
- [50] Tsuji, S.; Swenson, D. C.; Jordan, R. F., *Organometallics* **1999**, *18*, 4758.
- [51] Canty, A. J.; Minchin, N. J.; Engelhardt, L. M.; Skelton, B. W.; White, A. H., *J. Chem. Soc., Dalton* **1986**, 645.
- [52] Sanchez-Mendez, A.; Silvestri, G. F.; de Jesus, E.; de la Mata, F. J.; Flores, J. C.; Gomez, R.; Gomez-Sal, P., *Eur. J. Inorg. Chem.* **2004**, 3287.
- [53] Feth, M. P.; Klein, A.; Bertagnolli, H., *Eur. J. Inorg. Chem.* **2003**, 839.
- [54] Hu, Y.-Z.; Chamchoumis, C.; Grebowicz, J. S.; Thummel, R. P., *Inorg. Chem.* **2002**, *41*, 2296.
- [55] Drahos, B.; Rohlik, Z.; Kotek, J.; Cisarova, I.; Hermann, P., *Dalton Trans.* **2009**, 4942.
- [56] Gillard, R. D.; Pilbrow, M. F., *J. Chem. Soc., Dalton* **1974**, 2320.
- [57] Adams, D. M.; Chatt, J.; Gerratt, J.; Westland, A. D., *Journal of the Chemical Society* **1964**, 734.
- [58] Goggin, P. L.; Goodfellow, R. J., *Journal of the Chemical Society* **1966**, 1462.

- [59] Goodfellow, R. J.; Evans, J. G.; Goggin, P. L.; Duddell, D. A., *Journal of the Chemical Society* **1968**, 1604.
- [60] Mastin, S. H., *Inorg. Chem.* **1974**, *13*, 1003.

4 Salicylamidate ligands: a new N₂O class of chelating phenol ligands

Table of contents

Abstract	148
4.1 New class of salicylamidate ligands	149
4.2 H-bonded salicylamidate ligands	152
4.2.1 Synthesis and characterisation of phenolates [NBu ₄][^{OHNH} L] (42), [NBu ₄][^{NHMe} L] (43) and [NBu ₄][^{NMe2} L] (44)	154
4.2.1.1 X-ray structures	155
4.2.1.2 ¹ H-NMR spectra	157
4.2.1.3 IR spectra	159
4.2.1.3 Electrochemistry	160
4.2.1.4 EPR spectra	163
4.2.1.5 UV/vis spectra	165
4.2.2 Overview	166
4.2.4 Conclusions	170
References	171

Abstract

A new class of phenol-based ligands (salicylamides) has been designed and prepared to mimic the role of the tyrosyl moiety (*ie.* Tyr), namely able to support and stabilize its oxidated form (*ie.* phenoxyl radical) in many redox enzymatic processes.

These salicylamide compounds show important characteristics and their easy synthesis allows to prepare different derivatives, being potentially multidentate, polianionic, bridging and chelating ligands.

In particular, a series of salicylamides (monomethyl **(43)**, dimethyl **(44)** and N-ethanol amides **(42)**) has been prepared in order to investigate the potential stabilization of their corresponding phenolates (*ie.* **(42⁻)**-**(44⁻)**) and phenoxyl radicals (*ie.* **(42[•])**-**(44[•])**). The latter, in fact, display an appreciable stability.

Their characterisation (*ie.* by X-ray, electrochemical studies and ¹H-¹³C-NMR, IR, UV-vis and EPR spectroscopies) and the study of the electronic structure of these species clarify the crucial effect of the intramolecular H-bond in phenolates (**(42⁻)** and **(43⁻)**) and in the electrochemically generated phenoxyl radicals (**(42[•])** and **(43[•])**). Moreover, a quantitative estimate of the H-bond effect has been tentatively carried out and revealed that it exerts a stronger stabilisation on the phenolate form and not (or little) on the oxidized derivative, thus being indicative of an increase of the redox potential.

4.1 New class of salicylamidate ligands

There is a growing interest in the chemistry of phenol-based ligands that can be grouped in a large number of categories with many different features.

We selected a class of phenol ligands based on the 2-hydroxybenzoyl backbone (Figure 4.1). This family of compounds has been object of a wide investigation¹ and many studies² clarified the chemical properties of this molecular scaffold.

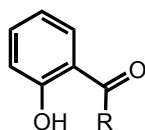
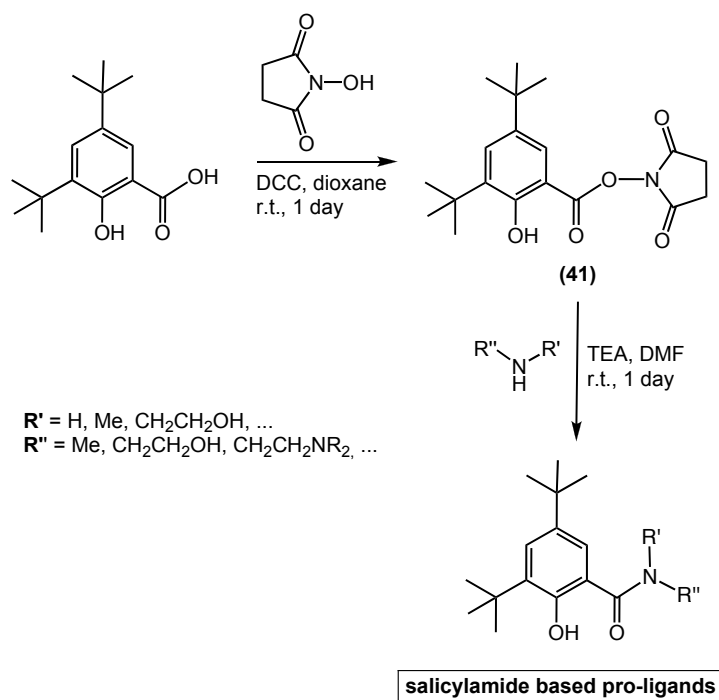


Figure 4.1 The 2-hydroxybenzoyl scaffold.

As reported in the introduction of this thesis, highly oriented syntheses of ligands with peculiar functions is a main interest of this work. Within this family of compounds, the attention has been addressed to the large variety of phenol-based ligands with applications in bioinorganic chemistry.

Their main ability is to be stable to redox conditions and resist in their oxidated forms. For this purpose, in order to fortify the ligand to oxidative degradation, *ortho*- and *para*- positions of the aromatic ring have been substituted with *tert*-butyl groups that confer stability against the decomposition of the oxidized derivative (*i.e.* the 2,4,6-^tBu₃C₆H₂O[•] radical, for instance, is stable in solution, see also Figure 7 of the General Introduction).³

Moreover, to easily achieve a large variety of compounds and extend their diversity toward a multidentate ability, the amidic functionalization of the carbonyl moiety has been planned (Scheme 4.1). The feasibility of the synthetic pathway derives, clearly, from the reduced number of synthetic steps that diversifies just at the last stage. For this reason, a simply large scale reaction to prepare the N-3,5-di-*tert*-butylsalicyloxysuccinimide (**41**) leads to the potential preparation of a large variety of salicylamides.



Scheme 4.1 Synthesis of salicylamide pro-ligands.

In this class of compounds, several pro-ligands have been prepared and hold interesting functionalities (Figure 4.2).

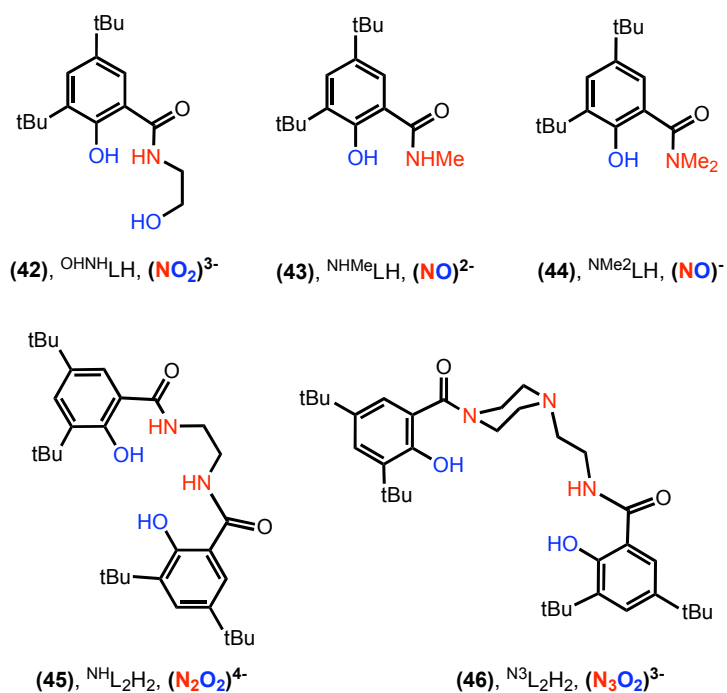


Figure 4.2 Salicyl amidate ligands ((number), abbreviation and denticity) prepared in this study.

From one side, the secondary salicylamides (**42**) and (**43**) upon deprotonation, form polinegative species capable of stabilizing higher oxidation states of the metal centers, and, as will be described in Section 4.2, able to form an H-bond stabilisation of the phenolate derivative for important studies of the phenoxyl radical analogues. On the other side, the multidentated salicylamides (**45**) and (**46**) offer the opportunity to test their coordination chemistry to generate stable metal complexes *e.g.* for potential catalytic applications.

A main intention for the synthesis of this new family of phenol-amide ligands is, indeed, to study their promising character to form a metal-complex able to mimic catalytic redox processes observed in biological systems (Chapter 5). These compounds, in fact, are expected to coordinate and sustain redox metal transitions generating stable phenoxyl radical species. This is a subject of primary interest, since the discovery of a Cu^{II}-tyrosyl radical entity in the active site of the galactose oxidase (GAO) (Figure 4.3),⁴⁻⁶ and these compounds have been designed for this purpose.

4.2 H-bonded salicylamidate ligands

Tyrosyl radical plays a crucial role in many biological systems^{7,8} e.g, it is essential to the catalytic activity of (a) galactose oxidase (GAO), which active site involves a copper(II) ion; (b) the class of iron-dependant ribonucleotide reductase (I RNR) enzymes that play a central role in DNA replication and DNA repair; and of (c) the photosystem II (PSII) which is a highly sophisticated plant-machinery that uses sunlight to split water to O₂ through photosynthesis.

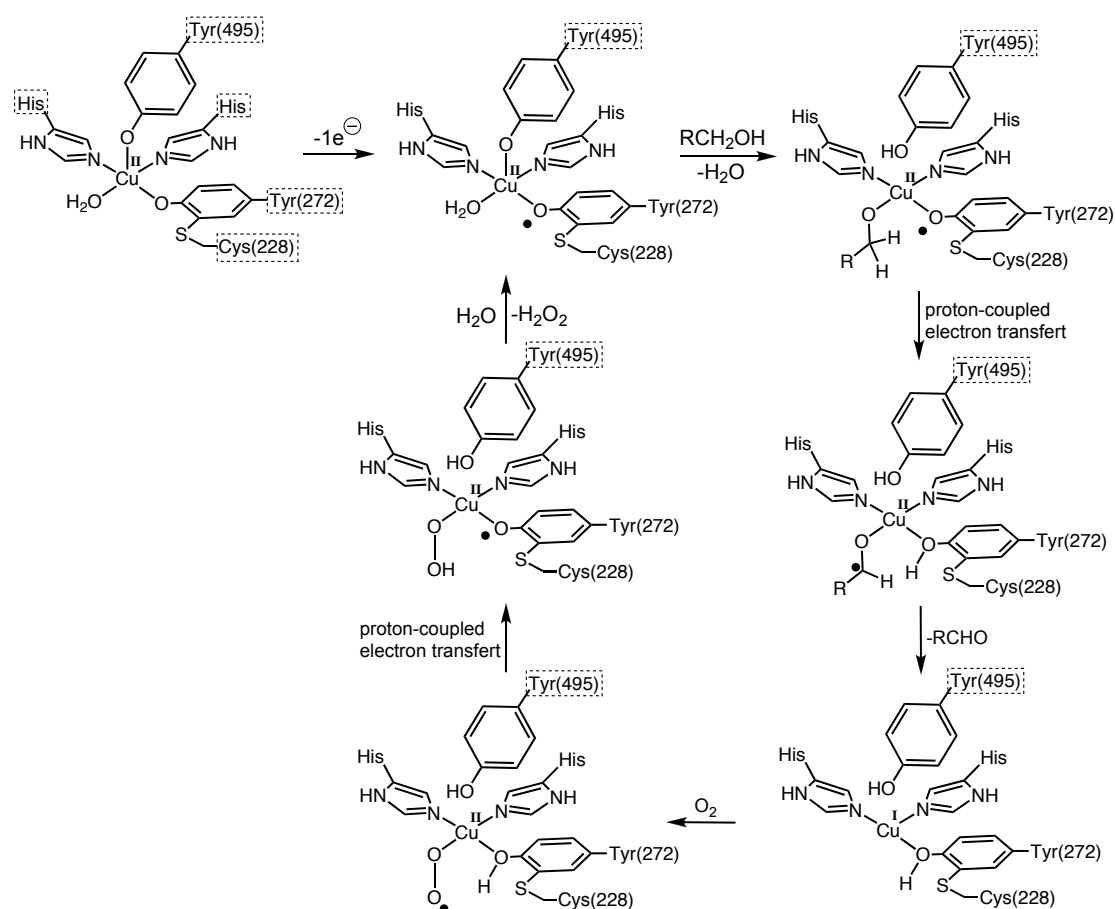


Figure 4.3 Galactose oxidase mechanism.

The local protein environment is expected to exert a considerable influence on the physicochemical properties of the tyrosyl radical. As a matter of fact, the potential of the Tyr[•]/Tyr redox couple varies as: 1.00 V (vs. NHE) for Tyr₁₂₂ in RNR,⁹ 0.72–0.76 V for Tyr_D in PSII¹⁰ and 0.40 V for Tyr₂₇₂ in GAO.^{11,12} Such electrostatic local

environmental changes induce a spin redistribution that affects the radical properties. However, the factors that determine these properties remain to be defined.

Thus, the production of chemical analogues of Tyr[•] in various local environments is of much current theoretical and experimental interest; in particular the studies of the influence of local H-bonding to phenol(ate) and its corresponding phenoxyl radical, are essential to understand the physico-chemical properties of the biological tyrosyl radicals. Remarkably, in less than a decade, relatively stable hydrogen-bonded phenoxyl radicals have been successfully generated by the one electron oxidation of *o,p*-^tBu-protected phenol compounds that are intramolecularly H-bonded to a nitrogen atom from amino, imidazole or pyridine groups.¹²⁻²² This oxidation process is (quasi)-reversible and occurs at much lower potential than for non-hydrogen bonded phenol; both observation has been shown to be a direct consequence of a concerted proton-coupled electron transfer (PCET) mechanism,¹⁹ where both electron and proton are transferred simultaneously to produce an R-O[•]⋯H-N⁺ arrangement. These radicals have also been shown to act as H-atom abstractor.¹⁷⁻¹⁹ However, due to the PCET mechanism involved in these compounds, the understanding of the effect of O-H⋯N H-bonding on the oxidation potential of the phenol and that of R-O[•]⋯H-N⁺ on the stability of the resulting phenoxyl radical has been proved to be difficult.

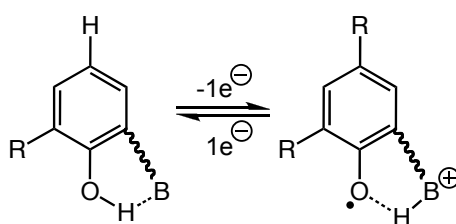


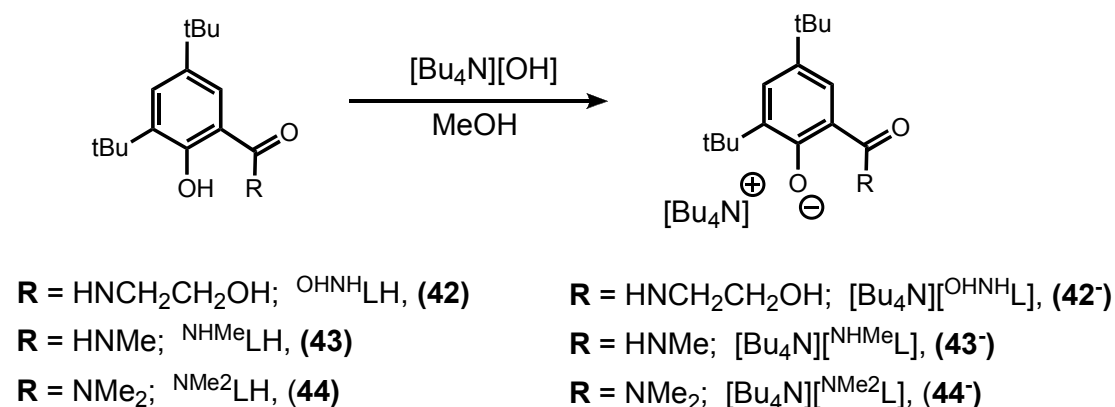
Figure 4.4 Proton-coupled electron transfer (PCET) occurring in redox process of phenols bearing basic pendant.

On the other hand, Kanamori et al.²³ have recently reported that relatively strong (phenolate)O⁻⋯H-N(amide) H-bonding occurs in salicylamidate and isophthalate compounds. These results have prompted us to design and synthesize several unprecedented H-bonded (or not) *o,p*-^tBu-protected salicylamidate compounds, in order to assess the influence of the H-bonding on their oxidation process and their resulting phenoxyl radical species. Thus, phenolates ^{OHNH}L⁻ (**42**),

$^{\text{NHMe}}\text{L}^-$ (**43⁻**) and $^{\text{NMe}_2}\text{L}^-$ (**44⁻**) were prepared to evaluate the effect of H-bonding on the oxidation potential of the phenolate (Scheme 4.2).

4.2.1 Synthesis and characterisation of phenolates $[\text{NBu}_4][^{\text{OHNH}}\text{L}]$ (**42⁻**), $[\text{NBu}_4][^{\text{NHMe}}\text{L}]$ (**43⁻**) and $[\text{NBu}_4][^{\text{NMe}_2}\text{L}]$ (**44⁻**)

The *o,p*-*t*Bu-protected salicylamide compounds, $^{\text{OHNH}}\text{LH}$ (**42**), $^{\text{NHMe}}\text{LH}$ (**43**) and $^{\text{NMe}_2}\text{LH}$ (**44**) have been readily synthesized in high yield²⁴ by the condensation of ethanolamine, methylamine and dimethylamine respectively, onto succinimide-activated 3,5-di-*tert*-butyl salicylic acid (Scheme 4.1). Deprotonation of the phenol moieties using equimolar amount of $[\text{NBu}_4][\text{OH}]$ in MeOH, yields quantitatively the corresponding phenolate salts, $[\text{NBu}_4][^{\text{OHNH}}\text{L}]$ (**42⁻**), $[\text{NBu}_4][^{\text{NHMe}}\text{L}]$ (**43⁻**) and $[\text{NBu}_4][^{\text{NMe}_2}\text{L}]$ (**44⁻**) (Scheme 4.2).



Scheme 4.2 Synthesis of phenolates (**42⁻**), (**43⁻**) and (**44⁻**).

These phenolates exhibit a remarkable stability in air, in solution and in solid state. In particular, is relevant to report the surprising crystalline nature of compounds (**42⁻**) and (**43⁻**) in comparison with (**44⁻**), that allow the determination of the solid state X-ray diffraction crystal structures, performed by Dr. M. Fátima C. Guedes da Silva, of the former phenolates (Section 4.2.1.1). This characteristic could be, essentially, associated to the intramolecular H-bond interaction that occurs for compounds (**42⁻**) and (**43⁻**), between the oxygen of phenolate and the amidic proton that is absent for the tertiary amide in (**44⁻**) (Figure 4.5).

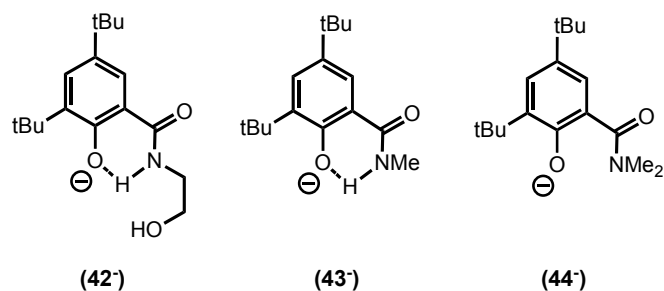
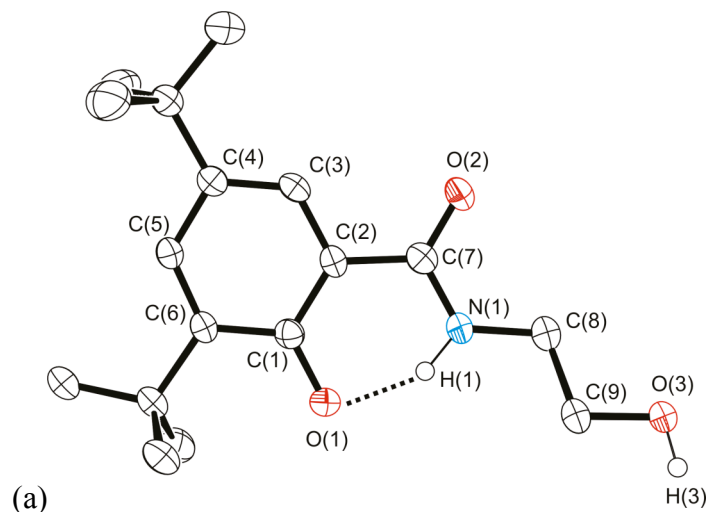
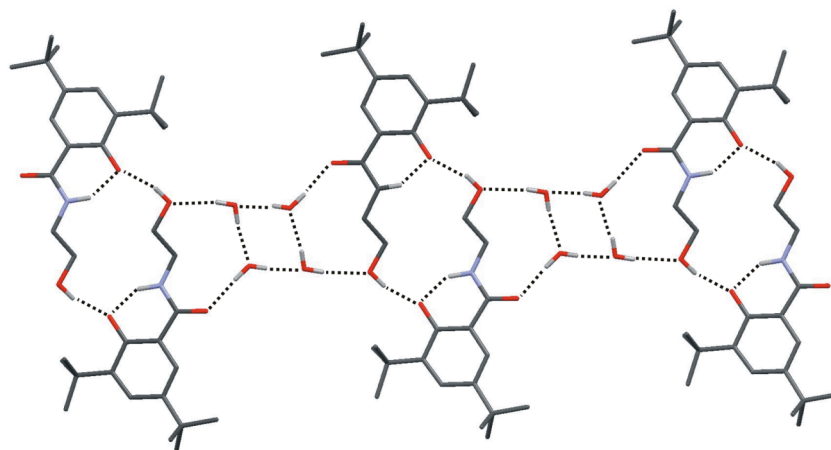


Figure 4.5 H-bonded and no H-bonded phenolates

4.2.1.1 X-ray structures

The molecular structures of both $[\text{NBu}_4][^{\text{OHNH}}\text{L}]\cdot 2\text{H}_2\text{O}$, **(42⁻)** $\cdot 2\text{H}_2\text{O}$, and $[\text{NBu}_4][^{\text{NHMe}}\text{L}]$ **(43⁻)** have been determined by X-ray crystallography (Figures 4.6 and 4.7 and Experimental part). The bond lengths and angles within both structures are as expected for phenolate compounds.²³ Both structures reveal a relatively strong intramolecular $\text{O}^-\cdots\text{H}-\text{N}$ hydrogen bonding²⁵ between the phenolate-O atom and the adjacent N-H amide group, as evidenced by the short $\text{O}\cdots\text{N}$ distance and the $\langle \text{O}(1)\cdots\text{H}(1)-\text{N}(1) \rangle$ angle (*i.e.* 2.585 Å and 145.59° for **(42⁻)** $\cdot 2\text{H}_2\text{O}$ and 2.576 Å and 138.86° for **(43⁻)**, correspondingly).





(b)

Figure 4.6 X-ray structures of $[\text{OHNH L}][\text{NBu}_4] \cdot 2\text{H}_2\text{O}$, the tetrabutylammonium counter anion is omitted for clarity: (a) ORTEP plot, with ellipsoids shown at 50% probability Only the H-atoms of NH and OH groups are shown. (b) MERCURY plot of H-bonding network crystal packing.

These geometrical parameters are comparable to other O-(oxyanion)⋯H-N(amide)/H-O(carboxylic) intramolecular H-bonding in deprotonated salicylamide^{23,26,27}/salicylate^{28,29} compounds. In both structures, the molecule is quasi-planar with a twist angle between the phenolate and CONH plane of ca. 6° and 5.5°, respectively in $[\text{NBu}_4][\text{OHNH L}] \cdot 2\text{H}_2\text{O}$ and $[\text{NBu}_4][\text{NHMe L}]$. In $[\text{NBu}_4][\text{OHNH L}] \cdot 2\text{H}_2\text{O}$, quasi-planar dimers are formed through mutual intermolecular H-bonding interaction between the alcohol pendant arm O(3)-H(3) of one molecule and phenolate-O(1) from another molecule. Additionally, the latter dimer $[\text{OHNH L}]_2$ is connected via H-bonding with tetramer water clusters (Figure 4.6(B)), giving rise to a sort of hydrophilic H-bonding chain sandwiched by hydrocarbon shell generated by the *tert*butyl groups.

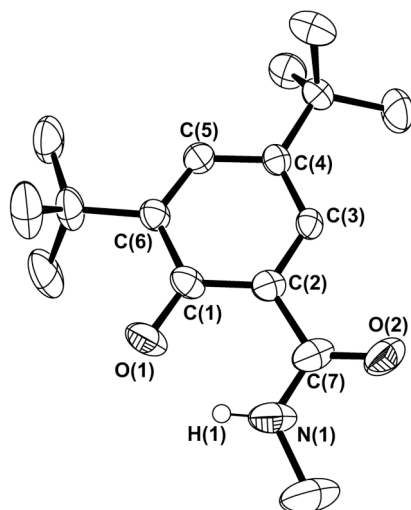


Figure 4.7 ORTEP plot of $[NBu_4][^{MeNH}L]$; with ellipsoids shown at 50% probability.

Table 4.1 Selected bond distances [\AA], angles [$^\circ$] and torsion angles [$^\circ$] compounds $[NBu_4][^{OHNH}L] \cdot 2H_2O$ (**42**) and $[NBu_4][^{MeNH}L]$ (**43**).

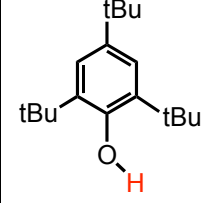
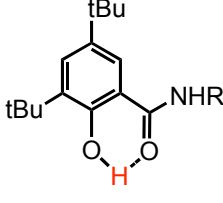
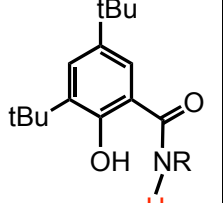
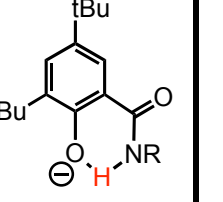
	(42) $\cdot 2H_2O$	(43)		(42) $\cdot 2H_2O$	(43)
C(1)-O(1)	1.303(3)	1.293(5)	N(1)-H(1)	0.93(3)	0.882(2)
C(1)-C(2)	1.426(4)	1.427(6)	O(1) \cdots N(1)	2.585	2.566
C(2)-C(3)	1.399(4)	1.403(6)	O(1) \cdots H(1)-N(1)	145.59	139.02
C(3)-C(4)	1.375(4)	1.374(5)	C(7)N(1)H(1)O(1)	8.36	4.21
C(4)-C(5)	1.406(4),	1.410(6)	C(7)C(2)C(1)O(1)	0.45	5.09
C(5)-C(6)	1.371(4),	1.373(6)			
C(6)-C(1)	1.444(4)	1.443(6)			
C(2)-C(7)	1.482(4)	1.475(6)			
C(7)-O(2)	1.251(3)	1.248(6)			
C(7)-N(1)	1.331(3)	1.325(6)			
C(8)-N(1)	1.443(4)	1.463(6)			

4.2.1.2 ^1H -NMR spectra.

The ^1H NMR spectra of the phenol compounds ^{OHNH}LH (**42**), ^{NHMe}LH (**43**) and $^{NMe_2}LH$ (**44**), in CD_3CN solution, exhibit an phenolic O-H proton resonance in the δ 10-13 ppm range (*i.e.* δ 13.31, 13.39, and 10.33 ppm respectively) characteristic of a O-H \cdots O=C intramolecular H-bonding of the phenol;^{23,27} whereas the amide N-H proton resonance observed in the aromatic region (δ 7.37, 7.48 ppm respectively for

($^{\text{NHMe}}\text{LH}$, $^{\text{OHNH}}\text{LH}$) are typically indicative of a non-hydrogen bonded amide NH (Tables 4.2 and 4.3).

Table 4.2 Selected $^1\text{H-NMR}$ (δ) (CD_3CN) resonances of H-bonded and non H-bonded phenolic and amidic protons.

				
$^1\text{H-NMR}$	ca. 5 ppm	ca. 11-13 ppm	ca. 7 ppm	ca. 12-13 ppm

In contrast, the $^1\text{H-NMR}$ spectra in CD_3CN of each of the corresponding phenolate salts $[\text{NBu}_4][^{\text{NRR}'}\text{L}^-]$ (**42** $^-$) and (**43** $^-$), display N-H proton resonances at much lower field (*i.e.* ca. 13 ppm for $^{\text{OHNH}}\text{L}^-$ and $^{\text{MeNH}}\text{L}^-$), typically indicating that the N-H proton is involved in an intramolecular $\text{O}^-\cdots\text{H-N}$ hydrogen bonding.²³ Moreover the $^1\text{H}/^{14}\text{N}$ -HSQC NMR experiment validated the assignment for (**42** $^-$) that incorporates a second hydroxyl moiety: the sharp singlet at 13.90 ppm could be effectively ascribed to the H-bonded amidic proton.

This assignment is further confirmed by the absence of the NH proton neither for the $^{\text{NMe}_2}\text{L}^-$ (**44** $^-$) in CD_3CN (which does not possess N-H group) nor for $^{\text{OHNH}}\text{L}^-$ and $^{\text{MeNH}}\text{L}^-$ in proton-exchangeable solvent such as MeOD. These NMR data demonstrate that the $\text{O}^-\cdots\text{H-N}$ H-bonding identified in the solid state, *i.e.* in the X-ray structure of $[\text{NBu}_4][^{\text{OHNH}}\text{L}^-]\cdot 2\text{H}_2\text{O}$ (**42** $^-$) and $[\text{NBu}_4][^{\text{MeNH}}\text{L}^-]$ (**43** $^-$), is preserved in solution.

Recently, theoretical studies performed by Dr. Maxim Kuznetsov allow to explain the atypical difference on the phenolic O-H proton resonances in the $^1\text{H-NMR}$ spectra of (**43**) and (**44**) (*i.e.* δ 13.39, and 10.33 ppm, respectively). Considering the most favorite conformations of (**43**) and (**44**), there is a significant twist of the CO bond from the ArOH plane in the (**44**) conformation due to a steric interaction of the amidic methyl group with a aromatic *meta*-hydrogen (Figure 4.8). This deviation could weaken the H-bond interaction and explain the shift to higher field (δ 10.33 ppm) in $^1\text{H-NMR}$ spectrum.

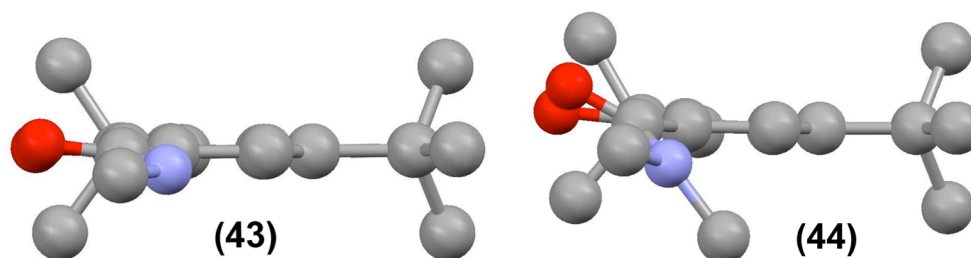


Figure 4.8 Schematic representation of the most favorite conformations for phenols $^{\text{NHMe}}\text{LH}$ (43) and $^{\text{NMe}_2}\text{LH}$ (44) (hydrogens are omitted for clarity).

4.2.1.3 IR spectra

The IR spectra (KBr pellets and in CH_3CN solution, Table 4.3) of the phenol compounds, $^{\text{OHNH}}\text{LH}$ (42), $^{\text{NHMe}}\text{LH}$ (43) and $^{\text{NMe}_2}\text{LH}$ (44), confirm the H-bonded effect^{30,31} (*i.e.* with CO oxygen) on the frequency of the O-H bonds (*i.e.* in KBr: 3313, 3328, and 3127 cm^{-1} , respectively) that are expected to downshift to lower wavenumbers. The same bands were not detected in the corresponding IR spectra in acetonitrile solution, where the O-H vibration could be conceivably suppressed by the H-bond interaction.

On the other hand, the $\nu(\text{NH})$ appears to downshift moving from phenols to phenolates (*i.e.* for the couples $^{\text{NHMe}}\text{LH}/^{\text{NHMe}}\text{L}^-$ (43)/(43⁻) and $^{\text{OHNH}}\text{LH}/^{\text{OHNH}}\text{L}^-$ (42)/(42⁻) in KBr: 3419/3274 and 3486/3114 cm^{-1} respectively and similarly in acetonitrile) indicating the influence of $\text{O}^-\cdots\text{H}-\text{N}$ hydrogen bonding to the stretching frequency of N-H bond.

Table 4.3 Selected $^1\text{H-NMR}$ (δ) (CD_3CN) resonances and IR (KBr and CH_3CN) bands of phenols (42)-(44) and phenolates (42⁻)-(44⁻).

	$^1\text{H NMR}$ (CD_3CN)		IR (KBr)			IR (CH_3CN)		
	<i>HO-Ar</i>	<i>HNCO</i>	<i>H-OAr</i>	<i>H-NCO</i>	<i>C=O</i>	<i>H-OAr</i>	<i>H-NCO</i>	<i>C=O</i>
(42)	13.31	7.48 ^a	3313	3486	1624	n.d.	3411	1634
(43)	13.39	7.37 ^a	3328	3419	1620	n.d.	3413	1639
(44)	10.31	-	3127	-	1612	n.d.	-	1622
(42 ⁻)	-	13.902	-	3114	1617	-	3005 ^b	1623
(43 ⁻)	-	13.198	-	3274	1623	-	3009 ^b	1625
(44 ⁻)	-	-	-	-	1638 ^a	-	-	1633

(^a) in nujol; (^b) weak bands.

This effect is even more pronounced for IR spectra in solution that apparently display the $\nu(\text{NH})$ of the H-bonded N-H bond at 3005-9 cm^{-1} for **(42⁻)** and **(43⁻)**, respectively (Table 4.3). These IR-bands appear more tenuous than the corresponding $\nu(\text{CH})$ bands, since the bond vibration is possibly attenuated by the H-bond. Nevertheless, the assignment was confirmed by the shifting of the frequency upon exchange* with deuterium (Figure 4.9).

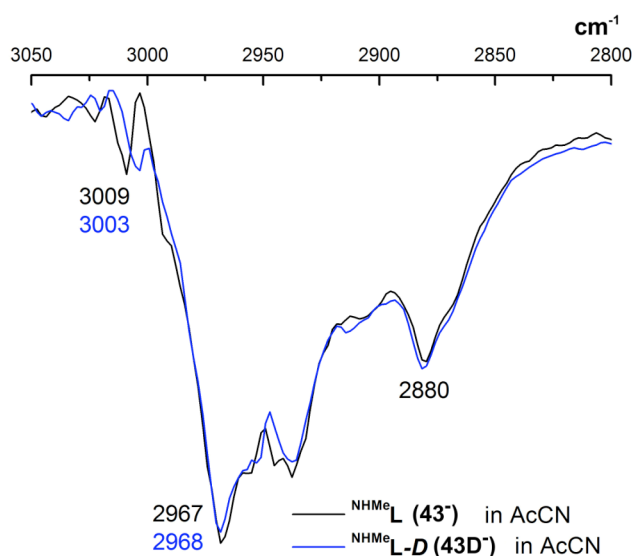
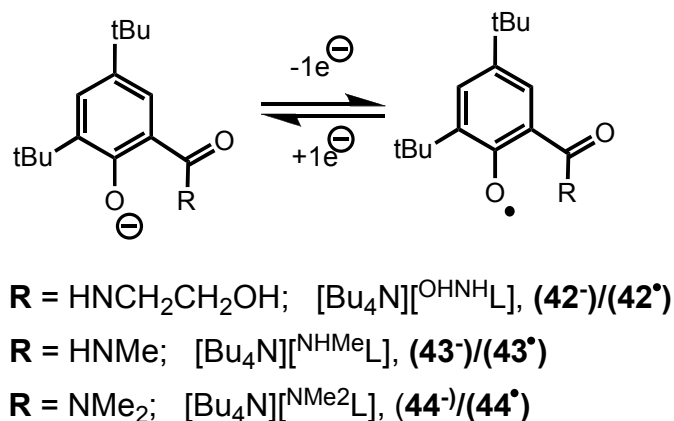


Figure 4.9 IR (CH_3CN) spectra ($3050\text{-}2800\text{ cm}^{-1}$) of phenolate (**43⁻**) and its corresponding deuterated derivative (**43D⁻**).

4.2.1.4 Electrochemistry

The cyclic voltammogram of each phenolate salts $\text{NRR}'\text{L}^-$ (**42⁻**), (**43⁻**) and (**44⁻**), in CH_3CN at 298 K containing $[\text{NBu}_4][\text{BF}_4]$ (0.2 M), exhibits a fully reversible one-electron oxidation process (see Figure 4.10 and Experimental part) associated with the formation of the corresponding phenoxyl radical compounds (Scheme 4.3). This oxidation process occurs at $E_{1/2}^{\text{ox}}/\text{V}$ vs. $\text{Fc}^{0/+}$ ($\text{Fc} = [\text{Fe}(\eta^5\text{-C}_5\text{H}_5)_2]$) = -0.119; -0.161 and -0.423 respectively for OHNHL^- (**42⁻**), NHMeL^- (**43⁻**) and NMe_2L^- (**44⁻**) (Table 4.4).

(*) Compounds (*i.e.* **(42⁻)** and **(43⁻)**) were dissolved in $\text{MeOH-}d_4$, stirred for 30 minutes and evaporated under vacuum.



Scheme 4.3 Reversible oxidation of phenolates (**42**⁻), (**43**⁻) and (**44**⁻) to the corresponding (**42**[•]), (**43**[•]) and (**44**[•]) phenoxyl radicals.

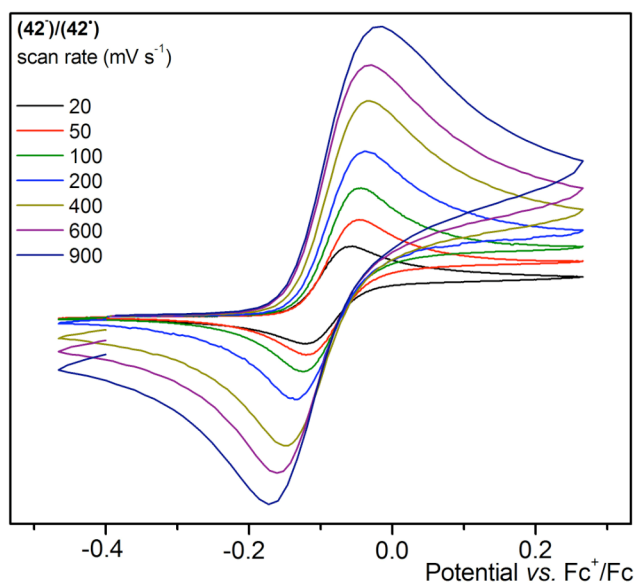


Figure 4.10 Cyclic voltammograms of a 1mM solution of phenolates (**42**⁻) in CH₃CN with 0.2 M [NBu₄][BF₄], at a platinum disc electrode (*d* = 0.5 mm).

For comparative purposes, the tetrabutylammonium 2,4,6-tris-*tert*-butylphenolate salt (*i.e.* [Bu₄N][^{tBu}L]) has been prepared and studied. It is described,^{32,33} in fact, the remarkable stability of the corresponding phenoxyl radical (^{tBu}L[•]), mainly due to its *ortho tert*-butyl groups (*i.e.* at 2 and 6-positions) that play an efficient steric shielding. The oxidation potentials $E_{1/2}^{\text{ox}}$ of these phenolates highlight the difference among them: the oxidation wave for (^{tBu}L⁻)/(^{tBu}L[•]) couple appears at the lowest potential (*i.e.* -0.572 V vs. Fc^{0/+}) in comparison to the others amide-based phenolates, *i.e.* the dimethylamide derivative (**44**⁻) at -0.423 V vs. Fc^{0/+} and finally the

two H-bonded amides (*i.e.* at -0.161 and -0.119 V vs. $\text{Fc}^{0/+}$ for **(43⁻)** and **(42⁻)**, respectively) (Figure 4.11).

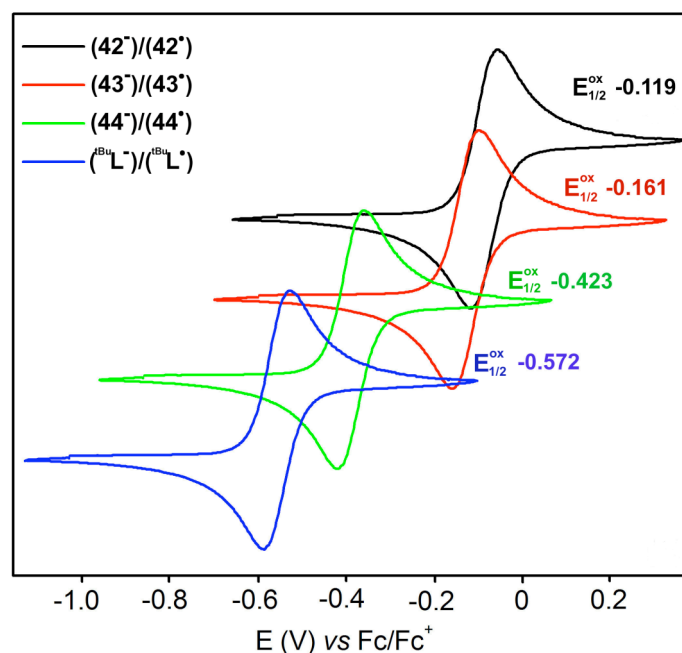


Figure 4.11 Comparative representation of cyclic voltammograms ($v = 120 \text{ mV s}^{-1}$) of 1 mM solutions in CH_3CN of phenolates **(42⁻)** (black line), **(43⁻)** (red), **(44⁻)** (green) and $(^{\text{tBu}}\text{L}^-)$ ($(^{\text{tBu}}\text{L}^-)$ = tetrabutylammonium 2,4,6-tris-tertbutylphenolate salt) (blue) in CH_3CN with 0.2 M $[\text{NBu}_4][\text{BF}_4]$, at a platinum disc electrode ($d = 0.5 \text{ mm}$).

In particular, a great attention should be dedicated to the parallel between **(43⁻)** and **(44⁻)**: the two phenolates differ only at just the methyl group onto the amide moiety. The effect on the potential of the electronic donation of the extra methyl group on the corresponding electron density of phenolate is expected to be minimal. Consequently, this difference of potentials (*i.e.* $\Delta E = 0.262 \text{ mV}$) should depend exclusively on the presence of the intramolecular H-bond, between the phenolate and the amidic proton. This interaction could, indeed, decrease the electron density of the O-phenolate making it harder to oxidize. This consideration could be extended to the H-bonded phenolate **(42⁻)** that, in fact, shows a comparable oxidation potential.

Additionally, the oxidation of the non-hydrogen bonded phenolate **(44⁻)** ($E_{1/2}^{\text{ox}} = -0.423 \text{ V vs. Fc}^{0/+}$) occurs at a higher potential than that of $(^{\text{tBu}}\text{L}^-)$ ($E_{1/2}^{\text{ox}} = -0.572 \text{ V vs. Fc}^{0/+}$ in CH_3CN ³²), and can be explained by taking into account (a) the electron donating properties of the additional *ortho*-tBu group which increase the electron

density at the oxygen atom in ArO^- and (b) the electron withdrawing effect of the amide functionality in **(44⁻)** which decreases the electron density at the O atom in **(44⁻)**). Both effects contribute to increase the difference between the oxidation potentials up to 149 mV.

Table 4.4 Potentials (vs. $\text{Fc}^{0/+}$ at 120 mVs^{-1}) for compounds **(42⁻)**, **(43⁻)** and **(44⁻)** in acetonitrile and dichloromethane.

	$E_{1/2}^{\text{ox}} / \text{V}^{(a)}$	$E_p^{\text{ox}} / \text{mV}^{(b)}$	$\Delta E / \text{mV}^{(c)}$	$E_{1/2}^{\text{ox}} / \text{V}^{(d)}$
(42⁻)	-0.119	-89	61	-0.248
(43⁻)	-0.161	-129	65	-0.300
(44⁻)	-0.423	-385	77	-0.544

^(a) in CH_3CN . ^(b) oxidation peak potential. ^(c) $\Delta E = E_p^{\text{ox}} - E_p^{\text{red}}$. ^(d) in CH_2Cl_2 .

It is noteworthy to verify the same shift of the oxidation potentials for these compounds when performing the CV in dichloromethane (Table 4.4). In this solvent a uniform cathodic shifting (*ca.* 130 mV) could be noticed for all compounds with respect of reference potential (*i.e.* that of Ferrocene/Ferricinium), indicating a possible effect of the solvent on these organic phenolates in comparison to ferrocene; but the relative differences among **(42⁻)**, **(43⁻)** and **(44⁻)** persist.

The remarkable reversibility obtained for the hydrogen-bonded salts $^{\text{NHMe}}\text{L}^-$ and $^{\text{OHNH}}\text{L}^-$ implies that the H-bonding interaction is presumably preserved in its corresponding radical form. On the contrary, if the H-bonded would be broken upon oxidation, the corresponding reduction would be, in principle, at a lower potential and then the process would lose its full reversibility.

The electrochemical one-electron oxidation of each $^{\text{NRR}}\text{L}^-$, in CH_3CN at room temperature, leads to the corresponding stable (for several hours under inert atmosphere, as indicated by the persistency of their visible spectra) bright-green-coloured phenoxyl radical species $^{\text{NRR}}\text{L}^\bullet$, as indicated by their UV/vis and EPR spectra (Sections 4.2.1.4 and 4.2.1.5).

4.2.1.5 EPR spectra

The X-band EPR measurements in fluid (room temperature) and frozen (120K) acetonitrile solution of each of the electrochemically generated phenoxyl radicals

$^{\text{NRR}}\text{L}^\bullet$ in CH_3CN exhibit a typical isotropic radical signal centered at $g_{\text{iso}}^{(*)} = 2.0043$ ($^{\text{OHNH}}\text{L}^\bullet$) (**(42')**), 2.0042 ($^{\text{NHMe}}\text{L}^\bullet$) (**(43')**), and 2.0046 ($^{\text{NMe}_2}\text{L}^\bullet$) (**(44')**), a peak-to-peak linewidth of 3.4, 4.0 and 4.2 G, respectively (see Figure 4.12).

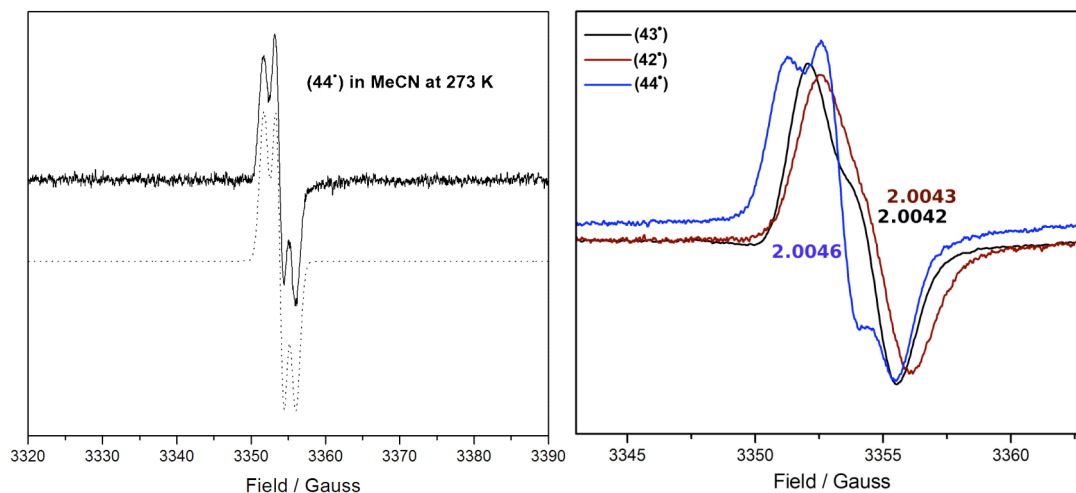


Figure 4.12 (right) EPR spectra of CH_3CN fluid solutions of the electrochemically generated (**(42')**), (**(43')**), (**(44')**), recorded at 263K. (left) EPR spectrum of the CH_3CN fluid solution of (**(44')**) at 270K (0.3 modulation amplitude) and simulated spectrum (dashed line).

The small line width of each signal indicates that there is no significant coupling with the N-atom from the amide function, implying thus that the unpaired electron is not (or very little) delocalized on the amide group (Figure 4.12 left). The nitrogen atom (^{14}N) has, in fact, a nuclear magnetic moment, $I = 1$, which, in case of hyperfine coupling, should triple the multiplicity of the EPR signal. The latter exhibits an hyperfine coupling with both meta-protons of the phenoxy ring. Each of the EPR spectra was simulated (Figure 4.12, left, dashed line) and as expected for a o,p- ^tBu -phenoxy radical, the hyperfine coupling to the meta-proton is relatively small ($<2\text{G}$)³⁴ in agreement with the odd alternant pattern where the electron density is mainly spread on the O-atom, at both *ortho*- and *para*-positions of the phenoxy ring.

The EPR data indicate a relatively large g_{iso} -shift of 0.0005-6 between the signals of the non-hydrogen bonded $^{\text{NMe}_2}\text{L}^\bullet$ (**(44')**) ($g = 2.0046$) and those of $^{\text{OHNH}}\text{L}^\bullet$ (**(42')**) ($g = 2.0043$) and $^{\text{NHMe}}\text{L}^\bullet$ (**(43')**) ($g = 2.0042$) (Figure 4.12 right). Since theoretical³⁵⁻³⁸ and experimental studies^{13,22,39-41} have indicated that hydrogen bonding

* The suffix 'iso' indicates the isotropic character of the signal that is independent from the three orientations (g_x , g_y and g_z) of the magnetic field.

to a phenoxyl (or tyrosyl) radical results in a considerable lowering of the g_x value but leaves g_y and g_z essentially unaffected, one can assume that the g_y and g_z are identical for ${}^{\text{NMe}_2}\text{L}^\bullet$, ${}^{\text{NHMe}}\text{L}^\bullet$ and ${}^{\text{OHNH}}\text{L}^\bullet$. Consequently, a Δg_{iso} of 0.0005 would give a $\Delta g_x = 3\Delta g_{\text{iso}} = 0.0015$. Such a g_x shift is in good agreement with the g_x -shift observed between H-bonded phenoxyl (tyrosyl) radical ($2.0061 < g_x < 2.0068$, phenoxyl^{13,22,40,42} and $2.0075 < g_x < 2.0076$ ^{43,44}, biological Tyr radicals) and non-hydrogen bonding phenoxyl radical such as (tBu)3-phenoxyl radical ($g_x = 2.00735$)⁴⁰ or "free" tyrosyl radicals Tyr \bullet ($g_x = 2.0087-89$)⁴¹⁻⁴⁵. Thus, the g_{iso} -shift observed between **(44'**) and **(42'**) or **(43'**) evidences the presence of the H-bond N-H \cdots O H-bonding in ${}^{\text{NHMe}}\text{L}^\bullet$ and ${}^{\text{OHNH}}\text{L}^\bullet$.

4.2.1.6 UV/vis spectra

The UV/vis spectrum of each oxidized species ${}^{\text{NRR}'}\text{L}^\bullet$ exhibits two intense bands at *ca.* 400 nm ($\epsilon > 1000 \text{ M}^{-1}\text{cm}^{-1}$) and a weak NIR (near infra red) broad band at 600-700 nm (ϵ *ca.* $250 \text{ M}^{-1}\text{cm}^{-1}$), which are characteristics of free or H-bonded phenoxyl radicals transitions (Figure 4.13).^{3,12,14,16,22}

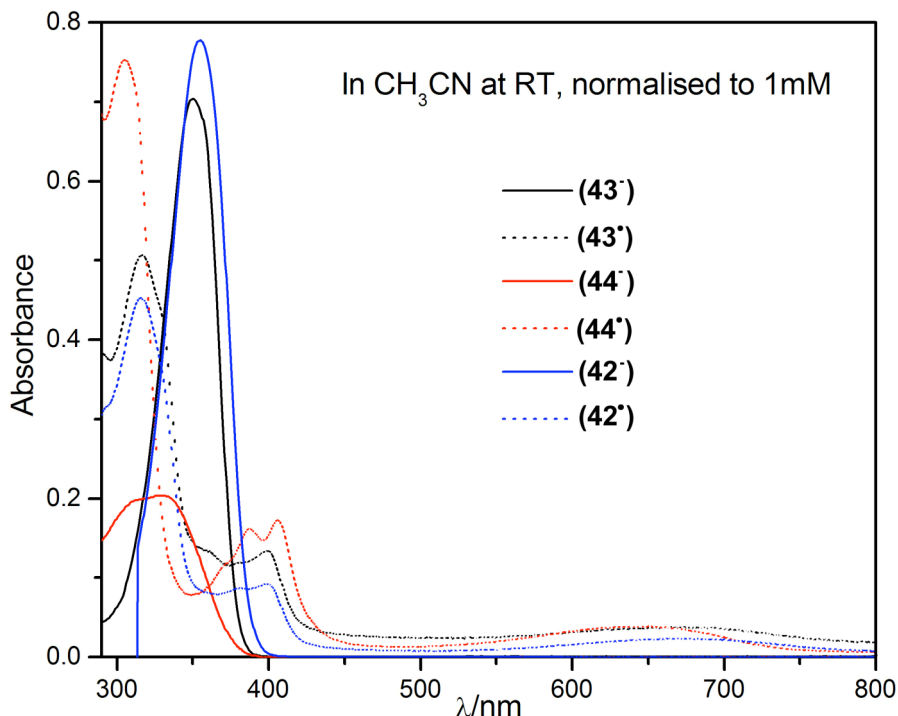


Figure 4.13 Room-temperature UV/vis spectra of CH_3CN solutions of **(42)**, **(43)**, **(44)** (*ca.* 1mM) and their corresponding electrochemically generated radicals **(42')**, **(43')** and **(44')** in CH_3CN containing $[\text{NBu}_4][\text{BF}_4]$ (0.2 M).

The $\epsilon_{400}/\epsilon_{700}$ ratio between the intensities of the *ca.* 400 nm (π - π^* transitions) and the *ca.* 700 nm bands appears to be indicative of the delocalization of the phenoxyl unpaired electron; *i.e.* for the "pure" phenoxyl radical $\epsilon_{400}/\epsilon_{700}$ is *ca.* 5, whereas for the highly delocalized radical $\epsilon_{400}/\epsilon_{700}$ can even be < 1 .¹² Thus, the $\epsilon_{400}/\epsilon_{700}$ ratio observed for each of the studied radicals strongly indicates that there is no or very little delocalization of the unpaired electron in $^{\text{NRR}}\text{L}^\bullet$ onto the amide backbone, and that the electronic structure of the $^{\text{NRR}}\text{L}^\bullet$ resembles that of a phenoxyl radical.

4.2.2 Overview

In view of the above results, clearly the one-electron oxidation of the H-bonded phenolate salts $^{\text{OHNH}}\text{L}^-$ (**42**⁻) and $^{\text{NHMe}}\text{L}^-$ (**43**⁻) and of the non-hydrogen-bonded analogue $^{\text{NMe}_2}\text{L}^-$ (**44**⁻) produces stable radical species, which are identified as phenoxyl radicals. Moreover, the experimental data are consistent with the oxidized products $^{\text{OHNH}}\text{L}^\bullet$ (**42**[•]) and $^{\text{NHMe}}\text{L}^\bullet$ (**43**[•]) being **H-bonded phenoxyl radicals**.

Indeed (a) the remarkable reversibility of the oxidation process of their phenolate precursors (*i.e.* (**42**⁻) and (**43**⁻)) most likely indicates a retention of the N-H \cdots (-/ \bullet O) H-bond upon oxidation. The large difference in the redox potential between the H-bonded and the non H-bonded phenolate, $\Delta E = E(^{\text{NMe}_2}\text{L}^{0/-}) - E(^{\text{NHMe}}\text{L}^{0/-}) = 0.262\text{V}$, further emphasizes this point; (b) the most striking effect resulting from the N-H \cdots (-/ \bullet O) H-bonding in these compounds is revealed by the analysis of the redox potentials (Scheme 4.3). As established above, $^{\text{NHMe}}\text{L}^-$ (**43**⁻) possesses a strong O \cdots H-N hydrogen bond but $^{\text{NMe}_2}\text{L}^-$ (**44**⁻) does not. This difference is correlated by an increase of the oxidation potential by 262 mV from $^{\text{NMe}_2}\text{L}^-$ to $^{\text{NHMe}}\text{L}^-$ which corresponds to a difference in energy of $25.3 \text{ kJ}\cdot\text{mol}^{-1}$ or *ca.* $6 \text{ kcal}\cdot\text{mol}^{-1}$. Since most hydrogen bonding are $3 - 8 \text{ kcal}\cdot\text{mol}^{-1}$, the difference observed clearly results from the H-bonding interaction.

This result is in great contrast with recent observations by Mayer *et al.*¹⁹ that H-bonding does not induce significant redox shift since the potential value ($E_{1/2} = -0.57 \text{ V vs. Fc}^+/\text{Fc}$) for the intramolecularly hydrogen-bonded phenoxide $^-\text{OAr-NH}_2$ in CH_3CN was essentially identical to that of ArO^- (Figure 4.14), although no X-ray structure of the phenolate salt $^-\text{OAr-NH}_2$ has been reported. Since the difference

between the two latter compounds is very small, it has been suggested that H-bond does not exert a significant effect on the oxidation potential of the phenolate.

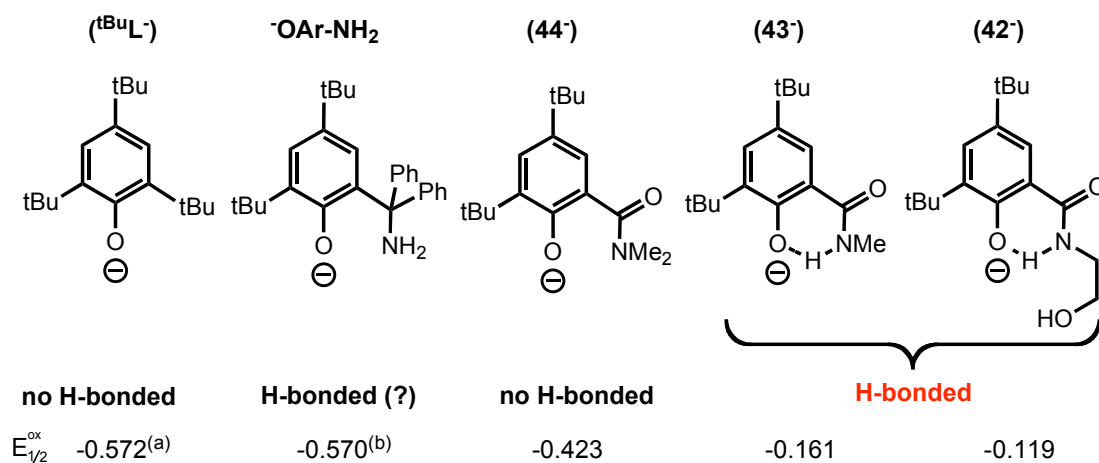


Figure 4.14 Parallel representation of different H-bonded and non-H-Bonded phenolates.

$E_{1/2}^{ox}$ values in V vs. $Fc^{0/+}$ (^(a) = ref³², ^(b) = ref¹⁹).

On the contrary, our compounds are oxidised at some 450 mV higher than the phenolate compound cited above; this difference could be partially ascribed to the presence of an amide functionality at the *ortho* position of the phenolate group, which exerts an electron withdrawing effect, but the crucial difference between (43⁻) and (44⁻) described above is a stronger proof for the evidence of the H-bond effect.

Moreover, in the Mayer's work no experimental confirmations of the permanent H-bonding are presented for ⁻OAr-NH₂, that in this case should assume a not-conjugated six-member ring (Figure 4.15 left) drastically different from the conjugated H-bonds phenols (Resonance Assisted Hydrogen Bonding, RAHB, Figure 4.15 right).⁴⁶ In the latter, the presence of conjugated bonds allows strengthening the hydrogen-bond ability of the two terminations.² This stronger H-bond interaction (RAHB) of our phenolates could be directly correlated to their higher oxidation potential in comparison to the Mayer example, ⁻OAr-NH₂.

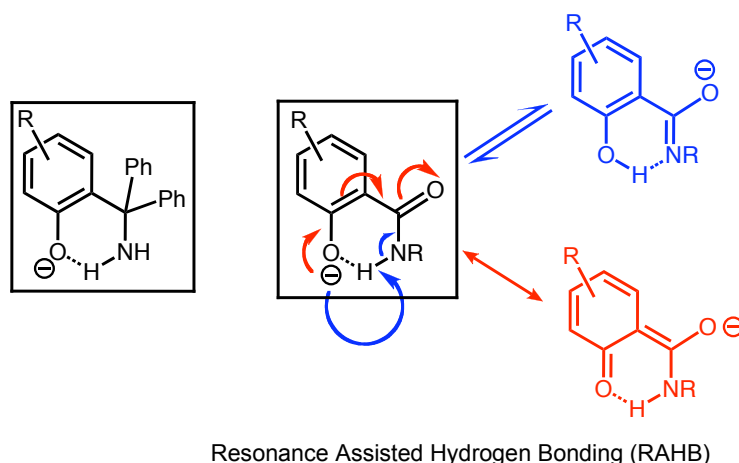
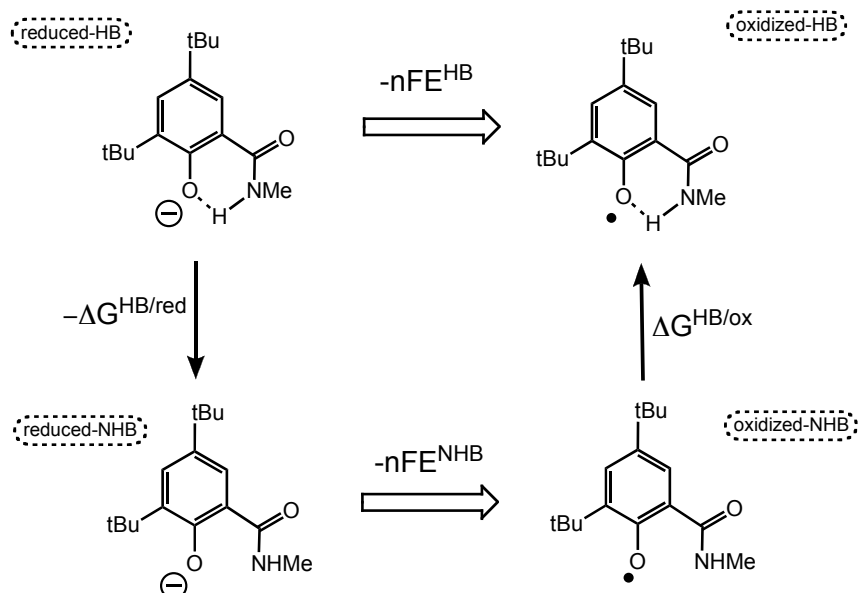


Figure 4.15 Representation of non-conjugated intramolecular H-bond (left) and the Resonance Assisted H-bond (RAHB, right).

The oxidation of the hydrogen-bonded phenolate can be described by the thermochemical cycle depicted in Scheme 4.4, which clearly shows that the difference in redox potential between non-hydrogen bonded and hydrogen-bonded phenolate ($\Delta E = E^{\text{HB}} - E^{\text{NHB}}$) is related to the difference $\Delta\Delta G (= \Delta G^{\text{HB/red}} - \Delta G^{\text{HB/ox}})$ between the H-bonding energy in the phenolate, reduced form ($\Delta G^{\text{HB/red}}$), and that in the phenoxy radical, oxidised form ($\Delta G^{\text{HB/ox}}$).¹⁹



Scheme 4.4 Thermochemical cycle indicating the effect of hydrogen bonding on redox potentials.

Since ${}^{\text{NHMe}}\text{L}^-$ (**43**⁻) and ${}^{\text{NMe}_2}\text{L}^-$ (**44**⁻) only differ (assuming that the electronic induction donating effect of the methyl ring is minimal) by the presence of hydrogen bonding, $\Delta E = E^{\text{HB}} - E^{\text{NHB}}$ is approximated to $E({}^{\text{NHMe}}\text{L}^{0/-}) - E({}^{\text{NMe}_2}\text{L}^{0/-}) = 0.262\text{V}$ which corresponds to a difference in energy of $25.3 \text{ kJ}\cdot\text{mol}^{-1}$ (or ca. $6 \text{ kcal}\cdot\text{mol}^{-1}$). This implies that in our case the determination of the energy difference between the hydrogen bonded (HB) and the non hydrogen bonded (NHB) phenolates should consider the following four species (Scheme 4.4): reduced-HB, reduced-NHB, oxidized-NHB and oxidized HB. Thus, for the thermochemical cycle in Scheme 4.4, it is possible to consider¹⁹ the equation:

$$-nFE^{\text{HB}} = -\Delta G^{\text{HB/red}} - nFE^{\text{NHB}} + \Delta G^{\text{HB/ox}} \quad [1]$$

where $-nFE^{\text{HB}}$ and $-nFE^{\text{NHB}}$ are the energies^(*) of the oxidation processes of HB (hydrogen bonded) and NHB (non hydrogen bonded) species, respectively; and $\Delta G^{\text{HB/red}}$ and $\Delta G^{\text{HB/ox}}$ are the H-bonding energies of the reduced and oxidized forms. Then, we can rewrite [1] replacing the potential for our case:

$$-nF(-E^{\text{NHMeL}}) = -\Delta G^{\text{HB/red}} - nF(-E^{\text{NMe}_2\text{L}}) + \Delta G^{\text{HB/ox}} \quad [2]$$

and we obtain

$$-nF(E^{\text{NHMeL}} - E^{\text{NMe}_2\text{L}}) = \Delta G^{\text{HB/red}} - \Delta G^{\text{HB/ox}}$$

$$-96485(0.262) = \Delta G^{\text{HB/red}} - \Delta G^{\text{HB/ox}}$$

$$\Delta\Delta G = |\Delta G^{\text{HB/red}} - \Delta G^{\text{HB/ox}}| = 25.3 \text{ kJ}\cdot\text{mol}^{-1} = \text{ca. } 6 \text{ kcal}\cdot\text{mol}^{-1}$$

Thus, the difference in H-bonding energies, $\Delta\Delta G$, is of ca. $6 \text{ kcal}\cdot\text{mol}^{-1}$. Since most hydrogen bonding energies are $3 - 8 \text{ kcal}\cdot\text{mol}^{-1}$, these results indicate that the H-bonding interaction is much stronger for the phenolate (*i.e.* the reduced form) than for its corresponding phenoxyl radical (*i.e.* the oxidized form) and considering the scale

* Considering the free energy equation $\Delta G = -nFE$ ($n = n^\circ$ of moles, $F = \text{Faraday's constant}$; for a spontaneous process, $\Delta G < 0$ and $E > 0$, where $E = E_{\text{ref}} - E_{\text{sample}} = -E_{\text{sample}}$).

of hydrogen bonding energy, the latter H-bond appears to be relatively weak (2-3 kcal).

This, in turn, means that the effect of the H-bonding on the redox potential is mainly exerted on the phenolate and not (or a little) on the phenoxyl radical. Also, it is probable that it is the decrease of the O-phenolate electron density atom anion upon H-bonding that makes the latter to be harder to oxidise (increase of redox potential). Therefore, the redox potential of the phenoxyl radical can be tuned through the H-bonding interaction.

Recently, a theoretical and an experimental estimate of pK_a values of **(43)** and **(44)** has been planned. This study could, in principle, give a definitive support to the previous discussion: assuming that the pK_a values of the phenol/phenolates couples for **(43)**/**(43⁻)** and **(44)**/**(44⁻)** could exclusively depend on the stabilisation of phenolate form that occurs for **(43⁻)** and not for **(44⁻)**. Thus, the resulting difference on pK_a could be correlated to the H-bonding energy of phenolate ($\Delta G^{HB/red}$) to calculate the absolute value of $\Delta G^{HB/red}$ and allow to estimate the stabilisation of H-bond on the phenoxyl radical species, $\Delta G^{HB/ox}$.

4.2.4 Conclusions

These results emphasized the fascinating research around this type of phenol-based ligands. As illustrated in the introduction, the description of the electronic structures of these compounds and their corresponding oxidized derivatives is of a crucial interest for the development of knowledge of these phenol-ligands in bioinorganic chemistry. The study of stability of these phenoxyl radical systems contributes to have a better overview on the physicochemical properties of the tyrosyl radical in biological systems.^{7,8}

Moreover, with this research it has been possible to get a good method to easily achieve H-bonded stable phenoxyl radical species for further investigations on radical chemistry.

The detailed characterisation of compounds **(42)**, **(43)** and **(44)** and their derivatives represent an excellent platform to extend the study toward their potential metal complexes.

References

- [1] Palomar, J.; De Paz, J. L. G.; Catalan, J., *Chem. Phys.* **1999**, *246*, 167.
- [2] *The Chemistry of Phenols, Chapter 8*. John Wiley & Sons, Ltd 2003; p 529.
- [3] Altwicker, E. R., *Chem. Rev.* **1967**, *67*, 475.
- [4] Borman, C. D.; Saysell, C. G.; Sokolowski, A.; Twitchett, M. B.; Wright, C.; Sykes, A. G., *Coord. Chem. Rev.* **1999**, *771*, 190.
- [5] Thomas, F., *Eur. J. Inorg. Chem.* **2007**, 2379.
- [6] Que, L.; Tolman, W. B., *Nature* **2008**, *455*, 333.
- [7] Stubbe, J.; van der Donk, W. A., *Chem. Rev.* **1998**, *98*, 705.
- [8] Stubbe, J.; Nocera, D. G.; Yee, C. S.; Chang, M. C. Y., *Chem. Rev.* **2003**, *103*, 2167.
- [9] Silva, K. E.; Elgren, T. E.; Que, L. J.; Stankovich, M. T., *Biochemistry* **1995**, *34*, 14093.
- [10] Vass, I.; Styring, S., *Biochemistry* **1991**, *30*, 830.
- [11] Wright, C.; Sykes, A. G., *Journal Inorganic Biochemistry* **2001**, *85*, 237.
- [12] Benisvy, L.; Bill, E.; Blake, A. J.; Collison, D.; Davies, E. S.; Garner, C. D.; McArdle, G.; McInnes, E. J. L.; McMaster, J.; Ross, S. H. K.; Wilson, C., *Dalton Trans.* **2006**, 258.
- [13] Benisvy, L.; Bittl, R.; Bothe, E.; Garner, C. D.; McMaster, J.; Ross, S.; Teutloff, C.; Neese, F., *Angew. Chem., Int. Ed.* **2005**, *44*, 5314.
- [14] Benisvy, L.; Hammond, D.; Parker, D. J.; Davies, E. S.; Garner, C. D.; McMaster, J.; Wilson, C.; Neese, F.; Bothe, E.; Bittl, R.; Teutloff, C., *J. Inorg. Biochem.* **2007**, *101*, 1859.
- [15] Costentin, C.; Robert, M.; Saveant, J. M., *J. Am. Chem. Soc.* **2006**, *128*, 4552.
- [16] Maki, T.; Araki, Y.; Ishida, Y.; Onomura, O.; Matsumura, Y., *J. Am. Chem. Soc.* **2001**, *123*, 3371.
- [17] Markle, T. F.; Mayer, J. M., *Angew. Chem., Int. Ed.* **2008**, *47*, 738.
- [18] Markle, T. F.; Rhile, I. J.; DiPasquale, A. G.; Mayer, J. M., *Proceedings of the National Academy of Sciences of the United States of America* **2008**, *105*, 8185.

- [19] Rhile, I. J.; Markle, T. F.; Nagao, H.; DiPasquale, A. G.; Lam, O. P.; Lockwood, M. A.; Rotter, K.; Mayer, J. M., *J. Am. Chem. Soc.* **2006**, *128*, 6075.
- [20] Rhile, I. J.; Mayer, J. M., *J. Am. Chem. Soc.* **2004**, *126*, 12718.
- [21] Rhile, I. J.; Mayer, J. M., *Angew. Chem., Int. Ed.* **2005**, *44*, 1598.
- [22] Thomas, F.; Jarjayes, O.; Jamet, M.; Hamman, S.; Saint-Aman, E.; Duboc, C.; Pierre, J. L., *Angew. Chem., Int. Ed.* **2004**, *43*, 594.
- [23] Kanamori, D.; Furukawa, A.; Okamura, T.; Yamamoto, H.; Ueyama, N., *Organic & Biomolecular Chemistry* **2005**, *3*, 1453.
- [24] Jimenez, C. A.; Belmar, J. B., *Tetrahedron* **2005**, *61*, 3933.
- [25] Jeffrey, G. A., *An Introduction to Hydrogen Bonding* Oxford University Press: Oxford, 1997.
- [26] Kanamori, D.; Okamura, T.; Yamamoto, H.; Shimizu, S.; Tsujimoto, Y.; Ueyama, N., *Bull. Chem. Soc. Jpn.* **2004**, *77*, 2057.
- [27] Kanamori, D.; Okamura, T. A.; Yamamoto, H.; Ueyama, N., *Angew. Chem., Int. Ed.* **2005**, *44*, 969.
- [28] Benisvy, L.; Mutikainen, I.; Quesada, M.; Turpeinen, U.; Gamez, P.; Reedijk, J., *Chem. Commun.* **2006**, 3723.
- [29] Benisvy, L.; Gamez, P.; Fu, W. T.; Kooijman, H.; Spek, A. L.; Meijerink, A.; Reedijk, J., *Dalton Trans.* **2008**, 3147.
- [30] Laurence, C.; Berthelot, M.; Lucon, M.; Morris, D. G., *Journal of the Chemical Society-Perkin Transactions 2* **1994**, 491.
- [31] Wayland, B. B.; Drago, R. S., *J. Am. Chem. Soc.* **1964**, *86*, 5240.
- [32] Bordwell, F. G.; Cheng, J. P., *J. Am. Chem. Soc.* **1991**, *113*, 1736.
- [33] Manner, V. W.; Markle, T. F.; Freudenthal, J. H.; Roth, J. P.; Mayer, J. M., *Chem. Commun.* **2008**, 256.
- [34] Xie, C. P.; Lahti, P. M.; George, C., *Org. Lett.* **2000**, *2*, 3417.
- [35] O'Malley, P. J., *J. Am. Chem. Soc.* **1998**, *120*, 11732.
- [36] Engstrom, M.; Himo, F.; Graslund, A.; Minaev, B.; Vahtras, O.; Agren, H., *J. Phys. Chem. A* **2000**, *104*, 5149.
- [37] Kaupp, M.; Gress, T.; Reviakine, R.; Malkina, O. L.; Malkin, V. G., *J. Phys. Chem. B* **2003**, *107*, 331.
- [38] Asher, J. R.; Doltsinis, N. L.; Kaupp, M., *J. Am. Chem. Soc.* **2004**, *126*, 9854.

- [39] Faller, P.; Goussias, C.; Rutherford, A. W.; Un, S., *Proceedings of the National Academy of Sciences of the United States of America* **2003**, *100*, 8732.
- [40] Lachaud, F.; Quaranta, A.; Pellegrin, Y.; Dorlet, P.; Charlot, M.-F.; Un, S.; Leibl, W.; Aukauloo, A., *Angew. Chem., Int. Ed.* **2005**, *44*, 1536.
- [41] Un, S.; Atta, M.; Fontecave, M.; Rutherford, A. W., **1995**.
- [42] Maniero, A. L.; Chis, V.; Zoleo, A.; Brustolon, M.; Mezzetti, A., *J. Phys. Chem. B* **2008**, *112*, 3812.
- [43] Dorlet, P.; Rutherford, A. W.; Un, S., *Biochemistry* **2000**, *39*, 7826.
- [44] van Dam, P. J.; Willems, J. P.; Schmidt, P. P.; Potsch, S.; Barra, A. L.; Hagen, W. R.; Hoffman, B. M.; Andersson, K. K.; Graslund, A., *J. Am. Chem. Soc.* **1998**, *120*, 5080.
- [45] Allard, P.; Barra, A. L.; Andersson, K. K.; Schmidt, P. P.; Atta, M.; Graslund, A., *J. Am. Chem. Soc.* **1996**, *118*, 895.
- [46] Gilli, G.; Bellucci, F.; Ferretti, V.; Bertolasi, V., *J. Am. Chem. Soc.* **1989**, *111*, 1023.

5 Salicylamidate ligands: coordination chemistry

Table of contents

Abstract	176
5.1 Introduction	177
5.2 Polianionic ligands	178
5.3 Ni^{II}-complex	179
5.3.1 Synthesis and characterisation of [NBu ₄] ₂ [Ni ₂ (^{OHNH} L) ₂]	179
Scheme 5.3. Synthesis of [NBu ₄] ₂ [Ni ₂ (^{OHNH} L) ₂] (47)	179
5.3.2 Oxidation of [NBu ₄] ₂ [Ni ₂ (^{OHNH} L) ₂]	181
5.3.2.1 Electrochemical studies of [NBu ₄] ₂ [Ni ₂ (^{OHNH} L) ₂]	182
5.3.2.2 Generation of (47 ⁺) and (47 ⁺⁺)	185
5.3.2.3 Electronic structures of (47 ⁺) and (47 ⁺⁺)	186
5.4 Overview	193
References	196

Abstract

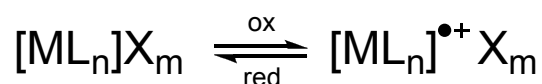
The synthesis, upon triple deprotonation of N-ethanol salicylamide (**42**) and reaction with Ni(OAc)₂, of the di-nickel complex [NBu₄]₂[Ni₂(^{OHNH}L)₂] (**47**) is reported. Compound (**47**) has been fully characterized (¹H, ¹³C-NMR, MS, IR, elemental and X-ray diffraction analyses) and its electrochemical behavior has been studied (CV and CPE).

Carefully preparation and investigation of the corresponding oxidized species (**47**⁺) and (**47**⁺⁺) has been carried out in acetonitrile and dichloromethane. Compounds (**47**⁺) and (**47**⁺⁺) show interesting properties in their corresponding EPR and UV/vis spectra. The investigation of their corresponding electronic structures is relevant to account for the potential properties of this system for future applications in bioinorganic chemistry and catalysis.

5.1 Introduction

In Chapter 4, a new class of potentially chelating salicylamidate ligands has been presented. Their redox properties and the corresponding study of the electronic structures of the oxidized derivatives represent an important description of their prospective capacity to mimic the redox function of the tyrosyl group (Tyr/Tyr⁻/Tyr[•]) in biological systems.¹⁻⁴

Naturally, the upcoming topic to explore would be the coordination chemistry of these new ligands toward those metal centers that, widely present in Nature, occupy a central role in different enzymes and catalytic systems (*i.e.* Cu, Fe, Zn, Ni...). Furthermore, an effort should be devoted to investigate the capacity of the resulting metal complexes to sustain oxidative conditions, in particular when being a redox reversible system (Scheme 5.1).



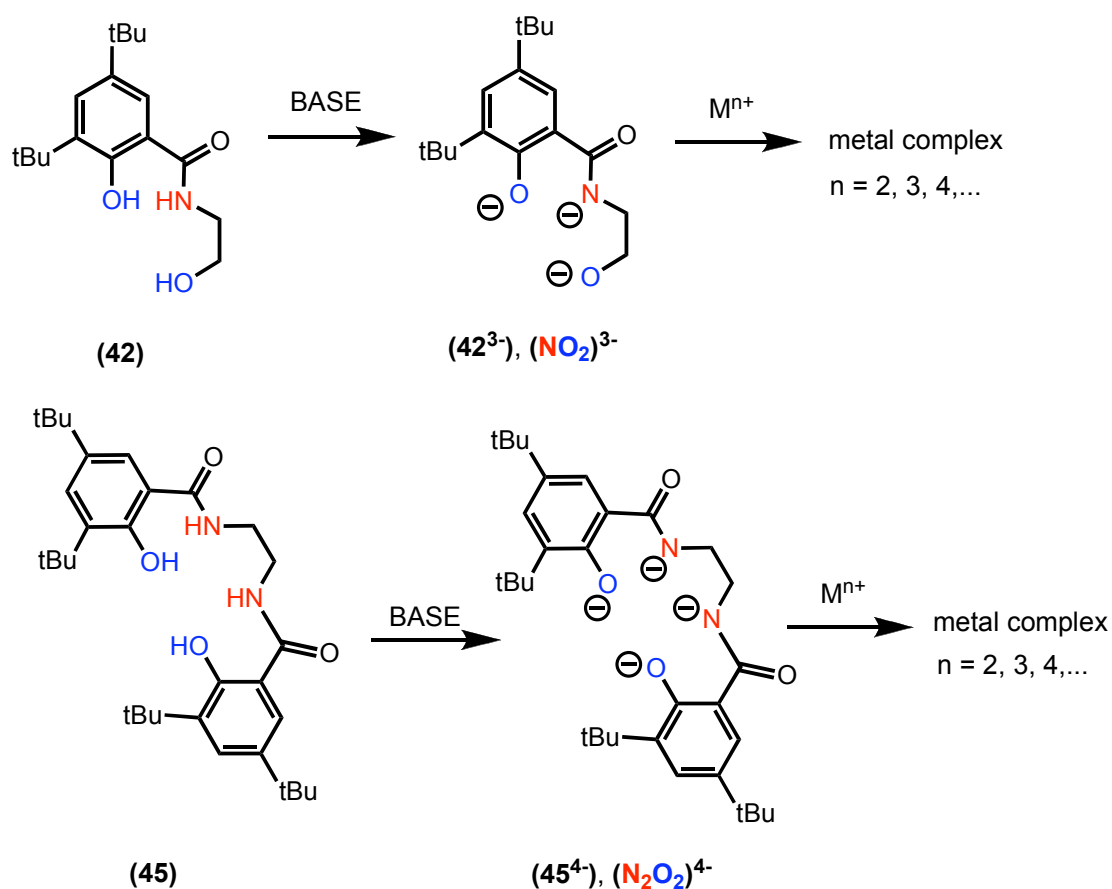
Scheme 5.1 Schematical representation of redox reversible metal complex

The detailed study of the electronic characteristics of phenoxy radical derivatives (**42**[•]), (**43**[•]) and (**44**[•]) (Chapter 4) was decisive for many aspects: (i) defining the characteristics and properties (*i.e.* nature, delocalisation, stability...) of these radicals; (ii) confirming the possible redox stabilisation of the corresponding metal complexes and (iii) assuring an excellent reference for further comparative studies.

Hence, in this chapter the coordination chemistry of the potentially tridentate ligand (**42**) has been investigated.

5.2 Polianionic ligands

As briefly anticipated in Chapter 4, the class of salicylamidate ligands has been designed also taking into account its potential polianionic character. For this reason different deprotonable sites have been introduced (see also Section 4.1) and, for instance, derivatives **(42)** and **(45)** represent two examples of $(\text{NO}_2)^{3-}$ and $(\text{N}_2\text{O}_2)^{4-}$ type chelating pro-ligands, respectively (Scheme 5.2).



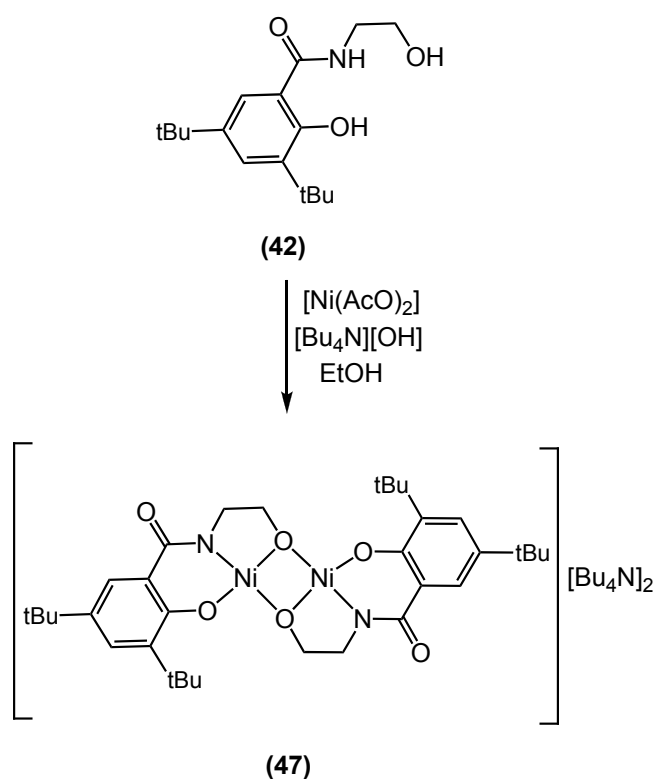
Scheme 5.2 Polianionic character of the salicylamidate ligands **(42)** and **(45)**.

Consequently, it is expected that these anionic derivatives should be able to stabilize high oxidation states of metal ions (*i.e.* M^{n+} , Scheme 5.2) and support the redox processes occurring in the resulting complexes.

5.3 Ni^{II}-complex

5.3.1 Synthesis and characterisation of [NBu₄]₂[Ni₂(^{OHNH}L)₂]

The coordination chemistry of the triply deprotonated N-ethanolamide derivative [^{OHNH}L]³⁻ (**42**³⁻) has been studied toward Ni⁺⁺ ion. Compound (**42**³⁻) has been prepared *in situ* and reacted with Ni(AcO)₂ in a 1:1 stoichiometric ratio affording compound (**47**) (Scheme 5.3).



Scheme 5.3. Synthesis of [NBu₄]₂[Ni₂(^{OHNH}L)₂] (**47**)

The di-nickel complex [NBu₄]₂[Ni₂(^{OHNH}L)₂] (**47**) is stable in air in the solid state and in solution and has been fully characterised by ¹H and ¹³C-NMR, IR and UV-vis spectroscopies, elemental analysis and single crystal X-ray diffraction (see next Sections and Experimental Part).

The ¹H-NMR spectrum of the pink powder of (**47**) rapidly revealed the diamagnetic nature of the nickel complex (*i.e.* square planar Ni^{II}, *d*⁸, low spin, *S* = 0)

that presents one set of resonances for the protons of the salicylamide ligands, indicating their equivalence.

The X-ray diffraction structure, performed by Dr. Fátima C. Guedes da Silva, (Figure 5.1), of **(47)** shows each of the nickel nuclei in a NO_3 -square planar geometry (Table 5.1). The pendant alkoxy groups of the ligands act as bridging moieties, being coordinated to both Ni centers (*i.e.* O(12) and O(32), Figure 5.1). **(47)** is almost planar (*i.e.* angle between the $\langle \text{N}(3)\text{O}(2)\text{Ni}(2) \rangle$ and $\langle \text{O}(32)\text{O}(12)\text{Ni}(2) \rangle$ planes is 0.09° , Figure 5.1) with the exception of the *tert*butyl groups and the alkyl chains that bend from the plane (*i.e.* $\text{N}(3)\text{C}(31)\text{-C}(32)\text{O}(32)$ and $\text{O}(12)\text{C}(12)\text{-C}(11)\text{N}(1)$ torsion angles are 46.29° and 40.76° , respectively, Figure 5.1 bottom).

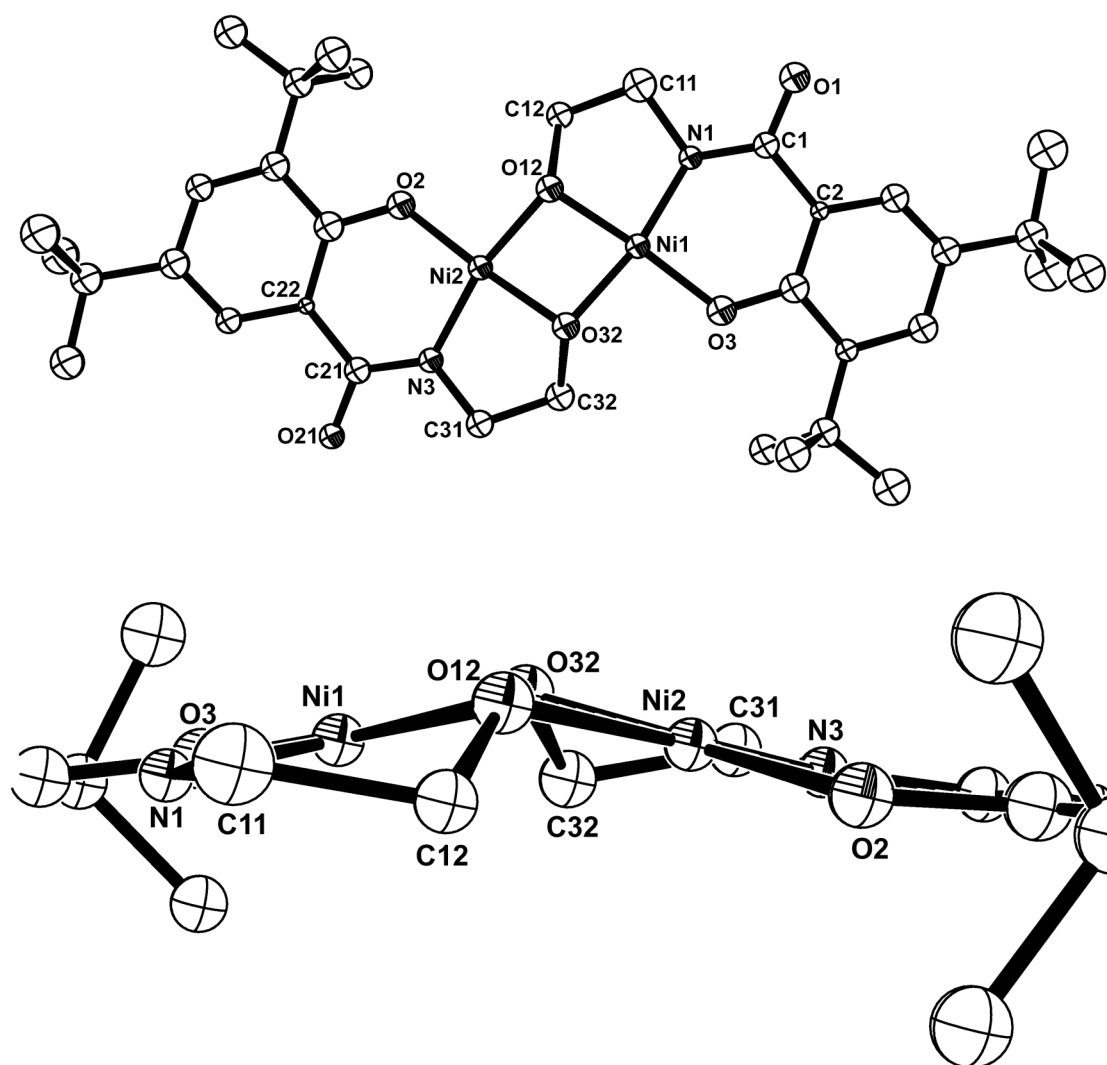


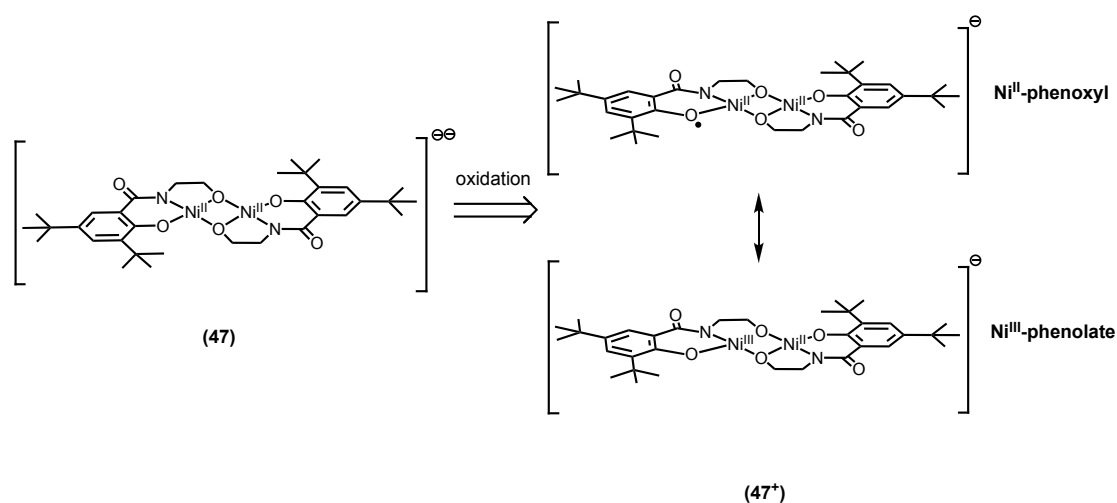
Figure 5.1 ORTEP plots of $[\text{NBu}_4]_2[\text{Ni}_2(\text{OHNL})_2]$ (**47**), where the ellipsoids are shown at 50% probability (hydrogens and two molecules of $[\text{NBu}_4]^+$ are omitted for clarity).

Table 5.1 Selected bond distances [\AA] and angles [$^\circ$] for $[\text{NBu}_4]_2[\text{Ni}_2(\text{O}^{\text{HNH}}\text{L})_2]$ (**47**).

distances		angles		torsion angles	
Ni(1)-Ni(2)	2.763(3)	O(12)Ni(1)O(32)	79.93	N(3)C(31)C(32)O(32)	46.29
Ni(1)-N(1)	1.813(10)	O(32)Ni(1)O(3)	95.13	N(1)C(11)C(12)O(12)	40.76
Ni(1)-O(3)	1.845(10)	O(3)Ni(1)N(1)	95.97	Ni(1)O(32)O(12)Ni(2)	151.74
Ni(1)-O(32)	1.893(9)	N(1)Ni(1)O(12)	88.85	O(12)Ni(1)Ni(2)O(32)	147.59
Ni(1)-O(12)	1.835(9)	O(12)Ni(2)O(32)	80.23		
Ni(2)-N(3)	1.859(11)	O(32)Ni(2)N(3)	86.59		
Ni(2)-O(2)	1.827(10)	N(3)Ni(2)O(2)	97.35		
Ni(2)-O(12)	1.860(9)	O(2)Ni(2)O(12)	95.84		
Ni(2)-O(32)	1.857(10)				

5.3.2 Oxidation of $[\text{NBu}_4]_2[\text{Ni}_2(\text{O}^{\text{HNH}}\text{L})_2]$

As previously mentioned, the study of the oxidation of (**47**) is crucial and could clarify potential bioinorganic applications of this new class of complexes.⁵ The presence of two metal centers could, in principle, lead to single or double oxidized derivatives carrying the $\text{Ni}^{\text{II}}/\text{Ni}^{\text{III}}$ or $\text{Ni}^{\text{III}}/\text{Ni}^{\text{III}}$ pairs, respectively. Moreover, it should be highlighted that the electron removal in (**47**) could, formally, affect (i) the ligand leading to a Ni^{II} -phenoxyl radical species or (ii) the nickel center affording a Ni^{III} -complex bearing the phenolate ligand (Scheme 5.4).

Scheme 5.4 Schematic representation of the oxidation of (**47**).

In general, the electronic structures of oxidized species of various metal-phenolate complexes have been shown⁶⁻⁸ to be dependent on the nature of the metal ions (*i.e.* oxidation of Fe^{III}-phenolate complexes was indentified as Fe^{III}-phenoxy radical species, whereas oxidation of V^{III}-analogues gave exclusively the V^{IV} and V^V complexes, where no oxidation of the phenolate moiety was observed) but also on the nature of the phenolate moiety coordinated.⁶ Examples^{5,9} of Ni^{II}-complexes reported the possibility to observe a valence tautomerism of the one-electron oxidized derivative, between Ni^{II}-phenoxy and Ni^{III}-phenolate species (Scheme 5.4 and Figure 5.2).

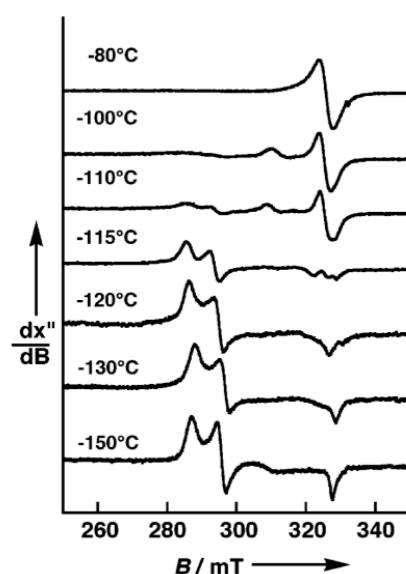


Figure 5.2 Example of the temperature dependence the EPR spectrum of Ni^{II}-phenoxy/Ni^{III}-phenolate species: at -150°C is visible the typical Ni^{III} EPR-profile, while from -110°C is predominant the organic radical EPR signal.¹⁰

The investigation of the mono- and di-oxidized derivatives of (47) could hold a great significance and the localisation of unpaired electrons allows understanding the electronic behavior both of the ligand and the metal center.

5.3.2.1 Electrochemical studies of [NBu₄]₂[Ni₂(^{OHNH}L)₂]

The cyclic voltammogram of (47), in CH₃CN at 298 K containing [NBu₄][BF₄] (0.2 M), displays two reversible one-electron oxidation waves (Figures 5.3 left, and 5.4) associated with the formation of the corresponding oxidized

compounds. These oxidation processes occur at $E_{1/2}^{ox}/V$ vs. $Fc^{0/+}$ ($Fc = [Fe(\eta^5-C_5H_5)_2]$) = -0.120 and 0.110.^(*)

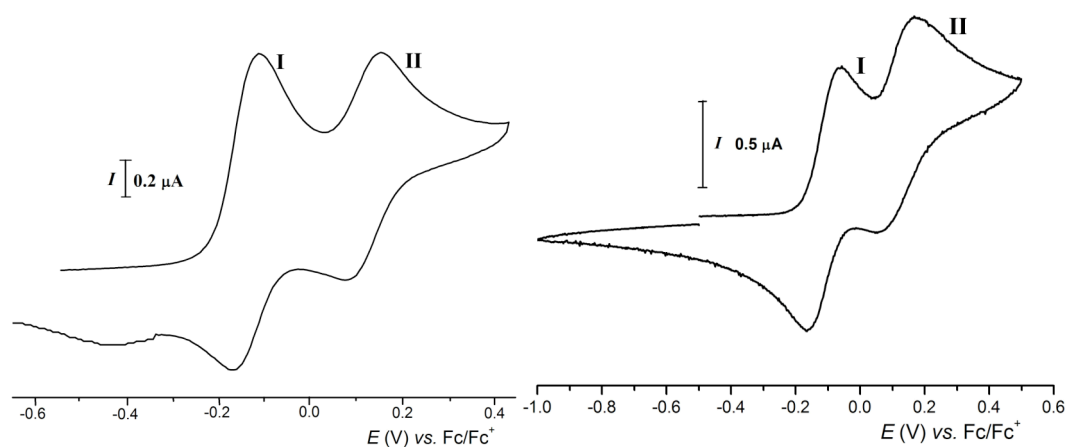
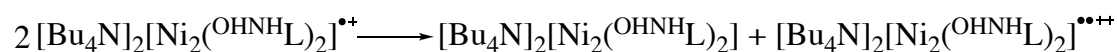


Figure 5.3 Cyclic voltammogram ($v = 120 \text{ mV s}^{-1}$) of a ca. 1mM solution of (47) in CH_3CN (left) and in CH_2Cl_2 (right) with 0.2 M $[NBu_4][BF_4]$, at a platinum disc electrode ($d = 0.5 \text{ mm}$).

The quasi-reversibility of the oxidation processes indicates that the oxidized species of Ni-complex, (47^+) and (47^{++}) , are stable in the timescale of the CV measurements. In particular, the cyclic voltammogram in dichloromethane displays a slightly shorter separation between the two oxidations (*i.e.*, $\Delta E_{1/2} = 202 \text{ mV}$ for CH_2Cl_2 and 230 mV for CH_3CN ; where $\Delta E_{1/2} = E_{1/2}^{II} - E_{1/2}^I$, and $E_{1/2}^I$ and $E_{1/2}^{II}$ are the redox potentials for the $(47)/(47^+)$ and $(47^+)/(47^{++})$ couples, respectively) in comparison with that in acetonitrile (Figure 5.3). This small difference could, in principle, be related to a different solvation effect of the two solvents, and, in this case, the acetonitrile appears to stabilize better the mono-oxidized form (47^+) . In particular, associated to these considerations the possible estimate¹¹ of the disproportionation constant (K_d) could be attempted. The latter (corresponding to a comproportionation constant $K_c = K_d^{-1}$) for the equilibrium between the monocationic derivative (47^+) and their neutral and dicationic forms:



* When necessary, to avoid overlapping redox couples, the $\{[Fe(TpmPy)](BF_4)_2\}^{0/+}$ (**(30)**, see Chapter 3) couple was used as the internal reference and the potentials of the redox process(es) were referenced to the $[Fc]^{0/+}$ couple by an independent calibration ($\Delta E_{1/2}, [Fc]^{0/+} - \text{(30)}^{0/+} = 0.642 \text{ V}$).

can be calculated by the use eq [5.1]

$$K_d = \exp(nF(E_{1/2}^{\text{II}} - E_{1/2}^{\text{I}})/RT) = \exp((E_{1/2}^{\text{II}} - E_{1/2}^{\text{I}})/0.059) \quad [5.1]$$

and the values are listed in Table 5.2. Despite the small difference between the disproportionation constants in the two solvents, the higher value calculated for dichloromethane could partially explain the observed instability of (**47**⁺) in this solvent (see next Sections).

Table 5.2 Redox potentials of (**47**)/(**47**⁺) and (**47**⁺)/(**47**⁺⁺) couples and disproportionation constant (K_d) for compound (**47**⁺) in acetonitrile and dichloromethane.

	$E_{1/2}^{\text{I}}$	$E_{1/2}^{\text{II}}$	K_d
CH₃CN	-0.120	+0.110	$2.28 \cdot 10^{-2}$
CH₂Cl₂	-0.124	+0.078	$3.26 \cdot 10^{-2}$

$E_{1/2}^{\text{I}}$ and $E_{1/2}^{\text{II}}$ vs. $\text{Fc}^{0/+}$ ($\text{Fc} = [\text{Fe}(\eta^5\text{-C}_5\text{H}_5)_2]$) (at r.t. at 120 mVs^{-1}) are the redox potentials for the (**47**)/(**47**⁺) and (**47**⁺)/(**47**⁺⁺) couples, respectively. The disproportionation constant K_d was calculated from eq. (5.1).

The CPE (controlled potential electrolysis) experiment has confirmed the one-electron process for each oxidation wave. It was also verified that under controlled temperature (not above 253 K) the species are stable under dinitrogen atmosphere for hours.

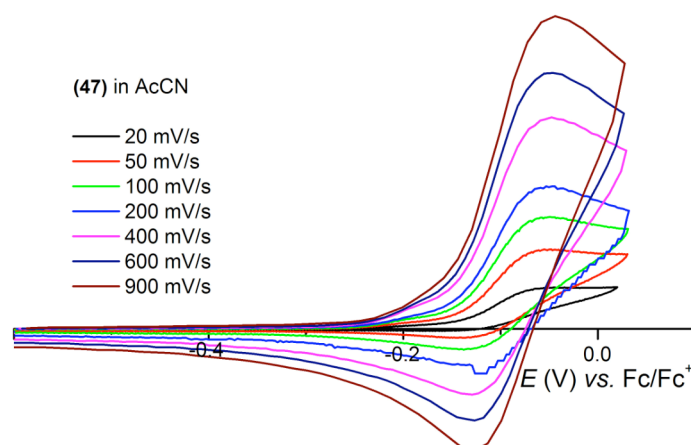


Figure 5.4 Reversibility tests for first oxidation of (**47**).

5.3.2.2 Generation of (47⁺) and (47⁺⁺)

Similarly to the study of the ligand (42) and its analogues in Chapter 4, the electrochemical method to prepare the mono- and di-oxidized compounds (47⁺) and (47⁺⁺) appears to be an excellent procedure to synthesize these radical species in carefully controlled conditions.

Compounds (47⁺) and (47⁺⁺) have then been generated both in CH₂Cl₂ and CH₃CN to verify any possible effect of the solvent. In fact, the cyclic voltammetry and CPE experiments in these solvents have suggested an eventual role of the solvent on the stability of the oxidized products. Whereas (47⁺) prepared in acetonitrile, is stable for hours under dinitrogen at 0 °C, the analogue generated in dichloromethane exhibits a higher instability and needed a more careful handling. In fact, in the presence of acetonitrile a possible coordination of the solvent molecule to the square planar Ni complexes could occur (Figure 5.5).

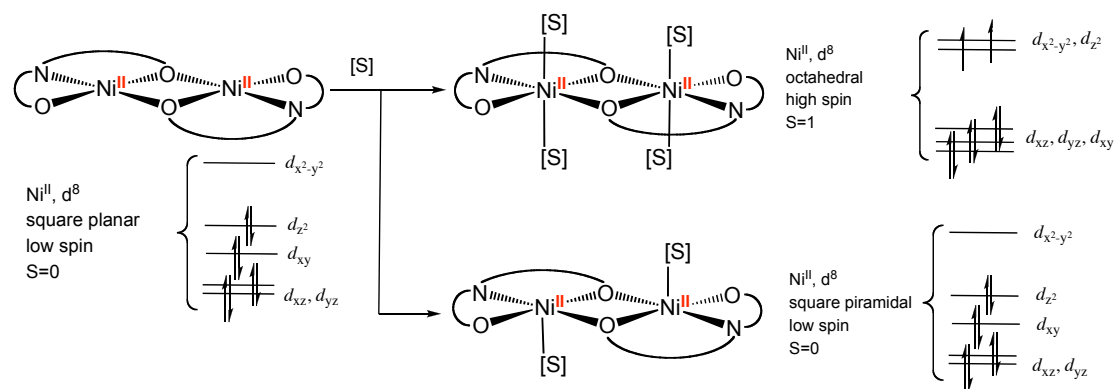


Figure 5.5 Schematic representation of the possible effect of solvent in Ni^{II} square planar metal complexes.

However, the stability of (47) in acetonitrile has been verified in ¹H-NMR: the absence of paramagnetic species has been confirmed. In fact, the coordination of an extra ligand to (47) would lead, in principle, to a modification of the coordination geometry of the metal center and consequently of its *d*-orbitals energies: the square planar Ni^{II}, *d*⁸, low spin, has no unpaired electrons (*i.e.* *S* = 0) and results in a ¹H-NMR spectrum typical of a diamagnetic compound, whereas a double axial coordination of two solvent molecules for each nickel center could result in an

octahedral Ni^{II} , d^8 , high spin, with two unpaired electrons for each nucleus ($S = 1$). The latter configuration is a triplet ground state and should affect the ^1H -NMR resonances.

The oxidized derivatives (47^+) and (47^{++}) have been electrochemically generated at low temperature under dinitrogen (see Experimental Chapter) and their corresponding EPR and UV/vis spectra have been run. The combined interpretation of EPR and UV/vis spectra turned out to be an important strategy for a better understanding of the electronic structures of these compounds. The results are presented in the next section.

5.3.2.3 Electronic structures of (47^+) and (47^{++})

(47^+) in CH_3CN . The EPR spectrum of a frozen acetonitrile solution of the mono-oxidized (47^+) exhibits a typical isotropic radical signal centered at $g_{\text{iso}} = 2.0032$ with a peak-to-peak linewidth of 11.2 G (Figure 5.6, black line), that reveals an hyperfine interaction when melted: a double signal with ca 5 G constant (Figure 5.6, red line).

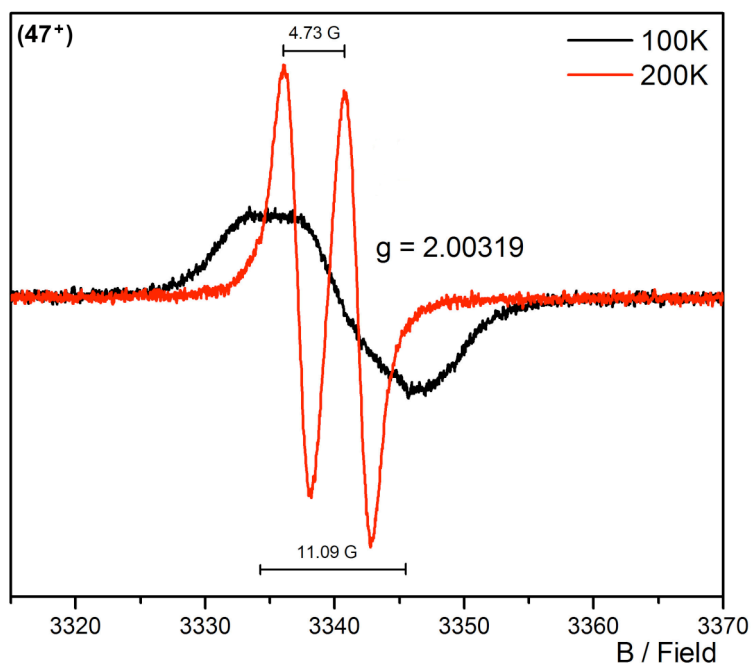


Figure 5.6 EPR spectra of CH_3CN frozen (black) and fluid solutions (red) of the electrochemically generated (47^+) recorded at 100 and 200K, respectively.

This value of g , that appears really close to those observed for the salicylamide radicals (**42** \cdot), (**43** \cdot) and (**44** \cdot) (Chapter 4), could be associated to a phenoxyl radical of the coordinated ligand, being the isotropic profile and the g value typical of an organic radical species, near to the free electron (*i.e.*, $g_e = 2.0023139$).

The doublet hyperfine coupling observed for the acetonitrile fluid solution of (**47** $^+$) (Figure 5.6, red line) corresponds to a single interaction with a *meta*-proton of the aromatic ring, whereas in the case of the free ligands the unpaired electron of the phenoxyl radical coupled with both *meta*-H nuclei generating a triplet (see Chapter 4, Figure 4.12). This difference should be further investigated but it is reasonable to associate the reduced aromatic delocalisation of the unpaired electron with the presence of the coordination to the Ni center (Figure 5.7).

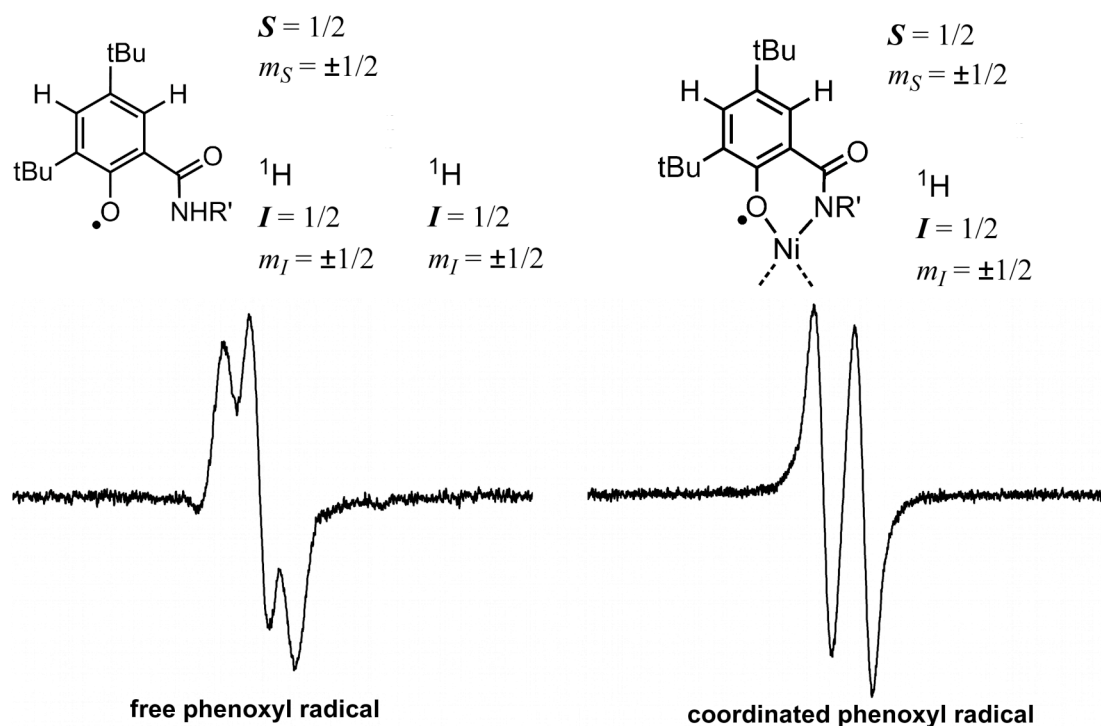


Figure 5.7 Comparative representation of the EPR spectra of the two protons hyperfine coupled radical (**42** \cdot) (left) and the one proton hyperfine coupled radical (**47** $^+$) (right).

The corresponding UV/vis spectrum of (**47** $^+$) displays the typical bands associated to the presence phenoxyl radical species (*ie.* at 439(955) and 670(290), $\lambda/\text{nm}(\epsilon/\text{M}^{-1} \text{cm}^{-1})$) (see also Section 4.2.1.5 for the free ligands), thus confirming its formation in the oxidation of (**47**) in acetonitrile.

(47⁺) in CH₂Cl₂. On the other hand, compound **(47⁺)** electrochemically prepared in CH₂Cl₂ shows, as previously mentioned, an higher instability compared to its analogue in CH₃CN. Despite this low stability, traces of product **(47⁺)** could be detected in the EPR spectrum (Figure 5.8) indicating the absence of an organic radical. In fact, the plausible interpretation of the EPR spectrum consists in a non-symmetrical profile (*i.e.* anisotropy) that could belong to a metal-centered paramagnet with a possible distortion of the different components of *g*: the rhombic ($g_{xx} \neq g_{yy} \neq g_{zz}$) or axial ($g_{\parallel} < g_{\perp}$) EPR symmetrical patterns (see also Figure 5.2, T= -150 °C).¹⁰

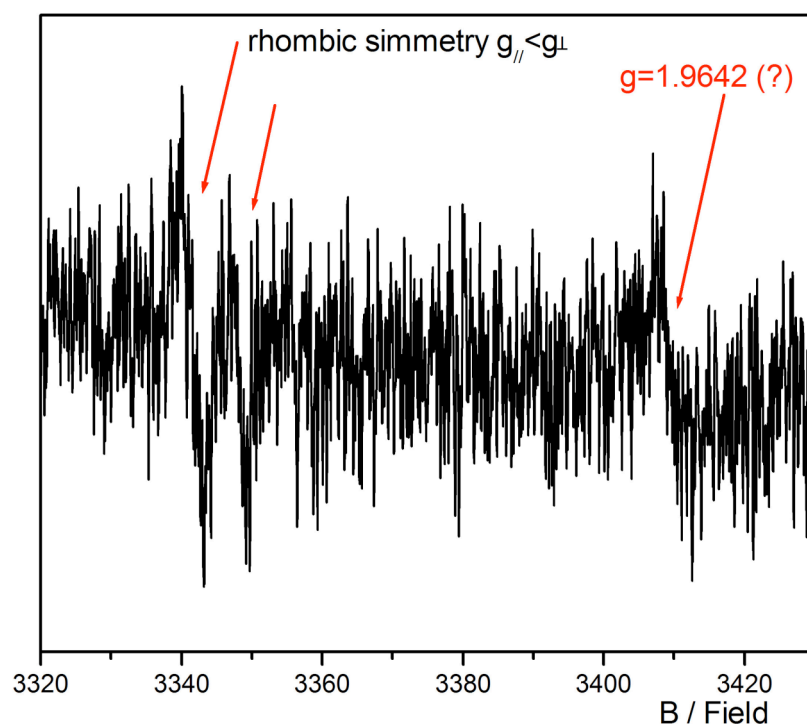


Figure 5.8 EPR spectrum of CH₂Cl₂ frozen solution of the electrochemically generated **(47⁺)** recorded at 90 K.

At the same time, the corresponding UV/vis/NIR spectrum exhibits a broad band in the *near-IR* region, at 1193 nm (ϵ *ca.* 445 M⁻¹cm⁻¹), that is characteristic for Ni^{III}-species (Figure 5.9).^{7,10,12}

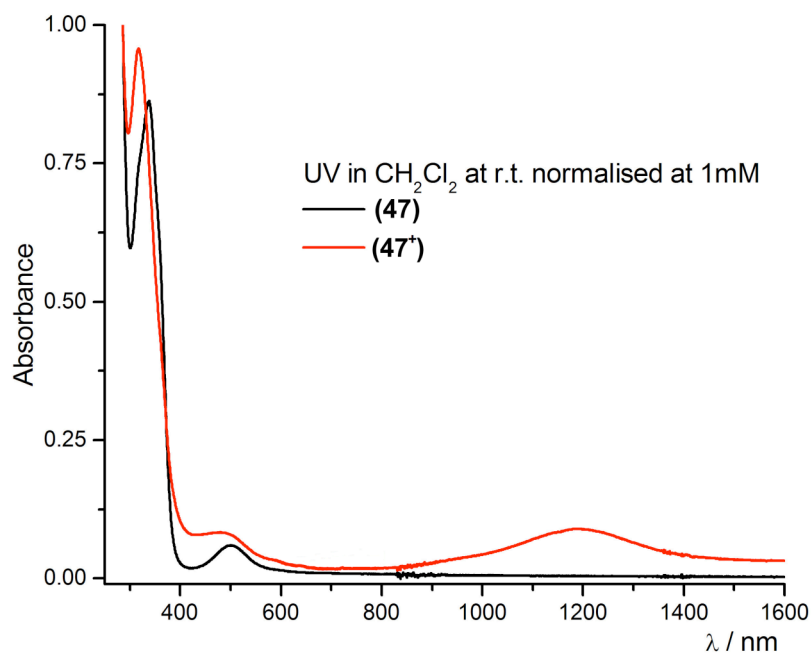


Figure 5.9 UV/vis/NIR spectrum* of (47) (black) and (47⁺) (red) in CH₂Cl₂.

These results could suggest the formation of the highly unstable mixed Ni^{II}/Ni^{III} complex. Additionally, a DFT theoretical study performed by Dr. M. L. Kuznetsov (see Experimental Part) of the SOMO (singly occupied molecular orbital) of (47⁺), based on the X-ray structural data of (47) (Figure 5.1), indicates that the mainly contribution to the total spin density for the unpaired electron is located on the nickel-atoms (Figure 5.10 and Experimental part). Thus, in the absence of extra ligands (*i.e.* solvent molecule), the calculations suggest the formation of the monooxidized (phenolate)-Ni^{II}-Ni^{III}-(phenolate) complex, as confirmed by these experimental results that indicate a metal-based oxidation.

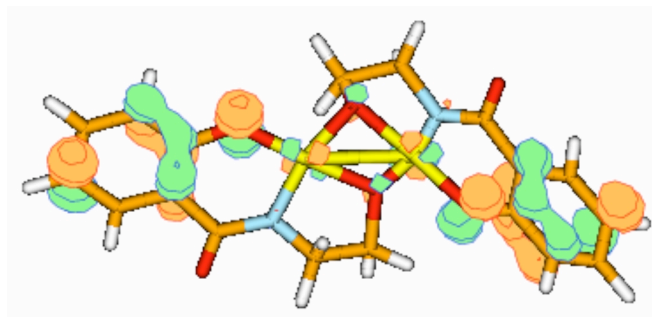


Figure 5.10 SOMO orbital of (47⁺).

* Due to the high instability, the spectrum has been recorded into two separated blocks 1600-800 and 800-200 nm and plotted together.

The fast decomposition of this Ni^{III}-Ni^{II} species has been observed, even if it has been difficult to discern the nature of this process. In fact, as previously described (Section 5.3.2.1) the disproportionation could occur for this type of compounds leading, in principle, to equimolar amounts of the starting complex (**47**) and of the doubly oxidized Ni^{III}-Ni^{III} derivative, and it is not even possible to exclude that the evidence for the presence of a Ni^{III}-species can come directly from one of these decomposition products (*i.e.* the Ni^{III}-Ni^{III} derivative). However, based on the experimental and theoretical results it is possible to rule out the formation of the Ni^{II}-phenoxyl species for the mono-oxidation product (**47**⁺) in dichloromethane.

(47⁺⁺) in CH₃CN. Analogously, the two-electrons-oxidized compound (**47⁺⁺**) has been prepared both in CH₃CN and CH₂Cl₂. The former solvent stabilise better the oxidized product and (**47⁺⁺**) shows a consistent UV/vis spectrum to its analogue mono-oxidized (**47⁺**) (*i.e.* 374, 492, 750 nm, Figure 5.11), confirming the presence of the phenoxyl radical moieties.^{8,13} Moreover, the UV/vis/NIR spectrum presents a ‘silent’ profile in the 1000-1600 nm region, thus excluding the formation of a Ni^{III}-species.

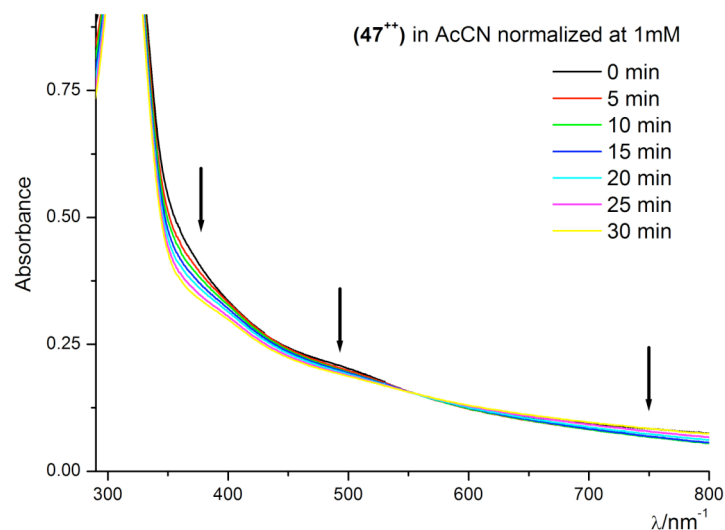


Figure 5.11 UV/vis spectrum of (**47⁺⁺**) in CH₃CN.

On the other hand, the silent EPR spectrum detected for (**47⁺⁺**) could be accounted for the antiferromagnetic coupling of two phenoxyl radical moieties. In fact, similarly to its (**47⁺**), the second electron removal could affect the other phenolate group and lead to a final compound (**47⁺⁺**) bearing two Ni^{II}-phenoxyl radical fragments. The latter,

could, in principle, antiferromagnetically couple to give a silent EPR spectrum ($S = 0$).

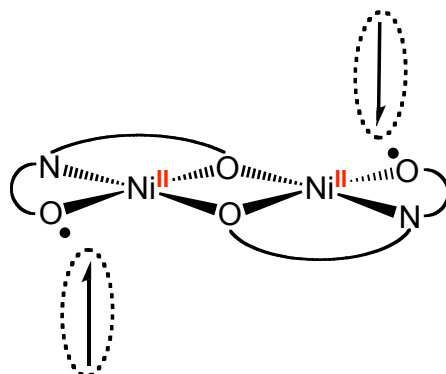


Figure 5.12 Electronic structure of (47^{++}) generated in CH_3CN .

(47^{++}) in CH_2Cl_2 . Surprisingly, the parallel between the mono- and di-oxidations does not match for the two-electrons oxidized product (47^{++}) in dichloromethane. The latter, in fact, would be expected to favour the double formation of a more stable (phenolate)- Ni^{III} - Ni^{III} -(phenolate) complex, but the isotropic signal detected in the EPR spectrum of (47^{++}) in CH_2Cl_2 could be ascribed to the presence of the $\cdot O$ -phenoxy radical species (Figure 5.13). Analogously, to compound (47^+) (Figure 5.6) generated in acetonitrile, the dichloromethane fluid solution EPR spectrum of (47^{++}) displays a doublet hyperfine interaction with the typical *ca.* 5 G constant ascribed at the coupling with a *meta*-proton (Figure 5.13 and also Figure 5.7).

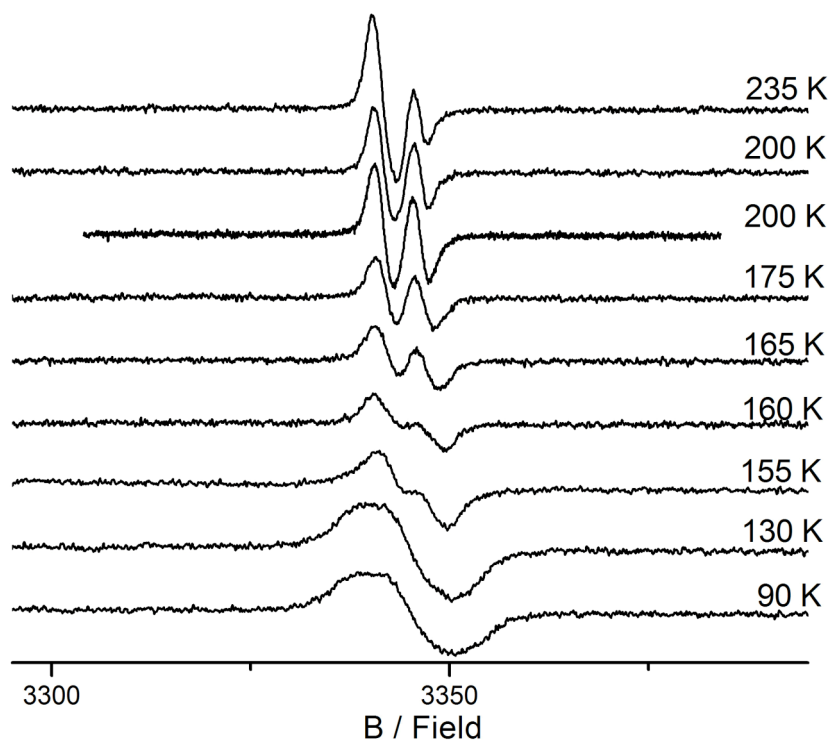


Figure 5.13 Variable temperature EPR spectra of (47^{++}) in CH_2Cl_2 .

Furthermore, the corresponding UV/vis spectrum shows the contemporary presence of the Ni^{III} -absorption band at 1193 nm (analogous to that observed for (47^{++}) in CH_2Cl_2 , Figure 5.9) together with the typical bands ascribed to the organic radical moiety. Then, compound (47^{++}) generated in CH_2Cl_2 , in the absence of further experimental data, could be described as the mixed (phenoxy)- $\text{Ni}^{\text{II}}/\text{Ni}^{\text{III}}$ -(phenolate) complex. However, the simultaneous presence, in EPR and UV spectra, of Ni^{III} and phenoxy radical species could also be explained by thermal equilibrium between them, as reported in various examples.¹⁰

Compound **(47)**, itself, is a complicated system due to the presence of its double Ni-phenolate scaffold. In Scheme 5.5 are summarized the previous results that describe a peculiar behavior for this new class of complexes.

5.4 Overview

These results, even if they are recently collected and preliminarily considered, represent a good indication for further studies:

(i) both in the mono and di-oxidations the acetonitrile solvent appears to favour the formation of phenoxyl radical species, probably holding a chemical function. However, it is important to consider that the cyclic voltammetric profile of **(47)** in this solvent displays two reversible oxidation waves, thus excluding a possible coordination of the acetonitrile molecule(s) to **(47⁺)** or **(47⁺⁺)** derivatives, since, in such a case, it should lead to a chemical modification of the compound (Figure 5.14, **(47a⁺)**) that consequently would be reduced at a different potential (**(47a)**).

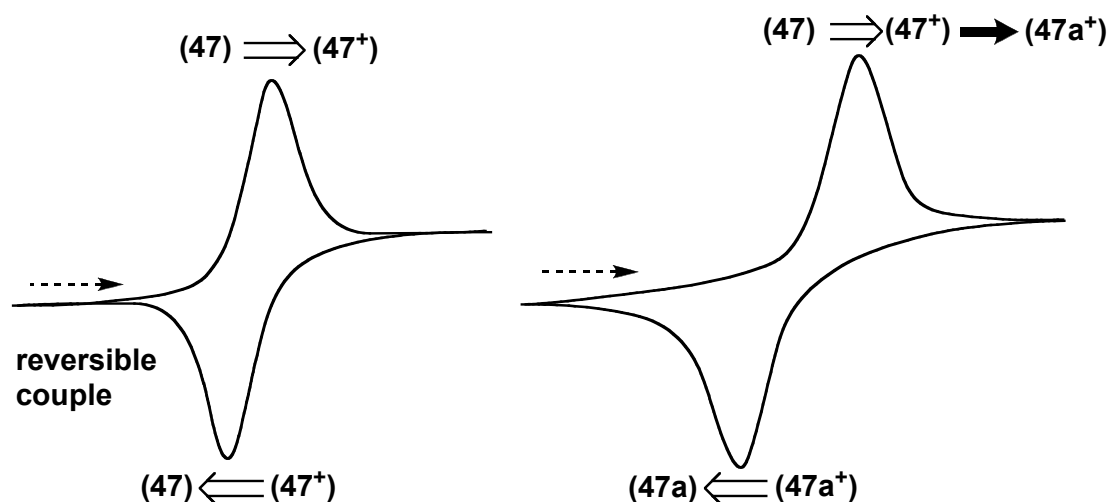
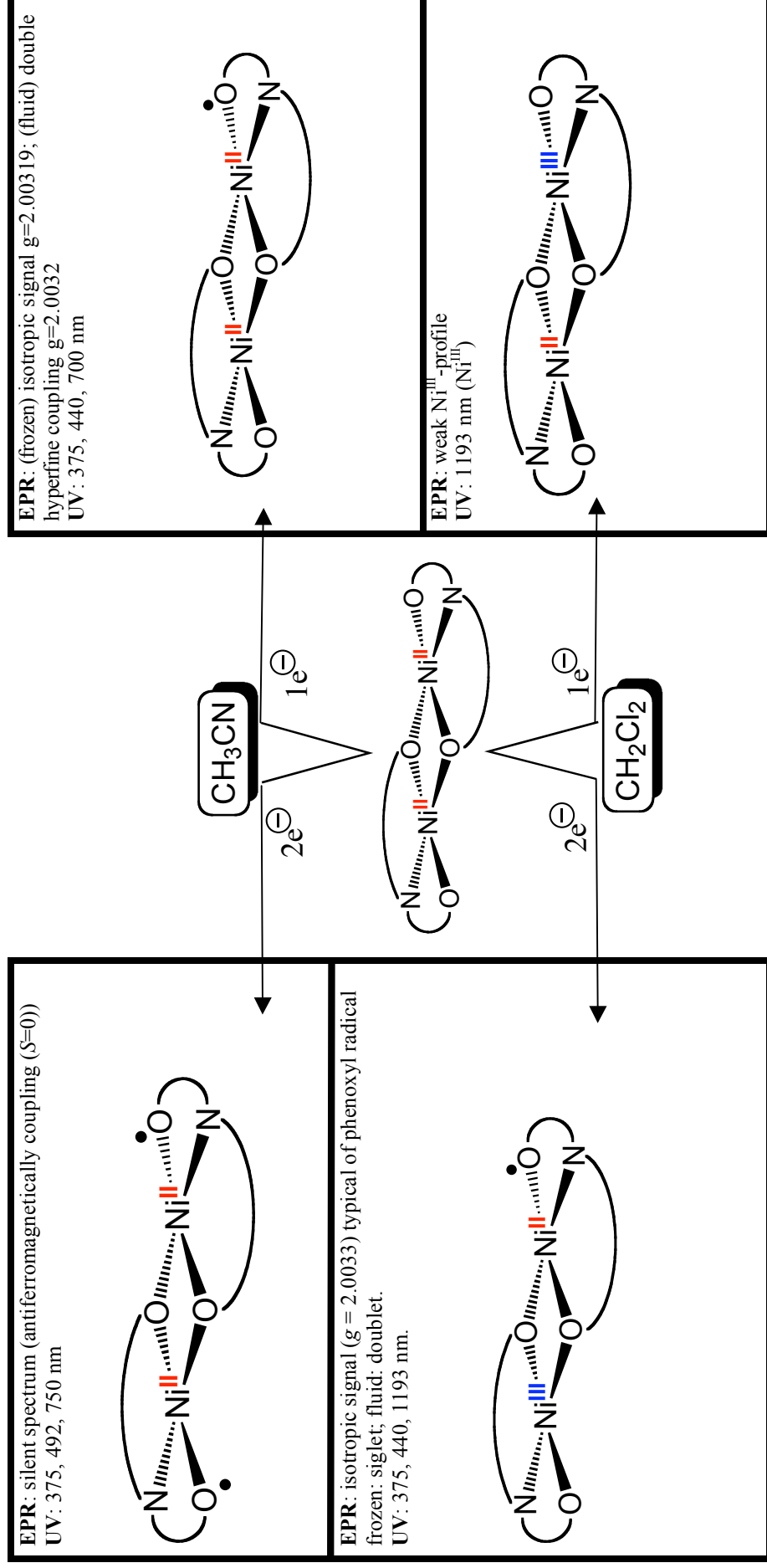


Figure 5.14 Representation of the expected effect of a chemical modification in the cyclic voltammetric profile of **(47)**.

Then, it is reasonable to consider exclusively a sort of stabilisation effect of the acetonitrile solvent to the oxidized derivatives of **(47)** that favours the Ni^{II}-phenoxyl system.

(ii) On the other hand, the oxidation in dichloromethane leads to more unstable products (in the case of **(47⁺)**) with evidences of formation of the Ni^{III}-phenolate species. In particular the two-electron oxidized product (**(47⁺⁺)**) in CH₂Cl₂ appears to hold both of the electronic structures, in a conceivable (phenolate)-Ni^{III}/Ni^{II}-(phenoxyl) system (Scheme 5.5).



Scheme 5.5 Electronic structures of (47^+) and (47^{++}) in CH_2Cl_2 and CH_3CN .

Many aspects of this work have still to be developed and leave open a pathway to further investigations: in particular for additional studies on the properties of compounds (**47⁺**) and (**47⁺⁺**) the high-field EPR technique (HF-EPR) is of a crucial interest for bioinorganic studies of the metal-complexes;¹⁴ the potential application in catalysis should also be studied, in view of the promising redox stability of this system.

Moreover, this class of metal-salicylamidate complexes has been further studied in our group confirming the good affinity of deprotonated ligand (**42³⁻**) toward Cu^{II} and Zn^{II}.

References

- [1] Stubbe, J.; van der Donk, W. A., *Chem. Rev.* **1998**, *98*, 705.
- [2] Stubbe, J.; Nocera, D. G.; Yee, C. S.; Chang, M. C. Y., *Chem. Rev.* **2003**, *103*, 2167.
- [3] Thomas, F., *Eur. J. Inorg. Chem.* **2007**, 2379.
- [4] Que, L.; Tolman, W. B., *Nature* **2008**, *455*, 333.
- [5] Kahn, O.; Martinez, C. J., *Science* **1998**, *44*, 279.
- [6] Rotthaus, O.; Jarjayes, O.; Del Valle, C. P.; Philouze, C.; Thomas, F., *Chem. Commun.* **2007**, 4462.
- [7] Shimazaki, Y.; Yajima, T.; Tani, F.; Karasawa, S.; Fukui, K.; Naruta, Y.; Yamauchi, O., *J. Am. Chem. Soc.* **2007**, *129*, 2559.
- [8] Benisvy, L.; Kannappan, R.; Song, Y.-F.; Milikisyants, S.; Huber, M.; Multikainen, I.; Turpeinen, U.; Gamez, P.; Bernasconi, L.; Baerends, E. J.; Hartl, F.; Reedijk, J., *Eur. J. Inorg. Chem.* **2007**, 637.
- [9] Glaser, T.; Heidemeier, M.; Frohlich, R.; Hildebrandt, P.; Bothe, E.; Bill, E., *Inorg. Chem.* **2005**, *44*, 5467.
- [10] Shimazaki, Y.; Tani, F.; Fukui, K.; Naruta, Y.; Yamauchi, O., *J. Am. Chem. Soc.* **2003**, *125*, 10513.
- [11] Blanchard, S.; Neese, F.; Bothe, E.; Bill, E.; Weyhermuller, T.; Wieghardt, K., *Inorg. Chem.* **2005**, *44*, 3636.
- [12] De Castro, B.; Freire, C., *Inorg. Chem.* **1990**, *29*, 5113.
- [13] Altwicker, E. R., *Chem. Rev.* **1967**, *67*, 475.
- [14] Andersson, K. K.; Schmidt, P. P.; Katterle, B.; Strand, K. R.; Palmer, A. E.; Lee, S. K.; Solomon, E. I.; Graslund, A.; Barra, A. L., *J. Biol. Inorg. Chem.* **2003**, *8*, 235.

6 Experimental data

Table of contents

6.1 Synthetic procedures	198
6.2 Crystallographic data	239
6.3 Electrochemical experiments	243
6.3.1 Cyclic Voltammetry	243
Apparatus	243
Internal standard:	243
General Procedure:	243
Reversibility tests:	244
6.3.2 Coulometry:	245
6.3.3 Electrochemical results	246
6.3.3.1 Results of reversibility studies of the oxidation/reduction processes for (42 ⁻), (43 ⁻) and (44 ⁻).	250
6.3.3.2 Reversibility of the oxidation/reduction process of Fc ^{0/+}	251
6.3.3.3 Reversibility of the oxidation/reduction process of (42 ^{•-})/(42 ⁻)	252
6.3.3.4 Reversibility of the oxidation/reduction processes of (43 ^{•-})/(43 ⁻) and (44 ^{•-})/(44 ⁻).	255
6.4 EPR conditions	258
6.5 Computational data	259
6.6 Catalytic studies	261
6.7 Compounds	263
References	280

6.1 Synthetic procedures

General Materials and Experimental Procedures

All syntheses were carried out under an atmosphere of dinitrogen, using standard Schlenk techniques. All solvents were dried, degassed and distilled prior to use. The reagents $\text{Fe}(\text{BF}_4)_2 \cdot 6\text{H}_2\text{O}$, $\text{NiCl}_2 \cdot 6\text{H}_2\text{O}$, ZnCl_2 , $[\text{Cu}(\text{MeCN})_4][\text{PF}_6]$, 4-bromomethylpyridine hydrobromide, triethylamine, methanesulfonyl chloride, NaHCO_3 , hexamethylenetetramine (HMT), $\text{Na}[\text{BPh}_4]$, 3-phenyl-1*H*-pyrazole, sulfur trioxide-trimethylamine complex, $[\text{NBu}_4][\text{OH}]$ 1.0 M methanolic solution, BuLi 1.6 M solution in hexane (Aldrich) and vanadium trichloride (Acros) were purchased and used without further purification. Where indicated, the reagents were synthesized in accordance with literature methods. C, H and N analyses were carried out by the Microanalytical Service of the Instituto Superior Técnico. Infrared spectra (4000–400 cm^{-1}) were recorded on a BIO-RAD FTS 3000MX instrument in KBr pellets and far infrared spectra (400–200 cm^{-1}) were recorded on a Vertex 70 spectrophotometer, in polyethylene and cesium iodide pellets. Vibrational frequencies are expressed in cm^{-1} ; abbreviations (intensity, shape): s, m and w, strong, medium and weak; s and br, sharp and broad. UV/vis/NIR spectra (1600–200 nm) were recorded on a Shimadzu UV-3101PC UV-VIS NIR spectrophotometer. ^1H , ^{13}C NMR spectra were measured on Bruker 300 and 400 UltraShieldTM spectrometers. ^1H and ^{13}C chemical shifts δ are expressed in ppm relative to $\text{Si}(\text{Me})_4$. Coupling constants are in Hz; abbreviations: s, singlet; d, doublet; m, complex multiplet; vt, virtual triplet; br, broad. EPR spectra were recorded on a Bruker ESP 300E X-band spectrometer equipped with an ER 4111 VT variable-temperature unit; g values were calculated from the formula $\nu = 1.39962 \cdot g \cdot B'$, where ν is the frequency measured (GHz) and B' is the corrected* value of Field (kGauss). SimFonia software was used to simulate the EPR spectra. $\text{ESI}^+/\text{ESI}^-$ mass spectra were obtained on a VARIAN 500-MS LC ion trap mass spectrometer (solvents: acetonitrile/methanol; flow: 20 $\mu\text{L}/\text{min}$; needle spray voltage: ± 5 Kv, capillarity voltage: ± 100 V; nebulizer gas (N_2): 35 psi; drying gas (N_2): 10

(*) The correction factor (*i.e.* ΔB) of field was calculated from the difference of theoretical and experimental values of field ($B' - B^{\text{exp}}$) of a reference compound (*i.e.* perylene radical in conc. sulfuric acid) with known g value: $\nu^{\text{exp}} = 1.39962 \cdot 2.002569 \cdot B'$.

psi; drying gas temperature (N₂): 350 °C). For the MS spectra description, M denotes the complex part of the compound.

Synthesis of hydrotris(pyrazolyl)methane, Tpm, HC(pz)₃ (1) (pz = pyrazolyl).

This compound was synthesized according to a published procedure¹ except for the final purification stage. The crude product (**1**) was crystallized from diethylether, leading to a white pure crystalline product (45%). Additionally, the crystallisation mother liquor was evaporated and the yellowish residue was purified by column chromatography (acetone/pentane 2/8) to afford an additional batch (29%) of (**1**), in good purity. ¹H-NMR (CDCl₃): δ 8.44 (s, 1H, HC(pz)), 7.72 (d, 3H, *J*_{HH} = 2.6 Hz, 3-H (pz)), 7.60 (d, 3H, *J*_{HH} = 2.6 Hz, 5-H (pz)), 6.40 (dd, 3-H, *J*_{HH} = 2.6 Hz, 4-H (pz)).

Synthesis of tris-2,2,2-(1-pyrazolyl)ethanol, HOCH₂C(pz)₃ (2) (pz = pyrazolyl).

This compound was synthesized according to a published procedure¹ except for a few details. Compound (**1**) (1.0 g 4.7 mmol, 1 eq), kept in a Shlenk under vacuum for 2 h, was dissolved in dry THF (60 mL) under dinitrogen. Fresh potassium *tert*-butoxide (1.4 g, 12.5 mmol, 2.6 eq) was added portionwise to the scorpionate solution and the resulting yellow/orange mixture was stirred under dinitrogen for 15 min., whereafter *para*-formaldehyde (0.38 g, 12 mmol, 2.6 eq) was added to the solution and the final mixture was stirred at room temperature overnight. Water (100 mL) was added and the mixture was extracted with diethyl ether (3 × 50 mL). The organic extracts were combined and dried over sodium sulfate and filtered. The solvent was removed under vacuum resulting in a pale yellow solid (1.0 g, 89%). ¹H-NMR (CDCl₃): δ 7.70 (d, 3H, *J*_{HH} = 2.5 Hz, 3-H (pz)), 7.11 (d, 3H, *J*_{HH} = 2.5 Hz, 5-H (pz)), 6.36 (dd, 3H, *J*_{HH} = 2.6 Hz, 4-H (pz)), 5.08 (s, 2H, CH₂). Compound (**2**) could crystallize by slow evaporation of a dichloromethane solution affording pure transparent crystals that show the following ¹H-NMR (CDCl₃) resonances: δ 7.70 (d, 3H, *J*_{HH} = 2.6 Hz, 3-H (pz)), 7.11 (d, 3H, *J*_{HH} = 2.6 Hz, 5-H (pz)), 6.36 (dd, 3H, *J*_{HH} = 2.6 Hz, 4-H (pz)), 5.08 (d, 2H, *J*_{HH} = 6.8 Hz, CH₂), 4.86 (t, 1H, *J*_{HH} = 6.8 Hz, OH).

Synthesis of 2,2,2-tris(pyrazol-1-yl)ethyl methanesulfonate, $\text{H}_3\text{CSO}_2\text{OCH}_2\text{C}(\text{pz})_3$ (2-Ms**) (pz = pyrazolyl).**

To a dichloromethane solution (20 mL) of 2,2,2-tris(pyrazol-1-yl)ethanol (**2**), (1 g, 4.10 mmol, 1 eq.) cooled at -15°C , triethylamine (0.75 mL, 5.38 mmol, 1.3 eq.) was added. The solution is stirred for 5 min. at -15°C then methanesulfonyl chloride (0.41 mL, 5.30 mmol, 1.3 eq.) was added dropwise. After addition the solution was allowed to warm to room temperature, during which time (10 min.) a precipitate appeared. The final mixture was stirred at room temperature for 1.5 h. Then water (ca. 10 mL) was added and the organic phase was washed with $\text{NaHCO}_{3\text{aq}}$, brine and dried over Na_2SO_4 . The solvent was evaporated in vacuum to give (**2-Ms**) as pale yellow solid (1.25 g, 95%). $\text{C}_{12}\text{H}_{14}\text{N}_6\text{O}_3\text{S}$, Anal. Calc.: C: 44.71%, H: 4.38%, N: 26.07%, S: 9.95%. Found: C: 44.23%, H: 4.80%, N: 25.89%, S: 9.23%. $^1\text{H-NMR}$ (400 MHz, CDCl_3): 7.69 (d, 3H, J_{HH} 1.7 Hz, 5-H (pz)), 7.30 (d, 3H, J_{HH} 2.2 Hz, 3-H (pz)), 6.38 (dd, 3H, J_{HH} 2.2 Hz, 4-H (pz)), 5.74 (s, 2H, CH_2), 2.94 (s, 3H, H_3C). Crystals suitable for X-ray diffraction are obtained by slow evaporation of (**2-Ms**) compound in dichloromethane

Synthesis of 4-((tris-2,2,2-(pyrazol-1-yl)ethoxy)methyl)pyridine, **TpmPy, (**4-py**) $\text{CH}_2\text{OCH}_2\text{C}(\text{pz})_3$ (**3**) (py = pyridyl, pz = pyrazolyl).**

Sodium hydride (159 mg, 3.98 mmol, 2 eq, 60% dispersion in mineral oil) was washed with dry pentane (2 x 10 mL) and then suspended in dry THF (15 mL). A THF (20 mL) suspension of tris-2,2,2-(pyrazol-1-yl)ethanol (**2**) (482 mg, 1.98 mmol, 1 eq) and 4-bromomethyl pyridine hydrobromide (502 mg, 1.98 mmol, 1 eq) was added portionwise to the hydride mixture under nitrogen; during this time, gaseous H_2 was formed. The resulting pale brown milky suspension was refluxed overnight. Then the mixture was allowed to cool down to room temperature and H_2O (20 mL) and Et_2O (20 mL) were added. The organic phase was separated and the aqueous phase was washed with Et_2O (5 mL). The organic phases were collected, washed with brine and dried over Na_2SO_4 , whereafter they are filtered and the solvent removed under vacuum to leave a pale yellow solid, that was crystallized in Et_2O to give colorless crystals of (**3**) (78%). Compound (**3**) is well soluble in all common organic solvents, e.g., Me_2CO , CHCl_3 , CH_2Cl_2 , MeOH, EtOH and DMSO, and less soluble in H_2O ($S_{25^\circ\text{C}} \approx 10 \text{ mg}\cdot\text{mL}^{-1}$). $\text{C}_{17}\text{H}_{17}\text{N}_7\text{O}$ (335.36): calcd. C 66.88, N 29.23, H 5.10; found. C 65.89,

N 29.02, H 5.41. IR (KBr): 3113 (m s), 3041, 2959, 2935 (m s), 2880 (m br), 1601 (s s, $\nu(\text{C}=\text{N})$), 1564 (s s, $\nu(\text{C}=\text{N})$), 1517 (s s, $\nu(\text{C}=\text{C})$), 1426 (m s), 1387 (m br), 1124 (s br), 863 (m s), 753 (s s), 688 (s s), 612 (s s), 489 (m s) cm^{-1} . ^1H NMR (300MHz, CDCl_3): δ 8.53 (d, 2H, $J_{\text{HH}} = 6.2$ Hz, 2-H (py)), 7.67 (d, 3H, $J_{\text{HH}} = 2.5$ Hz, 5-H (pz)), 7.40 (d, 3H, $J_{\text{HH}} = 2.5$ Hz, 3-H (pz)), 7.06 (d, 2H, $J_{\text{HH}} = 6.2$ Hz, 3-H (py)), 6.36 (dd, 3H, $J_{\text{HH}} = 2.5$ Hz, 4-H (pz)), 5.20 (s, 2H, $\text{CH}_2\text{-C}(\text{pz})_3$), 4.56 (s, 2H, $\text{CH}_2\text{-py}$). ^1H NMR (MHz, methanol- d_4): δ 8.43 (d, 2H, $J_{\text{HH}} = 5.7$ Hz, 2-H (py)), 7.66 (d, 3H, $J_{\text{HH}} = 2.5$ Hz, 5-H (pz)), 7.50 (d, 3H, $J_{\text{HH}} = 2.5$ Hz, 3-H (pz)), 7.20 (d, 2H, $J_{\text{HH}} = 5.7$ Hz, 3-H (py)), 6.41 (dd, 3H, $J_{\text{HH}} = 2.5$ Hz, 4-H (pz)), 5.15 (s, 2H, $\text{CH}_2\text{-C}(\text{pz})_3$), 4.64 (s, 2H, $\text{CH}_2\text{-py}$). ^{13}C NMR (100.6 MHz, CDCl_3): δ 148.79 (2-C (py)), 145.26 (4-C(py)), 140.46 (3-C(pz)), 129.73 (5-C (pz)), 120.57 (3-C (py)), 105.69 (4-C (pz)), 88.71 ($\text{C}(\text{pz})_3$), 73.11 (s, 2H, $\text{CH}_2\text{-C}(\text{pz})_3$), 71.50 (s, 2H, $\text{CH}_2\text{-py}$). X-ray quality single crystals were grown by slow cooling to 15°C of a concentrated diethyl ether solution of (**3**).

Synthesis of (tris-2,2,2-(pyrazol-1-yl)ethoxy)benzyl, $\text{PhCH}_2\text{OCH}_2\text{C}(\text{pz})_3$ (4**) (pz = pyrazolyl).**

Sodium hydride (75 mg, 1.88 mmol, 1 eq, 60% dispersion in mineral oil) was washed with dry pentane (2 x 15 mL) and then suspended in dry THF (15 mL). A THF (20 mL) solution of tris-2,2,2-(pyrazol-1-yl)ethanol (**2**) (456 mg, 1.87 mmol, 1 eq) was added dropwise to the hydride mixture under dinitrogen; during this time, gaseous H_2 was formed. A THF (5 mL) solution of benzyl chloride (388 μL , 3.36 mmol, 1.8 eq) was added dropwise to the final solution. The resulting pale brown solution was refluxed overnight. Then the mixture was allowed to cool down to room temperature and H_2O (20 mL) and Et_2O (30 mL) were added. The organic phase was separated and the aqueous phase was washed with Et_2O (10 mL). The organic extracts were collected, washed with brine and dried over Na_2SO_4 , whereafter they were filtered and the solvent removed under vacuum to leave a pale yellow solid that was purified by column chromatography (acetone/pentane 4/6) leading to a white powder of (**4**) (41%). Compound (**4**) is well soluble in all common organic solvents Me_2CO , CHCl_3 , CH_2Cl_2 , MeOH, EtOH and DMSO, and no soluble in H_2O . IR (KBr): 3101 (m s), 3022, 2951, 1534 (s s, $\nu(\text{C}=\text{N})$), 1519 (s s, $\nu(\text{C}=\text{C})$), 1413 (m s), 858 (m s), 738 (s s), 482 (m s) cm^{-1} . ^1H NMR (300MHz, CDCl_3): δ 7.63 (d, 3H, $J_{\text{HH}} = 2.4$ Hz, 5-H (pz)),

7.42 (d, 3H, $J_{HH} = 2.4$ Hz, 3-H (pz)), 7.29 (m, 3H, m,p -H (Ph)), 7.18 (d, 2H, $J_{HH} = 6.0$ Hz, o -H (Ph)), 6.31 (dd, 3H, $J_{HH} = 2.5$ Hz, 4-H (pz)), 5.11 (s, 2H, CH_2 -C(pz)₃), 4.49 (s, 2H, CH_2 -Ph).

Synthesis of TsNHCH₂CH₂OCH₂C(pz)₃ (5) (Ts = *para*-toluenesulfonyl, pz = pyrazolyl).

(i) Synthesis of N,O-bistosylethanolamine, TsNHCH₂CH₂OTs. To a stirred solution of tosylchloride (6.17 g, 32.36 mmol, 2.1 eq) in pyridine (4 mL) cooled at -30°C was added dropwise a solution of ethanolamine (993 μL, 16.18 mmol, 1 eq) in pyridine (3 mL). The resulting mixture was stirred 1h at -10°C, overnight, at 0°C. Crushed ice and CHCl₃ (10 mL) were added and the mixture stirred for 15 minutes. The organic phase was separated and washed with H₂O (3 x 10 mL), glacial acetic acid (5 mL) and water (10 mL), dried over Na₂SO₄ and evaporated to yield an orange oil that was triturated in pentane affording a white off solid (81%). ¹H-NMR (300 MHz, CDCl₃): 7.75 (d, 2H, $J_{HH} = 8$ Hz, m -H(Ts-O)), 7.70 (d, 2H, $J_{HH} = 8$ Hz, m -H(Ts-N)), 7.36 (d, 2H, $J_{HH} = 8$ Hz, o -H(Ts-O)), 7.31 (d, 2H, $J_{HH} = 8$ Hz, o -H(Ts-N)), 4.87 (tr br, 1H, $J_{HH} = 6$ Hz, NH), 4.05 (tr, 2H, $J_{HH} = 6$ Hz, CH₂-O), 3.23 (q, 2H, $J_{HH} = 6$ Hz, CH₂-NH), 2.47 (br, 3H, H₃C(Ts-O)), 2.44 (s, 3H, H₃C(Ts-N)).

(ii) Synthesis of N-tosylaziridine. To a toluene solution (40 mL) of N,O-bistosylethanolamine (4.83 g, 13.07 mmol, 1 eq) stirred vigorously, a solution of KOH (3.30 g, 58.90 mmol, 4.5 eq) in H₂O was added dropwise for 1h. The mixture was stirred for 2h at room temperature, then the organic layer was separated washed with H₂O (15 mL), dried over Na₂SO₄, filtered and evaporated. The crude residue was triturated in pentane (20 mL) and dried under vacuum affording a white/yellow solid (89%). ¹H-NMR (300 MHz, CDCl₃): 7.84 (d, 2H, $J_{HH} = 8$ Hz, m -H(Ts)), 7.36 (d, 2H, $J_{HH} = 8$ Hz, o -H(Ts)), 2.38 (m, 4H, CH₂-CH₂), 2.48 (br, 3H, H₃C(Ts)).

(iii) Synthesis of TsNHCH₂CH₂OCH₂C(pz)₃ (5). Sodium hydride (202 mg, 5.07 mmol, 1 eq, 60% dispersion in mineral oil) was washed with dry pentane (2 x 15 mL) and then suspended in dry THF (20 mL). A THF (20 mL) solution of tris-2,2,2-(pyrazol-1-yl)ethanol (**2**) (1.23 g, 5.07 mmol, 1 eq) was added dropwise to the hydride mixture under dinitrogen for 20 min.; during this time, gaseous H₂ was formed. A THF (10 mL) solution of N-tosylaziridine (1 g, 5.07 mmol, 1 eq) was added dropwise to the final solution. The resulting pale yellow solution was heated at 50°C for 2h.

Then the mixture was allowed to cool down to room temperature and H₂O (20 mL) and CHCl₃ (30 mL) were added. The organic phase was separated and the aqueous phase was washed with CHCl₃ (10 mL). The organic extracts were collected, washed with brine and dried over Na₂SO₄, whereafter they were filtered and the solvent removed under vacuum to leave a pale yellow oil. Compound **(5)** was isolated by column chromatography of this oil (acetone/pentane 1/2) leading to a white powder of **(5)** (52%). Compound **(5)** is well soluble in all common organic solvents, Me₂CO, CHCl₃, CH₂Cl₂, MeOH, EtOH and DMSO, and no soluble in H₂O. ¹H NMR (400MHz, CDCl₃): δ 7.68 (d, 3H, *J*_{HH}= 2.5 Hz, 5-H (pz)), 7.56 (d, 2H, *J*_{HH} = 8 Hz, *m*-H(Ts)), 7.14 (d, 2H, *J*_{HH} = 8 Hz, *o*-H(Ts)), 7.04 (d, 3H, *J*_{HH}= 2.5 Hz, 3-H (pz)), 6.30 (dd, 3H, *J*_{HH}= 2.5 Hz, 4-H (pz)), 6.09 (tr br, 1H, *J*_{HH} = 6 Hz, NH), 4.90 (s, 2H, CH₂-C(pz)₃), 3.56 (tr, 2H, *J*_{HH} = 6 Hz, CH₂-O), 2.97 (q, 2H, *J*_{HH} = 6 Hz, CH₂-NH), 2.48 (br, 3H, H₃C(Ts)). ¹³C NMR (400MHz, CDCl₃): δ 143.12 (H₃C-C(Ts)), 141.92 (3-C(pz)), 136.87 (O₂S-C(Ts)), 130.45 (5-C(pz)), 129.58 (*m*-C(Ts)), 127.06 (*o*-C(Ts)), 106.93 (4-C(pz)), 89.53 (C(pz)₃), 73.78 (H₂C-C(pz)₃), 69.77 (CH₂-O), 42.25 (CH₂-NH), 21.50 (H₃C(Ts)).

Synthesis of TsNHCH₂CH₂TsNCH₂CH₂OCH₂C(pz)₃ (**(6)** (pz = pyrazolyl)).

Compound **(6)** was isolated (23%) from chromatographic purification of **(5)** at the final stage. Higher yield (41%) of **(6)** could be obtained modifying the preparation of **(5)** in the following way: the solution of sodium tris-2,2,2-(pyrazol-1-yl)ethanoate is then added dropwise to a solution of N-tosylaziridine. Compound **(6)** is well soluble in all common organic solvents, Me₂CO, CHCl₃, CH₂Cl₂, MeOH, EtOH and DMSO, and no soluble in H₂O. ¹H NMR (400MHz, CDCl₃): δ 7.65 (d, 3H, *J*_{HH}= 2.5 Hz, 5-H (pz)), 7.60 (d, 2H, *J*_{HH} = 8 Hz, *m*-H(Ts)), 7.29 (d, 2H, *J*_{HH} = 8 Hz, *o*-H(Ts)), 7.18 (d, 3H, *J*_{HH}= 2.5 Hz, 3-H (pz)), 6.32 (dd, 3H, *J*_{HH}= 2.5 Hz, 4-H (pz)), 5.82 (tr br, 1H, *J*_{HH} = 6 Hz, NH), 5.00 (s, 2H, CH₂-C(pz)₃), 3.63 (tr, 2H, *J*_{HH} = 6 Hz, CH₂-O), 3.21 (tr, 2H, *J*_{HH} = 6 Hz, O-CH₂-CH₂-NTs), 3.21 (tr, 2H, *J*_{HH} = 6 Hz, NH-CH₂-CH₂-NTs), 2.96 (q, 2H, *J*_{HH} = 6 Hz, CH₂-NH), 2.44 (br, 3H, H₃C(Ts)).

Synthesis of the twitterionic tris(3,5-dimethylpyrazolyl)methane lithium tetrahydrofurane complex, $[\{^-\text{C}(\text{pz}^{\text{Me}2})_3\}\text{Li}^+(\text{thf})]$ (7) ($\text{pz}^{\text{Me}2}$ = 3,5-dimethylpyrazolyl).

A 1.6 M solution of butyllithium (230 μL , 0.37 mmol, 1.1 eq) in cyclohexane was added dropwise to tris(3,5-dimethylpyrazolyl)methane $\text{HC}(\text{pz}^{\text{Me}2})_3$ (100 g, 0.34 mmol, 1.0 eq) in dry THF (10 mL) at -70°C . The solution was stirred for 1h at -60°C then was allowed to warm to 0°C and all volatile components were removed under vacuum. The red oily residue was dissolved in a minimum amount of dry THF and cooled at -30°C . After 2 days a red solid of (7) formed (80%). $^1\text{H-NMR}$ (400 MHz, $\text{THF-}d_6$): 5.55 (s, 3H, 4-H (pz)), 2.51 (br, 12H, 3- H_3C (pz)), 2.15 (s, 12H, 5- H_3C (pz)).

Synthesis of the cationic tris(3,5-dimethylpyrazolyl)methane lithium tetrahydrofurane radical, $[\{^{\bullet}\text{C}(\text{pz}^{\text{Me}2})_3\}\text{Li}(\text{thf})]^+$ (7 $^+$) ($\text{pz}^{\text{Me}2}$ = 3,5-dimethylpyrazolyl).

A 1.6 M solution of butyllithium (230 μL , 0.37 mmol, 1.1 eq) in cyclohexane was added dropwise to tris(3,5-dimethylpyrazolyl)methane $\text{HC}(\text{pz}^{\text{Me}2})_3$ (100 g, 0.34 mmol, 1.0 eq) in dry THF (10 mL) at -70°C . The solution was stirred for 1h at -60°C , then cooled down to -90°C and a THF solution (2 mL) of I_2 (43 mg, 0.17 mmol, 0.5 eq) was added dropwise, via a cannula; the colour turned immediately to dark intense green and the mixture was kept stirred under argon atmosphere at -90°C . The solution was carefully transferred at -80°C to an EPR tube (kept under argon at -80°C); the tube was then immediately cooled (and the solution frozen) in liquid nitrogen (77 K). No colour change has been detected during or after the transfer: X-band EPR (center field: 3343.56; modulation frequency: 100 KHz; modulation amplitude: 0.1 Gpp; receiver gain: $4 \cdot 10^{-4}$; conversion time: 20 ms; time constant: 20 ms; ST : 42 s) of a 1 mM THF frozen solution of (7 $^+$), recorded at 95 K, exhibits an intense single isotropic signal at $g = 2.0026$ (with a peak-to-peak line width of *ca.* 15 G and no resolved hyperfine splitting).

Synthesis of tetrakis(3,5-dimethylpyrazolyl)methane, $C(pz^{Me_2})_4$ (pz^{Me_2} = 3,5-dimethylpyrazolyl) (8).

A 1.6 M solution of butyllithium (7.24 mL, 11.58 mmol, 1.15 eq) in cyclohexane was added dropwise to tris(3,5-dimethylpyrazolyl)methane (3.00 g, 10.08 mmol, 1 eq) in dry THF (100 mL) at -70°C . The solution turned orange-red and was stirred for 20 min at -60°C , then cooled down to -80°C . A solution of I_2 (1.28 g, 5.03 mmol, 0.5 eq) in dry THF (50 mL) was added dropwise to the red mixture under vigorous stirring at -80°C , causing a drastic colour change to deep intense green. The reaction mixture was stirred for a further 10 min at -80°C , and then allowed to warm to room temperature in 3 h; during this time the solution turned gradually to brown/yellow and a pale brown solid precipitate formed. The solvent was evaporated from the mixture to yield a brown solid. This was dissolved in CH_2Cl_2 (40 mL) and the solution was washed with water (2 x 20 mL), dried over Na_2SO_4 , filtered and evaporated, yielding a brown solid. The residue was rapidly purified by flash chromatography passing through a silica column (100% pentane as eluent). The product was isolated as a white crystalline solid in 27% yield with respect to $HC(pz^{Me_2})_3$. Slow evaporation of a chloroform solution over two days yielded single crystals of $C(pz^{Me_2})_4$ that were suitable for X-ray crystallography analysis. $C_{21}H_{28}N_8$, 392.5. IR (KBr): 3102 (m), 2961, 2926 (s br, CH), 1568 (vs, $\nu_{C=N}$), 1413 (s), 1243 (vs, br), 924 (vs), 899 (vs), 793 (s), 758 (s) cm^{-1} . MS-EI m/z : 297 [$C(pz^{Me_2})_3$] $^+$, 415 [$C(pz^{Me_2})_4+Na$] $^+$. 1H -NMR (400 MHz, $CDCl_3$, 298 K): 5.93 (s, 4H, 4-H (pz)), 2.14 (s, 12H, 3- H_3C (pz)), 1.67 (s, 12H, 5- H_3C (pz)). 1H -NMR (400 MHz, acetone- d_6 , 298 K): 6.00 (s, 4H, 4-H (pz)), 2.08 (s, 12H, 3- H_3C (pz)), 1.64 (s, 12H, 5- H_3C (pz)). 1H -NMR (400 MHz, MeOD, 298 K): 6.14 (s, 4H, 4-H (pz)), 2.12 (s, 12H, 3- H_3C (pz)), 1.64 (s, 12H, 5- H_3C (pz)). 1H -NMR (400 MHz, $CDCl_3$, 213 K): 5.97 (s, 4H, 4-H (pz)), 2.14 (s, 12H, 3- H_3C (pz)), 1.62 (s, 12H, 5- H_3C (pz)). 1H -NMR (400 MHz, acetone- d_6 , 213 K): 6.06 (s, 4H, 4-H (pz)), 2.05 (s, 12H, 3- H_3C (pz)), 1.58 (s, 12H, 5- H_3C (pz)). ^{13}C -NMR (100 MHz, $CDCl_3$, 298 K): 147.21 (3-C (pz)), 144.67 (5-C (pz)), 109.22 (4-C (pz)), 97.98 ($C(pz^{Me_2})_4$), 14.16 (3- CH_3 (pz)), 11.94 (5- CH_3 (pz)).

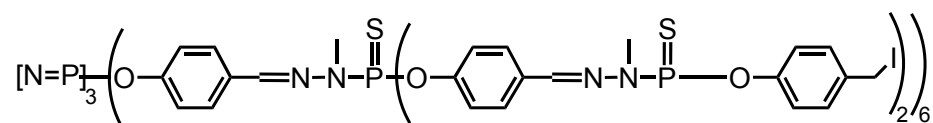
Synthesis of lithium tris(pyrazolyl)methanesulfonate, [Tpms]Li, [O₃SC(pz)₃]Li (9**) (pz = pyrazolyl).**

This compound was synthesized according to a published procedure² to afford (**9**) (62%). IR (KBr): 3136 (w), 2961, 1524 (m, $\nu(\text{C}=\text{N})$), (m), 1479, 1463 (s), 1398, 1331 (s), 1329 (s), 1105 (s), 1048 (s, $\nu(\text{S}-\text{O})$), 864 (s), 754 (s), 643 (s, $\nu(\text{C}-\text{S})$) cm^{-1} . ¹H-NMR (MeOD): δ 7.91 (d, 3H, $J_{\text{HH}} = 2.6$ Hz, 3-H (pz)), 7.58 (d, 3H, $J_{\text{HH}} = 2.6$ Hz, 5-H (pz)), 6.41 (dd, 3-H, $J_{\text{HH}} = 2.6$ Hz, 4-H (pz)). ¹H-NMR (DMSO-*d*₆): δ 8.11 (d, 3H, $J_{\text{HH}} = 2.6$ Hz, 3-H (pz)), 7.38 (d, 3H, $J_{\text{HH}} = 2.6$ Hz, 5-H (pz)), 6.31 (dd, 3-H, $J_{\text{HH}} = 2.6$ Hz, 4-H (pz)). ¹H-NMR (D₂O): δ 7.62 (d, 3H, $J_{\text{HH}} = 2.6$ Hz, 3-H (pz)), 7.55 (d, 3H, $J_{\text{HH}} = 2.6$ Hz, 5-H (pz)), 6.44 (dd, 3-H, $J_{\text{HH}} = 2.6$ Hz, 4-H (pz)).

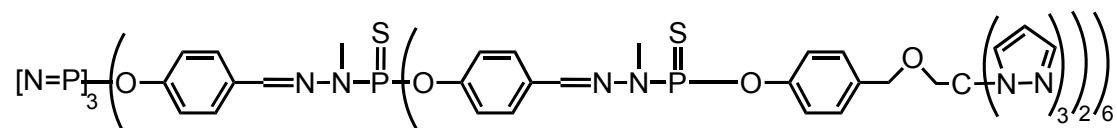
Synthesis of dendrimer, N₃P₃-G_{c1}-[CH₂C(pz)₃]₁₂ (10**).**

Sodium hydride (16 mg, 0.41 mmol, 24 eq, 60% dispersion in mineral oil) was washed with dry pentane (2 x 3 mL) and then suspended in dry THF (5 mL). A THF (5 mL) solution of tris-2,2,2-(pyrazol-1-yl)ethanol (**2**) (100 mg, 0.41 mmol, 24 eq) was added dropwise to the hydride mixture under dinitrogen; during this time, gaseous H₂ was formed. A THF (5 mL) solution of N₃P₃-G_{c0}-I₁₂ ([4198.38], 68 mg, 16.67·10⁻³ mmol, 1 eq) was added dropwise to the final solution. The resulting solution was stirred at 35°C overnight. The solvent was evaporated under vacuum and the residue was suspended in chloroform (8 mL), filtered and washed with ether (2 x 15 mL) affording to a pale yellow powder of (**10**) (32%).

N₃P₃-G_{c0}-I₁₂:



N₃P₃-G_{c1}-[CH₂C(pz)₃]₁₂:



(**10**), C₂₆₄H₂₅₂N₈₇O₃₀S₆P₉, (5594.68). ¹H NMR (300MHz, CDCl₃/THF-*d*₈): δ 7.55 (br s, 12H+36H, dendrimer + 5-H (pz)), 7.36-7.34 (br s, 36H, 3-H (pz)), 7.20-6.80 (m, 72H, dendrimer), 6.22-6.27 (m, 3H, 36H, 4-H (pz)), 5.11 (s br, 24H, CH₂-C(pz)₃), 4.41 (s,

24H, CH_2 -Ph), 2.88-3.10 (m, 18 H, dendrimer). $^{31}P\{^1H\}$ NMR (162.0 MHz, $CDCl_3/THF-d_8$): δ 10.79 (s, P_0), 64.87 (s, P_1).

Synthesis of tris(3,5-dimethylpyrazolyl)methane, Tpm^{Me_2} , $C(pz^{Me_2})_3$ (11**) (pz^{Me_2} = 3,5-dimethylpyrazolyl).**

This compound was synthesized according to a published procedure¹ except for the final purification stage. The organic extracts were collected and evaporated under vacuum and the residue was purified by column chromatography (acetone/pentane 1/9) leading to a white powder of (**11**) (61%). 1H -NMR ($CDCl_3$): δ 8.07 (s, 1H, $HC(pz)$), 5.87 (s, 3H, 4-H (pz)), 2.18 (d, 9H, 3- H_3C (pz)), 2.01 (s, 9H, 5- H_3C (pz)).

Synthesis of tris(3-phenylpyrazolyl)methane, Tpm^{Ph} , $C(pz^{Ph})_3$ (12**) (pz^{Ph} = 3-phenylpyrazolyl).**

To a vigorously stirred suspension of 3-phenyl-pyrazole (5.00 g, 34.7 mmol, 1 eq) and tetrabutylammonium bromide (0.56 g, 1.70 mmol, 0.05 eq) in water (70 mL), an excess of Na_2CO_3 (22.0 g, 208 mmol, 6 eq) was added during 30 min. Then chloroform (17 mL) was added and the final mixture was refluxed for 84 h (after 40 h a second amount of 17 mL of chloroform was added). After this time, the reaction mixture was then cooled to room temperature and toluene (20 mL) and water (15 mL) were added. The organic phase was separated, washed with water, brine, dried over Na_2SO_4 and evaporated under vacuum to give a brown oil. This crude oil was dissolved in toluene (40 mL) and a catalytic amount (*ca.* 80 μ L, 1.0 mmol) of trifluoroacetic acid (TFA) was added to this solution which was then refluxed for 1 day. After this, the solution was cooled down to room temperature, washed with water (2 x 15 mL) and neutralised with an aqueous solution of $NaHCO_3$. The organic phases were collected, washed with water and brine, then dried over Na_2SO_4 and evaporated. The crude solid was triturated in diisopropyl ether to give an off-white powder of (**12**) (3.2 g, 62%). The compound is well soluble in medium and high polarity solvents like Me_2CO , $CHCl_3$, CH_2Cl_2 , MeOH, EtOH and DMSO, and insoluble in H_2O . (**12**), $C_{28}H_{22}N_6$ (442.51): calcd. C 75.99, N 18.99, H 5.01; found C 75.86, N 18.71, H 5.39. IR (KBr): 3162 (w), 1529 (m, $\nu(C=N)$), 1502 (m), 1456 (s), 1240 (s), 1077 (s), 1050

(s), 809 (s), 756 (s), 693 (s) cm^{-1} . $^1\text{H-NMR}$ (300MHz, acetone- d_6): 8.86 (s, 1H, HC), 8.11 (d, 3H, $J_{\text{HH}}=2.6$ Hz, 5-H (pz)), 7.90 (d, 2H, $J_{\text{HH}}=8.1$ Hz, *o*-H (Ph)), 7.42 (dd, vt, 6H, *m*-H (Ph)), 7.35 (dd, vt, 3H, *p*-H (Ph)), 6.90 (d, 3H, $J_{\text{HH}}=2.6$ Hz, 4-H (pz)).

Synthesis of tris(3-*tert*-butylpyrazolyl)methane, Tpm^{tBu} , $\text{C}(\text{pz}^{\text{tBu}})_3$ (13) (pz^{tBu} = 3-*tert*-butylpyrazolyl).

(i) Synthesis of 3-*tert*-butyl-pyrazole. According to a published procedure³, freshly prepared (173 mg, 7.52 mmol, 0.96 eq of Na in methanol) sodium methoxide (0.96 eq) was dissolved in dry toluene (10 mL). To this solution a mixture of 3,3-dimethyl-2-butanone (1 mL, 7.85 mmol, 1eq) and ethyl formate (695 μL , 8.64 mmol, 1.1) was added. The resulting mixture was stirred under dinitrogen for 2h at room temperature. Then the solution was concentrated under gentle vacuum and all volatile products were removed (ca. 1 mL). Cold water was added (8 mL) and the biphasic mixture was stirred until the yellow color passed to the aqueous phase. The latter was separated and added to a water solution (5 mL) of monohydrate hydrazine (361 μL , 7.45 mmol, 0.95 eq). The final mixture was stirred overnight at room temperature. CH_2Cl_2 (15 mL) was added and the organic phase was separated, dried over Na_2SO_4 and evaporated to afford a yellow oil (54%). $^1\text{H-NMR}$ (300MHz, CDCl_3): 7.49 (m br, 1H+1H, 5-H(pz) + NH), 6.12 (d, 1H, $J_{\text{HH}} = 2.4$ Hz, 4-H (pz)), 1.35 (s, 9H, ^tBu).

(ii) Synthesis of tris(3-*tert*-butylpyrazolyl)methane, Tpm^{tBu} (13). To a vigorously stirred suspension of 3-*tert*-butyl-pyrazole (282 mg, 2.27 mmol, 1 eq) and tetrabutylammonium bromide (36.6 mg, 0.11 mmol, 0.05 eq) in water (10 mL), an excess of Na_2CO_3 (1.44 g, 13.58 mmol, 6 eq) was added during 30 min. Then chloroform (3 mL) was added and the final mixture was refluxed for 84 h (after 40 h a second amount of 3 mL of chloroform was added). The reaction mixture was then cooled to room temperature and toluene (10 mL) and water (8 mL) were added. The organic phase was separated, washed with water, brine, dried over Na_2SO_4 and evaporated under vacuum to give a brown oil. This crude oil was dissolved in toluene (15 mL) and a catalytic amount (ca. 5 μL , 0.07 mmol) of trifluoroacetic acid (TFA) was added to this solution which was then refluxed for 1 day. After this, the solution was cooled down to room temperature, washed with water (2 x 5 mL) and neutralised with an aqueous solution of NaHCO_3 . The organic phases were collected, washed with water and brine, then dried over Na_2SO_4 and evaporated. The crude residue was

purified by column chromatography (acetone/pentane 2/8) leading to a white powder of **(13)** (44%). The compound is well soluble all common organic solvents like Me₂CO, CHCl₃, CH₂Cl₂, MeOH, EtOH and DMSO, and insoluble in H₂O. **(13)**, C₂₂H₃₄N₆ (382.242): calcd. C 69.07, N 21.97, H 8.96; found C 69.26, N 21.78, H 9.13. IR (KBr): 3122 (w), 1519 (m, ν (C=N)), 1500 (m), 1436 (s), 1198 (m), 1054 (s), 819 (s), 736 (s) cm⁻¹. ¹H-NMR (300MHz, CDCl₃): 8.20 (s, 1H, HC), 7.20 (d, 3H, $J_{\text{HH}}=2.5$ Hz, 5-H (pz)), 6.14 (d, vt, 3H, $J_{\text{HH}}=2.5$ Hz, 4-H (pz)), 1.27 (s br, 27H, ^tBu). ¹H-NMR (300MHz, acetone-*d*₆): 8.38 (s, 1H, HC), 7.61 (d, 3H, $J_{\text{HH}}=2.5$ Hz, 5-H (pz)), 6.26 (d, vt, 3H, $J_{\text{HH}}=2.5$ Hz, 4-H (pz)), 1.26 (s br, 27H, ^tBu). ¹³C-NMR (300MHz, CDCl₃): 163.8 (s, 3-C (pz)), 129.3 (s, 5-C (pz)), 103.4 (s, 4-C (pz)), 99.9 (s, C(pz)₃), 32.4 (C(CH₃)₃), 29.9 (CH₃).

Synthesis of tris(3-*iso*-propylpyrazolyl)methane, Tpm^{iPr}, C(pz^{iPr})₃ (14)
(pz^{iPr} = 3-*iso*-propylpyrazolyl).

(i) Synthesis of 3-*iso*-propyl-pyrazole.⁴ An analogous procedure to that for the synthesis of 3-*tert*-butylpyrazole for **(13)** was followed, starting from 3-methyl-2-butanone, ethylformate and hydrazine. ¹H-NMR (300MHz, CDCl₃): 9.23 (s, 1H, NH), 7.34 (d, 1H, $J_{\text{HH}}=2.5$ Hz, 5-H (pz)), 6.09 (d, vt, 1H, $J_{\text{HH}}=2.5$ Hz, 4-H (pz)), 3.11 (m, 1H, CH(iPr)), 1.31 (d, 6H, ^tBu).

(ii) Synthesis of tris(3-*iso*-propylpyrazolyl)methane (14). An analogous procedure to that for the synthesis of **(13)** was followed, leading to **(14)** (51%). The compound is well soluble all common organic solvents like Me₂CO, CHCl₃, CH₂Cl₂, MeOH, EtOH and DMSO, and insoluble in H₂O. **(13)**, C₁₉H₂₅N₆ (337.447): calcd. C 67.63, N 24.90, H 7.47; found C 68.01, N 24.18, H 7.86. IR (KBr): 3180 (w), 3054, 2912, 1519 (m, ν (C=N)), 1431 (s), 1201 (m), 1063 (s), 823 (s), 765 (s) cm⁻¹. ¹H-NMR (300MHz, CDCl₃): 8.20 (s, 1H, HC), 7.20 (d, 3H, $J_{\text{HH}}=2.5$ Hz, 5-H (pz)), 6.14 (d, vt, 3H, $J_{\text{HH}}=2.5$ Hz, 4-H (pz)), 3.02 (m, 3H, CH(iPr)), 1.29 (d, 18H, ^tBu).

Synthesis of tris(3,5-diphenylpyrazolyl)methane, Tpm^{Ph2}, C(pz^{Ph2})₃ (15)
(pz^{Ph2} = 3,5-diphenylpyrazolyl).

To a vigorously stirred suspension of 3,5-diphenylpyrazole (3 g, 13.62 mmol, 1 eq) and tetrabutylammonium bromide (219 mg, 0.68 mmol, 0.05 eq) in water (35

mL), an excess of Na_2CO_3 (8.6 g, 81.76 mmol, 6 eq) was added during 30 min. Then chloroform (7 mL) was added and the final mixture was refluxed for 84 h (after 40 h a second amount of 7 mL of chloroform was added). After this time, the reaction mixture was then cooled to room temperature and toluene (18 mL) and water (10 mL) were added. The organic phase was separated, washed with water, brine, dried over Na_2SO_4 and evaporated under vacuum to give a brown oil. This crude oil was dissolved in toluene (30 mL) and a catalytic amount (*ca.* 40 μL , 0.5 mmol) of trifluoroacetic acid (TFA) was added to this solution which was then refluxed for 1 day. After this, the solution was cooled down to room temperature, washed with water (2 x 10 mL) and neutralised with an aqueous solution of NaHCO_3 . The organic phases were collected, washed with water and brine, then dried over Na_2SO_4 and evaporated. The $^1\text{H-NMR}$ of crude revealed the product (**15**) (20 %) with the presence of starting pyrazole (28%) and some byproducts of decomposition (46%) and the residue was not purified further.

Synthesis of lithium tris(3-phenylpyrazolyl)methanesulfonate, $[\text{Tpm}^{\text{Ph}}]_3\text{Li}$, $[\text{O}_3\text{SC}(\text{pz}^{\text{Ph}})_3]\text{Li}$ (16**) (pz^{Ph} = 3-phenylpyrazolyl).**

A 1.6 M solution of butyllithium (1.6 mL, 2.7 mmol, 1.1 eq) in hexane was added dropwise to tris(3-phenylpyrazolyl)methane Tpm^{Ph} (1.00 g, 2.26 mmol, 1.0 eq) in dry THF at -65°C . The solution turned red/brown and was stirred for 1 h at -60°C . Sulfur trioxide-trimethylamine complex (330 mg, 2.38 mmol, 1.05 eq) was added at -60°C and the reaction was allowed to warm to room temperature overnight. The solvent was evaporated and the residue was dried under vacuum at room temperature for 2 h. It was then suspended in THF and filtered to yield a white powder of (**1**) (0.66 g, 56%). The compound is well soluble in medium and high polarity solvents like H_2O ($S_{25^\circ\text{C}} \approx 90 \text{ mg}\cdot\text{mL}^{-1}$), Me_2CO , CHCl_3 , MeOH , EtOH and DMSO , and insoluble in Et_2O . $\text{Li}[\text{O}_3\text{SC}(\text{3Ph-pz})_3]$, $\text{C}_{28}\text{H}_{21}\text{N}_6\text{O}_3\text{SLi}$ (528.51): calcd. C 63.63, N 15.90, H 4.01, S 6.07; found C 63.12, N 15.71, H 4.39, S 5.91. IR (KBr): 3437 (s), 3060, 2980, 2882 (m br), 1534 (m, $\nu(\text{C}=\text{N})$), 1502 (m), 1456 (s), 1398 (m), 1354 (m), 1266 (s br), 1240 (s br), 1077 (s), 1048 (s, $\nu(\text{S}-\text{O})$), 888 (m), 866 (s), 760 (s), 698 (s), 643 (s, $\nu(\text{C}-\text{S})$) cm^{-1} . $^1\text{H-NMR}$ (300MHz, acetone- d_6): 8.22 (d, 3H, $J_{\text{HH}}=2.7$ Hz, 5-H (pz)), 7.77 (d, 6H, $J_{\text{HH}}=8.1$ Hz, *o*-H (Ph)), 7.37-7.24 (m, 9H, *m*-H and *p*-H (Ph)), 6.83 (d, 3H, $J_{\text{HH}}=2.7$ Hz, 4-H (pz)). $^{13}\text{C-NMR}$ (300MHz, acetone- d_6): 151.1 (s, 3-C (pz)), 134.4 (s,

5-C (pz)), 133.5 (s, pz-C (Ph)), 128.3 (s, o-C (Ph)), 127.6 (s, p-C (Ph)), 125.8 (s, m-C (Ph)), 103.5 (s, 4-C (pz)), 99.9 (s, O₃SC).

Synthesis of [(pz^{Me2})₃C-O-C(pz^{Me2})₃] (17) (pz^{Me2} = 3,5-dimethylpyrazolyl).

A 1.6 M solution of butyllithium (230 μ L, 0.37 mmol, 1.1 eq) in cyclohexane was added dropwise to tris(3,5-dimethylpyrazolyl)methane HC(pz^{Me2})₃ (100 g, 0.34 mmol, 1.0 eq) in dry THF (10 mL) at -70°C. The solution was stirred for 1h at -60°C, then cooled down to -90°C and a THF solution (2 mL) of I₂ (43 mg, 0.17 mmol, 0.5 eq) was added dropwise, via a cannula; the colour turned immediately to dark intense green and the mixture was kept stirred under argon atmosphere at -90°C. After the addition, O₂ was bubbled through the solution which turned instantaneously to deep red. The mixture was stirred at -90°C for 20 min and stored at -80°C overnight in a deep freezer. The reaction mixture was then allowed to warm to room temperature and the final solution (brown/red) was evaporated to give a brown solid. The product was purified by flash chromatography (acetone/pentane) to give a pale brown powder in 33 % yield. ¹H-NMR (400 MHz, CDCl₃): 5.83 (s, 3H, 4-H (pz)), 2.41 (br, 18H, 3-H₃C (pz)), 2.26 (s, 18H, 5-H₃C (pz)). MS-EI *m/z*: 611 [O(C(pz^{Me2})₃) + H]⁺, 305 [O(C(pz^{Me2})₃)]²⁺.

Synthesis of 4-((tris-2,2,2-(3-phenylpyrazol-1-yl)ethanol, HOCH₂C(pz^{Ph})₃) (18) (pz^{Ph} = 3-phenylpyrazolyl).

Tris(3-phenylpyrazolyl)methane (300 mg, 0.68 mmol, 1 eq) was dissolved in dry THF (8 mL) and potassium *tert*-butoxide (197 mg, 1.76 mmol, 2.6 eq) was added portionwise. After 5 minutes *para*-formaldehyde (52 mg, 1.74 mmol, 2.6 eq) was added and the resulting mixture stirred at room temperature overnight. Water (10 mL) was added and the mixture extracted with diethyl ether (3 x 20 mL). The organic extracts are combined, washed with brine and dried over sodium sulfate. The mixture was filtered off and the solvent was removed in vacuo leading to a white off powder (89%) of (18). The compound is well soluble in all common organic solvents, *e.g.*, Me₂CO, CHCl₃, CH₂Cl₂, MeOH, EtOH and DMSO, less soluble in H₂O. C₂₉H₂₄N₆O (472.55): calcd. C 73.71, N 17.78, H 5.12; found. C 73.89, N 18.01, H 5.33 IR (KBr): 3056, 2963, 2923 (m s), 2877 (m br), 1544 (m s, *n*(C=N)), 1514 (s s, *n*(C=C)), 1440

(m s), 1354 (m br), 1137 (s br), 862 (m s), 743 (s s), 648 (m s) cm^{-1} . $^1\text{H-NMR}$ (CDCl_3): δ 7.83 (d, 6H, $J_{\text{HH}}=8$ Hz, o-H (Ph)), 7.41 (dd, vt, 6H, $J_{\text{HH}}=8$ Hz, m-H(Ph)), 7.38 (dd, vt, 3H, $J_{\text{HH}}=8$ Hz, p-H (Ph)), 7.19 (d, 3H, $J_{\text{HH}}=2.6$ Hz, 5-H (pz)), 6.67 (dd, 3H, $J_{\text{HH}}=2.6$ Hz, 4-H (pz)), 5.29 (s, 2H, CH_2). $^{13}\text{C}\{^1\text{H}\}$ and HMQC $^{13}\text{C}-^1\text{H}$ NMR (100.6 MHz, CDCl_3): δ 153.68 (s, 3-C (pz)), 132.47 (s, pz-C (Ph)), 131.78 (s, 5-C (pz)), 128.81 (s, m-C (Ph)), 128.67 (s, p-C (Ph)), 126.17 (s, o-C (Ph)), 104.16 (s, 4-C (pz)), 90.04 (s, $\text{CH}_2\text{-C}(\text{pz})_3$), 68.15 (s, $\text{O-CH}_2\text{-C}(\text{pz})_3$).

Synthesis of 4-((tris-2,2,2-(3-phenylpyrazol-1-yl)ethoxy)methyl)pyridine, TpmPy^{Ph} (19).

Sodium hydride (159 mg, 3.98 mmol, 2 eq, 60% dispersion in mineral oil) was washed with dry pentane (2 x 10 mL) and then suspended in dry THF (15 mL). A THF (20 mL) suspension of tris-2,2,2-(3-phenylpyrazol-1-yl)ethanol (940 mg, 1.98 mmol, 1 eq) and 4-bromomethyl pyridine hydrobromide (502 mg, 1.98 mmol, 1 eq) are added portionwise to the hydride mixture under nitrogen. The resulting pale brown milky suspension was refluxed overnight. Then the mixture was allowed to cool down to room temperature, and H_2O (20 mL) and Et_2O (20 mL) are added. The organic phase was separated and the aqueous phase was washed with Et_2O (5 mL). The organic phases are collected, washed with brine and dried over Na_2SO_4 , Filtration and removal of solvent under vacuum leaves a transparent oil, that was purified by column chromatography (pentane/acetone 8/2) to give a white off solid (75%) of (19). Compound (2) is stable in air although being slightly hygroscopic. It is well soluble in all common organic solvents, e.g. Me_2CO , CHCl_3 , CH_2Cl_2 , MeOH, EtOH and DMSO, and is insoluble in H_2O . $\text{C}_{35}\text{H}_{29}\text{N}_7\text{O}$ (563.66): calcd. C 74.58, N 17.39, H 5.19; found. C 74.02, N 16.92, H 5.01. IR (KBr): 3132, 3059, 2923, 2853 (w s, $n(\text{C-H})$), 1603 (s s, $n(\text{C=N})$), 1561 (s s, $n(\text{C=N})$), 1530 (s s, $n(\text{C=C})$), 1499, 1455 (s s), 1219 (m br), 1124, 1101, 1071, 1042 (m s), 869 (s s), 751 (s s), 692 (s s), 616 (w s), 477 (m s) cm^{-1} . $^1\text{H-NMR}$ (CDCl_3 , 298 K): δ 8.47 (d, 2H, $J_{\text{HH}}=6.0$ Hz, 2,6-H (py)), 7.81 (d, 6H, $J_{\text{HH}}=7.6$ Hz, o-H (Ph)), 7.57 (d, 3H, $J_{\text{HH}}=2.6$ Hz, 5-H (pz)), 7.40 (dd, vt, 6H, $J_{\text{HH}}=7.6$ Hz, m-H (Ph)), 7.33 (dd, vt, 3H, $J_{\text{HH}}=7.6$ Hz, p-H (Ph)), 7.10 (d, 2H, $J_{\text{HH}}=6.0$ Hz, 3,5-H (py)), 6.67 (d, 3H, $J_{\text{HH}}=2.6$ Hz, 4-H (pz)), 5.40 (s, 2H, $\text{CH}_2\text{-C}(\text{pz})_3$), 4.64 (s, 2H, $\text{CH}_2\text{-py}$). $^1\text{H-NMR}$ (acetone- d_6 , 298 K): δ 8.41 (d, 2H, $J_{\text{HH}}=5.7$ Hz, 2,6-H (py)), 7.86 (d, 6H, $J_{\text{HH}}=7.7$ Hz, o-H (Ph)), 7.78 (d, 3H, $J_{\text{HH}}=2.7$ Hz, 5-H (pz)), 7.40 (t, 6H, $J_{\text{HH}}=$

7.7 Hz, *m*-H (Ph)), 7.32 (t, 3H, $J_{\text{HH}} = 7.2$ Hz, *p*-H (Ph)), 7.19 (d, 2H, $J_{\text{HH}} = 6.0$ Hz, 3,5-H (py)), 6.88 (d, 3H, $J_{\text{HH}} = 2.6$ Hz, 4-H (pz)), 5.42 (s, 2H, $\text{CH}_2\text{-C}(\text{pz})_3$), 4.79 (s, 2H, $\text{CH}_2\text{-py}$). $^{13}\text{C}\{^1\text{H}\}$ and HMQC $^{13}\text{C}\text{-}^1\text{H}$ NMR (100.6 MHz, CDCl_3 , 298 K): δ 153.08 (s, 3-C (pz)), 149.76 (s, 2,6-C (py)), 146.73 (s, 4-C (py)), 132.81 (s, pz-C (Ph)), 132.44 (s, 5-C (pz)), 128.70 (s, *m*-C (Ph)), 128.38 (s, *p*-C (Ph)), 126.03 (s, *o*-C (Ph)), 121.75 (s, 3,5-C (py)), 103.88 (s, 4-C (pz)), 90.17 (s, $\text{CH}_2\text{-C}(\text{pz})_3$), 74.07 (s, $\text{O-CH}_2\text{-C}(\text{pz})_3$), 72.54 (s, $\text{O-CH}_2\text{-py}$). ^{13}C -NMR (100.6 MHz, $\text{acetone-}d_6$, 298 K): δ 153.47 (s, 3-C (pz)), 150.46 (s, 2,6-C (py)), 147.51 (s, 4-C (py)), 133.72 (s, pz-C (Ph)), 133.65 (s, 5-C (pz)), 129.40 (s, *m*-C (Ph)), 129.00 (s, *p*-C (Ph)), 126.52 (s, *o*-C (Ph)), 122.38 (s, 3,5-C (py)), 104.43 (s, 4-C (pz)), 90.99 (s, $\text{CH}_2\text{-C}(\text{pz})_3$), 74.32 (s, $\text{O-CH}_2\text{-C}(\text{pz})_3$), 72.65 (s, $\text{O-CH}_2\text{-py}$).

Synthesis of $[\text{Cu}(\text{Tpms}^{\text{Ph}})(\text{MeCN})]$ (**20**).

Compound (**20**) was prepared by adding 5 mL of a methanolic solution of $\text{Li}(\text{Tpms}^{\text{Ph}})$ (**16**) (78.3 mg, 0.148 mmol) to a $[\text{Cu}(\text{MeCN})_4][\text{PF}_6]$ solution (55.2 mg, 0.148 mmol) in the same solvent (10 mL). The reaction mixture was stirred at room temperature for 10 min. and compound (**20**) precipitated as a white powder which was collected by filtration, washed with cold methanol (2 x 5 mL) and dried under vacuum (57 mg, 62%). It is well soluble in medium polarity solvents like Me_2CO , CHCl_3 and CH_2Cl_2 , less soluble in H_2O ($S_{25^\circ\text{C}} \approx 4 \text{ mg}\cdot\text{mL}^{-1}$), MeOH , EtOH and DMSO , and insoluble in C_6H_6 and Et_2O . (**2**), $\text{C}_{30}\text{H}_{24}\text{N}_7\text{O}_3\text{SCu}$ (626.17): calcd. C 57.55, N 15.66, H 3.86, S 5.12; found. C 57.36, N 15.09, H 3.71, S 4.95. IR (KBr): 3571 (s), 3158, 3126, 3060 (m br), 2930 (m br), 2316 (w br), 1534 (s, $\nu(\text{C}=\text{N})$), 1500 (s), 1458 (s), 1372 (m), 1237 (s br), 1045 (s, $\nu(\text{S}-\text{O})$), 853 (m), 767 (s), 696 (m), 639 (s, $\nu(\text{C}-\text{S})$), 540 (m) cm^{-1} . ^1H NMR (300MHz, $\text{acetone-}d_6$, 298 K): δ 8.07 (s, br, 3H), 7.95 (d, 6H, $J_{\text{HH}} = 7.7$ Hz, *o*-H (Ph)), 7.52-7.43 (m, 9H, *m*-H and *p*-H (Ph)), 6.94 (d, 3H, $J_{\text{HH}} = 2.8$ Hz, 4-H (pz)), 2.12 (s, 3H, H_3CCN). ^1H NMR (300MHz, $\text{acetone-}d_6$, 188 K): δ 8.87 (s, br, 1H, 5-H (pz)), 8.09 (d, 4H, $J_{\text{HH}} = 7.4$ Hz, *o*-H (Ph)), 7.99 (d, 2H, $J_{\text{HH}} = 7.4$ Hz, *o*-H (Ph)), 7.63-7.47 (m, 9H, *m*-H and *p*-H (Ph)), 7.35 (s, br, 1H 4-H (pz)), 7.27 (s, br, 2H, 5-H (pz)), 7.00 (s, br, 2H, 4-H (pz)). $^{13}\text{C}\{^1\text{H}\}$ and HMQC $^{13}\text{C}\text{-}^1\text{H}$ NMR (300MHz, $\text{acetone-}d_6$, 298 K): 153.7 (s, 3-C (pz)), 135.8 (s, 5-C (pz)), 131.5 (s, pz-C (Ph)), 129.1 (s, *p*-C (Ph)), 128.5 (s, *m*-C (Ph)), 126.9 (s, *o*-C (Ph)), 116.18 (s, NCCH_3), 104.71 (s, 4-C (pz)), 100.0 (s, O_3SC), 0.91 (s, NCCH_3). X-ray quality single

crystals were grown by slow evaporation under nitrogen at room temperature of an acetone solution of **(20)**.

Synthesis of [Cu(Tpms^{Ph})(PTA)] (**21**).

To a methanolic solution (15 mL) of [Cu(MeCN)₄][PF₆] (42.0 mg, 0.113 mmol, 1 eq.) was added a solution (5 mL) of Li(Tpms^{Ph}) (**16**) (60 mg, 0.113 mmol, 1 eq.) in the same solvent. The transparent colourless solution was stirred for 10 minutes at room temperature to allow the formation *in situ* of complex **(20)** that remains in solution. Then PTA (prepared according to published procedure^{5,6}) (16 mg, 0.10 mmol) was slowly added portionwise and stirring of the reaction mixture was continued at room temperature for 1 h. The formed white powder of **(21)** was collected by filtration, washed with cold methanol (2 x 10 mL), then recrystallized from acetone at 4°C (73.7 mg, 87.5%). Complex **(21)** is well soluble in medium polarity solvents like Me₂CO, CHCl₃ and CH₂Cl₂, less soluble in H₂O (*S*_{25°C} ≈ 6 mg·mL⁻¹), MeOH, EtOH and DMSO, and insoluble in C₆H₆, and Et₂O. **(3)**·0.5CH₂Cl₂, C_{34.5}H₃₄ClN₉O₃PSCu (784.74): calcd. C 52.80, N 16.06, H 4.36, S 4.08; found C 53.36, N 16.19, H 4.50, S 4.01. IR (KBr): 3168 (s), 2943(m br), 1532 (m, ν(C=N)), 1414 (s), 1328 (m), 1246 (s br), 1054 (s, ν(S-O)), 1015 (s), 972 (m), 854 (m), 770 (s), 633 (s, ν(C-S)), 534 (m) cm⁻¹. ¹H NMR (300 MHz, acetone-*d*₆, 298 K): 8.50 (s, br, 3H), 7.73 (d, 6H, *J*_{HH} = 8.0 Hz, *o*-H (Ph)), 7.61 (dd, vt, 6H, *m*-H (Ph)), 7.54 (dd, vt, 3H, *p*-H (Ph)), 6.92 (d, 3H, *J*_{HH} = 2.8 Hz, 4-H (pz)), 4.16 H^A and 3.96 H^B (*J*_{AB} = 13.0 Hz, 6H, NCH^AH^BN (PTA)), 2.97 (s, br, 6H, PCH₂N (PTA)). ¹H NMR (300 MHz, acetone-*d*₆, 188 K): δ 8.85 (s, br, 3H, 5-H (pz)), 8.02-7.50 (m, 15H, *o*-H, *m*-H and *p*-H (Ph)), 7.12 (s, br, 3H, 4-H (pz)), 4.09 H^A and 3.72 H^B (6H, *J*_{AB} = 12.0 Hz, NCH^AH^BN (PTA)), 2.57 (s, br, 6H, PCH₂N (PTA)). ¹³C{¹H} and HMQC ¹³C-¹H NMR (300MHz, acetone-*d*₆, 298 K): 154.4 (s, 3-C (pz)), 135.5 (s, 5-C (pz)), 132.3 (s, pz-C (Ph)), 129.33 (s, *p*-C (Ph)), 129-29 (s, *m*-C (Ph)), 127.3 (s, *o*-C (Ph)), 105.6 (s, 4-C (pz)), 72.2 (s, PCH₂N), 48.70 (s, NCH₂N). ³¹P{¹H}-NMR (acetone-*d*₆, 298 K): -93.3 (s, br PTA). X-ray quality single crystals were grown by slow evaporation under nitrogen at room temperature of an acetone solution of **(21)**.

Synthesis of [Cu(Tpms^{Ph})(HMT)] (22).

A solution of Li(Tpms^{Ph}) (16) (78.3 mg, 0.148 mmol) in methanol (15 mL) was added to a [Cu(MeCN)₄][PF₆] solution (55.2 mg, 0.148 mmol) in the same solvent (5 mL). The solution was stirred for 10 min. to allow the formation *in situ* of [Cu(Tpms^{Ph})(MeCN)] (20) that remains in solution. Then a methanolic solution (8 mL) of hexamethylenetetramine (HMT) (20.8 mg, 0.148 mmol) was added to the reaction mixture and the final solution was stirred at room temperature for 1 h. The white powder of crude (22) was collected by filtration, washed with cold methanol (2 x 10 mL), then recrystallized from acetone at 4°C. The final white microcrystalline solid was dried under vacuum to afford (22)·0.5Me₂CO (97 mg, 87%). Complex (22) is well soluble in medium polarity solvents like Me₂CO, CHCl₃ and CH₂Cl₂, less soluble in H₂O (*S*_{25°C} ≈ 6 mg·mL⁻¹), MeOH, EtOH and DMSO, and insoluble in C₆H₆ and Et₂O. (22)·0.5Me₂CO, C_{35.5}H₃₆N₁₀O_{3.5}SCu (754.34): calcd. C 56.52, N 18.57, H 4.81, S 4.25; found C 56.24, N 18.23, H 4.63, S 4.05. IR (KBr): 3571 (s), 3151, 3107, 3070 (m br), 2980 (m br), 2951(m br), 2926(m br), 2883 (m br), 1534 (m, ν(C=N)), 1499 (m), 1457 (s), 1376 (m), 1240 (s br), 1046 (s, ν(S-O)), 1023 (s), 991 (m), 852 (m), 760 (s), 705 (m), 637 (s, ν(C-S)), 533 (m) cm⁻¹. ¹H NMR (300 MHz, acetone-*d*₆, 298 K): δ 7.94 (d, 6H, *J*_{HH} = 7.4 Hz, *o*-H (Ph)), 7.84 (s, br, 3H, 5-H (pz)), 7.60-7.52 (m, 12H, *m*-H *p*-H (Ph)), 6.92 (s, br, 3H, 4-H (pz)), 4.29 (s, br, 12H, NCH₂N (HMT)). ¹H NMR (300 MHz, acetone-*d*₆, 188 K): δ 8.91 (s, br, 1H, 5-H (pz)), 8.14 (d, 4H, *J*_{HH} = 7.0 Hz, *o*-H (Ph)), 7.95 (s, br, 2H, *o*-H (Ph)), 7.76-7.66 (m, 6H, *m*-H (Ph)), 7.45 (m, 3H, *p*-H (Ph)), 7.35 (s, br, 1H, 4-H (pz)), 7.22 (s, br, 2H, 5-H (pz)), 6.90 (s, br, 2H, 4-H (pz)), 4.39 H^A and 4.09 H^B (*J*_{AB} = 12.0 Hz, 6H, NCH^AH^BN (HMT)), 4.19 (s, br, 6H, N^{coord}CH₂N (HMT)). ¹³C{¹H} and HMQC ¹³C-¹H NMR (75.4 MHz, acetone-*d*₆, 298 K): 153.9 (s, 3-C (pz)), 136.0 (s, 5-C (pz)), 132.47 (s, pz-C (Ph)) 129.7 (s, *p*-C (Ph)), 129.2 (s, *m*-C (Ph)), 127.0 (s, *o*-C (Ph)) 104.9 (s, 4-C (pz)), 74.3 (s, br (HMT)). X-ray quality single crystals were grown by slow evaporation under nitrogen at room temperature of the acetone solution of (22).

Synthesis of [Cu(Tpms^{Ph})(mPTA)][PF₆] (23).

(i) **Synthesis of (mPTA)[BPh₄]**. A methanolic solution (25 mL) of Na[BPh₄] (342 mg, 1.00 mmol) was added to a solution (25 mL) of [mPTA]I ((prepared

according to published procedure^{5,6}) (300 mg, 1.00 mmol) in the same solvent. The resulting white suspension was stirred for 15 min. and the solid was then filtered off, washed with methanol (3 × 10 mL) and dried under vacuum giving a white powder, which was crystallized from acetone/methanol leading to the colourless crystalline product (mPTA)[BPh₄], in *ca.* 80% yield. The compound is well soluble in medium polarity solvents like Me₂CO, CHCl₃ and CH₂Cl₂, sparingly soluble in H₂O (*S*_{25°C} = 0.2 mg·mL⁻¹), MeOH, EtOH and DMSO, and insoluble in C₆H₆ and Et₂O. (mPTA)[BPh₄]·0.25MeOH, BC_{31.25}H₃₆N₃OP (499.41): calcd. C 75.16, N 8.41, H 7.21; found C 75.03, N 8.80, H 7.24. IR (KBr): 3052 (m br), 2996 (m br), 2984 (m br), 2965 (m br), 2921 (m br), 1580 (m, ν (C=C)), 1478 (m), 1452 (w), 1426 (m), 1311 (m), 1271 (m), 1247 (m), 1123 (m), 1099 (m), 1025 (m), 982 (m), 913 (m), 804 (m), 751 (s), 737 (s, ν (BPh₄⁻)), 709 (s, ν (BPh₄⁻)), 602 (m), 554 (m) cm⁻¹. ¹H NMR (300MHz, acetone-*d*₆): δ 7.34 (br s, 8H, *o*-H (Ph)), 6.92 (dd, vt, *J*_{HH} = 6.9 Hz 8H, *m*-H (Ph)), 6.78 (dd, vt, 4H, *p*-H (Ph)), 5.13 and 5.04 (*J*(H^AH^B) = 13.2 Hz, 4H, NCH^AH^BN⁺), 4.70 and 4.52 (*J*(H^AH^B) = 14.0 Hz, 2H, NCH^AH^BN), 4.54 (s, 2H, PCH₂N⁺), 4.09 and 3.94 (*J*(H^AH^B) = 15.0 Hz, ³*J*(H^A-P) = 15.0 Hz, ³*J*(H^B-P) = 9.6 Hz, 4H, PCH^AH^BN), 2.81 (s, 3H, N⁺CH₃). ³¹P{¹H} NMR (162.0 MHz, acetone-*d*₆): -85.4 (s). ³¹P{¹H} NMR (162.0 MHz, DMSO-*d*₆): -87.0 (s). ¹³C{¹H} and HMQC ¹³C-¹H NMR (100.6 MHz, acetone-*d*₆): 165.7 - 164.2 (4s, 1-C, BPh₄), 137.0 (s, 2-C, BPh₄), 126.1 - 126.0 (4s, 3-C, BPh₄), 122.3 (s, 4-C, BPh₄), 81.9 (s, NCH₂N⁺), 70.6 (s, NCH₂N), 57.3 (dd, vt, ¹*J*(C-P) = 33.6 Hz, PCH₂N⁺), 50.4 (s, N⁺CH₃), 46.6 (dd, vt, ¹*J*(C-P) = 20.8 Hz, PCH₂N).

(ii) Synthesis of [Cu(Tpms^{Ph})(mPTA)][PF₆] (23). To a stirred methanolic solution (45 mL) of [Cu(MeCN)₄][PF₆] (186 mg, 0.50 mmol) were added 10 mL of a methanolic solution of Li(Tpms^{Ph}) (264 mg, 0.50 mmol). After 10 min. to allow the formation *in situ* of [Cu(Tpms^{Ph})(MeCN)] (20) that remains in solution, a dichloromethane solution (10 mL) of (mPTA)[BPh₄] (246 mg, 0.50 mmol) was added. The reaction mixture was stirred at room temperature for 1 h and then concentrated to half volume under vacuum. The mixture was kept at 4°C for two days. A white microcrystalline solid was collected, washed with cold methanol (2 × 10 mL) and dried under vacuum to yield (23) (315 mg, 70 %). Complex (23) is well soluble in medium polarity solvents like Me₂CO, CHCl₃ and CH₂Cl₂, less soluble in H₂O (*S*_{25°C} ≈ 7.5 mg·mL⁻¹), MeOH, EtOH and DMSO, and insoluble in C₆H₆ and Et₂O. (5)·1.5CH₂Cl₂, C_{36.5}H₃₉F₆Cl₃N₉O₃P₂SCu (1029.67): calcd. C 42.61, N 12.24, H

3.82, S 3.11; found C 42.58, N 12.79, H 4.06, S 3.34. IR (KBr): 3651 (s), 3154 (m br), 3107 (m br), 3075 (m br), 2990 (m br), 2930 (m br), 1535 (m, $\nu(\text{C}=\text{N})$), 1450 (m), 1459 (s), 1386 (m), 1355 (m), 1280 (s br), 1247 (s), 1077 (s), 1049 (s, $\nu(\text{S}-\text{O})$), 985 (m), 924 (m), 844 (s), 762 (m), 698 (m), 629 (m, $\nu(\text{C}-\text{S})$), 558 (m) cm^{-1} . ^1H NMR (300 MHz, acetone- d_6 , 298 K): δ 8.05-7.89 (m, br, 6H+3H, *o*-H (Ph) + 5-H (pz)), 7.61-7.56 (m, 9H, *m*-H *p*-H (Ph)), 6.96 (s, br, 3H, 4-H (pz)), 5.01 (s, br, 4H, $\text{NCH}^{\text{A}}\text{H}^{\text{B}}\text{N}^+$), 4.47 and 4.40 ($J(\text{H}^{\text{A}}\text{H}^{\text{B}}) = 14.0$ Hz, 2H, $\text{NCH}^{\text{A}}\text{H}^{\text{B}}\text{N}$), 3.98 (s, 2H, PCH_2N^+), 3.61 and 3.43 ($J(\text{H}^{\text{A}}\text{H}^{\text{B}}) = 13$ Hz, 4H, $\text{PCH}^{\text{A}}\text{H}^{\text{B}}\text{N}$), 2.79 (s, 3H, N^+CH_3). ^1H NMR (300 MHz, acetone- d_6 , 213 K): δ 8.94 (d, 1H, $J_{\text{HH}} = 2.83$ Hz, 5-H (pz)), 8.04 (d, 4H, $J_{\text{HH}} = 7.4$ Hz, *o*-H (Ph)), 7.95 (d, 2H, $J_{\text{HH}} = 7.0$ Hz, *o*-H (Ph)), 7.72-7.58 (m, 6H, *m*-H (Ph)), 7.52-7.38 (m, 3H, *p*-H (Ph)), 7.35 (d, 1H, 4-H (pz)), 7.28 (d, $J_{\text{HH}} = 2.70$ Hz, 2H, 5-H (pz)), 6.96 (d, 2H, 4-H (pz)), 5.08 and 5.00 ($J(\text{H}^{\text{A}}\text{H}^{\text{B}}) = 13.0$ Hz, 4H, $\text{NCH}^{\text{A}}\text{H}^{\text{B}}\text{N}^+$), 4.56 and 4.36 ($J(\text{H}^{\text{A}}\text{H}^{\text{B}}) = 14.0$ Hz, 2H, $\text{NCH}^{\text{A}}\text{H}^{\text{B}}\text{N}$), 4.15 (s, 2H, PCH_2N^+), 3.78 and 3.20 ($J(\text{H}^{\text{A}}\text{H}^{\text{B}}) = 14$ Hz, 4H, $\text{PCH}^{\text{A}}\text{H}^{\text{B}}\text{N}$), 2.81 (s, 3H, N^+CH_3). $^{31}\text{P}\{^1\text{H}\}$ NMR (121.4 MHz, acetone- d_6 , 298 K): $\delta = -70.9$ (br s), -144.2 (septet, PF_6). $^{13}\text{C}\{^1\text{H}\}$ and HMQC $^{13}\text{C}-^1\text{H}$ NMR (100.6 MHz, acetone- d_6 , 298 K): 155.8 (s, 3-C (pz)), 137.2 (s, 5-C (pz)), 130.5 (s, *p*-C (Ph)), 130.2 (s, *m*-C (Ph)), 128.3 (s, *o*-C (Ph)), 106.3 (s, 4-C (pz)), 81.6 (s, NCH_2N^+), 69.9 (s, NCH_2N), 55.8 (s, PCH_2N^+), 50.1 (s, N^+CH_3), 46.7 (s, PCH_2N). X-ray quality single crystals were grown by slow evaporation under nitrogen at room temperature of an acetone solution of (**23**).

Synthesis of $[\text{Cu}(\text{Tpms}^{\text{Ph}})(\text{CyNC})]$ (**24**) (CyNC = cyclohexyl isocyanide).

To a methanolic solution (10 mL) of $[\text{Cu}(\text{MeCN})_4][\text{PF}_6]$ (32 mg, 0.086 mmol, 1 eq.) were added 3 mL of a solution of $\text{Li}(\text{Tpms}^{\text{Ph}})$ (**16**) (45 mg, 0.085 mmol, 1 eq.) in the same solvent. The colourless solution was stirred for 5 minutes at room temperature and precipitation of complex (**20**) occurred. The suspension was then stirred for 15 minutes and cyclohexyl isocyanide (CyCN) (11 μL , 0.089 mmol, 1.1 eq) was slowly added portionwise, and the stirring of the reaction mixture was continued at room temperature overnight. The formed white powder of (**24**) was collected by filtration, washed with cold methanol (2 x 10 mL), then recrystallized from cold acetone at 5°C (73.7 mg, 87.5%). Complex (**24**) is well soluble in medium polarity solvents like Me_2CO , CHCl_3 and CH_2Cl_2 , less soluble in H_2O ($S_{25^\circ\text{C}} \approx 3$

mg·mL⁻¹), MeOH, EtOH and DMSO, and insoluble in C₆H₆ and Et₂O. **(24)**, C₃₅H₃₂N₇SO₃Cu (694.29): calcd. C 60.55, N 14.12, H 4.64, S 4.61; found C 61.03, N 14.09, H 4.80, S 4.34. IR (KBr): 3150 (w s), 2935(m s), 2860 (w s), 2191 (s s, $\nu(\text{CN})$), 1535 (m s, $\nu(\text{C}=\text{N})$), 1500 (m s), 1458 (m s), 1358 (m s), 1274 (s s), 1235 (s s), 1077 (s, $\nu(\text{S}-\text{O})$), 1059 (m s), 856 (w m), 758 (s s), 641 (s s, $\nu(\text{C}-\text{S})$), 534 (w s) cm⁻¹. ¹H NMR (300 MHz, CDCl₃, 298 K): 8.20-7.66 (m br, 3H+6H, 5H (pz) + *o*-H (Ph)), 7.46-7.39 (m br, 9H, *m,p*-H (Ph)), 6.69 (d, 3H, $J_{\text{HH}}=2.7$ Hz, 4-H (pz)), 3.38 (m, 1H, *CH*(cy)), 1.50-1.27 (m, 10H, (CH₂)₅ (cy)). ¹H NMR (300 MHz, CDCl₃, 213 K): 9.04 (s br, 1H, 5-H (pz)), 7.85 (m br, 6H, *o*-H (Ph)), 7.47 (m br, 9H, *m,p*-H (Ph)), 7.02 (s br, 2H, 5-H (pz)), 6.96 (s br, 1H, 4-H (pz)), 6.66 (s br, 2H, 4-H (pz)), 3.16 (m, 1H, *CH*(cy)), 1.81-1.12 (m br, 10H, (CH₂)₅ (cy)). X-ray quality single crystals were grown by slow diffusion of dry diethylether in a concentrated solution of the titled compound in dichloromethane, under dinitrogen.

Synthesis of [Cu(Tpms^{Ph})(XyNC)] (25) (XyCN = 2,6-dimethylphenyl isocyanide).

To a methanolic suspension (10 mL) of **(20)** (20 mg, 0.032 mmol, 1 eq.) was added 2,6-dimethylphenyl isocyanide (XyNC) (4.6 mg, 0.035 mmol, 1.1 eq.) portionwise. The milky mixture was stirred at room temperature overnight under dinitrogen atmosphere. The formed white powder of **(25)** was collected by filtration, washed with cold methanol (2 x 5 mL) to afford **(25)** (78%). Complex **(25)** is well soluble in medium polarity solvents like Me₂CO, CHCl₃ and CH₂Cl₂, less soluble in H₂O ($S_{25^\circ\text{C}} \approx 3$ mg·mL⁻¹), MeOH, EtOH, and insoluble in Et₂O. **(25)**, C₃₇H₃₀N₇O₃SCu (716.30): calcd. C 62.04, N 13.69, H 4.22, S 4.47; found C 62.43, N 13.13, H 4.43, S 4.14. IR (KBr): 3142 (w s), 3059 (w b), 2922 (m s), 2153 (s s, $\nu(\text{CN})$), 1535 (m s, $\nu(\text{C}=\text{N})$), 1500 (m s), 1459 (m s), 1375 (m s), 1280 (s s), 1236 (s s), 1057 (s, $\nu(\text{S}-\text{O})$), 858 (w m), 757 (s s), 630 (s s, $\nu(\text{C}-\text{S})$), 539 (w s) cm⁻¹. ¹H NMR (300 MHz, CDCl₃, 298 K): 7.82 (d, 6H, $J_{\text{HH}} = 7.5$ Hz, *o*-H (Ph)), 7.76 (d, 1H, $J_{\text{HH}} = 8.0$ Hz, *p*-H(XyNC)), 7.70 (d, 1H, $J_{\text{HH}} = 2.5$ Hz, 5-H (pz)), 7.46-7.29 (m br, 9H+2H, *m*-H(XyNC) + *m,p*-H (Ph)), 7.19 (d, 2H, $J_{\text{HH}} = 2.5$ Hz, 5-H (pz)), 6.67 (m br, 3H, 4-H (pz)), 2.17 (s, 6H, (CH₃)₂ (XyNC)).

Synthesis of [Cu(Tpms^{Ph})(L)] (**26**) (L = MeC(=NH)NHMe).

To a dichloromethane solution (3 mL) of (**20**) (40 mg, 0.064 mmol, 1 eq.) was added a 2.0 M THF solution of monomethylamine (32 μ L, 0.064 mmol, 1 eq.). The resulting colourless solution was stirred at room temperature for 3 h under dinitrogen. The solvent was removed under vacuum and the residue was washed with cold methanol (5 mL) to afford (**26**) (61%). Complex (**26**) is well soluble in medium polarity solvents like Me₂CO, CHCl₃ and CH₂Cl₂, less soluble in H₂O ($S_{25^\circ\text{C}} \approx 4$ mg·mL⁻¹), MeOH, EtOH, and insoluble in Et₂O. (**26**), C₃₁H₂₉N₈O₃SCu (657.23): calcd. C 56.65, N 17.04, H 4.45, S 4.87; found C 57.10, N 16.98, H 4.67, S 4.12. IR (KBr): 3323, 3276 (m s, $\nu(\text{NH})$), 3127 (w b), 3059 (m s), 1604, 1532 (m s, $\nu(\text{C}=\text{N})$), 1499 (m s), 1458 (m s), 1372 (m s), 1268 (s s), 1237 (s s), 1104, 1078, 1044 (s, $\nu(\text{S}-\text{O})$), 854 (w m), 697 (s s, $\nu(\text{C}-\text{S})$), 539 (w s) cm⁻¹. ¹H NMR (300 MHz, CDCl₃, 298 K): 7.87 (m br, 6H + 3H, 5-H (pz) + *o*-H (Ph)), 7.43 (m br, 9H, *m,p*-H (Ph)), 6.71 (s br, 3H, 4-H (pz)), 3.75 (s b, 1H, NH-CH₃) 2.17 (s, 3H, CH₃-C), 1.85 (s br, 3H, CH₃-NH).

Synthesis of [Cu(Tpms^{Ph})(CO)] (**27**).

In a stainless steel vessel, 3 mL of a methanolic solution of Li(Tpms^{Ph}) (**16**) (42 mg, 0.081 mmol, 1 eq.) were added to a solution (10 mL) of [Cu(MeCN)₄][PF₆] (30 mg, 0.081 mmol, 1 eq.) in the same solvent. The vessel was closed and final solution was saturated with 20 atm of carbon monoxide and stirred at room temperature overnight. Then, the solvent was removed under vacuum, washed with cold methanol (5 mL), to afford (**27**) as a white powder (68 %). Complex (**27**) is soluble Me₂CO, CHCl₃ and CH₂Cl₂, less soluble in H₂O ($S_{25^\circ\text{C}} \approx 3$ mg·mL⁻¹), MeOH, EtOH, and insoluble in Et₂O. (**27**), C₂₉H₂₁N₆O₄SCu (613.13). IR (KBr): 3158, 3125 (w s), 2960, 2935(m s), 2860 (w s), 2107 (m s, $\nu(\text{CO})$), 1535 (m s, $\nu(\text{C}=\text{N})$), 1500 (m s), 1459 (m s), 1356 (m s), 1271 (s s), 1237 (s s), 1078 (s, $\nu(\text{S}-\text{O})$), 1044 (m s), 867 (w m), 758 (s s), 639 (s s, $\nu(\text{C}-\text{S})$), 540 (w s) cm⁻¹. ¹H NMR (300 MHz, CDCl₃, 298 K): 8.02 (s br, 3H, 5-H (pz)), 7.94 (d, 6H, $J_{\text{HH}} = 7.5$ Hz, *o*-H (Ph)), 7.49-7.44 (m br, 9H, *m,p*-H (Ph)), 6.96 (d, 3H, $J_{\text{HH}} = 2.6$ Hz, 4-H (pz)).

Synthesis of $[\text{Cu}(\mu\text{-O})(\text{TpmS}^{\text{Ph}})]_2$ (**28**).

Deep dark gree/blue crystals of compound (**28**) were grown in a cooled methanolic solution of (**20**) in presence of 1 eq of hexamethylenetetramine (HMT) in air. The compound was not characterized further. $\text{C}_{56}\text{H}_{42}\text{N}_{12}\text{O}_8\text{S}_2\text{Cu}_2$, (1202.25).

Synthesis of $[(\mu\text{-Cu}^{\text{II}})\{\text{Cu}^{\text{I}}(\text{TpmS}^{\text{Ph}})(\mu\text{-OH}_2)(\mu\text{-OMe})\}_2]$ (**29**).

Compound (**29**), in pale green crystals, was grown in a cooled methanolic solution of (**20**) in air. The compound was not characterized further. $\text{C}_{58}\text{H}_{50}\text{N}_{12}\text{O}_{10}\text{S}_2\text{Cu}_3$, (1329.88).

Synthesis of $[\text{Fe}(\text{TpmPy})_2][\text{BF}_4]_2$ (**30**).

To a methanolic solution (2 mL) of $\text{Fe}(\text{BF}_4)_2 \cdot 6\text{H}_2\text{O}$ (50 mg, 0.148 mmol, 1 eq) is added portionwise a solution of Tpm^{Py} (**3**) (99 mg, 0.296 mmol, 2 eq) in MeOH (2 mL). The colorless solution turns immediately to pink and after a few minutes a pink solid precipitates. The mixture is stirred under nitrogen for 15 min. and then filtered. The solid is washed with methanol (2 x 5 mL) to leave a pale pink solid of (**30**) (91%). Compound (**30**) is well soluble in acetonitrile and DMSO, sparingly soluble in CH_2Cl_2 , CHCl_3 , MeOH, and less soluble in H_2O ($S_{25^\circ\text{C}} \approx 4.0 \text{ mg} \cdot \text{mL}^{-1}$). (**30**) $\cdot 2\text{CH}_3\text{CN}$, $\text{C}_{38}\text{H}_{40}\text{N}_{16}\text{O}_2\text{FeB}_2\text{F}_8$ (982.30): calcd. C 46.46, N 22.81, H 4.10; found. C 46.50, N 22.98 H 3.99. IR (KBr): 3158, 3126, 3060 (m br), 2918 (m br), 1562 (m s, $\nu(\text{C}=\text{N})$), 1518 (m s, $\nu(\text{C}=\text{C})$), 1419 (s s), 1341 (s s), 1231 (s br), 1119-1050 (s br, $\nu(\text{BF}_4)$), 867 (m s), 770 (s s), 607 (m s), 521 (m s) cm^{-1} . $^1\text{H-NMR}$ (CD_3CN , 298 K): δ 8.71-8.40 (m, 30H), 7.53 (br s, 12H), 7.39-7.23 (br m, 18H), 6.57 (br s, 18H), 5.76 (br s, 12H, $\text{CH}_2\text{-C}(\text{pz})_3$), 5.24 (br s, 12H, $\text{CH}_2\text{-py}$). $^1\text{H-NMR}$ (CD_3CN , 233 K): δ 8.65-8.60 (m, 24H, 5-H(pz) + 2,6-H(py)), 8.41 (br s, 6H, 5-H(pz)), 7.53 (d, 12H, $J_{\text{HH}} = 6.0 \text{ Hz}$, 2,6-H(py)), 7.43 (d, 4H, $J_{\text{HH}} = 1.6 \text{ Hz}$, 3-H(pz)), 7.40 (d, 2H, $J_{\text{HH}} = 1.6 \text{ Hz}$, 3-H(pz)), 7.28 (d, 8H, $J_{\text{HH}} = 1.6 \text{ Hz}$, 3-H(pz)), 7.24 (d, 4H, $J_{\text{HH}} = 1.6 \text{ Hz}$, 3-H(pz)), 6.55 (m, 6H, 4-H(pz)), 6.52 (m, 12H, 4-H(pz)) 5.73 (br s, 12H, $\text{CH}_2\text{-C}(\text{pz})_3$), 5.23 (br s, 12H, $\text{CH}_2\text{-py}$). $^{13}\text{C}\{^1\text{H}\}$ and HMQC $^{13}\text{C-}^1\text{H}$ NMR (100.6 MHz, CD_3CN , 298 K): δ 153.08 (s, 3-C (pz)), 149.76 (s, 2,6-C (py)), 146.73 (s, 4-C (py)), 132.81 (s, pz-C (Ph)), 132.44 (s, 5-C (pz)), 128.70 (s, m-C (Ph)), 128.38 (s, p-C (Ph)), 126.03 (s, o-C (Ph)), 121.75 (s, 3,5-C (py)), 103.88 (s, 4-C (pz)), 90.17 (s, $\text{CH}_2\text{-C}(\text{pz})_3$), 74.07 (s, $\text{O-CH}_2\text{-C}(\text{pz})_3$),

72.54 (s, O-CH₂-py). X-ray quality single crystals were grown by slow evaporation under nitrogen, at room temperature, of an acetonitrile solution of **(30)**.

Synthesis of [ZnCl₂(TpmPy)₂] (**31**).

To a methanolic solution of ZnCl₂ (15 mg, 0.11 mmol, 1 eq) is added dropwise a solution of **(3)** (74 mg, 0.22 mol, 2 eq) in MeOH. The colorless solution is stirred at room temperature for 3h, during which time a white solid precipitates. The product **(31)** is filtered off, washed with a small amount of cold methanol and dried (78%). The compound **(31)** is soluble in CHCl₃, sparingly soluble in MeOH, EtOH, acetone and acetonitrile, insoluble in Et₂O and less soluble in H₂O (*S*_{25°C} ≈ 2.5 mg·mL⁻¹). **(31)** C₃₄H₃₄Cl₂N₁₄O₂Zn (807.03) calcd. C 50.58, H 4.25, N 24.30; found. C. 49.58, H 4.23, N 24.07. IR (KBr): 3155, 2930, 2900 (m s, ν(C-H)), 1621 (s s, ν(C=N)), 1563, 1518 (m s, ν(C=N), ν(C=C)), 1430 (s s), 1390 (s s), 1133, 1112 (s s), 869 (m s), 754 (s s), 614 (m s), 508, 478 (m s) cm⁻¹. MS-EI *m/z*: 434 [ZnCl(Tpm^{Py})]⁺, 367 [Zn(Tpm^{Py})₂]⁺⁺. ¹H-NMR (300MHz, methanol-*d*₄): δ 8.51 (d, 2H, *J*_{HH}= 5.7 Hz, 2-H (py)), 7.67 (d, 3H, *J*_{HH}= 2.5 Hz, 5-H (pz)), 7.50 (d, 3H, *J*_{HH}= 2.5 Hz, 3-H (pz)), 7.30 (d, 2H, *J*_{HH}= 5.7 Hz, 3-H (py)), 6.42 (dd, 3H, *J*_{HH}= 2.5 Hz, 4-H (pz)), 5.17 (s, 2H, CH₂-C(pz)₃), 4.68 (s, 2H, CH₂-py). ¹H NMR (300MHz, acetone-*d*₆): δ 8.67 (d, 2H, *J*_{HH}= 5.7 Hz, 2-H (py)), 7.67 (d, 3H, *J*_{HH}= 2.3 Hz, 5-H (pz)), 7.56 (d, 3H, *J*_{HH}= 2.4 Hz, 3-H (pz)), 7.52 (d, 2H, *J*_{HH}= 5.7 Hz, 3-H (py)), 6.41 (dd, vt, 3H, *J*_{HH}= 2.4 Hz, 4-H (pz)), 5.25 (s, 2H, CH₂-C(pz)₃), 4.83 (s, 2H, CH₂-py). ¹³C-NMR (100.6 MHz, acetone-*d*₆, 298 K): δ 153.04 (s, 4-C (py)), 149.54 (s, 2,6-C (py)), 142.05 (s, 3-C (pz)), 133.70 (s, pz-C (Ph)), 132.16 (s, 5-C (pz)), 123.85 (s, 3,5-C (py)), 107.24 (s, 4-C (pz)), 90.84 (s, CH₂-C(pz)₃), 74.61 (s, O-CH₂-C(pz)₃), 72.12 (s, O-CH₂-py).

Synthesis of [Ni(TpmPy)₂]Cl₂ (**32**).

To a water solution of NiCl₂·6H₂O (22 mg, 0.09 mmol, 1 eq) is added portionwise **(3)** (61 mg, 0.18 mol, 2 eq). The solid partially dissolves during the addition. After addition, the blue-violet solution is stirred at room temperature overnight, after which time the solvent is left to evaporate. The product crystallizes from the concentrated mixture as pale violet crystals that are separated by filtration (80%). The compound **(32)** is soluble in CHCl₃, sparingly soluble in MeOH, EtOH,

acetone and acetonitrile, insoluble in Et₂O and well soluble in H₂O ($S_{25^{\circ}\text{C}} \approx 50 \text{ mg}\cdot\text{mL}^{-1}$). **(32)** C₃₄H₃₄Cl₂N₁₄O₂Ni (800.34) calcd. C 51.03, H 4.28, N 24.50; found. C. 49.57, H 4.21, N 24.09. IR (KBr): 2965, 2927 (m s, $\nu(\text{C-H})$), 1568, 1522 (m s, $\nu(\text{C=N})$), $\nu(\text{C=C})$). MS-EI m/z : 364 [Ni(Tpm^{Py})₂]⁺⁺. X-ray quality single crystals were grown by slow evaporation of a concentrated methanol solution of **(32)**.

Synthesis of [ZnCl₂(TpmPy^{Ph})₂] (**33**).

To a methanolic solution of ZnCl₂ (15 mg, 0.11 mmol, 1 eq) is added dropwise a solution of **(19)** (124 mg, 0.22 mmol, 2 eq) in MeOH. An immediate precipitation of a pale yellow solid occurs. The mixture is stirred for 10 minutes, then the solid is filtered off and washed with a small amount of cold methanol, to yield a pale yellow solid of **(33)** (81%). The compound is well soluble in CHCl₃ and acetone, moderately soluble in MeOH, EtOH and acetonitrile and less soluble in H₂O ($S_{25^{\circ}\text{C}} \approx 0.8 \text{ mg}\cdot\text{mL}^{-1}$). **(33)** CH₃OH, C₇₁H₆₂Cl₂N₁₄O₃Zn (1295.66) calcd. C 65.81, H 4.82, N 15.13; found. C. 65.74, H 4.67, N 15.31. IR (KBr): 3148, 3060, 2928 (w s, $\nu(\text{C-H})$), 1620 (s s, $\nu(\text{C=N})$), 1531 (m s, $\nu(\text{C=C})$), 1500 (m s, $\nu(\text{C=C})$), 1456 (s s), 1222 (s br), 871, 776, 694 (s s), 616 (w s), 477 (m s) cm⁻¹. *far*-IR (Cesium Iodide): 336-301 cm⁻¹ (m s, $\nu(\text{Zn-Cl})$). MS-EI m/z : 564 [Tpm^{PyPh} + H]⁺, 662 [ZnCl(Tpm^{PyPh})]⁺. ¹H-NMR (CDCl₃, 298 K): δ 8.56 (d, 2H, $J_{\text{HH}} = 6.0 \text{ Hz}$, 2,6-H (py)), 7.76 (d, 6H, $J_{\text{HH}} = 7.5 \text{ Hz}$, *o*-H (Ph)), 7.44 (d, 3H, $J_{\text{HH}} = 2.6 \text{ Hz}$, 5-H (pz)), 7.40-7.28 (m, 11H, *m*-H, *p*-H(Ph) + 3,5-H (py)), 6.34 (d, 3H, $J_{\text{HH}} = 2.6 \text{ Hz}$, 4-H (pz)), 5.40 (s, 2H, CH₂-C(pz)₃), 4.73 (s, 2H, CH₂-py). ¹H-NMR (acetone-*d*₆, 298 K): δ 8.55 (d, 2H, $J_{\text{HH}} = 6.2 \text{ Hz}$, 2,6-H (py)), 7.83 (d, 6H, $J_{\text{HH}} = 7.0 \text{ Hz}$, *o*-H (Ph)), 7.76 (d, 3H, $J_{\text{HH}} = 2.6 \text{ Hz}$, 5-H (pz)), 7.53 (d, 2H, $J_{\text{HH}} = 6.0 \text{ Hz}$, 3,5-H (py)), 7.38 (dd, vt, 6H, $J_{\text{HH}} = 7.6 \text{ Hz}$, *m*-H (Ph)), 7.31 (dd, vt, 3H, $J_{\text{HH}} = 7.6 \text{ Hz}$, *p*-H (Ph)), 6.86 (d, 3H, $J_{\text{HH}} = 2.6 \text{ Hz}$, 4-H (pz)), 5.47 (s, 2H, CH₂-C(pz)₃), 4.97 (s, 2H, CH₂-py). ¹³C-NMR (100.6 MHz, CDCl₃, 298 K): δ 153.22 (s, 3-C (pz)), 151.90 (s, 4-C (py)), 148.46 (s, 2,6-C (py)), 132.46 (s, pz-C (Ph)), 132.27 (s, 5-C (pz)), 128.79 (s, *m*-C (Ph)), 128.55 (s, *p*-C (Ph)), 125.94 (s, *o*-C (Ph)), 122.97 (s, 3,5-C (py)), 104.08 (s, 4-C (pz)), 89.91 (s, CH₂-C(pz)₃), 74.37 (s, O-CH₂-C(pz)₃), 71.83 (s, O-CH₂-py). ¹³C-NMR (100.6 MHz, acetone-*d*₆, 298 K): δ 153.69 (s, 3-C (pz)), 153.28 (s br, 4-C (py)), 149.35 (s, 2,6-C (py)), 133.78 (s, pz-C (Ph)), 132.06 (s, 5-C (pz)), 129.58 (s, *m*-C (Ph)), 129.19 (s, *p*-C (Ph)), 126.66 (s, *o*-C (Ph)), 123.88 (s,

3,5-C (py)), 104.67 (s, 4-C (pz)), 90.37 (s, CH₂-C(pz)₃), 75.14 (s, O-CH₂-C(pz)₃), 72.40 (s, O-CH₂-py).

Synthesis of [NiCl₂(TpmPy^{Ph})₂] (34).

To a methanolic solution of NiCl₂·6H₂O (22 mg, 0.09 mmol, 1 eq) is added dropwise a solution of (19) (104 mg, 0.18 mmol, 2 eq) in MeOH. An immediate precipitation of a white off solid occurs. The mixture is stirred for 10 minutes, then the solid is filtered off and washed with a small amount of cold methanol, to yield (34) (81%). The compound is well soluble in CHCl₃ and acetone, moderately soluble in MeOH, EtOH and acetonitrile and less soluble in H₂O (*S*_{25°C} ≈ 1.0 mg·mL⁻¹). (34), C₇₀H₅₈Cl₂N₁₄O₂Ni (1256.92) calcd. C 66.89, H 4.65, N 15.60; found. C. 67.03 H 4.82, N 15.19. IR (KBr): 3148, 3061, 2926 (w s, ν(C-H)), 1617 (s s, ν(C=N)), 1531 (m s, ν(C=C)), 1500 (m s, ν(C=C)), 1456 (s s), 1221 (s br), 871, 751, 693 (s s), 619 (w s), 489 (m s) cm⁻¹. MS-EI *m/z*: 564 [Tpm^{PyPh} + H]⁺, 656 [NiCl(Tpm^{PyPh})]⁺.

Synthesis of [VOCl₂(TpmPy)] (35).

To a solution of vanadium trichloride (0.20 g, 1.27 mmol) in THF (15 mL) is added (3) (0.430 g, 1.27 mmol) in THF (10 mL). The resulting pale blue solution is stirred overnight. The final pale blue solution is concentrated and upon addition of Et₂O a pale blue solid precipitates. The solid is collected by filtration, washed with Et₂O and dried in vacuo (52%). The compound (35) is soluble in DMSO, moderately soluble in MeOH and EtOH, and less soluble in H₂O (*S*_{25°C} ≈ 5.0 mg·mL⁻¹). (35) VO₂Cl₂C₁₇H₁₇N₇ (473.21) calcd. C 43.15, H 3.62, N 20.72. found: C 42.92, H 3.53, N 20.81. IR (KBr): 3170, 3148 (s s, ν(C-H)), 1519-1517 (s br, ν(C=C), ν(C=N)), 971 (m, ν(V=O)). *far*-IR (polyethylene): 391, 348 cm⁻¹ (m s, ν(V-Cl)). EPR (DMSO, r.t. modulation amplitude: 0.1 Gpp; receiver gain: 4·10⁻⁴; conversion time: 20 ms; time constant: 40 ms): a = 101.6 G, g = 1.9989. MS-EI *m/z*: 406 [VOCl₂(Tpm^{Py}) - pz]⁺, 339 [VOCl₂(Tpm^{Py}) - 2 pz]⁺.

Synthesis of [PdCl₂(TpmPy)₂] (**36**).

To a dichloromethane solution (8 mL) of (**3**) (78 mg, 0.23 mmol, 2 eq) is added dropwise a suspension of *cis*-[PdCl₂(CH₃CN)₂] (30 mg, 0.11 mmol, 1 eq) in dichloromethane. The yellow resulting solution is stirred at room temperature for 1h, during which time a pale yellow solid precipitates. The product is filtered off washed with a small amount of cold CH₂Cl₂ and dried, yielding a pale yellow powder of (**36**) (75%). The compound is soluble in CH₂Cl₂, CHCl₃ and DMSO, sparingly soluble in MeOH and acetonitrile, and less soluble in H₂O (*S*_{25°C} ≈ 0.8 mg·mL⁻¹). (**36**) C₃₄H₃₄Cl₂N₁₄O₂Pd, (848.06) calcd. C 48.15, H 4.04, N 23.12. found. C 48.06, H 3.94, N 23.15. IR (KBr): 3128, 3050, 2923, 2851 (w s, ν(C-H)), 1619 (m s, ν(C=N)), 1561, 1517 (s s, ν(C=N), ν(C=C)), 1428, 1390 (s s), 1323 (s s), 1133, 1111, 1064 (s s), 867 (s s), 753 (s s), 616 (m s), 505 (m s) cm⁻¹. *far*-IR (polyethylene): 361 (m s, ν(Pd-Cl)), 308-296 cm⁻¹ (m s, ν(Pd-Cl)). MS-EI *m/z*: 811 [Pd(Tpm^{py})₂Cl]⁺. ¹H-NMR (300MHz, CDCl₃, 298 K): δ 8.68 (d, 2H, *J*_{HH}= 6.7 Hz, 2,6-H (py)), 7.67 (s, vd, 3H, 5-H (pz)), 7.34 (d, 3H, *J*_{HH}= 2.6 Hz, 3-H (pz)), 7.07 (d, 2H, *J*_{HH}= 6.0 Hz, 3,5-H (py)), 6.36 (m, vdd, 3H, 4-H (pz)), 5.22 (s, 2H, CH₂-C(pz)₃), 4.61 (s, 2H, CH₂-py). ¹³C-NMR (100.6 MHz, CDCl₃, 298 K): δ 153.11 (s, 2,6-C (py)), 150.25 (s, 4-C (py)), 141.75 (s, 3-C (pz)), 130.77 (s, 5-C (pz)), 122.54 (s, 3,5-C (py)), 107.01 (s, 4-C (pz)), 89.85 (s, CH₂-C(pz)₃), 74.72 (s, O-CH₂-C(pz)₃), 71.78 (s, O-CH₂-py). ¹³C-NMR (100.6 MHz, DMSO-*d*₆, 298 K): δ 152.61 (s, 2,6-C (py)), 150.75 (s, 4-C (py)), 141.01 (s, 3-C (pz)), 131.15 (s, 5-C (pz)), 122.60 (s, 3,5-C (py)), 106.57 (s, 4-C (pz)), 89.17 (s, CH₂-C(pz)₃), 73.16 (s, O-CH₂-C(pz)₃), 70.30 (s, O-CH₂-py). X-ray quality single crystals were grown by slow evaporation of a concentrated dichloromethane solution of (**36**).

Synthesis of [PdCl₂(TpmPy^{Ph})₂] (**37**).

To a dichloromethane solution (10 mL) of (**19**) (104 mg, 0.18 mmol, 2 eq) is added dropwise a suspension of *cis*-[PdCl₂(CH₃CN)₂] (24 mg, 0.09 mmol, 1 eq) in dichloromethane. The pale yellow resulting solution is stirred at room temperature for 1h. The solvent is removed under vacuum and the residue is washed with a small amount of cold methanol (2 mL), filtered off and dried yielding a pale yellow powder of (**37**) is collected (68%). The compound is well soluble in CH₂Cl₂, CHCl₃, CH₃CN and DMSO, moderately soluble in MeOH and EtOH, and insoluble in H₂O.

$C_{70}H_{58}N_{14}O_2PdCl_2$, (1304.65). calcd. C 65.66, H 2.68, N 15.31. found: C 65.89, H 2.91, N 15.02. IR (KBr): 3147, 3060, 2925, 2850 (w s, $\nu(C-H)$), 1621 (m s, $\nu(C=N)$), 1531 (s s, $\nu(C=N)$, $\nu(C=C)$), 1500, 1456 (s s), 1221 (s br), 1134, 1102, 1073, 1044 (m s), 871 (s s), 752 (s s), 694 (s s), 627 (w s), 503 (m s) cm^{-1} . *far*-IR (polyethylene): 365 (s s, $\nu(Pd-Cl)$). MS-EI m/z : 1268 $[PdCl(Tpm^{PyPh})_2]^+$, 1304 $[PdCl_2(Tpm^{PyPh})_2]^+$. 1H -NMR ($CDCl_3$, 298 K): δ 8.63 (d, 2H, J_{HH} = 6.7 Hz, 2,6-H (py)), 7.81 (d, 6H, J_{HH} = 7.9 Hz, *o*-H (Ph)), 7.48 (d, 3H, J_{HH} = 2.6 Hz, 5-H (pz)), 7.41 (dd, vt, 6H, J_{HH} = 7.6 Hz, *m*-H (Ph)), 7.33 (dd, vt, 3H, J_{HH} = 7.6 Hz, *p*-H (Ph)), 7.10 (d, 2H, J_{HH} = 6.6 Hz, 3,5-H (py)), 6.66 (d, 3H, J_{HH} = 2.6 Hz, 4-H (pz)), 5.40 (s, 2H, $CH_2-C(pz)_3$), 4.64 (s, 2H, CH_2 -py). $^{13}C\{^1H\}$ and HMQC ^{13}C - 1H NMR (100.6 MHz, $CDCl_3$, 298 K): δ 153.25 (s, 3-C (pz)), 152.97 (s, 2,6-C (py)), 150.36 (s, 4-C (py)), 132.69 (s, pz-C (Ph)), 132.31 (s, 5-C (pz)), 128.77 (s, *m*-C (Ph)), 128.47 (s, *p*-C (Ph)), 126.05 (s, *o*-C (Ph)), 122.54 (s, 3,5-C (py)), 104.06 (s, 4-C (pz)), 90.10 (s, $CH_2-C(pz)_3$), 74.56 (s, O- $CH_2-C(pz)_3$), 71.79 (s, O- CH_2 -py).

Synthesis of $[PdCl_2(\mu-TpmPy)_2Fe](BF_4)_2$ (**38**).

Method 1: To a yellow/brown solution of *cis*- $[PdCl_2(CH_3CN)_2]$ (12 mg, 0.046 mmol, 1 eq) in dichlorometane (5 mL) is added dropwise an acetonitrile solution (5 mL) of $[Fe(TpmPy)_2](BF_4)_2$ (**30**) (41 mg, 0.045 mmol, 1 eq). The resulting mixture is stirred at room temperature for 1h, during which time a pale orange-pink solid precipitates. The solid is filtered off, washed with acetonitrile and dried, yielding (**11**) (78%).

Method 2: To a dichloromethane solution (8 mL) of $[PdCl_2(TpmPy)_2]$ (**36**) (25 mg, 0.030 mmol, 1eq) is added dropwise a solution of $Fe(BF_4)_2 \cdot 6H_2O$ (10 mg, 0.030 mmol, 1 eq) in methanol. The pale pink resulting mixture is stirred at room temperature for 1h. The product is filtered off, washed with a small amount of methanol and dried, yielding a pale pink powder of (**38**) (69%). (**38**) $\cdot 4H_2O$, $C_{34}H_{42}N_{14}B_2F_8FeO_6PdCl_2$, (1149.58), calcd. C 35.52, H 3.68, N 17.05 found: C 35.36, H 3.22, N 17.10. IR (KBr): 3138, 2900 (w s, $\nu(C-H)$), 1621 (s s, $\nu(C=N)$), 1519-1513 (m br, $\nu(C=N)$, $\nu(C=C)$), 1420 (s s), 1339 (s s), 1231 (s s), 1106-1036 (s br, $\nu(BF_4)$), 866 (m s), 766 (m br) cm^{-1} . MS-EI m/z : 811/813 $[PdCl(Tpm^{Py})_2]^+$, 990 $[Pd(Tpm^{Py})Cl_2Fe]_2(BF_4)_2^{++}$. 1H -NMR (CD_3CN , 313 K): δ 8.78 (d, 2H, J_{HH} = 6.0 Hz,

2,6-H (py)), 8.58 (s br, 3H, 5-H (pz)), 7.58 (d, 2H, $J_{\text{HH}} = 6.0$ Hz, 3,5-H (py)), 7.30 (s br, 3H, 3-H (pz)), 6.57 (s, br, 3H, 4-H(pz)), 5.78 (s, 2H, $\text{CH}_2\text{-C}(\text{pz})_3$), 5.31 (s, 2H, $\text{CH}_2\text{-py}$). $^1\text{H-NMR}$ (CD_3CN , 253 K): δ 8.72 (d br, 2H, 2,6-H (py)), 8.62 (s br, 2H, 5-H (pz)), 8.41 (s br, 1H, 5-H (pz)), 7.58 (d br, 2H, 3,5-H (py)), 7.40 (s br, 1H, 4-H (pz)), 7.27 (s br, 2H, 4-H (pz)), 6.56 (s, br, 1H, 4-H(pz)), 6.51 (s, br, 2H, 4-H(pz)), 5.78 (s, 2H, $\text{CH}_2\text{-C}(\text{pz})_3$), 5.30 (s, 2H, $\text{CH}_2\text{-py}$).

Synthesis of $[\text{Fe}(\mu\text{-TpmPy})_2\text{Cu}(\text{NO}_3)_2](\text{BF}_4)_2$ (**39**).

To an acetonitrile solution (5 mL) of $[\text{Fe}(\text{TpmPy})_2](\text{BF}_4)_2$ (**30**) (89 mg, 0.1 mmol, 1 eq), a solution of $\text{Cu}(\text{NO}_3)_2 \cdot 2.5 \text{H}_2\text{O}$ (23 mg, 0.1 mmol, 1 eq) in acetonitrile (2 mL) is added. An immediate precipitation of a pale violet solid occurs. It is filtered off under nitrogen, washed with a small amount of cold acetonitrile (1 mL) and dried to leave compound (**39**) (69%). $\text{C}_{34}\text{H}_{34}\text{N}_{16}\text{B}_2\text{CuF}_8\text{FeO}_8$ (1087.75). calcd. C 37.54, H 3.15, N 20.60. found: C 36.47, H 3.30, N 20.02. IR (KBr): $\nu = 3137$ (m s, C-H), 1620 (m s, $\nu(\text{N}=\text{C})$), 1517-1515 (m br, $\nu(\text{N}=\text{C})$, $\nu(\text{C}=\text{C})$), 1384 (s s), 1107 (m s), 1082 (m s), 1035 (s s), 866 (s s), 767 (m s), 606 (w s) cm^{-1} . MS-EI m/z : 731 $[\{\text{Fe}(\text{Tpm}^{\text{Py}})_2\text{Cu}_2(\text{Tpm}^{\text{Py}})\}(\text{BF}_4)(\text{NO}_3)_3]^{++}$, 363 $[\text{Fe}(\text{Tpm}^{\text{Py}})_2]^{++}$

Synthesis of $[\text{PdCl}_2(\mu\text{-TpmPy}^{\text{Ph}})_2\text{Fe}_2(\text{H}_2\text{O})_6](\text{BF}_4)_4$ (**40**).

To an acetonitrile suspension (7 mL) of $[\text{PdCl}_2(\text{TpmPy}^{\text{Ph}})_2]$ (**37**) (30 mg, 0.023 mmol, 1 eq) is added dropwise a solution of $\text{Fe}(\text{BF}_4)_2 \cdot 6\text{H}_2\text{O}$ (8 mg, 0.024 mmol, 1 eq) in acetonitrile. The yellow resulting mixture is stirred at room temperature for 1h, during which time a pale yellow solid precipitated. The product is filtered off, washed with a small amount of acetonitrile and dried, yielding a pale yellow powder of (**40**) (59%). $\text{C}_{70}\text{H}_{70}\text{N}_{14} \text{B}_2\text{F}_8\text{Fe}_2\text{O}_8\text{PdCl}_2$ (1698.04). calcd. C 49.51, H 4.16, N 11.55. found: C 50.33, H 4.87, N 11.02. IR (KBr): 3441 (w s, $\nu(\text{OH})$), 3147, 3058, 2924 (w s, $\nu(\text{C-H})$), 1643 (w br, $\nu(\text{OH})$), 1620 (m s, $\nu(\text{C}=\text{N})$), 1531 (s s, $\nu(\text{C}=\text{N})$, $\nu(\text{C}=\text{C})$), 1499, 1455 (s s), 1429, 1392 (m s), 1220 (s br), 1134, 1133-1043 (s br, $\nu(\text{BF}_4)$), 871 (s s), 750 (s s), 693 (s s) cm^{-1} . MS-EI m/z : 1268 $[\text{PdCl}(\text{Tpm}^{\text{PyPh}})_2]^+$, 1366 $[\text{PdCl}(\text{Tpm}^{\text{PyPh}})_2\text{Fe}](\text{CH}_3\text{CN})^+$. $^1\text{H-NMR}$ (CDCl_3 , 298 K): δ 8.61 (d, 2H, $J_{\text{HH}} = 6.4$ Hz, 2,6-H (py)), 7.78 (d, 6H, $J_{\text{HH}} = 7.6$ Hz, *o*-H (Ph)), 7.46 (d, 3H, $J_{\text{HH}} = 2.6$ Hz, 5-H (pz)), 7.40 (dd, vt, 6H, $J_{\text{HH}} = 7.6$ Hz, *m*-H (Ph)), 7.33 (dd, vt, 3H, $J_{\text{HH}} = 7.6$ Hz, *p*-

H (Ph)), 7.11 (d, 2H, $J_{\text{HH}} = 6.6$ Hz, 3,5-H (py)), 6.65 (d, 3H, $J_{\text{HH}} = 2.6$ Hz, 4-H (pz)), 5.40 (s, 2H, $\text{CH}_2\text{-C}(\text{pz})_3$), 4.67 (s, 2H, $\text{CH}_2\text{-py}$). $^{13}\text{C}\{^1\text{H}\}$ and HMQC $^{13}\text{C}\text{-}^1\text{H}$ NMR (100.6 MHz, CDCl_3 , 298 K): δ 153.34 (s, 3-C (pz)), 153.07 (s, 2,6-C (py)), 149.91 (s, 4-C (py)), 132.76 (s, pz-C (Ph)), 132.39 (s, 5-C (pz)), 128.82 (s, m-C (Ph)), 128.53 (s, p-C (Ph)), 126.12 (s, o-C (Ph)), 122.62 (s, 3,5-C (py)), 104.12 (s, 4-C (pz)), 89.25 (s, $\text{CH}_2\text{-C}(\text{pz})_3$), 73.92 (s, O- $\text{CH}_2\text{-C}(\text{pz})_3$), 70.89 (s, O- $\text{CH}_2\text{-py}$).

Synthesis of N-3,5-di-*tert*-Butylsalicyloxysuccinimide (41).

Starting from 3,5-di-*tert*-butylsalicylic acid monohydrate (commercially available from Aldrich). This starting material was dissolved in diethylether and dried over Na_2SO_4 , the solution was filtered and evaporated to give the non-hydrated compound. The latter (18 g, 72.4 mmol) and N-hydroxysuccinimide (9.2 g, 79.6 mmol, 1.1 eq) were dissolved in 250 mL of dioxane. The solution was cooled to 0°C and dicyclohexylcarbodiimide (16.4 g, 79.6 mmol, 1.1 eq) in 200 mL of dioxane was added dropwise. The reaction mixture was left stirring at room temperature under inert atmosphere for 24 h, whereafter a white precipitate (urea derivative) was formed. The reaction mixture was filtered using a Buchner funnel and the filtrate was evaporated to dryness to give (41) as a white powder. Yield: 85 %. ^1H -NMR (400 MHz, CDCl_3): 10.11 (s, 1H, OH(phenol)), 7.82 (d, 1H, ArH, J^4 2.5 Hz), 7.64 (d, 1H, ArH, J^4 2.5 Hz), 2.92 (s, 4H, $-\text{CH}_2\text{-CH}_2-$), 1.41 (s, 9H, ^tBu), 1.30 (s, 9H, ^tBu). $^{13}\text{C}\{^1\text{H}\}$ -NMR (xx MHz, CDCl_3): 169.10 (CO), 159.75 (C-, Ar), 141.52 (Ar), 137.82 (Ar), 133.00 (HC(Ar)), 123.40 (HC(Ar)), 107.07 (Ar), 35.23 (C-, ^tBu), 34.37 (C-, ^tBu), 31.23 (CH_3 , ^tBu), 29.28 (CH_3 , ^tBu), 25.66 ($-\text{CH}_2\text{CH}_2-$).

Synthesis of 3,5-di-*tert*-butyl-2-hydroxy-N-(2-hydroxyethyl) benzamide, $^{\text{NHOH}}\text{LH}$ (42).

To a solution of N-3,5-di-*tert*-butylsalicyloxysuccinimide (41) (2.0 g, 5.7 mmol) in 10 mL of DMF, was added a solution of ethanolamine (0.4 g, 6.7 mmol) in 5 mL of DMF. Then, 6 mL of triethylamine (pre-dried over NaOH) was added to the reaction mixture. After few minutes a precipitate formed and the reaction mixture was left stirring for 24 h. The mixture was then poured into a cold (ice/water bath) 10% HCl aqueous solution (20 mL) and the white precipitate was filtered through a

Buchner funnel, collected and dried under vacuo to give **(42)** in 86 % yield; Anal. Elem. C₁₇H₂₇NO₃ [293.19]: Calcd C, 69.59, H, 9.28, N, 4.77. Found. C, 69.26, H, 8.82, N, 4.93. ¹H NMR (400 MHz, CDCl₃) 12.56 (s, 1H, OH(phenol)), 7.47 (d, 1H, ArH, J⁴ 2.5 Hz), 7.17 (d, 1H, ArH, J⁴ 2.5 Hz), 6.73 (br, 1H, NH), 3.86 (t, 2H, CH₂-OH), 3.64 (q, 2H, CH₂-NHCO), 2.20 (broad, 1H, OH), 1.42 (s, 9H, ^tBu), 1.34 (s, 9H, ^tBu). ¹H NMR ((CD₃)₂CO) 13.59 (s, 1H, OH(phenol)), 7.73 (d, 2H, ArH, J⁴ 2.5 Hz), 7.48 (d, 2H, ArH, J⁴ 2.5 Hz), 3.70 (t, 2H, CH₂-OH), 3.51 (m, 2H, CH₂-NHCO), 1.41 (s, 9H, ^tBu), 1.29 (s, 9H, ^tBu). ¹H NMR (MeOD) 7.55 (d, 2H, ArH, J⁴ 2.5 Hz), 7.46 (d, 2H, ArH, J⁴ 2.5 Hz), 3.72 (t, 2H, CH₂-OH), 3.51 (m, 2H, CH₂-NHCO), 1.41 (s, 9H, ^tBu), 1.32 (s, 9H, ^tBu). ¹H NMR (CD₃CN) 13.31 (s, 1H, OH(phenol)), 7.49-7.48 (m, 1H+1H, ArH+NH), 7.41 (d, 1H, ArH, J⁴ 2.5 Hz), 3.86 (broad, 2H, CH₂-OH), 3.46 (q, 2H, CH₂-NHCO), 2.97 (broad, 1H, OH), 1.40 (s, 9H, ^tBu), 1.31 (s, 9H, ^tBu). ¹³C{¹H}-NMR (100 MHz, CDCl₃) 172.01 (CO), 158.67 (C-OH, Ar), 139.90 (C-^tBu, Ar), 137.94 (C-^tBu, Ar), 128.81 (CH, (Ar)), 119.69 (CH, (Ar)), 113.10 (C-CO, Ar), 61.86 (CH₂-OH), 42.37 (CH₂-NH), 35.16 (C-(CH₃)₃), 34.31 (C-(CH₃)₃), 31.48 (CH₃, ^tBu), 29.35 (CH₃, ^tBu). MS (EI (+)) M/z 294 [M+H]⁺, 316 [M+Na]⁺. IR (KBr pellets): 3486 (N-H), 3313 (PhO-H), 1624 (C=O), 1586, 1554 cm⁻¹; (5 mM sol of MeCN): 3411 (N-H), 1634 cm⁻¹.

Synthesis of tetrabutyl ammonium salt of 2,4-di-*tert*-butyl-6-(2-hydroxyethylcarbamoyl)phenolate, [NBu₄][^{OHNH}L] (42**).**

To a solution of 3,5-di-*tert*-butyl-2-hydroxy-N-(2-hydroxyethyl)benzamide (**42**) (1.5 g, 5.1 mmol) in dry methanol (10 mL), was added a 1.0 M solution in methanol of tetrabutylammonium hydroxide (5.1 mL, 5.1 mmol). The transparent solution was stirred under N₂ for 5 h. Then the solvent was removed under vacuum leaving a white powder that is crystallized from CH₂Cl₂/Et₂O to give the corresponding salt [NBu₄][^{NHOH}L] (**42**) in 72% yield; Anal. Elem. C₃₃H₆₂N₂O₃ [534.47]: Calcd C 74.11, H 11.68, N 5.24. Found. C 74.10, H 12.48, N 5.33. ¹H NMR (400 MHz, CDCl₃) 7.68 (d, 1H, ArH, J⁴ 2.7 Hz), 7.23 (d, 1H, ArH, J⁴ 2.7 Hz), 3.65 (m, 2H, CH₂-OH), 3.45 (m, 2H, CH₂-NHCO), 3.13-3.06 (m, 8H, -CH₂-N, [NBu₄]), 2.06 (br, 1H, HO), 1.52-1.43 (m, 8H, -CH₂-, [NBu₄]), 1.33-1.24 (m, 9H+8H, ^tBu + [NBu₄]) 1.19 (s, 9H, ^tBu), 0.90-0.84 (m, 12H, CH₃-, [NBu₄]). ¹H NMR (MeOD) 7.60 (br, 1H, ArH), 7.42 (br, 1H, ArH), 3.72 (t, 2H, CH₂-OH, J³ 6.0 Hz), 3.49 (q, 2H, CH₂-NHCO, J³ 6.0

Hz), 3.28-3.20 (m, 8H, -CH₂-N, [NBu₄]), 1.72-1.61 (m, 8H, [NBu₄]), 1.48-1.35 (m, 9H+8H, ^tBu + [NBu₄]), 1.31 (s, 9H, ^tBu), 1.03 (t, 12H, CH₃-, [NBu₄]). ¹H NMR (CD₃CN) 13.90 (br, 1H, NH), 7.63 (br, 1H, ArH), 7.13 (br, 1H, ArH), 5.65 (br, 1H, OH), 3.58 (m, 2H, CH₂-OH), 3.42 (m, 2H, CH₂-NHCO), 3.10-3.04 (m, 8H, -CH₂-N, [NBu₄]), 1.65-1.54 (m, 8H, -CH₂-, [NBu₄]), 1.39-1.30 (m, 9H+8H, ^tBu + [NBu₄]), 1.25 (s, 9H, ^tBu), 0.99-0.93 (m, 12H, CH₃-, [NBu₄]). ¹³C{¹H}-NMR (100 MHz, CDCl₃) 172.18 (CO), 157.77 (C-OH, Ar), 137.72 (C-^tBu, Ar), 136.10 (C-^tBu, Ar), 127.42 (HC(Ar)), 122.19 (HC(Ar)), 114.75 (C-CO, Ar), 61.76 (CH₂-OH), 58.53 (-CH₂-N, [NBu₄]), 42.77 (CH₂-NH), 35.03 (C-, ^tBu), 34.12 (C-, ^tBu), 31.64 (CH₃, ^tBu), 29.54 (CH₃, ^tBu), 23.80 (-CH₂-, [NBu₄]), 19.54 (-CH₂-, [NBu₄]), 13.53 (-CH₃, [NBu₄]). ¹H/¹⁵N-HSQC (CD₃CN): 13.90 (br, 1H, NH). MS (EI (-)) M/z 292 [^{NHOH}L]⁻. MS (EI (+)) M/z 242 [NBu₄]⁺. IR (KBr pellets): 3400 (CH₂O-H), 3114 (N-H), 2945 (C-H), 1617 (C=O), 1583 cm⁻¹; (5 mM sol of MeCN): 3008 (N-H, weak), 2966, 2943, 1624 (C=O), 1572 cm⁻¹. UV/vis/NIR (λ/nm(ε/ M⁻¹cm⁻¹)): 355(7775). X-ray quality single crystals were grown by slow diffusion of dry diethylether in a concentrated solution of the title compound in dichloromethane, under a dinitrogen atmosphere.

Synthesis of 2,4-di-*tert*-butyl-6-(2-hydroxyethylcarbamoyl)phenoxyradical, [^{OHNH}L][•] (**42**[•]).

In a CPE electrochemical cell (see Section 6.3.2) stored under dinitrogen was added a 0.2 M solution (15 mL to each compartement) of [NBu₄][BF₄] in dry acetonitrile. The solution was degased with dinitrogen bubbling for 10 minutes. Compound (**42**) (8.0 mg, 0.015 mmol) was added to the electrolyte solution and a cyclic voltammogram (using Pt-disk working electrode) was run. Controlled potential coulometry of this solution of (**42**[•]) was performed at room temperature, under dinitrogen bubbling, at 0.360 V vs. Ag/AgCl until the current is almost zero (see Section 6.3.2). The obtained transparent clear green solution of (**42**[•]) was carefully transferred to a Schlenk and an EPR tube (kept under argon), that were then immediately cooled (and the solution frozen) in liquid nitrogen (77 K). No color change has been detected during or after the transfer, indicating that the bright green color characteristic of the radical remained. UV/vis/NIR (λ/nm(ε/M⁻¹cm⁻¹)): 676 (255), 399(1140), 384(1050), 317(5075), 294(3565), 283(3200). EPR (CH₃CN, 90 K/298 K): a = 3.4 G, g = 2.0043.

Synthesis of 3,5-di-*tert*-butyl-2-hydroxy-N-methyl benzamide, ^{NHMe}LH (43).

To a solution of N-3,5-di-*tert*-butylsalicyloxysuccinimide (**41**) (2.8 g, 8.1 mmol) in 15 mL of DMF, was added a 2.0 M solution of THF of methylamine (4.6 mL, 9.26 mmol). Then, 8 mL of triethylamine (pre-dried over NaOH) was added to the reaction mixture. After a few minutes the reaction mixture started to become milky and a powdery solid started to form. The suspension was left stirring for 24 h. After this time the pale yellow mixture was poured into a cold (ice/water bath) 10% HCl aqueous solution (30 mL) and the final mixture was stirred at 0°C for 5 minutes and filtered through a Buchner funnel, collected, washed with pentane and dried under vacuo to give ^{NHMe}LH (**43**) in 82% yield. Anal. Elem. C₁₆H₂₅NO₂ [263.18]: Calcd C 72.96, H 9.57, N 5.32. Found. C 72.89, H 10.09, N 5.29. ¹H NMR (CDCl₃): 12.70 (s, 1H, OH(phenol)), 7.45 (d, 2H, ArH, J⁴ 2.5 Hz), 7.15 (d, 2H, ArH, J⁴ 2.5 Hz), 6.39 (br, 1H, NH), 3.01 (d, 3H, H₃C-NH, J³ 4.8 Hz), 1.42 (s, 9H, ^tBu), 1.30 (s, 9H, ^tBu). ¹H NMR (CD₃CN): 13.39 (s, 1H, OH(phenol)), 7.47 (d, 1H, ArH, J⁴ 2.4 Hz), 7.37 (m, 1H+1H, ArH+NH), 2.87 (d, 3H, H₃C-NH, J³ 4.8 Hz), 1.40 (s, 9H, ^tBu), 1.30 (s, 9H, ^tBu). ¹³C{¹H}-NMR (100 MHz, CDCl₃) 172.01 (CO), 158.71 (C-OH, Ar), 139.93 (C-^tBu, Ar), 138.26 (C-^tBu, Ar), 128.80 (CH, (Ar)), 119.15 (CH, (Ar)), 113.42 (C-CO, Ar), 35.32 (C-(CH₃)₃), 34.41 (C-(CH₃)₃), 31.62 (CH₃, ^tBu), 29.50 (CH₃, ^tBu), 26.65 (H₃C-N). ¹³C{¹H}-NMR (100 MHz, CD₃CN) 172.70 (CO), 159.40 (C-OH, Ar), 140.89 (C-^tBu, Ar), 138.11 (C-^tBu, Ar), 129.24 (CH, (Ar)), 121.40 (CH, (Ar)), 114.34 (C-CO, Ar), 35.71 (C-(CH₃)₃), 35.04 (C-(CH₃)₃), 31.67 (CH₃, ^tBu), 29.61 (CH₃, ^tBu) 26.32 (H₃C-N), MS (EI (+)) M/z 264 [M+H]⁺, 286 [M+Na]⁺. IR (KBr pellets): 3419 (N-H), 3328 (PhO-H), 1620 (C=O), 1582, 1544 cm⁻¹. (5 mM sol of MeCN): 3413 (N-H), 2961, 1639 (C=O), 1592 cm⁻¹.

Synthesis of tetrabutyl ammonium salt of 2,4-di-*tert*-butyl-6-(2-methylcarbamoyl)phenolate, [NBu₄][^{NHMe}L] (43⁻).

To a solution of 3,5-di-*tert*-butyl-2-hydroxy-N-methylbenzamide (**43**) (1 g, 3.8 mmol) in dry methanol (5 mL), was added a 1.0 M solution in methanol of tetrabutylammonium hydroxide (3.8 mL, 3.8 mmol). The colorless solution turned to

pale yellow colour and was stirred under N₂ for 5 h. Then the solvent was removed under vacuum leaving a yellow oil. The crude oil was suspended in Et₂O, the mixture is stirred for 2 hrs and the solvent was gently decanted off. The sticky white off solid is dried under vacuum to leave the corresponding salt [NBu₄]⁻[^{NHMe}L] (43) in quantitative yield; Anal. Elem. C₃₂H₆₀N₂O₂ [504.47]: Calcd C 76.13, H 11.97, N 5.55. Found. C 75.63, H 10.20, N 5.90. ¹H NMR (400 MHz, CD₃CN) 13.20 (br, 1H, NH), 7.63-7.08 (br, 2H, ArH), 3.08-3.04 (m, 8H, -CH₂-N, [NBu₄]), 2.80 (s, 3H, CH₃-NH), 1.61-1.54 (m, 8H, -CH₂-, [NBu₄]), 1.38-1.29 (m, 9H+8H, ^tBu + [NBu₄]), 1.23 (s, 9H, ^tBu), 0.97 (t, 12H, CH₃-, [NBu₄], J³ 7.0 Hz). ¹H NMR (400 MHz, CDCl₃) 7.36 (br, 2H, ArH), 3.27-3.21 (m, 8H, -CH₂-N, [NBu₄]), 2.96 (s, 3H, CH₃-NH), 1.63-1.58 (m, 8H, -CH₂-, [NBu₄]), 1.44-1.33 (m, 9H+8H, ^tBu + [NBu₄]), 1.27 (s, 9H, ^tBu), 0.96 (t, 12H, CH₃-, [NBu₄], J³ 7.0 Hz). ¹H NMR (400 MHz, MeOD) 7.58 (s, 1H, ArH), 7.40 (s, 1H, ArH), 3.26-3.21 (m, 8H, -CH₂-N, [NBu₄]), 2.93 (s, 3H, CH₃-NH), 1.71-1.62 (m, 8H, -CH₂-, [NBu₄]), 1.46-1.34 (m, 9H+8H, ^tBu + [NBu₄]), 1.30 (s, 9H, ^tBu), 1.02 (t, 12H, CH₃-, [NBu₄], J³ 7.2 Hz). ¹³C{¹H}-NMR (100 MHz, CDCl₃): 171.92 (CO), xx (C-OH, Ar), 138.02 (C-^tBu, Ar), 128.12 (HC(Ar)), 120.46 (HC(Ar)), 114.23 (C-CO, Ar), 58.88 (-CH₂-N, [NBu₄]), 35.27 (C-, ^tBu), 34.32 (C-, ^tBu), 31.70 (CH₃, ^tBu), 29.58 (CH₃, ^tBu), 26.30 (CH₃-NH), 24.17 (-CH₂-, [NBu₄]), 19.79 (-CH₂-, [NBu₄]), 13.77 (-CH₃, [NBu₄]). ¹³C{¹H}-HSQC NMR (100 MHz, CD₃CN) 172.34 (CO), xx (C-OH, Ar), 139.52 (C-^tBu, Ar), 128.43 (C-^tBu, Ar), 125.86 (HC(Ar)), 124.04 (HC(Ar)), xx (C-CO, Ar), 59.19 (-CH₂-N, [NBu₄]), 35.85 (C-, ^tBu), 34.23 (C-, ^tBu), 32.32 (CH₃, ^tBu), 29.93 (CH₃, ^tBu), 25.32 (CH₃-NH), 24.23 (-CH₂-, [NBu₄]), 20.24 (-CH₂-, [NBu₄]), 13.74 (-CH₃, [NBu₄]). ¹³C{¹H}-NMR (100 MHz, MeOD) 173.73 (CO), 139.05 (C-^tBu, Ar), 128.83 (HC(Ar)), 122.60 (HC(Ar)), 115.93 (C-CO, Ar), 59.49 (-CH₂-N, [NBu₄]), 36.07 (C-, ^tBu), 35.15 (C-, ^tBu), 32.03 (CH₃, ^tBu), 30.20 (CH₃, ^tBu), 26.31 (CH₃-NH), 24.78 (-CH₂-, [NBu₄]), 20.70 (-CH₂-, [NBu₄]), 13.94 (-CH₃, [NBu₄]). MS (EI (-)) M/z 262 [^{NHMe}L]⁻. MS (EI (+)) M/z 242 [NBu₄]⁺. IR (nujol): 3274 (N-H), 1623 (C=O), 1584, 1531 cm⁻¹; (5 mM sol of MeCN): 3009 (N-H, weak) 1626 (C=O) cm⁻¹. UV/vis/NIR (λ/nm(ε/M⁻¹cm⁻¹)): 351(5736). X-ray quality single crystals were grown by slow diffusion of dry diethylether in a concentrated solution of the title compound in dichloromethane, under a dinitrogen atmosphere.

Synthesis of 2,4-di-*tert*-butyl-6-(2-methylcarbamoyl)phenoxyradical, [^{NHMe}L]• (43•).

In a CPE electrochemical cell (see Section 6.3.2) stored under dinitrogen was added a 0.2 M solution (15 mL to each compartement) of [NBu₄][BF₄] in dry acetonitrile. The solution was degased with dinitrogen bubbling for 10 minutes. Compound (43•) (7.6 mg, 0.015 mmol) was added to the electrolyte solution and a cyclic voltammogram (using Pt-disk working electrode) was run. Controlled potential coulometry of this solution of (43•) was performed at room temperature, under dinitrogen bubbling, at 0.320 V vs. Ag/AgCl until the current was almost zero (see Section 6.3.2). The obtained transparent clear green solution of (43•) was carefully transferred to a Schlenk and an EPR tube (kept under argon), that were then immediately cooled (and the solution frozen) in liquid nitrogen (77 K). No color change has been detected during or after the transfer, indicating that the bright green color characteristic of the radical remained. UV/vis/NIR (λ /nm(ϵ / M⁻¹cm⁻¹)): 666 (300), 400(1284), 380(1152), 317(5180). EPR (CH₃CN, 90 K/298 K): a = 4.0 G, g = 2.0042.

Synthesis of 3,5-di-*tert*-butyl-2-hydroxy-N-dimethyl benzamide, ^{NMe2}LH (44).

To a solution of N-3,5-di-*tert*-butylsalicyloxysuccinimide (41) (2 g, 5.7 mmol) in 13 mL of DMF, was added a mixture of 3 mL of DMF and a 2.0 M solution in THF of dimethylamine (3.45 ml, 6.9 mmol). Then, 3 mL of triethylamine (pre-dried over NaOH) was added to the reaction mixture. After a few minutes the reaction mixture start to become milky and a powdery solid started to form. The suspension was left stirring for 24 h then poured into a cold (ice/water bath) 10% HCl aqueous solution (20 mL) and the milky final mixture was stirred as 0°C for 10 minutes. A white precipitate was filtered off using a Buchner funnel, collected and dried under vacuo to give ^{NMe2}LH (44) in 80% yield. Anal. Elem. C₁₇H₂₇NO₂ [277.20]: Calcd C 73.60, H 9.81, N 5.05. Found. C 73.51, H 10.36, N 5.00. ¹H NMR (CDCl₃) 10.02 (s, 1H, OH(phenol)), 7.35 (d, 2H, ArH, J⁴ 2.5 Hz), 7.12 (d, 2H, ArH, J⁴ 2.5 Hz), 3.14 (s, 6H, (CH₃)₂N), 1.41 (s, 9H, ^tBu), 1.28 (s, 9H, ^tBu). ¹H NMR ((CD₃)₂CO) 10.65 (s, 1H, OH(phenol)), 7.42 (d, 2H, ArH, J⁴ 2.5 Hz), 7.30 (d, 2H, ArH, J⁴ 2.5 Hz), 3.15 (s, 6H, (CH₃)₂N), 1.41 (s, 9H, ^tBu), 1.30 (s, 9H, ^tBu). ¹H-NMR (CD₃CN) 10.33 (s, 1H,

OH(phenol)), 7.41 (d, 1H, ArH, J^4 2.4 Hz), 7.26 (d, 1H, ArH, J^4 2.4 Hz), 3.09 (s, 6H, (CH₃)₂N), 1.40 (s, 9H, ^tBu), 1.29 (s, 9H, ^tBu). ¹³C{¹H}-NMR (100 MHz, CDCl₃) 173.44 (CO), 159.82 (C-OH, Ar), 139.61 (C-^tBu, Ar), 137.52 (C-^tBu, Ar), 126.84 (CH, (Ar)), 123.16 (CH, (Ar)), 116.42 (C-CO, Ar), 36.49 ((CH₃)₂N), 35.24 (C-(CH₃)₃), 34.32 (C-(CH₃)₃), 31.57 (CH₃, ^tBu), 29.58 (CH₃, ^tBu). ¹³C{¹H}-NMR (100 MHz, CD₃CN) 173.51 (CO), 156.28 (C-OH, Ar), 140.78 (C-^tBu, Ar), 137.74 (C-^tBu, Ar), 127.52 (CH, (Ar)), 124.47 (CH, (Ar)), 117.84 (C-CO, Ar), 38.73 (broad, (CH₃)₂N), 35.74 (C-(CH₃)₃), 34.93 (C-(CH₃)₃), 31.62 (CH₃, ^tBu), 29.74 (CH₃, ^tBu). MS (EI (+)) M/z 278 [M+H]⁺, 300 [M+Na]⁺. IR (KBr pellets): 3127 (PhO-H), 1612 (C=O), 1586, 1478, 1406 cm⁻¹; (5 mM sol of MeCN): 1622 (C=O) cm⁻¹.

Synthesis of tetrabutyl ammonium salt of 2,4-di-*tert*-butyl-6-(2-dimethylcarbamoyl)phenolate, [NBu₄][^{NMe₂L}] (44).

To a solution of 3,5-di-*tert*-butyl-2-hydroxy-N-dimethylbenzamide (**44**) (2 g, 7.2 mmol) in dry methanol (10 mL), was added a 1.0 M solution in methanol of tetrabutylammonium hydroxide (7.2 mL, 7.2 mmol). The colorless solution turned to pale yellow and was stirred under N₂ for 5 h. Then the solvent was removed under vacuum leaving a yellow oil. The crude oil was suspended in Et₂O, the mixture was stirred for 2 h and the solvent was gently decanted off. The residue was dried under vacuum to leave the corresponding salt [NBu₄][^{NMe₂L}] in 89% yield; Anal. Elem. C₃₃H₆₂N₂O₂ [518.47]: Calcd C 76.40, H 12.04, N 5.40. Found. C 76.75, H 12.32, N 5.21. ¹H NMR (400 MHz, CDCl₃) 7.35 (d, 1H, ArH, J^4 2.6 Hz), 7.12 (d, 1H, ArH, J^4 2.6 Hz), 3.42-3.36 (m, 8H, -CH₂-N, [NBu₄]), 3.14 (s, 6H, (CH₃)₂-N), 1.74-1.62 (m, 8H, -CH₂-, [NBu₄]), 1.50-1.41 (m, 9H+8H, ^tBu + [NBu₄]), 1.28 (s, 9H, ^tBu), 1.00 (t, 12H, CH₃-, [NBu₄], J^3 7.1 Hz). ¹³C{¹H}-NMR (100 MHz, CDCl₃) 173.10 (CO), 159.01 (C-OH, Ar), 138.26 (C-^tBu, Ar), 136.76 (C-^tBu, Ar), 126.11 (CH, (Ar)), 124.39 (CH, (Ar)), 117.24 (C-CO, Ar), 59.12 (-CH₂-N, [NBu₄]), 36.21 ((CH₃)₂N), 35.87 (C-(CH₃)₃), 34.98 (C-(CH₃)₃), 31.23 (CH₃, ^tBu), 29.65 (CH₃, ^tBu), 23.71 (-CH₂-, [NBu₄]), 19.64 (-CH₂-, [NBu₄]), 13.48 (-CH₃, [NBu₄]). IR (nujol): 1638 (C=O) cm⁻¹; (5 mM sol of MeCN): 1633 (C=O) cm⁻¹. UV/vis/NIR (λ /nm(ϵ / M⁻¹cm⁻¹)): 333 (1220), 320 (1200).

Synthesis of 2,4-di-*tert*-butyl-6-(2-dimethylcarbamoyl)phenoxyradical, $[\text{NMe}_2\text{L}]^\cdot$ (44**).**

In a CPE electrochemical cell (see Section 6.3.2) stored under dinitrogen was added a 0.2 M solution (15 mL to each compartement) of $[\text{NBu}_4][\text{BF}_4]$ in dry acetonitrile. The solution was degased with dinitrogen bubbling for 10 minutes. Compound (**44**) (7.8 mg, 0.015 mmol) was added to the electrolyte solution and a cyclic voltammogram (using Pt-disk working electrode) was run. Controlled potential coulometry of this solution of (**44**) was performed at room temperature, under dinitrogen bubbling, at 0.320 V vs. Ag/AgCl until the current was almost zero (see Section 6.3.2). The obtained transparent clear green solution of (**44**) was carefully transferred to a Schlenk and an EPR tube (kept under argon), that were then immediately cooled (and the solution frozen) in liquid nitrogen (77 K). No color change has been detected during or after the transfer, indicating that the bright green color characteristic of the radical remained. UV/vis/NIR ($\lambda/\text{nm}(\epsilon/\text{M}^{-1}\text{cm}^{-1})$): 646 (305), 406(1350), 388(1260), 305 (5885). EPR (CH_3CN , 90 K/298 K): $a = 4.2$ G, $g = 2.0046$.

Synthesis of N,N'-(ethane-1,2-diyl)bis(3,5-di-*tert*-butyl-2-hydroxybenzamide), $^{\text{NH}}\text{L}_2\text{H}_2$ (45**).**

To a solution of N-3,5-di-*tert*-butylsalicyloxysuccinimide (**41**) (4.43 g, 12.75 mmol) in 50 mL of DMF, was added a solution of ethylene diamine (428 μL , 6.4 mmol) in 20 mL of DMF. Then, 10 mL of triethylamine (pre-dried over NaOH) was added to the reaction mixture. After a few minutes, a precipitate formed and the reaction mixture was left stirring for 24 h. The mixture was then poured into a cold (ice/water bath) 10% HCl aqueous solution (20 mL) and extracted with dichloromethane (3 x 15 mL). The organic phases were combined, dried over MgSO_4 , filtered and evaporated to give a white solid which was recrystallized from CH_2Cl_2 /pentane to give white crystalline powder of (**45**) in 70 % yield. Anal. Elem. $\text{C}_{32}\text{H}_{48}\text{N}_2\text{O}_4$ [524.74]: Calcd C, 73.24, H, 9.22, N, 5.34. Found. C, 73.12, H, 9.05, N, 5.28. ^1H NMR (CDCl_3 , 400 MHz): 12.66 (s, 2H, 2x(O-H)), 7.48-7.44 (m, 4H, 2x(Ar-H + NH)), 7.27 (vd^(*), 2H, 2x(Ar-H)), 3.73 (m, 4H, 2x(CH_2)), 1.41 (s, 18H, 2x(^tBu)),

* Overlapped with CHCl_3 residual peak.

1.31 (s, 18H, 2x(^tBu)). MS (EI (+)): M/z 525 [M+1]⁺. IR (KBr pellets): 3408 (PhO-H), 1641(C=O), 1580, 1512 cm⁻¹

Synthesis of 3,5-di-*tert*-butyl-2-hydroxy-N-(2-(4-(3,5-di-*tert*-butyl-2-hydroxybenzoyl)piperazin-1-yl)ethyl)benzamide, ^N₃L₂H₂ (46).

To a solution of N-3,5-di-*tert*-Butylsalicyloxysuccinimide (**41**) (2.97 g, 8.5 mmol) in 20 mL of DMF, was added a solution of 2-(piperazin-1-yl)ethanamine (1.1 g, 8.5 mmol) in 10 mL of DMF. Then, 8 mL of triethylamine (pre-dried over NaOH) was added to the reaction mixture. The reaction mixture was left stirring for 24 h, whereupon a white precipitate was formed. The mixture was then poured into water (30 mL) and extracted with dichloromethane (3 x 15 mL). The organic phases were combined, dried over Na₂SO₄, filtered and evaporated to give a clear oily material. This oily was vigorously stirred in pentane (50 mL) until a white solid formed. The solid was then filtered off and dried under vacuum to give (**46**) in 83 % yield (with respect to the phenol starting material). Anal. Elem. C₃₆H₅₅N₃O₄ [593.85]: Calcd C, 72.81, H, 9.34, N, 7.08. Found. C, 72.77, H, 9.28, N, 6.95. ¹H NMR (CDCl₃, 400 MHz): 12.32 (s br, 1H, O-H), 9.55 (s br, 1H, O-H), (s br, 7.42 (m, 2H, Ar-H), 7.36 (m, 2H, Ar-H), 7.07 (s br, 1H, N-H), 3.80 (m, 4H, 2x(CH₂)_{pip}), 3.58 (m, 2H, (CH₂)_{en}), 2.70 (t, 2H, J⁴ 5.89 Hz, (CH₂)_{en}), 2.61 (t, 4H, J⁴ 5.28 Hz, 2x(CH₂)_{pip}). MS (EI (+)): M/z 594 [M+1]⁺. IR (KBr pellets): 3432 (PhO-H), 3313(N-H), 1624(C=O), 1586, 1554 cm⁻¹.

Synthesis of [NBu₄]₂[Ni₂(^{OHNH}L)₂] (47).

To a pale green solution of [Ni(OAc)₂](H₂O)₄ (424 mg, 1.70 mmol, 1 eq) in ethanol (60 mL) was added dropwise a solution of (**42**) (500 mg, 1.70 mmol, 1 eq) in 35 mL of ethanol. The resulting solution was stirred under dinitrogen at room temperature for 30 minutes, after which time a 1.0 M solution of [Bu₄N][OH] in methanol (5.1 mL, 5.11 mmol, 3 eq) was added dropwise. The solution turned to pink/red and was stirred for 1 h at room temperature. The solvent was evaporated in vacuum yielding an orange/pink oil. This residue was partially dissolved in dry acetonitrile (45 mL) and filtered, via cannula. The resulting filtered solution was stored under a dinitrogen atmosphere at -18 °C for 2 days. The solvent was decanted

off leaving a pink crystalline solid of (**47**) that was washed with 5 mL of cold acetonitrile and dried (41 %) Anal. Elem. C₆₆H₁₂₀N₄O₆Ni₂ [1183.09]: Calcd C, 67.00, H, 10.22, N, 4.74. Found. C, 66.26, H, 10.32, N, 4.71. ¹H NMR (CDCl₃) 7.83 (d, 2H, ArH, J⁴ 2.5 Hz), 6.88 (d, 2H, ArH, J⁴ 2.5 Hz), 3.69-3.65 (m, 16H, -CH₂-N, [NBu₄]), 2.69 (s br, 4H, CH₂-OH), 2.60 (m, 4H, CH₂-NHCO), 1.86-1.80 (m, 16H, -CH₂-, [NBu₄]), 1.57-1.51 (m, 16H, -CH₂-, [NBu₄]), 1.20 (s, 18H, ^tBu), 1.18 (s, 18H, ^tBu), 0.95 (t, 24H, CH₃-, [NBu₄]). ¹H NMR ((CD₃)₂CO) 7.84 (d, 2H, ArH, J⁴ 2.5 Hz), 6.83 (d, 2H, ArH, J⁴ 2.5 Hz), 3.63-3.58 (m, 16H, -CH₂-N, [NBu₄]), 3.30 (s br, 4H, CH₂-OH), 2.58 (m, 4H, CH₂-NHCO), 1.89-1.84 (m, 16H, -CH₂-, [NBu₄]), 1.53-1.46 (m, 16H, -CH₂-, [NBu₄]), 1.20 (s, 18H, ^tBu), 1.18 (s, 18H, ^tBu), 0.98 (t, 24H, CH₃-, [NBu₄]). ¹H NMR (CD₃CN) 7.62 (d, 2H, ArH, J⁴ 2.4 Hz), 6.90 (d, 2H, ArH, J⁴ 2.5 Hz), 3.11 (m, 16H, -CH₂-N, [NBu₄]), 2.54-2.32 (m br, 8H, CH₂-OH + CH₂-NHCO), 1.66-1.56 (m, 16H, -CH₂-, [NBu₄]), 1.42-1.33 (m, 16H, -CH₂-, [NBu₄]), 1.20 (s, 18H, ^tBu), 1.16 (s, 18H, ^tBu), 0.96 (t br, 24H, CH₃-, [NBu₄]). MS (EI (+)). ¹³C {¹H}-NMR (100 MHz, CDCl₃) 175.84 (CO), 159.29 (C-OH, Ar), 135.06 (C-^tBu, Ar), 134.95 (C-^tBu, Ar), 124.01 (HC(Ar)), 123.54 (HC(Ar)), 117* (C-CO, Ar), 63.98 (CH₂-OH), 59.36 (-CH₂-N, [NBu₄]), *ca.* 43 (br, CH₂-NH), 35.26 (C-, ^tBu), 35.08 (C-, ^tBu), 32.21 (CH₃, ^tBu), 29.85 (CH₃, ^tBu), 24.42 (-CH₂-, [NBu₄]), 20.35 (-CH₂-, [NBu₄]), 13.85 (-CH₃, [NBu₄]). MS (EI (+)) M/z 1423 [M+NBu₄]⁺; (EI (-)) M/z 938 [M-NBu₄]⁻. IR (KBr pellets): 2960 (s s), 2903 (m s), 2875 (m s), 1637 (w s), 1604 (m s, C=O), 1555 (s s), 1479 (m s), 1431 (s s), 1282 (m s), 1254 (m s), 1064 (m s), 800 (w s), 663 (w s) cm⁻¹. UV/vis/NIR (λ/nm(ε/ M⁻¹cm⁻¹)): 500(525), 338(7550).

Synthesis of [{NBu₄}₂{Ni(^{OHNH}L)₂}]⁺ (**47**⁺).

In CH₃CN. In a CPE electrochemical cell (see Section 6.3.2) stored under dinitrogen was added a 0.2 M solution (15 mL to each compartment) of [NBu₄][BF₄] in dry acetonitrile. The solution was degassed with dinitrogen bubbling for 10 minutes. Compound (**47**) (18 mg, 0.015 mmol) was added to the electrolyte solution and the resulting mixture was cooled to 253 K, then a cyclic voltammogram (using Pt-disk working electrode) was run. Controlled potential coulometry of this solution of (**47**) was performed at room temperature, under dinitrogen bubbling, at 0.340 V vs. Ag/AgCl until the current was almost zero (see Section 6.3.2). The final transparent

* Partially overlapped with CH₃CN residual peak.

dark brown solution of (**47**⁺) was carefully transferred to a Schlenk and an EPR tube (kept under argon), that were then immediately cooled (and the solution frozen) in liquid nitrogen (77 K). No color change has been detected during or after the transfer.

In CH₂Cl₂. The procedure was analogue to that of the CPE in CH₃CN.

UV/vis/NIR ($\lambda/\text{nm}(\epsilon/ \text{M}^{-1}\text{cm}^{-1})$): (CH₃CN) 670(290), 439(955), 375(2450), 314(5850). (CH₂Cl₂) 1193(445), 481(410), 316(4765) EPR (CH₃CN, 90 K/298 K): $a = 5.0 \text{ G}$, $g = 2.0032$; (CH₂Cl₂, 90 K/298 K): weak isotropic signal at, $g = 2.0044$ and 1.9642 ;

Synthesis of $[\{\text{NBu}_4\}_2\{\text{Ni}_2(\text{OHNH}\text{L})_2\}]^{++}$ (**47**⁺⁺).

In CH₃CN. In a CPE electrochemical cell (see Section 6.3.2) stored under dinitrogen was added a 0.2 M solution (15 mL to each compartement) of [NBu₄][BF₄] in dry acetonitrile. The solution was degased with dinitrogen bubbling for 10 minutes. Compound (**47**) (18 mg, 0.015 mmol) was added to the electrolyte solution and the resulting mixture was cooled to 253 K, then a cyclic voltammogram (using Pt-disk working electrode) was run. Controlled potential coulometry of this solution of (**47**) was performed at room temperature, under nitrogen bubbling; at 0.589 V vs. Ag/AgCl until the current was almost zero (see Section 6.3.2). The obtained transparent dark brown solution of (**47**⁺⁺) was carefully transferred to a schlenk and an EPR tube (kept under argon), that were then immediately cooled (and the solution frozen) in liquid nitrogen (77 K). No color change has been detected during or after the transfer.

In CH₂Cl₂. The procedure was analogue to that of the CPE in CH₃CN, except for the temperature of the experiment. The final solution was electrolyzed at 243 K.

UV/vis/NIR ($\lambda/\text{nm}(\epsilon/ \text{M}^{-1}\text{cm}^{-1})$): (CH₃CN) 749(405), 492(850), 385(2750), 314(5900); (CH₂Cl₂) 1193(490), 788(342), 487(800), 387(2000), 316(7200). EPR (CH₃CN, 90 K/298 K): silent. (CH₂Cl₂, 90 K/298 K): $a = 5.0 \text{ g}$ $g = 2.0033$.

Synthesis of $[\text{Ag}(\text{HC}(\text{pz}^{\text{Me}_2})_3)_2][\text{BF}_4]$ (**48**) ($\text{pz}^{\text{Me}_2} = 3,5\text{-dimethylpyrazolyl}$).

To a stirred solution of tris(3,5-dimethylpyrazolyl)methane (100 mg, 0.34 mmol, 1 eq.) in dry THF (10 mL), a 1.6 M solution of butyllithium (240 μL , 0.39 mmol, 1.15 eq.) in cyclohexane was added dropwise at -70°C. The resulting solution turned orangish-red and was stirred for 20 min at -60°C, then cooled down to -80°C.

Solid Ag[BF₄] (65 mg, 0.33 mmol, 1 eq.) was added to the red mixture under vigorous stirring at -80°C, whereafter the colour of the mixture turned slowly to darker brown. The reaction mixture was stirred for a further 10 min at -80°C, and then allowed to warm until room temperature in 3 h. The solvent was evaporated to yield a brown solid. This was dissolved in CH₂Cl₂ (15 mL) and the solution was washed with water (2 x 5 mL), dried over Na₂SO₄, filtered and evaporated, yielding a brown solid. This solid was washed several times with THF and a slow evaporation of the THF solution yielded white single crystals of **(48)** in 30 % yield. (C₃₂H₄₄AgN₁₂BF₄). MS-EI(+) *m/z* (L = HC(pz^{Me2})₃): 405.2 [AgL]⁺, 703.2 [AgL₂]⁺; MS-EI(-) *m/z*: 87.3 [BF₄]⁻. ¹H-NMR (acetone-*d*₆): 1.96 (s, 24H, 5-CH₃), 2.50 (s, 24H, 3-CH₃), 6.09 (s, 6H, 4-H (pz)), 8.23 (s, 2H, HC(pz^{Me2})).

Synthesis of [(μ-Cu){Cu(μ-O)(Tpms^{Ph})₂}] (**50**).

Deep dark gree/blue crystals of compound **(50)** were grown in a cooled methanolic solution of **(26)** in air. The compound was not characterized further. C₅₆H₄₂N₁₂O₁₀S₂Cu₃, (1297.79).

6.2 Crystallographic data

Crystal data Intensity data were collected using a Bruker AXS-KAPPA APEX II diffractometer with graphite monochromated Mo-K α radiation. Data were collected at 150 K using omega scans of 0.5° per frame and a full sphere of data was obtained. Cell parameters were retrieved using Bruker SMART software and refined using Bruker SAINT⁷ on all the observed reflections. Absorption corrections were applied using SADABS.⁷ The structures were solved by direct methods by using the SHELXS-97 package⁸ and refined with SHELXL-97⁹. Calculations were performed using the WinGX System-Version 1.80.03.¹⁰ and PLATON/SQUEEZE¹¹ was used to correct the data.

	(3)	(2-Ms)	(8)
Crystal shape	block	prism	prism
Crystal colour	white	colourless	colourless
Empirical formula	C ₁₇ H ₁₇ N ₇ O	C ₁₂ H ₁₄ N ₆ O ₃ S	C ₂₁ H ₂₈ N ₈
Formula weight	335.38	322.35	392.51
Crystal system	triclinic	monoclinic	triclinic
Space Group	P -1	P21/n	P-1
<i>a</i> (Å)	8.3750(11)	7.7397(16)	8.7193(8)
<i>b</i> (Å)	9.6879(11)	12.757(3)	10.1915(12)
<i>c</i> (Å)	10.6197(14)	14.957(3)	12.5175(12)
α	92.074(7)	90	78.152(7)
β	106.285(8)	103.719(12)	84.766(5)
γ	91.599(7)	90	69.968(6)
<i>V</i> (Å ³)	825.88(18)	1434.7(5)	1022.52(19)
<i>Z</i>	2	4	2
ρ_{calc} (g cm ⁻³)	1.349	1.492	1.275
μ (Mo K α) (mm ⁻¹)	0.091	0.249	0.091
<i>F</i> (000)	352	672	420
Refl. Collected/unique	18468/4997	35129/3941	8098/3538
$R_1 = [I > 2\sigma(I)]$; wR2 (all data)	0.0425; 0.1200	0.0348; 0.1037	0.0558; 0.1496

	(20)	(21) · C ₃ H ₆ O	(22)	(23) · C ₃ H ₆ O
Crystal shape	plate	prism	prism	prism
Crystal colour	white	colourless	colourless	colourless
Empirical formula	C ₃₀ H ₂₄ CuN ₇ O ₃ S	C ₃₄ H ₃₃ CuN ₉ O ₃ P S · C ₃ H ₆ O	C ₃₇ H ₃₉ Cu N ₁₀ O ₄ S	C ₃₅ H ₃₆ CuN ₉ O ₃ PS, C ₃ H ₆ O · F ₆ P
Formula weight	626.18	800.36	783.38	960.37
Crystal system	orthorhombic	orthorhombic	orthorhombic	monoclinic
Space Group	Pbcn P2n2ab	Pbca	Pbca	P21/n
<i>A</i> (Å)	15.0997(15)	13.799(3)	11.4692(7)	16.056(6)
<i>B</i> (Å)	13.9691(14)	20.730(5)	21.8702(14)	15.889(6)
<i>C</i> (Å)	28.789(3)	26.676(7)	28.7465(16)	16.279(6)
β (°)	90	90	90	96.901(2)
<i>V</i> (Å ³)	6072.5(11)	7631(3)	7210.6(8)	4123(3)
<i>Z</i>	8	8	8	4
ρ_{calc} (g cm ⁻³)	1.370	1.393	1.443	1.547
μ (Mo K α) (mm ⁻¹)	0.831	0.721	0.720	0.738
<i>F</i> (000)	2576	3328	3264	1976
Refl. Collected/unique	26662/5543	28366/6974	35881/6595	7547/7547
$R_1 = [I > 2\sigma(I)]$; wR2 (all data)	0.0474; 0.1079	0.0615; 0.1386	0.0555 0.1200	0.1575; 0.2104

	(24)·(Et ₂ O) _{0.5}	(28)·(C ₂ H ₆ O) ₄	(29)
Crystal shape	orism	plate	prism
Crystal colour	colorless	green	blue
Empirical formula	(C ₃₅ H ₃₂ CuN ₇ O ₃ S) ₂ ·C ₄ H ₁₀ O	C ₅₆ H ₄₂ Cu ₂ N ₁₂ O ₈ S ₂ ·(C ₃ H ₆ O) ₄	C ₅₈ H ₅₂ Cu ₃ N ₁₂ O ₁₀ S ₂
Formula weight	1462.67	1434.53	1331.86
Crystal system	monoclinic	triclinic	monoclinic
Space Group	C2/c:b1	P-1	P21
<i>a</i> (Å)	27.422(2)	11.7576(5)	11.8383(12)
<i>b</i> (Å)	11.4315(7)	11.8670(6)	24.052(3)
<i>c</i> (Å)	23.0916(17)	11.8957(6)	11.838(3)
α	90.00	98.114(3)	90.00
β	106.675(2)	94.929(4)	101.01(8)
γ	90.00	90.750(4)	90.00
<i>V</i> (Å ³)	6934.2(8)	1636.55(14)	3308.8(10)

Z	4	1	2
ρ_{calc} (g cm ⁻³)	1.401	1.456	1.337
$\mu(\text{Mo K}\alpha)$ (mm ⁻¹)	0.740	0.787	1.080
<i>F</i> (000)	3048	744	1366
Refl. Collected/unique	28579/6331	19885/5560	12778/9940
$R_1 = [I > 2\sigma(I)]$; wR2 (all data)	0.0464; 0.1093	0.0687; 0.2090	0.0654; 0.1766

	(30)	(31)	(32)	(36)
Crystal shape	amorphous	cube	prism	plate
Crystal colour	red	colorless	pink	colorless
Empirical formula	C ₃₄ H ₃₄ FeN ₁₄ O ₂ 2(BF ₄)	C ₃₄ H ₃₄ Cl ₂ N ₁₄ O ₂ Zn	C ₃₄ H ₃₄ N ₁₄ NiO ₂	C ₃₄ H ₃₄ Cl ₂ N ₁₄ O ₂ Pd
Formula weight	900.22	807.02	729.46	848.05
Crystal system	monoclinic	monoclinic	monoclinic	monoclinic
Space Group	P21/ <i>c</i>	P21/ <i>c</i>	P21/ <i>c</i>	P21/ <i>c</i>
<i>a</i> (Å)	14.8596(12)	20.5210(12)	13.126(11)	13.266(3)
<i>b</i> (Å)	13.0034(10)	15.8868(17)	22.194(18)	9.2463(19)
<i>c</i> (Å)	20.7112(17)	11.0942(12)	20.15(2)	16.451(3)
α	90.00	90.00	90.00	90.00
β	105.932(3)	92.334(3)	104.03(4)	111.280(7)
γ	90.00	90.00	90.00	90.00
<i>V</i> (Å ³)	3848.2(5)	3613.9(6)	5695(9)	1880.3(7)
Z	4	4	4	2
ρ_{calc} (g cm ⁻³)	1.554	1.483	0.851	1.498
$\mu(\text{Mo K}\alpha)$ (mm ⁻¹)	0.485	0.882	0.374	0.688
<i>F</i> (000)	1840	1664	1520	864
Refl. Collected/unique	24714/6808	26666/7610	43838/12516	12587/3233
$R_1 = [I > 2\sigma(I)]$; wR2 (all data)	0.0618; 0.2117	0.0374; 0.1068	0.0675; 0.1806	0.0827; 0.2787

	(42) · 2H ₂ O	(43)	(47)	(48) ^(a)
Crystal shape	prism	prism	plate	plate
Crystal colour	colourless	colourless	pink	white
Empirical formula	C ₃₃ H ₆₆ N ₂ O ₅	C ₃₂ H ₆₀ N ₂ O ₂	C ₇₀ H ₁₂₈ N ₅ Ni ₂ O ₇	C ₃₂ H ₄₄ AgBF ₄ N ₁₂

Formula weight	570.88	504.82	1269.19	790.290
Crystal system	triclinic	monoclinic	triclinic	monoclinic
Space Group	P-1	P21/c	P-1	P21/c
a (Å)	8.9498(12),	11.268(4)	12.085(3)	8.9572(3)
b (Å)	13.4507(18)	16.369(6)	16.345(4)	12.8529(4)
c (Å)	15.964(2)	19.073(7)	20.368(5)	15.9160(5)
α	86.522(10)	90	69.892(10)	90
β	88.448(10)	115.31(2)	80.773(11)	92.188(2)
γ	72.232(9)	90	84.246(11)	90
V (Å ³)	1826.7(4)	3180(2)	3724.8(15)	1831.01(10)
Z	2	4	2	2
ρ_{calc} (g cm ⁻³)	1.038	1.054	1.131	1.278
μ (Mo K α) (mm ⁻¹)	0.068	0.064	0.556	0.589
F (000)	636	1128	1388	734
Refl. Collected/unique	23205/6675	19075/ 5799	13085/5194	14017/3199
$R_1 = [I > 2\sigma(I)]$; wR2 (all data)	0.0635; 0.1351	0.1278; 0.1862	0.0667; 0.1440	0.0337; 0.0820

^(a) Least square refinements with anisotropic thermal motion parameters for all the non-hydrogen atoms and isotropic for the remaining atoms were employed. The BF_4 anion is disordered in the structure and attempts were made to model it, but were unsuccessful. Potential volume of 214.8 Å³ were found. A total of 91 electrons per unit cell worth of scattering were located in the void. The stoichiometry is tentatively calculated as $1BF_4^-$ anion per unit cell.

6.3 Electrochemical experiments

Dichloromethane and acetonitrile solvents were freshly distilled from calcium hydride under dinitrogen. $[\text{NBu}_4][\text{BF}_4]$ was prepared by literature methods.¹²

6.3.1 Cyclic Voltammetry

Apparatus

The electrochemical experiments were carried out on an EG&G PAR 273A potentiostat/galvanostat connected to a personal computer through a GPIB interface. Cyclic voltammetry (CV) studies were undertaken in a two-compartment three-electrode cell, with platinum disk working ($d = 0.5$ mm) and counter electrodes. A Luggin capillary connected to a silver-wire pseudo-reference electrode was used to control the working electrode potential. The solutions were saturated with N_2 by bubbling this gas before each run and were 10^{-3} M in the test compound and 0.2 M in $[\text{NBu}_4][\text{BF}_4]$ as the supporting electrolyte.

Internal standard:

Redox potentials are quoted *versus* the $[\text{Fc}]/[\text{Fc}]^+$ ($\text{Fc} = [\text{Fe}(\eta^5\text{-C}_5\text{H}_5)_2]$, ferrocinium/ferrocene) couple used as an internal reference.¹³ When necessary (*e.g.* for the compounds **(42)**, **(43)** and **(47)** (see Chapters 4 and 5)), the $\{\text{Fe}(\text{TpmPy})\}[\text{BF}_4]_2\}^{0/+}$ (compound **(30)**, see Chapter 3) couple was used as the internal reference to avoid the overlapping redox couples. In these circumstances, the potentials of the redox processes were referenced to that of the $[\text{Fc}]^{0/+}$ couple by an independent calibration. The $\Delta E_{1/2}$ between $\text{Fc}^{0/+}$ and $\{\text{Fe}(\text{TpmPy})\}[\text{BF}_4]_2\}^{0/+}$ recorded under identical conditions was 0.642V.

General Procedure:

in a electrochemical cell stored under dinitrogen is added a 0.2 M solution (4-5 mL) of $[\text{NBu}_4][\text{BF}_4]$ in the suitable dry solvent. The solution is degassed with dinitrogen bubbling for 10 min. then a cyclic voltammogram is run to verify the electrochemical profile of the background solution. The compound (*ca.* 0.005 mmol) was added to the electrolyte solution and the CV is run.

Reversibility tests:

The parameters, E_p^{ox} and E_p^{red} (anodic and cathodic potential, respectively) and i_p^a , i_p^c (anodic and cathodic current, respectively) are shown in Figure 6.1. Three main tests were used to determine the reversibility of a redox process. Thus, a system is considered to have a reversible behavior if it obeys the following conditions: (i) $\Delta E = E_p^{ox} - E_p^{red}$ is constant with varying scan-rate and equal to ca. 59mV; (ii) the ratio i_p^a / i_p^c is equal to 1. (iii) a plot of i_p^a or i_p^c vs. (scan rate)^{1/2} is linear.

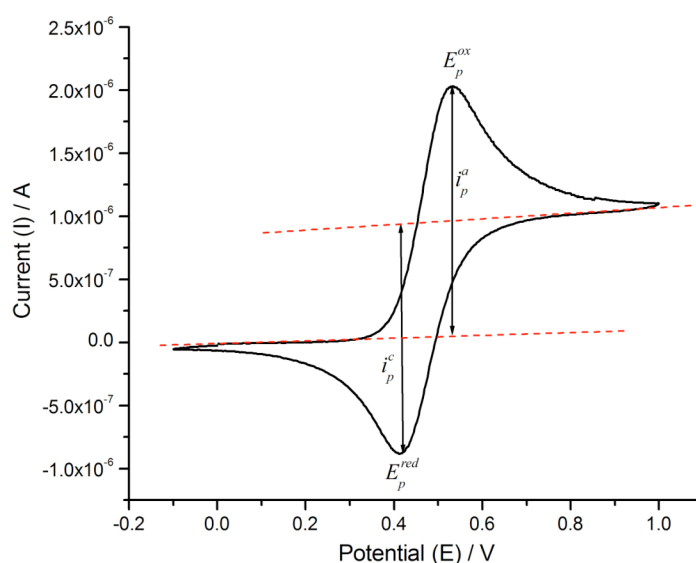


Figure 6.1 The cyclic voltammogram of a reversible redox process.

A system that obeys these conditions is considered to be showing a standard Nernstian response.¹⁴

It is important that each of these tests is carried out for both the test compound and the internal standard (which should behave as a fully reversible system). However, experimentally, the $[Fc]^{0/+}$ (or $\{Fe(TpmPy)\}[BF_4]_2\}^{0/+}$) couple exhibits a deviation from the standard Nernstian response,¹⁴ using the apparatus previously described. This deviation could be due to solvent, such as CH_2Cl_2 , for instance, that possesses a low dielectric constant, and produces a high cell resistance. Therefore, it was assumed that, if a test compound under the same conditions showed a similar deviation from an ideal Nernstian response to that of $[Fc]^{0/+}$ (or

{Fe(TpmPy)}[BF₄]₂}^{0/+}) couple, the redox process of the test compound would be considered to be electrochemically reversible.

Under these conditions, the formal redox potential for the redox couple is defined as:

$$E_{1/2}^{ox} = (E_p^{ox} + E_p^{red})/2$$

6.3.2 Coulometry:

Controlled potential electrolyses (CPE) were carried out in a two-compartment three-electrode cell with platinum-gauze working and counter electrodes in compartments separated by a glass frit; a Luggin capillary, probing the working electrode, was connected to a silver wire pseudo-reference electrode. The solutions were saturated with N₂ by bubbling this gas before each run and were 0.2 M in [NBu₄][BF₄] as supporting electrolyte and *ca.* 10⁻³ M in the test compound.

Method:

The CPE experiment consists of applying a constant potential at a value that is sufficiently high (or low) to oxidise (or reduce) a given compound. During the experiment, the test compound is electrolysed at the surface of the working electrode. Thus, electrons are transferred from the test compound to the working electrode (in the case of an oxidation) or from the working electrode to the test compound (in the case of a reduction). The charge (Q) accumulated during the experiment is recorded and Q can be plotted vs time (t) (Figure 6.2 left).

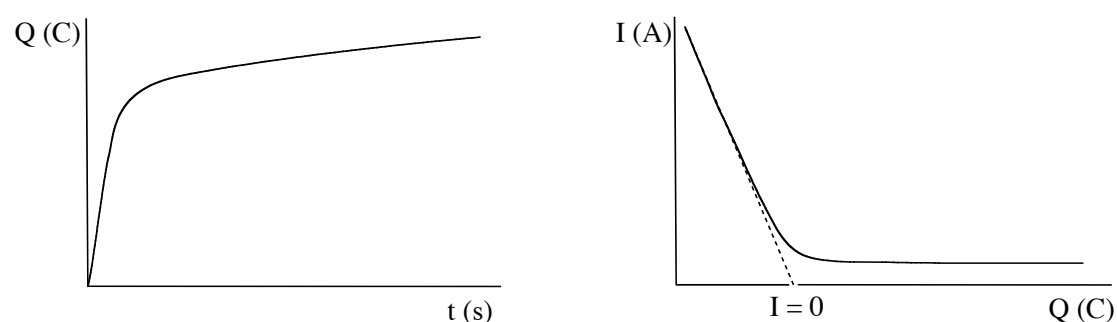


Figure 6.2 Plots of Q vs time (left) and I vs Q (right).

At the beginning of an experiment the current (I) response is high ($I = dQ/dt$) and reaches a plateau ($I = 0$) at the end of the experiment, as all the molecules have

been electrolysed. Experimentally there is a residual current (*i.e.* background current), hence Q keeps increasing. The total charge accumulated during the experiment is expressed as:

$$Q = NnF$$

N = number of moles of the test compound used; n = number of electron transferred per molecule of test compound; F = Faraday constant = 96500 C (coulombs).

Thus, from this expression, and the plot of current (I) vs Q can be extrapolated the correct value of Q for $I = 0$ (Figure 6.2, right) and n is readily obtained.

6.3.3 Electrochemical results

For compounds **(30)**, **(42⁻)**, **(43⁻)**, **(44⁻)** and **(47)** that exhibit, in the cyclic voltammogram, one (or two) reversible process(es) are reported (i) the half-wave oxidation potential $E_{1/2}^{ox}$ vs. $\text{Fc}^{0/+}$ (V), (ii) the peak oxidation potential E_p^{ox} vs. $\text{Fc}^{0/+}$ (mV), (iii) the difference between anodic and cathodic potentials $\Delta E = E_p^{ox} - E_p^{red}$ at different scan rates (20-900 mV s^{-1}), (iv) the ratio between anodic and cathodic currents i_p^a/i_p^c at different scan rates (20-900 mV s^{-1}), (v) the corresponding parameters for the reference compound (*i.e.* $\text{Fc}^{0/+}$) in analogue conditions and (iv) the number of electrons per molecule transferred in the CPE experiment.

For compounds **(20)** and **(21)** that, in the cyclic voltammogram, display irreversible process(es) are reported (i) the peak potential(s) of the genuine wave(s) (labelled as I, II, ...) with a possible attribution, (ii) the additional waves and (iii) the number of electrons per molecule transferred in the CPE experiment.

[Cu(Tpms^{Ph})(MeCN)] **(20)**

In CH₃CN at RT. CV displays (Figure 6.3) two genuine not reversible waves (*i.e.* **I**, **II**) $E_p^{Iox} = + 0.540$ V (oxidation, $\text{Cu}^{I/II}$); $E_p^{IIred} = - 0.893$ V (reduction $\text{Cu}^{I/0}$); $E_p^{red} = + 0.073$ V (not genuine reduction, $\text{Cu}^{II/I}$); $E_p^{ox} = - 0.530$ V (high intensity, sharp, not genuine oxidation, $\text{Cu}^{0/I}$). Controlled potential coulometry of **(20)** for **I** (E_p^{Iox}) process, performed in acetonitrile at room temperature at 1.09 V vs. Ag/AgCl indicated the transfer of 0.89 electrons per molecule.

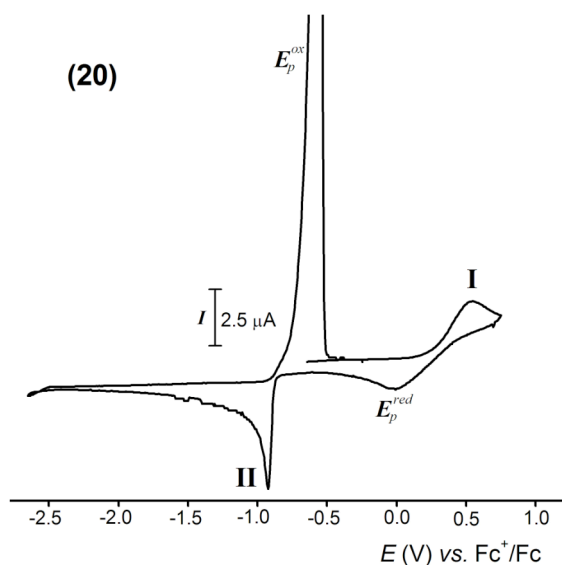


Figure 6.3 Cyclic voltammogram ($v = 120 \text{ mV s}^{-1}$) of a ca. 1 mM solution of **(20)** in CH_3CN with 0.2 M $[\text{NBu}_4][\text{BF}_4]$, at a platinum disc electrode ($d = 0.5 \text{ mm}$).

[Cu(Tpms^{Ph})(PTA)] (21)

In CH_3CN at RT. displays (Figure 6.4) two genuine not reversible waves (*i.e.* **I**, **II**) $E_p^{\text{Iox}} = +0.735 \text{ V}$ (oxidation, $\text{Cu}^{\text{I/II}}$); $E_p^{\text{IIred}} = -1.430 \text{ V}$ (reduction $\text{Cu}^{\text{I/0}}$), $E_p^{\text{ox}} = -0.547 \text{ V}$ (high intensity, sharp, not genuine oxidation, $\text{Cu}^{\text{0/I}}$). Controlled potential coulometry of **(21)** for **I** (E_p^{Iox}) process, performed in acetonitrile at room temperature at 1.30 V vs. Ag/AgCl indicated the transfer of 0.94 electrons per molecule.

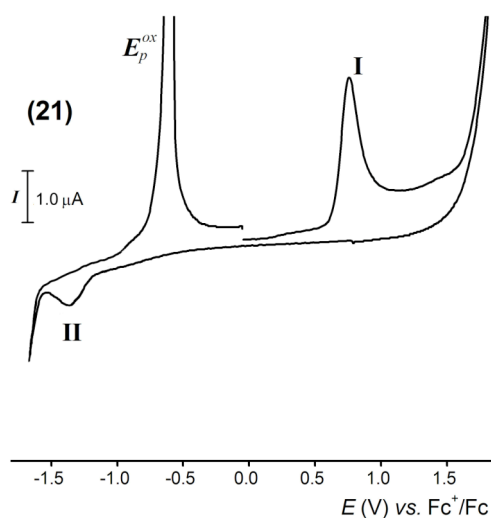


Figure 6.4 Cyclic voltammogram ($v = 120 \text{ mV s}^{-1}$) of a ca. 1 mM solution of **(21)** in CH_3CN with 0.2 M $[\text{NBu}_4][\text{BF}_4]$, at a platinum disc electrode ($d = 0.5 \text{ mm}$).

[Fe(Tpm^{Py})₂][BF₄]₂ (30)

In CH₃CN at RT. (see Figure 3.6) $E_{1/2}^{ox} = + 0.640$ V, $E_p^{ox} = +671$ mV, $\Delta E = 62$ mV at 120 mV s⁻¹. $\Delta E = 59 - 79$ mV (scan rate = $20 - 900$ mV s⁻¹); $i_p^a/i_p^c = 1 \pm 0.1$; (scan rate)^{1/2} $\propto i_p^c$ (and i_p^a). For Fc/Fc⁺: $\Delta E = 58 - 76$ mV (scan rate = $20 - 900$ mV.s⁻¹). Thus the process is considered to be fully reversible. Controlled potential coulometry of [Fe(Tpm^{Py})₂][BF₄]₂ performed in acetonitrile at room temperature at 1.20 V vs. Ag/AgCl indicated the transfer of 1.02 electrons per molecule. Thus, this is a one-electron oxidation process.

[^{NHOH}L][NBu₄] (42⁻)

In CH₃CN at RT. (see Figure 4.10 and 4.11) $E_{1/2}^{ox} = - 0.119$ V, $E_p^{ox} = -89$ mV, $\Delta E = 61$ mV at 120 mV s⁻¹. $\Delta E = 58 - 71$ mV (scan rate = $20 - 900$ mV s⁻¹); $i_p^a/i_p^c = 1 \pm 0.1$ at scan rate (s.r.) > 100 mV.s⁻¹, at $20, 50$ and 80 mVs⁻¹, i_p^a/i_p^c are $1.18, 1.34,$ and 1.29 respectively; (scan rate)^{1/2} $\propto i_p^c$ (and i_p^a). For Fc/Fc⁺: $\Delta E = 60 - 88$ mV (scan rate = $20 - 900$ mV s⁻¹). Thus the process is considered to be fully reversible. Controlled potential coulometry of [^{NHOH}L][NBu₄] performed in acetonitrile at room temperature at 0.360 V vs. Ag/AgCl indicated the transfer of 0.97 electrons per molecule. Thus, this is a one-electron oxidation process.

In CH₂Cl₂ at RT. $E_{1/2}^{ox} = - 0.248$ V, $E_p^{ox} = -206$ mV, $\Delta E = 67$ mV at a 120 mVs⁻¹. $\Delta E = 67 - 100$ mV (scan rate¹⁵ = $20 - 900$ mV s⁻¹); $i_p^a/i_p^c = 1.12 - 1.25$ (scan rate $> 20 - 900$ mV.s⁻¹); (scan rate)^{1/2} $\propto i_p^c$ (and i_p^a). For Fc/Fc⁺: $\Delta E = 82 - 100$ mV (scan rate = $20 - 900$ mV.s⁻¹). Thus the process is considered to be fully reversible. Controlled potential coulometry of [^{NHOH}L][NBu₄] performed in dichloromethane at room temperature at 0.430 V vs. Ag/AgCl indicated the transfer of 0.93 electrons per molecule. Thus, this is a one-electron oxidation process.

[^{NHMe}L][NBu₄] (43⁻)

In CH₃CN at RT. (see Figure 4.10 and 4.11) $E_{1/2}^{ox} = - 0.161$ V, $E_p^{ox} = -129$ mV, $\Delta E = 65$ mV at 120 mV s⁻¹. $\Delta E = 65 - 99$ mV (scan rate = $20 - 900$ mV s⁻¹); $i_p^c/i_p^a = 1 \pm 0.1$ at scan rate > 50 mV.s⁻¹, at 20 mV s⁻¹ i_p^c/i_p^a is 1.27 ; (scan rate)^{1/2} $\propto i_p^c$

(and i_p^a). For Fc/Fc⁺: $\Delta E = 69 - 89$ mV (scan rate = 20 - 900 mV.s⁻¹). Thus the process is considered to be fully reversible. Controlled potential coulometry of [^{NHMe}L][NBu₄] performed in acetonitrile at room temperature at 0.320 V vs. Ag/AgCl indicated the transfer of 0.99 electrons per molecule. Thus, this is a one-electron oxidation process. **In CH₂Cl₂ at RT.** $E_{1/2}^{ox} = -0.300$ V, $E_p^{ox} = -240$ mV, $\Delta E = 60$ mV at a 120 mVs⁻¹. $\Delta E = 69 - 92$ mV (scan rate¹⁵ = 20 - 900 mV s⁻¹); $i_p^a/i_p^c = 1.11 - 1.29$ (scan rate > 20 - 900 mV.s⁻¹); (scan rate)^{1/2} $\propto i_p^c$ (and i_p^a). For Fc/Fc⁺: $\Delta E = 71 - 94$ mV (scan rate = 20 - 900 mV.s⁻¹). Thus the process is considered to be fully reversible.

[^{NMe2}L][NBu₄] (44)

In CH₃CN at RT. (see Figure 4.10 and 4.11) $E_{1/2}^{ox} = -0.423$ V, $E_p^{ox} = -385$ mV, $\Delta E = 77$ mV at 120 mV s⁻¹. $\Delta E = 69 - 89$ mV (scan rate = 20 - 900 mV s⁻¹); $i_p^a/i_p^c = 1 \pm 0.1$ at scan rate > 100 mV.s⁻¹, at 20, 50, and 80 mV.s⁻¹, i_p^a/i_p^c are 1.21, 1.21, and 1.33 respectively; (scan rate)^{1/2} $\propto i_p^c$ (and i_p^a). For Fc/Fc⁺: $\Delta E = 72 - 90$ mV (scan rate = 20 - 900 mV.s⁻¹). Thus the process is considered to be fully reversible. Controlled potential coulometry of [^{NMe2}L][NBu₄] performed in acetonitrile at room temperature at 0.184 V vs. Ag/AgCl indicated the transfer of 0.98 electrons per molecule. Thus, this is a one-electron oxidation process.

In CH₂Cl₂ at RT. $E_{1/2}^{ox} = -0.544$ V, $E_p^{ox} = -508$ mV, $\Delta E = 72$ mV at a 120 mVs⁻¹. $\Delta E = 72 - 111$ mV (scan rate¹⁵ = 20 - 900 mV s⁻¹); $i_p^a/i_p^c = 1.05 - 1.31$ (scan rate > 20 - 900 mV.s⁻¹); (scan rate)^{1/2} $\propto i_p^c$ (and i_p^a). For Fc/Fc⁺: $\Delta E = 80 - 101$ mV (scan rate = 20 - 900 mV.s⁻¹). Thus the process is considered to be fully reversible.

[Ni(^{OHNH}L)]₂[NBu₄]₂ (47)

In CH₃CN at 253 K. (see Figure 5.3) $E_{1/2}^{Iox} = -0.120$ V, $E_p^{Iox} = -76$ mV, $\Delta E = 89$ mV at 120 mV s⁻¹. $\Delta E = 76 - 95$ mV (scan rate = 20 - 900 mV s⁻¹); $i_p^a/i_p^c = 1 \pm 0.3$; (scan rate)^{1/2} $\propto i_p^c$ (and i_p^a). $E_{1/2}^{IIox} = +0.110$, $E_p^{IIox} = 166$ mV, $\Delta E = 102$ mV at 120 mV s⁻¹. $\Delta E = 99 - 109$ mV (scan rate = 20 - 900 mV s⁻¹); $i_p^a/i_p^c = 1 \pm 0.2$; (scan rate)^{1/2} $\propto i_p^c$ (and i_p^a). For Fc/Fc⁺: $\Delta E = 77 - 89$ mV (scan rate = 20 - 900 mV.s⁻¹). Thus, these processes are considered to be *quasi* reversible. Controlled potential coulometry of (47) performed in acetonitrile at 253 K, for process $E_{1/2}^I$ at 0.340 V vs. Ag/AgCl and

for process $E_{1/2}^{\text{II}}$ at 0.589 V vs. Ag/AgCl indicated the transfer of 1.01 and 1.92 electrons per molecule, respectively. Thus, each of these processes are a one-electron oxidation processes.

In CH_2Cl_2 at 253 K. $E_{1/2}^{\text{Iox}} = -0.124$ V, $E_p^{\text{Iox}} = -82$ mV, $\Delta E = 81$ mV at 120 mV s^{-1} . $\Delta E = 81 - 94$ mV (scan rate = $20 - 900$ mV s^{-1}); $i_p^a/i_p^c = 1 \pm 0.1$ at scan rate > 100 mV.s^{-1} , at $20, 50,$ and 80 mV.s^{-1} , i_p^a/i_p^c are $1.24, 1.27,$ and 1.19 respectively; (scan rate) $^{1/2} \propto i_p^c$ (and i_p^a). $E_{1/2}^{\text{IIox}} = +0.078$, $E_p^{\text{IIox}} = 125$ mV, $\Delta E = 94$ mV at 120 mV s^{-1} . $\Delta E = 91 - 104$ mV (scan rate = $20 - 900$ mV s^{-1}); $i_p^a/i_p^c = 1 \pm 0.1$ at scan rate > 120 mV.s^{-1} , at $20, 50, 80$ and 120 mV.s^{-1} , i_p^a/i_p^c are $1.28, 1.22, 1.15$ and 1.19 respectively; (scan rate) $^{1/2} \propto i_p^c$ (and i_p^a). For Fc/Fc $^+$: $\Delta E = 77 - 109$ mV (scan rate = $20 - 900$ mV.s^{-1}). Thus, these processes are considered to be *quasi* reversible. Controlled potential coulometry of (47) performed in acetonitrile at 253 K, for process $E_{1/2}^{\text{I}}$ at 0.356 V vs. Ag/AgCl and for process $E_{1/2}^{\text{II}}$ at 0.553 V vs. Ag/AgCl indicated the transfer of 1.04 and 1.89 electrons per molecule, respectively. Thus, each of these processes are a one-electron oxidation processes.

6.3.3.1 Results of reversibility studies of the oxidation/reduction processes for (42 $^-$), (43 $^-$) and (44 $^-$)

The $[\text{NRR}^{\text{I}}\text{LH}]^+ / [\text{NRR}^{\text{I}}\text{LH}]^-$ couple (*i.e.* compounds (42 *)/(42 $^-$), (43 *)/(43 $^-$) and (44 *)/(44 $^-$)) and the Fc $^+$ /Fc couple show a similar magnitude and variation in ΔE with increasing scan rate. The i_p^a / i_p^c ratio of the $[\text{NRR}^{\text{I}}\text{LH}]^+ / [\text{NRR}^{\text{I}}\text{LH}]^-$ couple, in CH_3CN , is close to 1 (within 12%) for scan rate (s.r.) > 120 mV.s^{-1} and increases from 1.2 to 1.3 for s.r. $20, 50, 80$ mV.s^{-1} . In CH_2Cl_2 , the i_p^a / i_p^c ratio is in the range of 1.2-1.3, but the same effect was observed for the [Fc $^+$]/[Fc] couple. The peak currents, i_p^c and i_p^a , each vary linearly with the square root of the scan rate for the $[\text{NRR}^{\text{I}}\text{LH}]^+ / [\text{NRR}^{\text{I}}\text{LH}]^-$ couple.

Thus, under these experimental conditions; the $[\text{NRR}^{\text{I}}\text{LH}]^+ / [\text{NRR}^{\text{I}}\text{LH}]^-$ couple behaves the same as the [Fc $^+$]/[Fc] couple. Therefore, it is considered that the redox processes of compounds (42 *)/(42 $^-$), (43 *)/(43 $^-$) and (44 *)/(44 $^-$) are electrochemically reversible.

All Tables reported: s.r. (scan rate, $\text{mV}\cdot\text{s}^{-1}$); i_p^a (anodic current, 10^{-7} A); i_p^c (cathodic current, 10^{-7} A); ΔE ($\Delta E = E_p^{ox} - E_p^{red}$); and i_p^a / i_p^c .

6.3.3.2 Reversibility of the oxidation/reduction process of $\text{Fc}^{0/+}$ (ferrocene/ferrocinium)

Table 6.1 Electrochemical characteristics in CH_3CN of the couple $\text{Fc}^{0/+}$.

s.r.	i_p^a	$-i_p^c$	ΔE	i^a/i^c
20	5.69	5.85	0.088	0.97
50	8.04	8.20	0.078	0.98
80	9.39	9.83	0.070	0.96
120	11.31	11.68	0.070	0.9
200	14.50	14.84	0.064	0.98
300	16.99	17.17	0.067	0.99
400	19.62	20.01	0.067	0.98
500	21.50	21.65	0.066	0.99
700	25.55	25.17	0.067	1.02
900	28.91	28.37	0.060	1.02

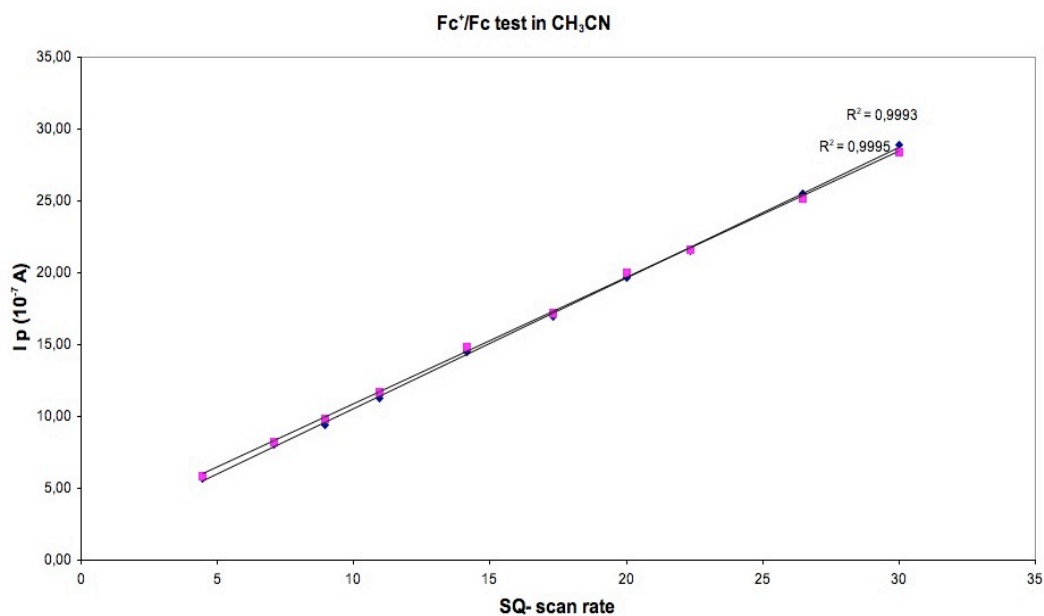


Figure 6.5 Plot of i_p^a (blue dots) vs. $\sqrt{\text{scan rate}}$ and $-i_p^c$ (purple dots) vs. $\sqrt{\text{scan rate}}$ for $\text{Fc}^{0/+}$ couple in CH_3CN

Table 6.2 Electrochemical characteristics in CH_2Cl_2 of the couple $\text{Fc}^{0/+}$

s.r.	i_p^a	$-i_p^c$	ΔE	i^a/i^c
20	6.12	5.60	0.137	1.09
50	8.73	6.38	0.084	1.37
80	10.67	8.61	0.087	1.24
120	12.77	10.29	0.087	1.24
200	15.25	12.30	0.082	1.24
300	17.50	13.74	0.080	1.27
400	19.70	14.91	0.085	1.32
500	21.38	17.22	0.080	1.24
700	23.69	19.48	0.099	1.22
900	26.93	21.60	0.082	1.25

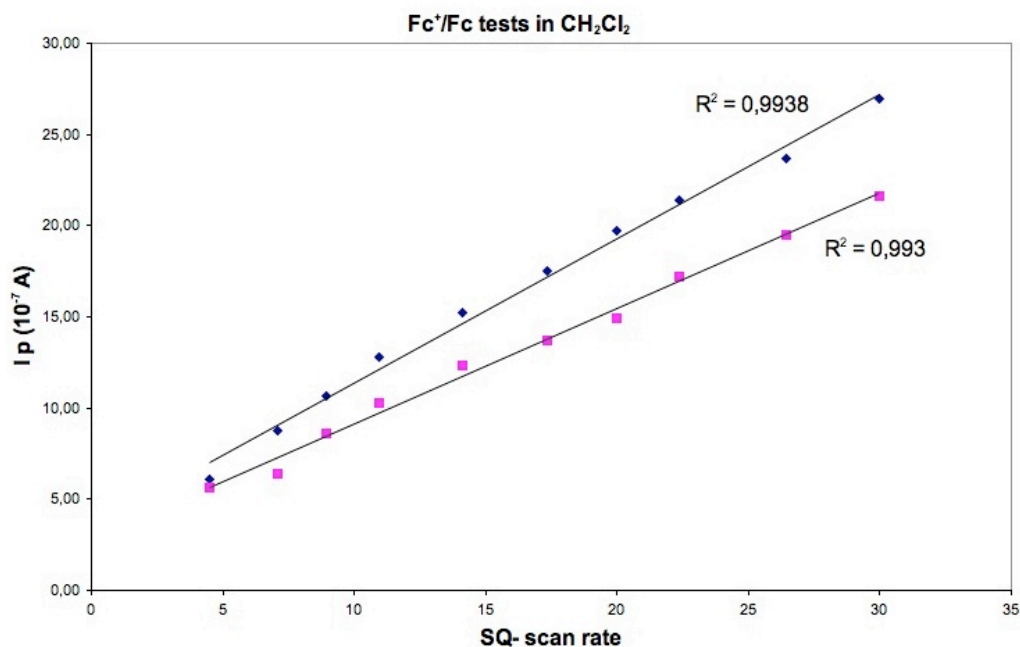


Figure 6.6 Plot of i_p^a (blue dots) vs. $\sqrt{\text{scan rate}}$ and $-i_p^c$ (purple dots) vs. $\sqrt{\text{scan rate}}$ for $\text{Fc}^{0/+}$ couple in CH_2Cl_2

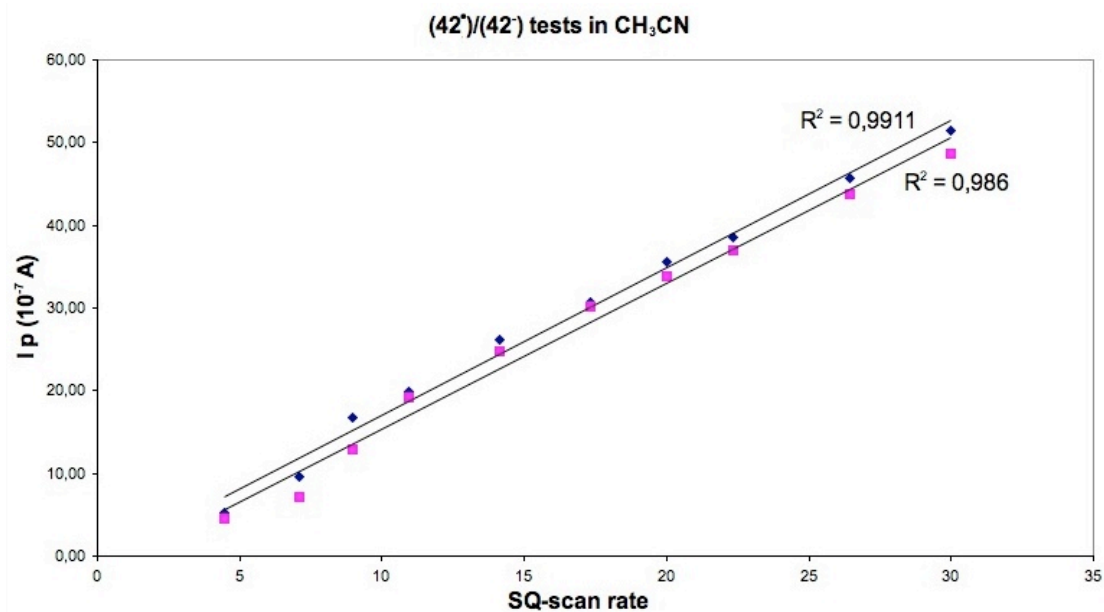
6.3.3.3 Reversibility of the oxidation/reduction process of $(42^{\cdot-})/(42^{\cdot})$

$(42^{\cdot-})/(42^{\cdot})$ pair shows very similar electrochemical behaviour in CH_3CN to that of the Fc^+/Fc couple (Tables 6.1 and 6.3); although it was observed that for low scan rates (*i.e.* 20, 50 and 80 $\text{mV}\cdot\text{s}^{-1}$) the i_p^a / i_p^c ratios were higher (Table 6.1).

However, for the $(42^{\bullet+})/(42^-)$ couple, i_p^c and i_p^a each varied linearly with the square root of the scan rate (Figure 6.7).

Table 6.3 Electrochemical characteristics in CH_3CN of the couple $(42^{\bullet+})/(42^-)$.

s.r.	i_p^a	$-i_p^c$	ΔE	i^a/i^c
20	5.23	4.45	0.071	1.18
50	9.52	7.10	0.061	1.34
80	16.77	12.97	0.055	1.29
120	19.86	19.19	0.060	1.03
200	26.11	24.76	0.059	1.05
300	30.71	30.16	0.062	1.02
400	35.56	33.86	0.057	1.05
500	38.59	36.96	0.059	1.04
700	45.73	43.71	0.061	1.05
900	51.52	48.66	0.058	1.06



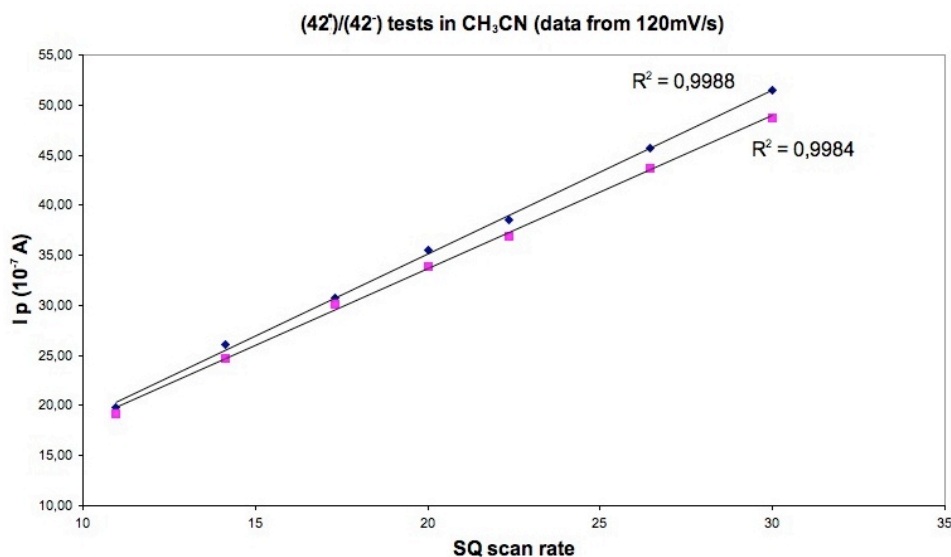


Figure 6.7 Plots of all data (previous page) and data for $s.r. > 120 \text{ mVs}^{-1}$ (this page) of i_p^a (blue dots) vs. $\sqrt{\text{scan rate}}$ and $-i_p^c$ (purple dots) vs. $\sqrt{\text{scan rate}}$ for (42[•])/(42⁻) in CH₃CN

Analogous considerations could be indicated for CV measurements in dichloromethane (Tables 6.2 and 6.4). The i_p^a/i_p^c ratio is higher than 1 (*i.e.* *ca.* 1.20) both for the Fc⁺/Fc and the (42[•])/(42⁻) couples.

Table 6.4 Electrochemical characteristics in CH₂Cl₂ of the couple (42[•])/(42⁻).

s.r.	i_p^a	$-i_p^c$	ΔE	i^a/i^c
20	7.59	6.46	0.076	1.18
50	11.03	9.53	0.079	1.16
80	13.25	11.83	0.077	1.12
120	15.37	13.56	0.067	1.13
200	19.54	15.66	0.082	1.25
300	23.22	18.95	0.076	1.23
400	25.23	20.83	0.085	1.21
500	28.49	23.62	0.094	1.21
700	31.86	27.03	0.099	1.18
900	35.25	29.80	0.100	1.18

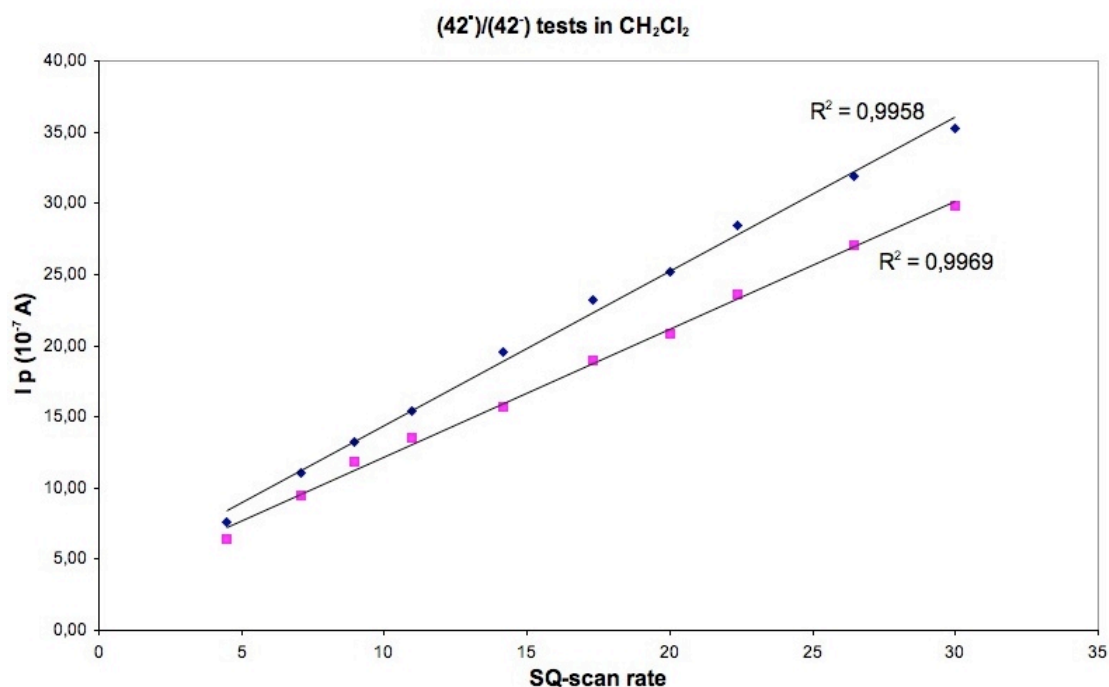


Figure 6.8 Plot of i_p^a (blue dots) vs. $\sqrt{\text{scan rate}}$ and $-i_p^c$ (purple dots) vs. $\sqrt{\text{scan rate}}$ for (42[•])/(42⁻) in CH₂Cl₂

6.3.3.4 Reversibility of the oxidation/reduction processes of (43[•])/(43⁻) and (43⁻)/(44[•])

(43[•])/(43⁻) and (44[•])/(44⁻) couples shows very similar electrochemical behaviour in CH₃CN to that of the Fc⁺/Fc couple (Tables 6.5 and 6.6); although it was observed that for low scan rates the i_p^a / i_p^c ratios were higher (for (43[•])/(43⁻) pair at 20 mV s⁻¹ i_p^c / i_p^a is 1.27, Table 6.5; and for (44[•])/(44⁻) at 20, 50, and 80 mV.s⁻¹, i_p^a / i_p^c are 1.21, 1.21, and 1.33 respectively). However, for the both (43[•])/(43⁻) and (44[•])/(44⁻) couples, i_p^c and i_p^a each varied linearly with the square root of the scan rate (Figures 6.9 and 6.10).

Table 6.5 Electrochemical characteristics in CH₃CN of the couple (43[•])/(43⁻)

s.r.	i_p^a	$-i_p^c$	ΔE	i^a/i^c
20	5.28	4.16	0.082	1.27
50	7.43	6.58	0.078	1.13
100	10.16	8.87	0.065	1.14

200	13.14	12.20	0.085	1.08
400	17.24	15.76	0.099	1.09
600	21.93	19.38	0.092	1.13
900	25.25	22.55	0.090	1.12

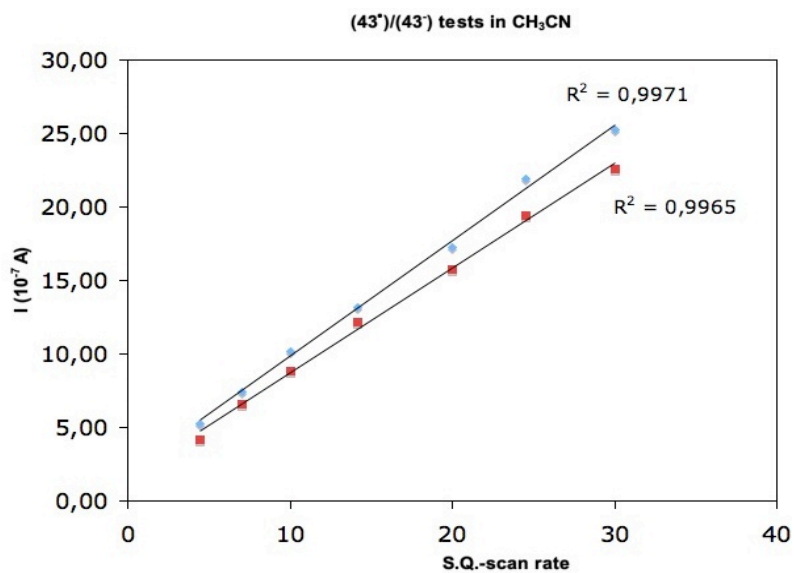


Figure 6.9 Plot of i_p^a (blue dots) vs. $\sqrt{\text{scan rate}}$ and $-i_p^c$ (red dots) vs. $\sqrt{\text{scan rate}}$ for (43⁺)/(43⁻) in CH₃CN

Table 6.6 Electrochemical characteristics in CH₃CN of the couple (44⁺)/(44⁻).

s.r.	i_p^a	$-i_p^c$	ΔE	i^c/i^a
20	4.97	4.11	0.080	1.21
50	6.94	5.72	0.089	1.21
80	8.41	6.30	0.078	1.33
120	9.68	8.22	0.073	1.19
200	11.24	9.49	0.069	1.18
300	13.18	11.11	0.077	1.19
400	14.64	13.58	0.078	1.08
500	15.30	14.44	0.077	1.06
700	16.81	16.12	0.080	1.04
900	18.77	18.75	0.089	1.00

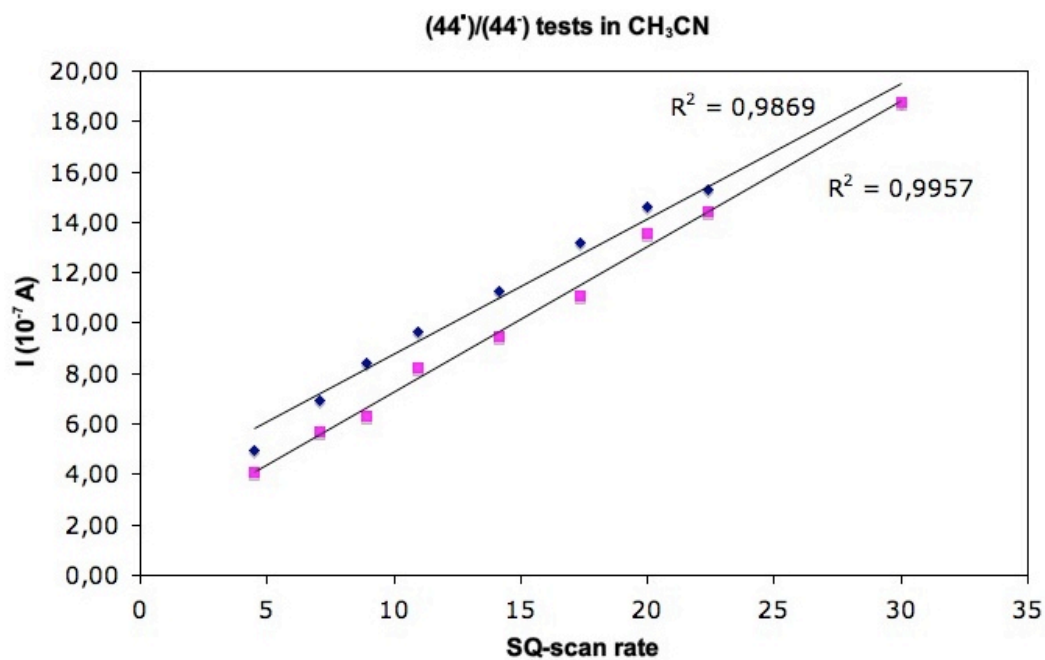


Figure 6.10 Plot of i_p^a (blue dots) vs. \sqrt{v} (scan rate) and $-i_p^c$ (purple dots) vs. \sqrt{v} (scan rate) for (44^{•+})/(44⁻) in CH₃CN.

Analogous reversibility tests of (43^{•+})/(43⁻) and (44^{•+})/(44⁻) couples in CH₂Cl₂ have furnished comparable results.

6.4 EPR conditions

(42^{*}), [^{NHOH}L]^{*} (in CH₃CN at 253-270 K): center field: 3354.3358; modulation frequency: 100 KHz; modulation amplitude: 1.0-0.1 Gpp; receiver gain: $4.48 \cdot 10^{-4}$; conversion time: 40.96 ms; time constant: 81.92 ms; ST : 40 s. **Calculation for 263 K:** *g* values were calculated from the formula $\nu = 1.39962 \cdot g \cdot B'$, where ν is the frequency measured (GHz) and B' is the corrected value of field (kGauss). The correction factor (ΔB) of field was calculated from the difference of theoretical and experimental values of field ($B' - B^{\text{exp}}$) of a reference compound (i.e. perylene radical in conc. sulphuric acid) with known *g* value (i.e. 2.002569): $B' = \nu^{\text{exp}} / (1.39962 \cdot g)$
Perylene radical in conc. sulfuric acid: *g* = 2.002569; B^{exp} = 3345.5890; ν^{exp} = 9.409219 GHz; $B' = 3357.0356$; $\Delta B = 11.4466$. [^{NHOH}L]^{*} : B^{exp} = 3341.3852; ν^{exp} = 9.405720 GHz; $B' = 3352.8318$; *g* = 2.00433.

(43^{*}), [^{NHMe}L]^{*} (in CH₃CN at 253-270 K): center field: 3354.6030; modulation frequency: 100 KHz; modulation amplitude: 1.0-0.1 Gpp; receiver gain: $4.48 \cdot 10^{-4}$; conversion time: 40.96 ms; time constant: 81.92 ms; ST : 40 s. **Calculation for 263 K: perylene radical in conc. sulfuric acid:** *g* = 2.002569; B^{exp} = 3347.2468; ν^{exp} = 9.411541 GHz; $B' = 3357.8641$; $\Delta B = 10.6172$. [^{NHMe}L]^{*} : B^{exp} = 3343.9866; ν^{exp} = 9.410058GHz; $B' = 3354.6038$; *g* = 2.00420.

(44^{*}), [^{NMe2}L]^{*} (in CH₃CN at 253-270 K): center field: 3353.3816; modulation frequency: 100 KHz; modulation amplitude: 1.0-0.1 Gpp; receiver gain: $4.48 \cdot 10^{-4}$; conversion time: 40.96 ms; time constant: 81.92 ms; ST : 40 s. **Calculation for 263 K: perylene radical in conc. sulfuric acid:** *g* = 2.002569; B^{exp} = 3348.1435; ν^{exp} = 9.414326 GHz; $B' = 3358.8577$; $\Delta B = 10.7142$. [^{NMe2}L]^{*} : B^{exp} = 3343.2112; ν^{exp} = 9.410179 GHz; $B' = 3353.9254$; *g* = 2.00463.

(47⁺), [^{NBu4}]₂[Ni₂(^{OHNH}L)₂]⁺ (in CH₃CN at 253-270 K): center field: 3350.9832; modulation frequency: 100 KHz; modulation amplitude: 1.0-0.2 Gpp; receiver gain: $4.48 \cdot 10^{-4}$; conversion time: 40.96 ms; time constant: 81.92 ms; ST : 40 s. **Calculation for 263 K: perylene radical in conc. sulfuric acid:** *g* = 2.002569; B^{exp} = 3345.1501; ν^{exp} = 9.407328 GHz; $B' = 3356.3632$; $\Delta B = 11.2131$. [^{NBu4}]₂[Ni₂(^{OHNH}L)₂]⁺ : B^{exp} = 3340.2201; ν^{exp} = 9.396430 GHz; $B' = 3351.4332$; *g* = 2.00319.

6.5 Computational data

(7⁺)

Computational Details. The full geometry optimization of (7) and (7⁺) has been carried out in Cartesian coordinates at the DFT level of theory using the Gaussian 98¹⁶ package. The calculations have been performed using Becke's three-parameter hybrid exchange functional¹⁷ in combination with the gradient-corrected correlation functional of Lee, Yang, and Parr¹⁸ (B3LYP) and the 6-31G* basis set. Restricted approximations for the structure with closed electron shells and unrestricted methods for the structure with open electron shells have been employed. Symmetry operations were not applied. The Hessian matrix was calculated analytically to prove the location of correct minimum (no imaginary frequencies were found). The hybridization of atomic orbitals has been calculated using the natural bond orbital (NBO) partitioning scheme.¹⁹ The experimental X-ray geometry of (7) was taken as a basis for the initial geometry of the optimization processes.

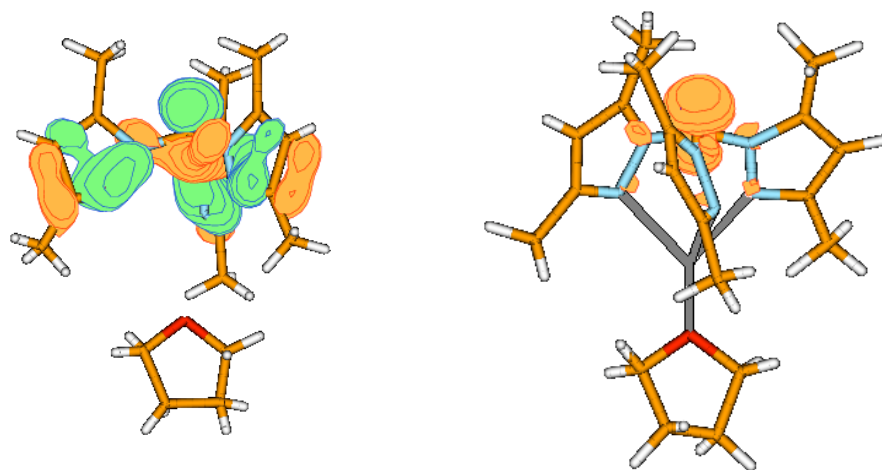


Figure 6.11 Plots of SOMO orbital (left) and spin density (right) for (7⁺).

atom/ Mulliken atomic spin densities					
1 N	-0,000149	21 H	-0,000106	41 C	0,032189
2 C	0,73872	22 C	-0,000046	42 C	0,000311
3 O	-0,000019	23 H	-0,000083	43 H	-0,000002

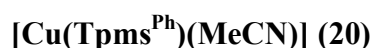
4 Li	-0,003669	24 H	0,000585	44 H	0,003345
5 N	0,018811	25 H	0,000424	45 H	0,000007
6 N	0,001029	26 C	0,001377	46 C	0,000007
7 N	0,01995	27 C	0,031243	47 H	-0,000001
8 N	0,000174	28 H	-0,001546	48 H	-0,000002
9 N	0,019598	29 C	0,03206	49 C	-0,000001
10 C	-0,000111	30 C	0,000361	50 H	0
11 H	0,000012	31 H	-0,000105	51 H	0
12 H	0,00059	32 H	0,000217	52 C	-0,000002
13 H	0,000456	33 H	0,003244	53 H	0,000002
14 C	0,002777	34 C	-0,000056	54 H	0
15 C	0,030316	35 H	-0,00004	55 C	0,000001
16 H	-0,0015	36 H	0,000585	56 H	-0,000001
17 C	0,033578	37 H	0,00044	57 H	0
18 C	0,000166	38 C	0,001905		
19 H	0,000325	39 C	0,030902		
20 H	0,003268	40 H	-0,001536		

(47⁺)

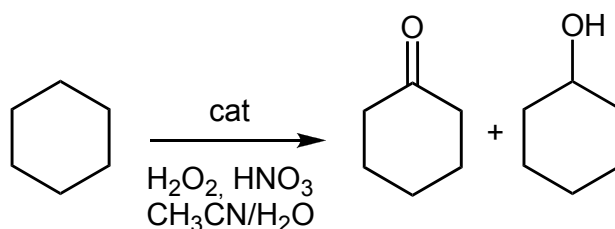
atom/ Mulliken atomic spin densities					
1 C	-0,019906	16 H	-0,001919	31 H	0,001043
2 C	0,047606	17 H	-0,002733	32 C	-0,007461
3 C	-0,005166	18 N	0,11126	33 H	0,001829
4 C	0,038557	19 O	0,004805	34 H	0,011925
5 C	-0,020783	20 O	0,066528	35 C	-0,00387
6 H	0,000704	21 O	0,066118	36 H	0,000418
7 C	0,058448	22 Ni	0,172852	37 H	0,010203
8 C	-0,030314	23 C	-0,019882	38 H	-0,001922
9 H	0,001042	24 C	0,047642	39 H	-0,002736
10 C	-0,007469	25 C	-0,005194	40 N	0,11107
11 H	0,001832	26 C	0,038605	41 O	0,004753
12 H	0,01194	27 C	-0,020815	42 O	0,06642
13 C	-0,003861	28 H	0,000705	43 O	0,06619
14 H	0,000415	29 C	0,058501	44 Ni	0,17276
15 H	0,010194	30 C	-0,030337		

6.6 Catalytic studies

Gas chromatographic (GC) measurements were carried out using a FISON Instruments GC 8000 series gas chromatograph with a FID detector and a capillary column (DB-WAX, column length: 30 m; internal diameter: 0.32 mm). The temperature of the injector was 240 °C. The initial temperature was maintained at 100 °C for 1 min, then raised 10 °C/min to 180 °C and held at this temperature for 1 min. Helium was used as the carrier gas.



Oxidation of cyclohexane to cyclohexanol and cyclohexanone.

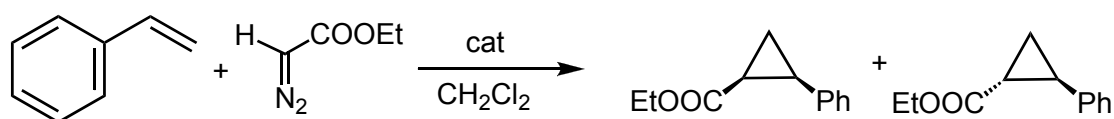


entry	n(cat)/n(C ₆ H ₁₂) *10 ³	n(H ₂ O ₂)/n(cat) *10 ⁻³	Acid	yield (%) (one/ol)	TON (one/ol)	T (° C)
1	2	0.5	yes	0.18/0.06	0.9/0.3	r.t.
2	2	0.5	yes	0.26/0.10	1.3/0.5	40° C
3	1	1	yes	0.10/0.03	1.0/0.3	r.t.
4	0.5	2	yes	0.07/-	1.4/-	r.t.
5	2	0.5	no	-/-	-	r.t.
6	5	0.2	yes	0.32/0.11	0.64/0.22	40° C

The oxidation reactions were carried out in Schlenk tubes and under dinitrogen. In typical conditions the reaction mixtures were prepared as follows: a suitable amount of catalyst precursor (**20**) was dissolved in 3 mL of MeCN. A 30% water solution of H₂O₂ (0.50 mL, 5.00 mmol) and cyclohexane (540 μL, 5.0 mmol) were then added and the reaction mixture was stirred for 6 h, at the desired

temperature and atmospheric pressure. In the experiments with HNO₃, this acid was added immediately before the addition of the substrate. For the analysis of the products, 90 μL of cycloheptanone (internal standard) and 6.5 mL of diethyl ether (to extract the substrate and the organic products from the reaction mixture) were added. The obtained mixture was stirred during 10 min and then a sample (1 μL) was taken from the organic phase and analyzed by GC by the internal standard method.

Cyclopropanation of styrene with ethyldiazoacetate.



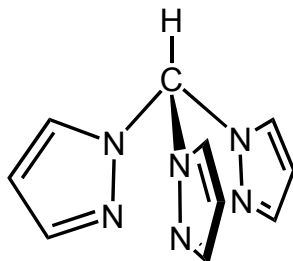
entry	mol styrene/EDA/cat	yield (byproducts) ^a	yield ^b (%)	time (h)	T (° C)
1	500/10/1	78 %	5.4 %	20 h	r.t.
2	500/10/2	82 %	7 %	20 h	r.t.

(a) total yield of diethylfumarate and diethylmaleate based on ¹H-NMR. (b) based on ¹H-NMR.

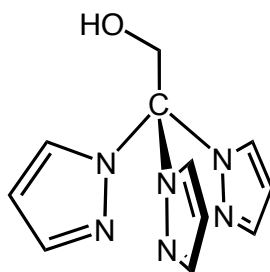
To a dichloromethane solution (3 mL) of styrene, a suitable amount of catalyst and diazocompound were added. The final solution was stirred at room temperature for 20 h. The solvent was removed under vacuum and the crude was analysed by ¹H-NMR in CDCl₃.

6.7 Compounds

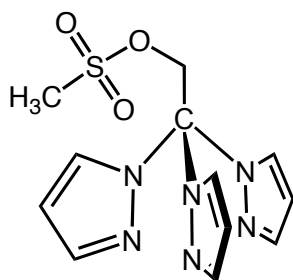
(1), hydrotris(pyrazolyl)methane, Tpm, $\text{HC}(\text{pz})_3$ (pz = pyrazolyl).



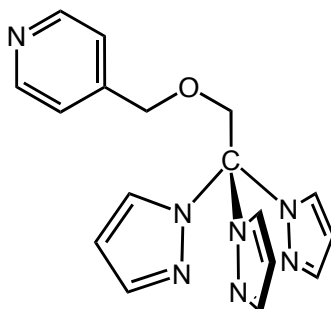
(2), tris-2,2,2-(1-pyrazolyl)ethanol, $\text{HOCH}_2\text{C}(\text{pz})_3$ (pz = pyrazolyl).



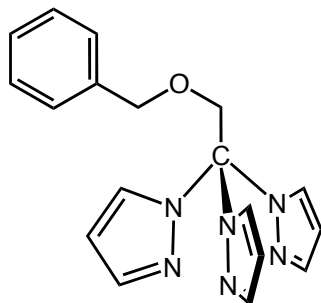
(2-Ms) 2,2,2-tri(pyrazol-1-yl)ethyl methanesulfonate, $\text{H}_3\text{CSO}_2\text{OCH}_2\text{C}(\text{pz})_3$ (pz = pyrazolyl).



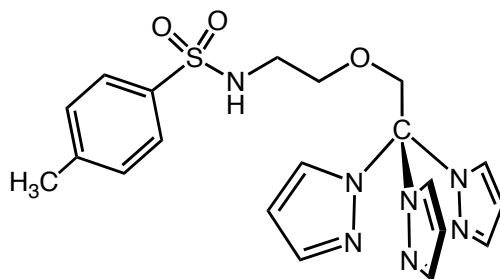
(3), 4-((tris-2,2,2-(pyrazol-1-yl)ethoxy)methyl)pyridine, TpmPy, (4-py)CH₂OCH₂C(pz)₃ (pz = pyrazolyl).



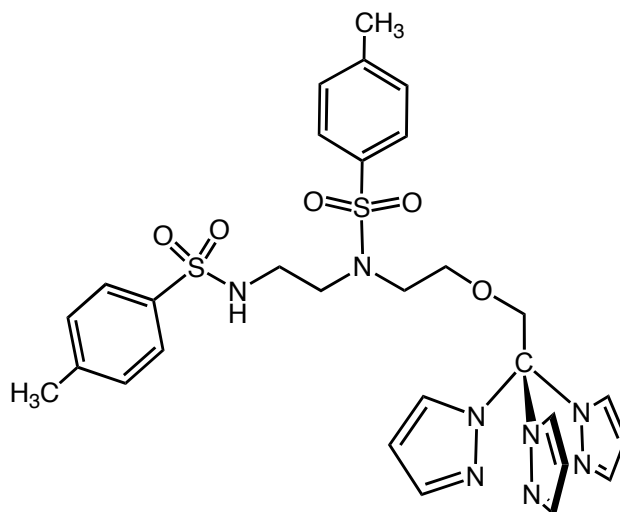
(4), (tris-2,2,2-(pyrazol-1-yl)ethoxy)benzyl, $\text{PhCH}_2\text{OCH}_2\text{C}(\text{pz})_3$ (pz = pyrazolyl).



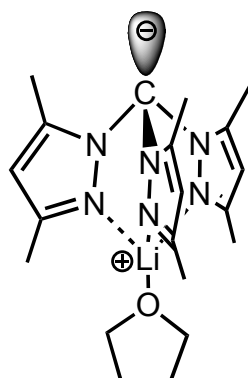
(5), $\text{TsNHCH}_2\text{CH}_2\text{OCH}_2\text{C}(\text{pz})_3$ (Ts = *para*-toluenesulfonyl, pz = pyrazolyl).



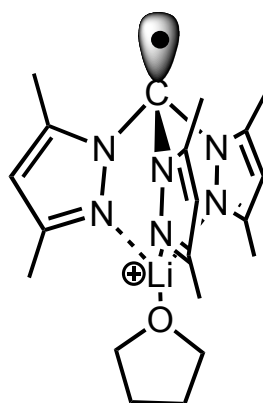
(6), $\text{TsNHCH}_2\text{CH}_2\text{TsNCH}_2\text{CH}_2\text{OCH}_2\text{C}(\text{pz})_3$ (Ts = *para*-toluenesulfonyl, pz = pyrazolyl).



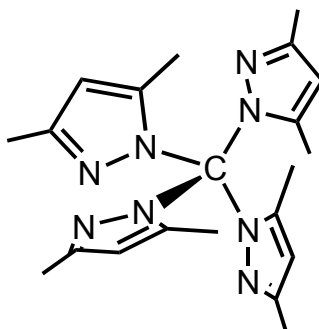
(7), twitterionic tris(3,5-dimethylpyrazolyl)methane lithium tetrahydrofuran complex, $[\{C(pz^{Me_2})_3\}Li^+(thf)]$, ($pz^{Me_2} = 3,5$ -dimethylpyrazolyl).



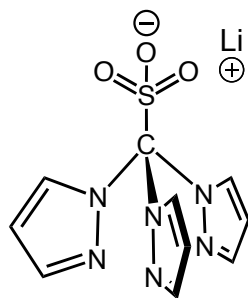
(7⁺), cationic tris(3,5-dimethylpyrazolyl)methane lithium tetrahydrofuran radical, $[\{C(pz^{Me_2})_3\}Li(thf)]^+$, ($pz^{Me_2} = 3,5$ -dimethylpyrazolyl).



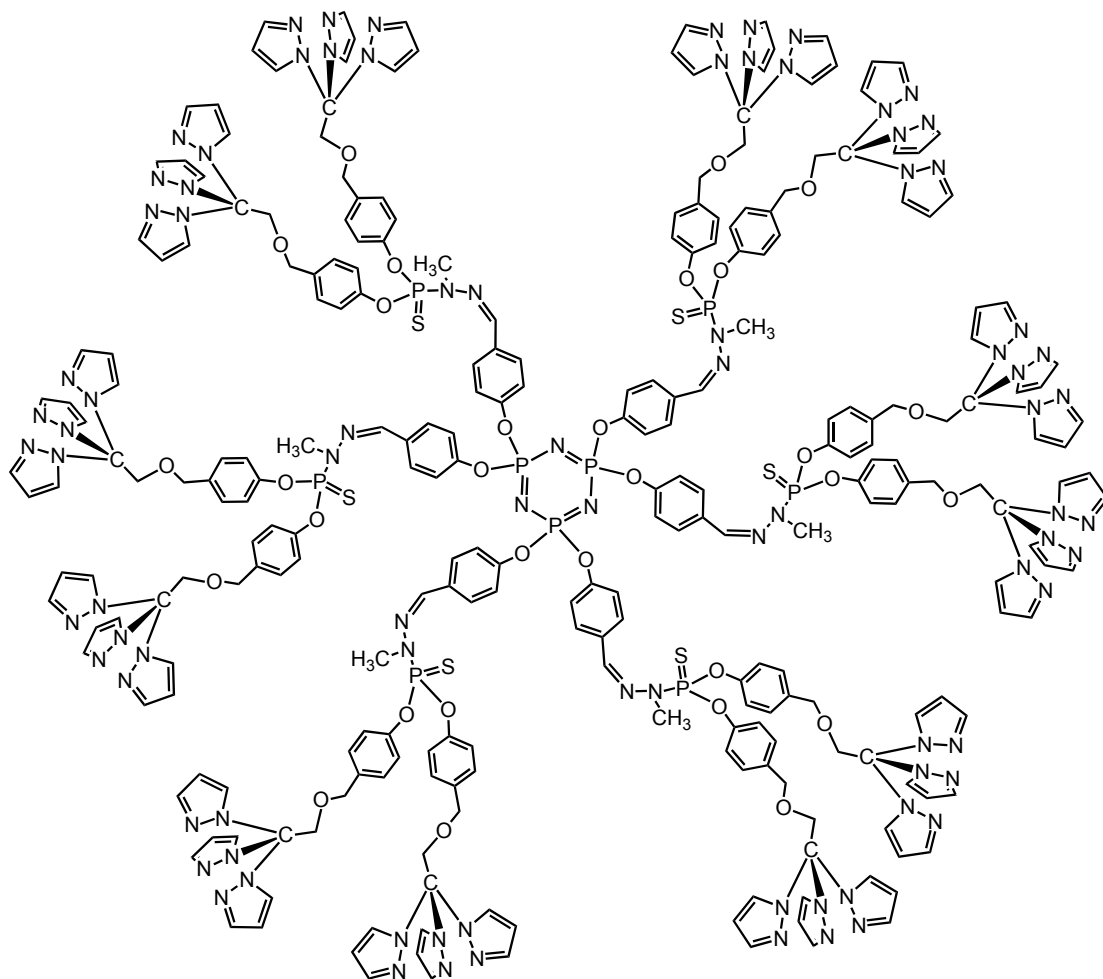
(8), Synthesis of tetrakis(3,5-dimethylpyrazolyl)methane, $C(pz^{Me_2})_4$ ($pz^{Me_2} = 3,5$ -dimethylpyrazolyl).



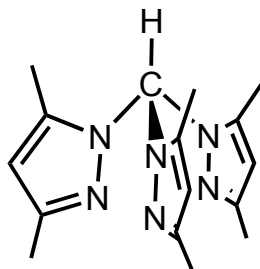
(9), lithium tris(pyrazolyl)methanesulfonate, [Tpms]Li, [O₃SC(pz)₃]Li, (pz = pyrazolyl).



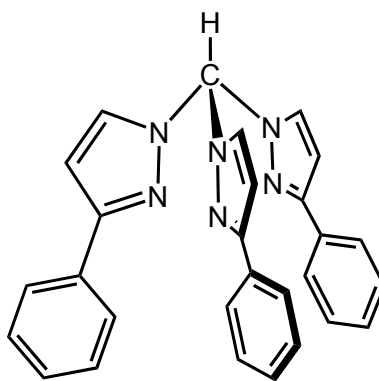
(10), N₃P₃-G_{c1}-[CH₂C(pz)₃]₁₂.



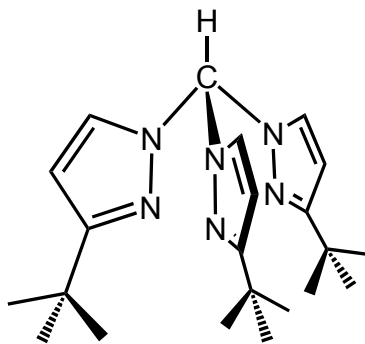
(11), tris(3,5-dimethylpyrazolyl)methane, Tpm^{Me_2} , $\text{C}(\text{pz}^{\text{Me}_2})_3$ (pz^{Me_2} = 3,5-dimethyl-pyrazolyl).



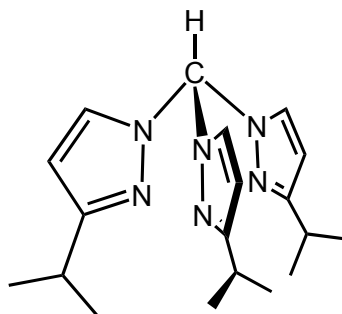
(12), tris(3-phenylpyrazolyl)methane, Tpm^{Ph} , $\text{C}(\text{pz}^{\text{Ph}})_3$ (pz^{Ph} = 3-phenyl-pyrazolyl).



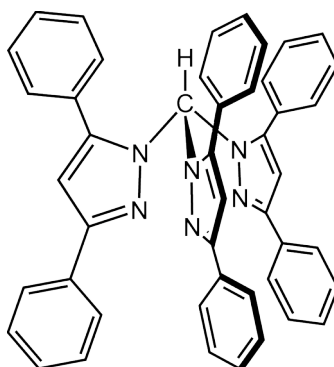
(13), tris(3-*tert*-butylpyrazolyl)methane, Tpm^{tBu} , $\text{C}(\text{pz}^{\text{tBu}})_3$ (pz^{tBu} = 3-*tert*-butyl-pyrazolyl).



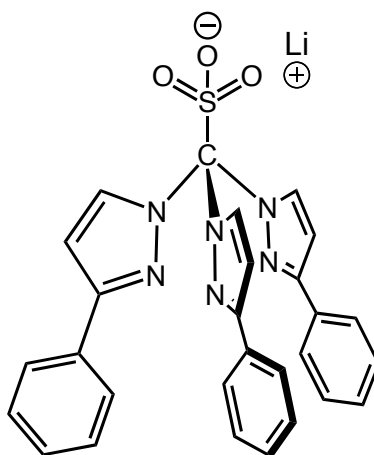
(14), tris(3-*iso*-propylpyrazolyl)methane, Tpm^{iPr} , $\text{C}(\text{pz}^{\text{iPr}})_3$ (pz^{iPr} = 3-*iso*-propyl-pyrazolyl).



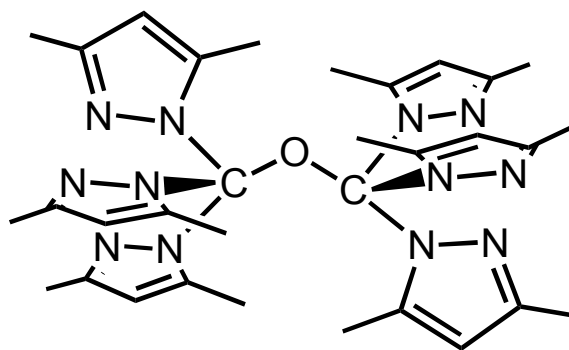
(15), tris(3,5-diphenylpyrazolyl)methane, Tpm^{Ph_2} , $\text{C}(\text{pz}^{\text{Ph}_2})_3$ (pz^{Ph_2} = 3,5-diphenyl-pyrazolyl).



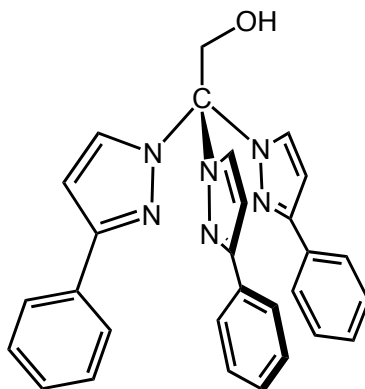
(16), lithium tris(3-phenylpyrazolyl)methanesulfonate, $[\text{Tpms}^{\text{Ph}}]\text{Li}$, $[\text{O}_3\text{SC}(\text{pz}^{\text{Ph}})_3]\text{Li}$, (pz^{Ph} = 3-phenyl-pyrazolyl).



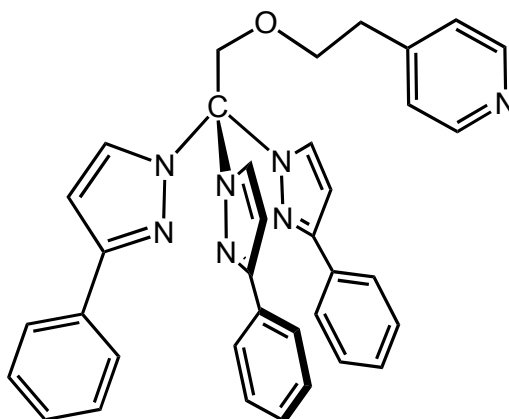
(17), $[(\text{pz}^{\text{Me}_2})_3\text{C}-\text{O}-\text{C}(\text{pz}^{\text{Me}_2})_3]$ (pz^{Me_2} = 3,5-dimethylpyrazolyl).



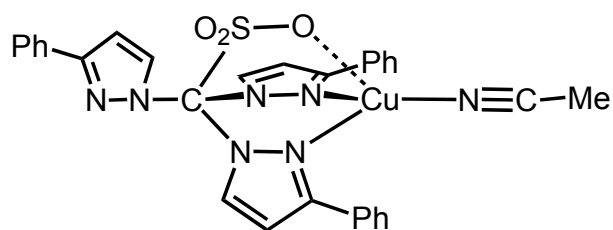
(18), 4-((tris-2,2,2-(3-phenylpyrazol-1-yl)ethanol, $\text{HOCH}_2\text{C}(\text{pz}^{\text{Ph}})_3$ (pz^{Ph} = 3-phenyl-pyrazolyl).



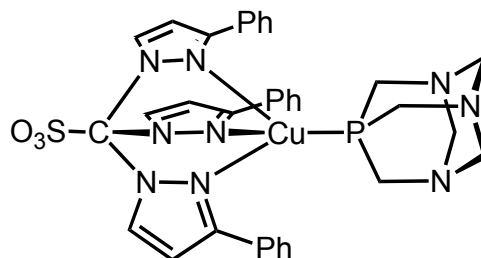
(19), TpmPy^{Ph} , 4-((tris-2,2,2-(3-phenylpyrazol-1-yl)ethoxy)methyl)pyridine,



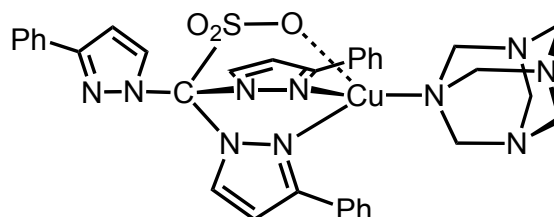
(20), [Cu(Tpms^{Ph})(MeCN)].



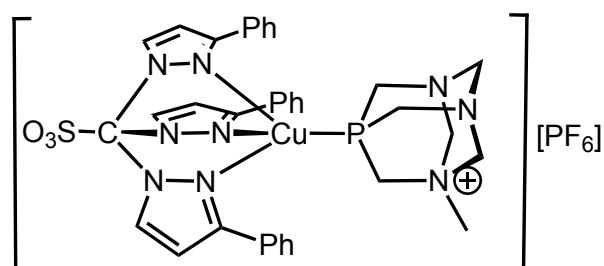
(21), [Cu(Tpms^{Ph})(PTA)].



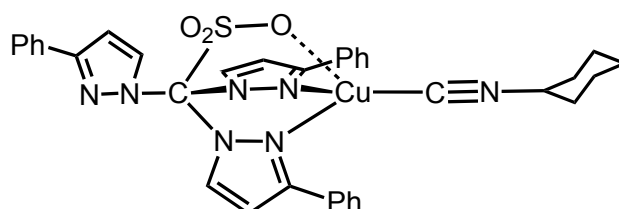
(22), [Cu(Tpms^{Ph})(HMT)].



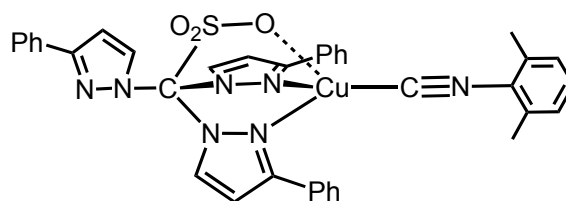
(23), [Cu(Tpms^{Ph})(mPTA)][PF₆].



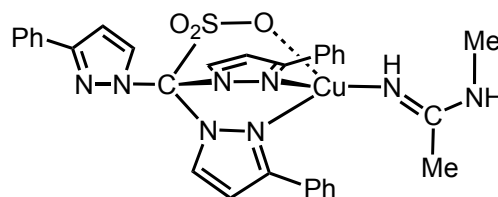
(24), [Cu(Tpms^{Ph})(CyNC)] (CyNC = cyclohexyl isocyanide)



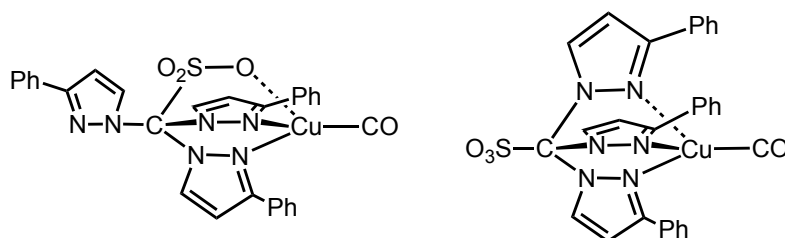
(25), [Cu(Tpms^{Ph})(XyNC)] (XyCN = 2,6-dimethylphenyl isocyanide)



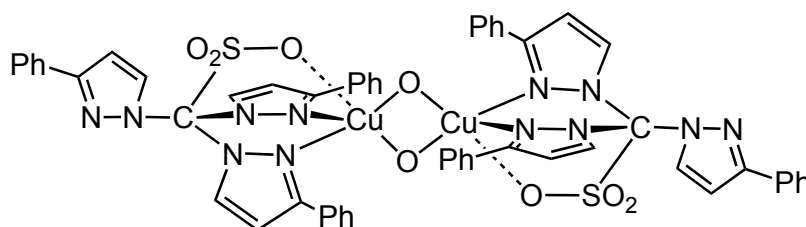
(26), [Cu(Tpms^{Ph})(L)] (L = MeC(=NH)NHMe).



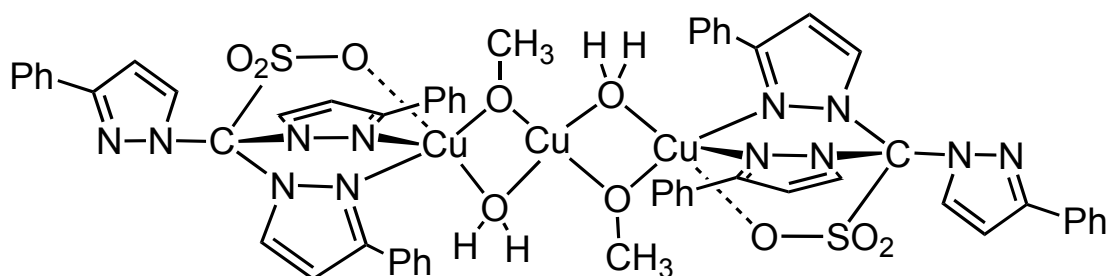
(27), [Cu(Tpms^{Ph})(CO)]

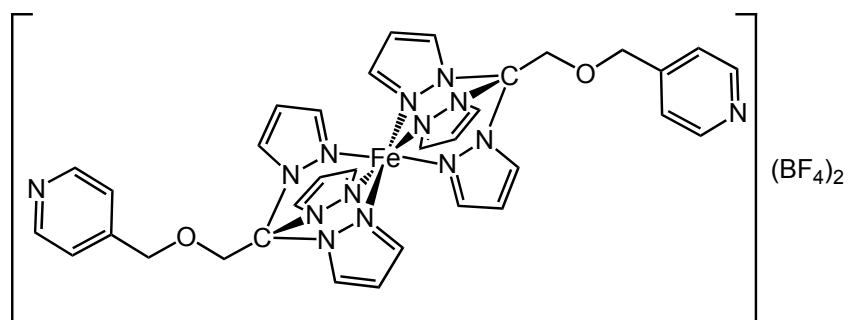
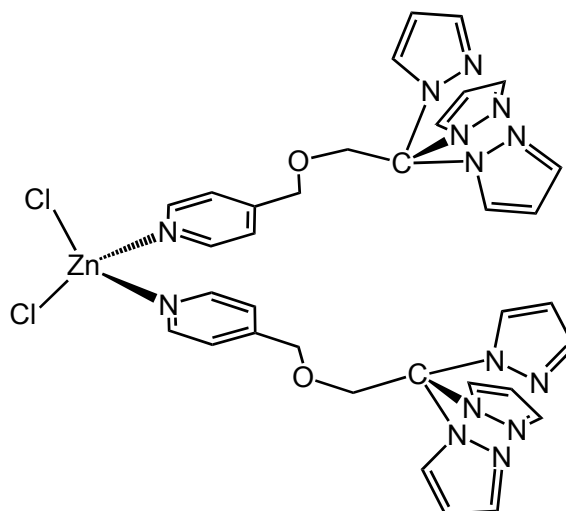
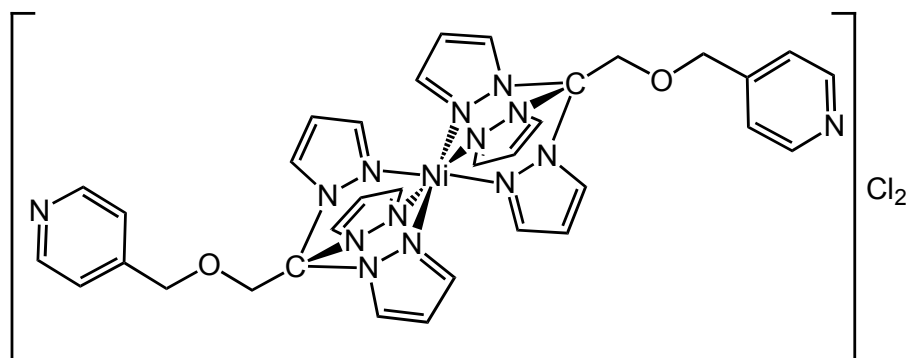


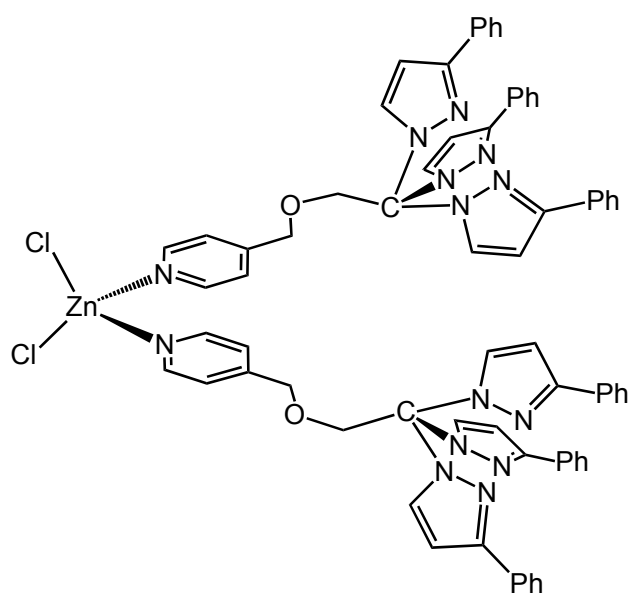
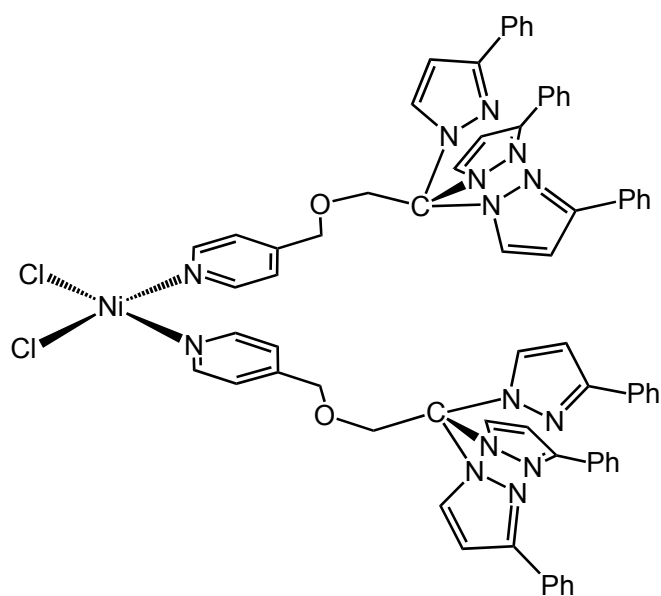
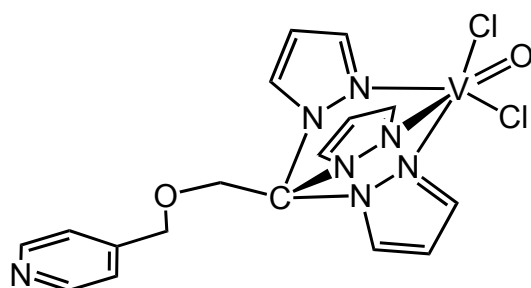
(28), [Cu(μ-O)(Tpms^{Ph})₂].

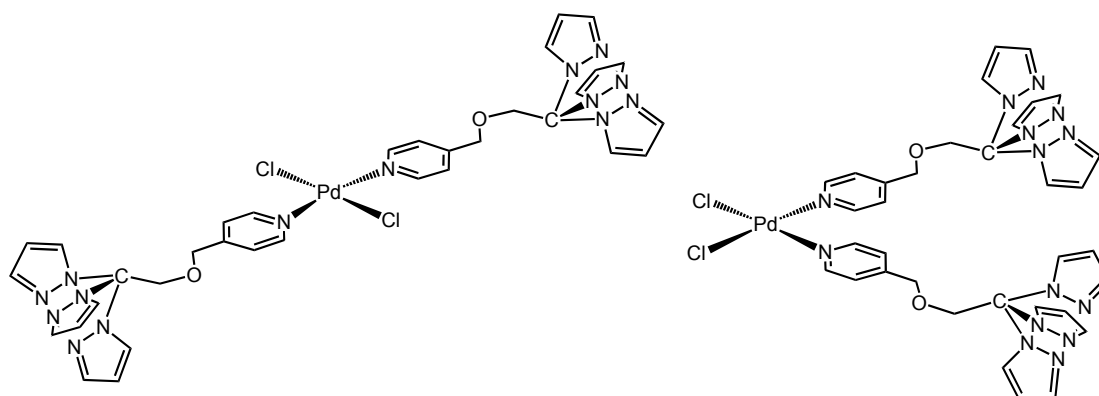
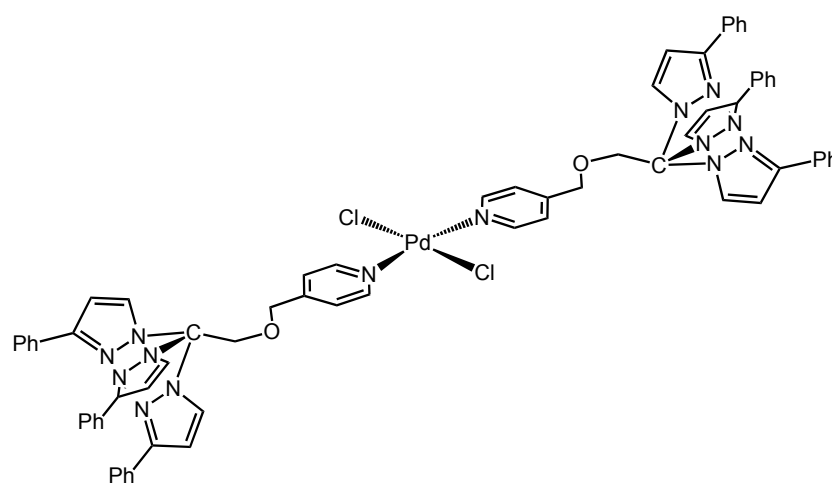
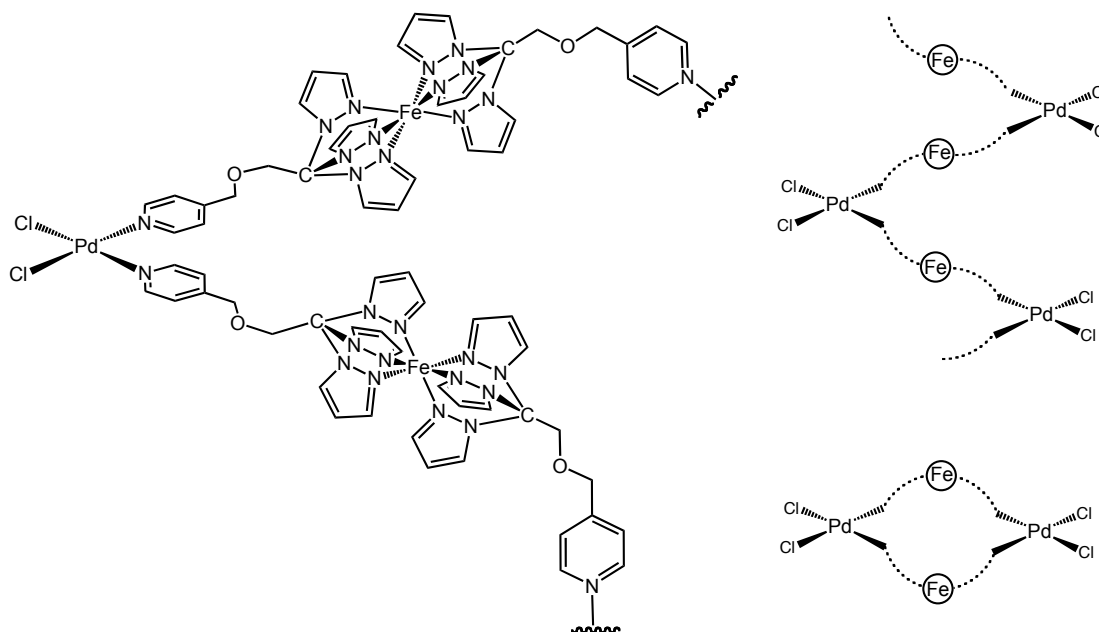


(29), [(μ-Cu^{II}){Cu^I(Tpms^{Ph})(μ-OH₂)(μ-OMe)}₂]

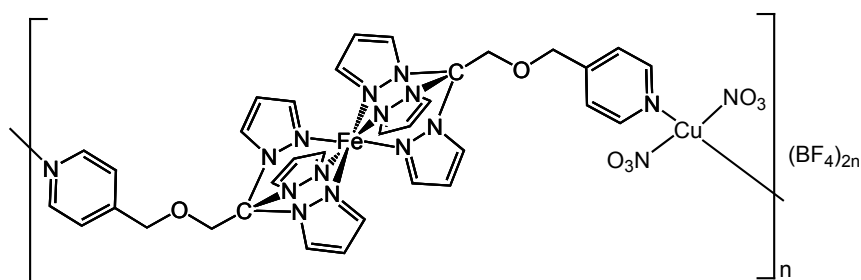


(30), [Fe(TpmPy)₂][BF₄]₂.**(31), Synthesis of [ZnCl₂(TpmPy)₂].****(32), [Ni(TpmPy)₂Cl₂].**

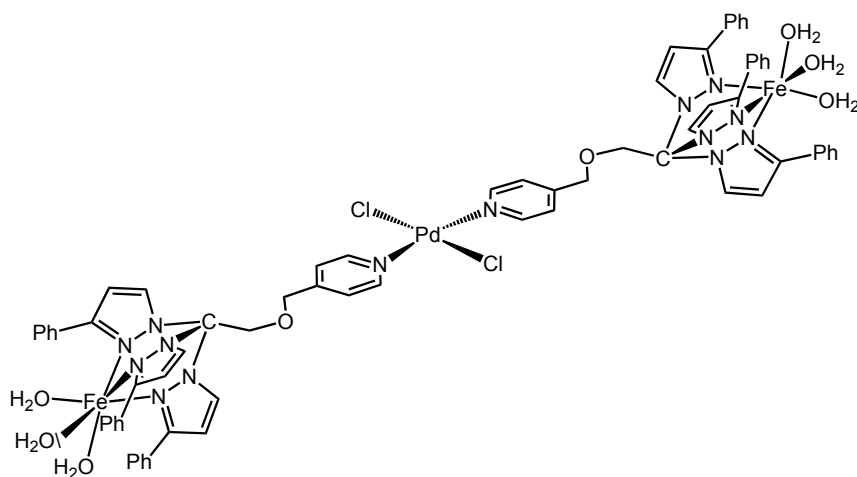
(33), [ZnCl₂(TpmPy^{Ph})₂].**(34), [NiCl₂(TpmPy^{Ph})₂].****(35), [VOCl₂(TpmPy)].**

(36), [PdCl₂(TpmPy)₂].**(37), [PdCl₂(TpmPy^{Ph})₂].****(38), [PdCl₂(μ-TpmPy)₂Fe](BF₄)₂ (proposed).**

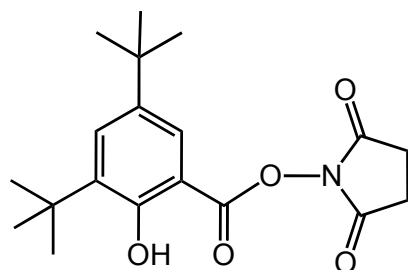
(39), $[\text{Fe}(\mu\text{-TpmpPy})_2\text{Cu}(\text{NO}_3)_2](\text{BF}_4)_2$ (proposed).



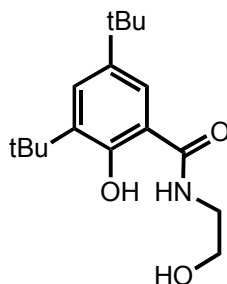
(40), $[\text{PdCl}_2(\mu\text{-TpmpPy}^{\text{Ph}})_2\text{Fe}_2(\text{H}_2\text{O})_6](\text{BF}_4)_4$.



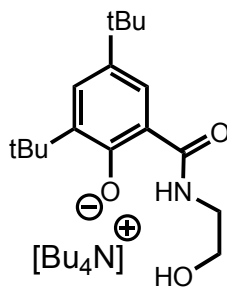
(41), N-3,5-di-*tert*-butylsalicyloxysuccinimide.



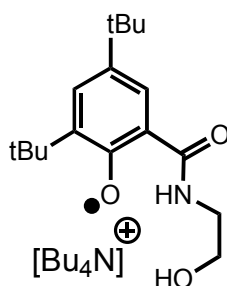
(42), 3,5-di-*tert*-butyl-2-hydroxy-N-(2-hydroxyethyl) benzamide, ^{NHOH}LH.



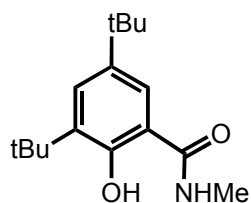
(42⁻), tetrabutyl ammonium salt of 2,4-di-*tert*-butyl-6-(2-hydroxyethylcarbamoyl)phenolate, $[\text{NBu}_4][^{\ominus}\text{OHNH}_2\text{L}]$.



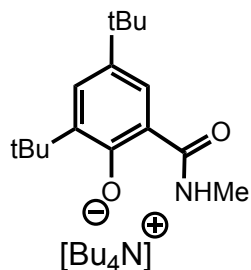
(42[']), 2,4-di-*tert*-butyl-6-(2-hydroxyethylcarbamoyl)phenoxyradical, $[\text{OHNH}_2\text{L}]^{\bullet}$.



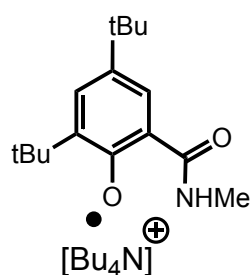
(43), 3,5-di-*tert*-butyl-2-hydroxy-N-methyl benzamide, $^{\text{NHMe}}\text{LH}$.



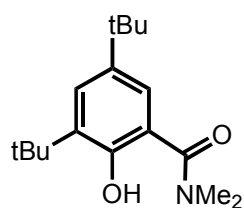
(43⁻), tetrabutyl ammonium salt of 2,4-di-*tert*-butyl-6-(2-methylcarbamoyl)phenolate, $[\text{NBu}_4][^{\ominus}\text{NHMeL}]$.



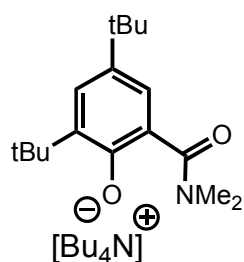
(43'), 2,4-di-*tert*-butyl-6-(2-methylcarbamoyl)phenoxyradical, [^{NHMe}L][•].



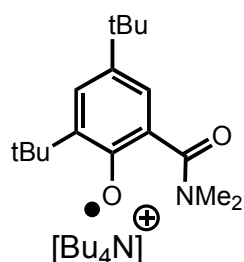
(44), 3,5-di-*tert*-butyl-2-hydroxy-N-dimethyl benzamide, ^{NMe2}LH.



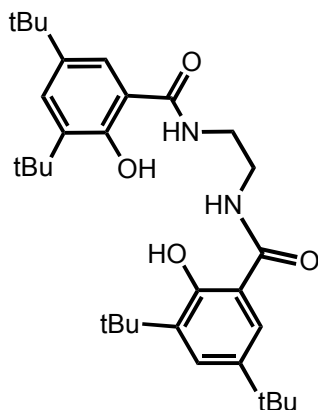
(44'), tetrabutyl ammonium salt of 2,4-di-*tert*-butyl-6-(2-dimethylcarbamoyl)phenolate, [NBu₄][^{NMe2}L]



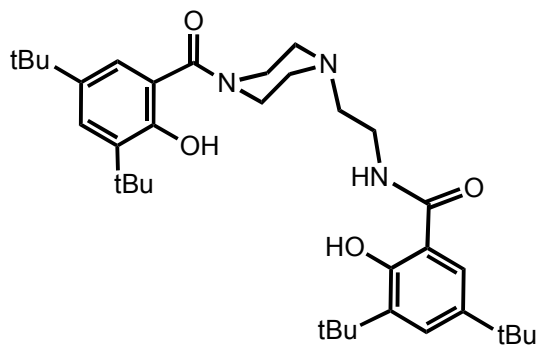
(44'), 2,4-di-*tert*-butyl-6-(2-dimethylcarbamoyl)phenoxyradical, [^{NMe2}L][•].



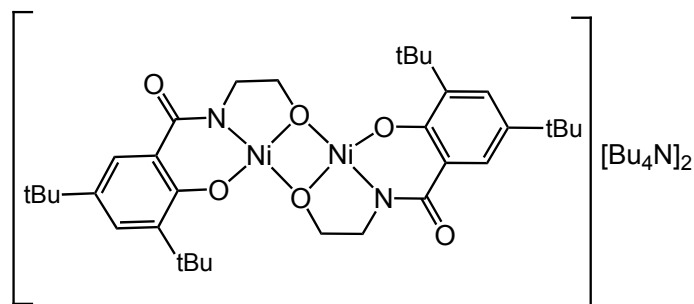
(45), N,N' -(ethane-1,2-diyl)bis(3,5-di-*tert*-butyl-2-hydroxybenzamide), $^{\text{NH}}\text{L}_2\text{H}_2$.

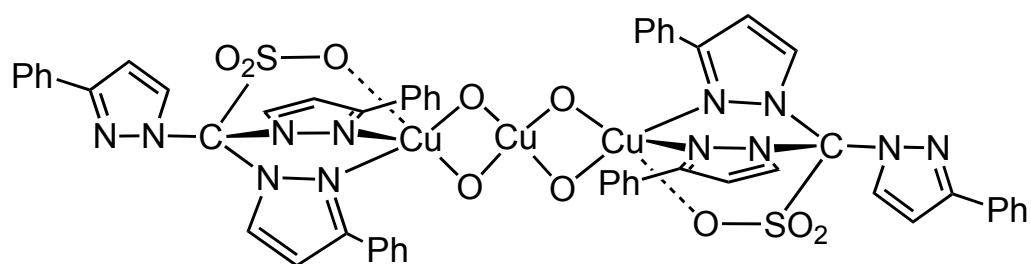
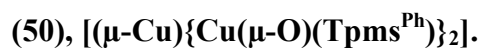
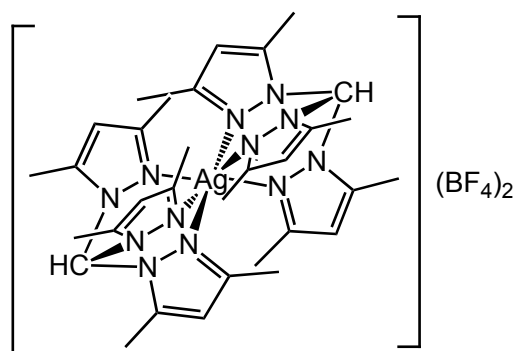
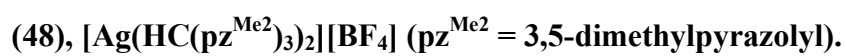
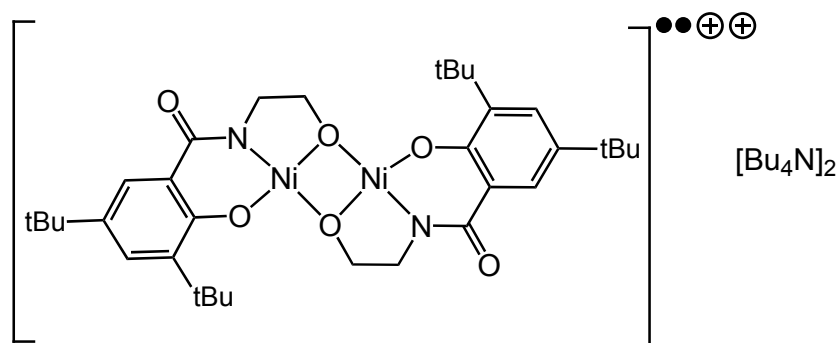
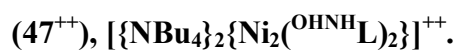
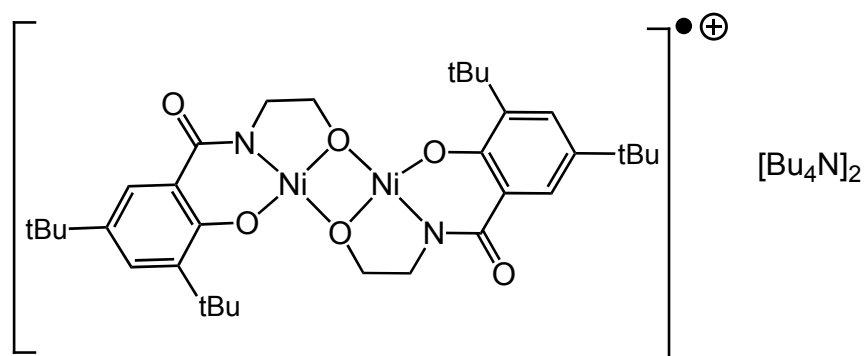
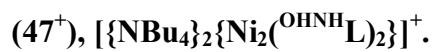


(46), 3,5-di-*tert*-butyl-2-hydroxy-N-(2-(4-(3,5-di-*tert*-butyl-2-hydroxybenzoyl)piperazin-1-yl)ethyl)benzamide, $^{\text{N}^3}\text{L}_2\text{H}_2$.



(47), $[\text{NBu}_4]_2[\text{Ni}_2(\text{OHNH}\text{L})_2]$.





References

- [1] Reger, D. L.; Grattan, T. C.; Brown, K. J.; Little, C. A.; Lamba, J. J. S.; Rheingold, A. L.; Sommer, R. D., *J. Organomet. Chem.* **2000**, *607*, 120.
- [2] Klaui, W.; Berghahn, M.; Rheinwald, G.; Lang, H. R., *Angew. Chem., Int. Ed.* **2000**, *39*, 2464.
- [3] Trofimenko, S.; Calabrese, J. C.; Thompson, J. S., *Inorg. Chem.* **1987**, *26*, 1507.
- [4] Trofimenko, S.; Calabrese, J. C.; Domaille, P. J.; Thompson, J. S., *Inorg. Chem.* **1989**, *28*, 1091.
- [5] Daigle, D. J.; Decuir, T. J.; Robertson, J. B.; Darenbourg, D. J., *Inorg. Synth.* **1998**, *32*, 40.
- [6] Daigle, D. J.; Pepperma, Ab; Vail, S. L., *J. Heterocycl. Chem.* **1974**, *11*, 407.
- [7] Bruker, *APEX2 & SAINT*. Madison, Wisconsin, USA, 2004.
- [8] Sheldrick, G. M., *Acta Crystallogr., Sect. A: Found. Crystallogr.* **1990**, *46*, 467.
- [9] Sheldrick, G. M., *Acta Crystallogr., Sect. A: Found. Crystallogr.* **2008**, *A64*, 112.
- [10] Farrugia, L. J., *J. Appl. Crystallogr.* **1999**, *32*, 837.
- [11] Spek, A. L., *Acta Crystallogr., Sect. C* **1990**, *46*, C34.
- [12] Kubas, G. J., *Inorg. Synth.* **1990**, *28*, 68.
- [13] Gagné, R. R.; Koval, C. A.; Lisensky, G. C., *Inorg. Chem.* **1980**, *19*, 2854.
- [14] Bard, A. J.; Faulkner, L. R., *Electrochemical methods, Fundamentals and Applications*. 2001.
- [15] Bordwell, F. G.; Cheng, J. P., *J. Am. Chem. Soc.* **1991**, *113*, 1736.
- [16] T. Frisch, M. J.; Trucks, G. W.; Schlegel, H. B.; Scuseria, G. E.; Robb, M. A.; Cheeseman, J. R.; Zakrzewski, V. G.; Montgomery, J. A.; Stratmann, R. E.; Burant, J. C.; Dapprich, S.; Millam, J. M.; Daniels, A. D.; Kudin, K. N.; Strain, M. C.; Farkas, O.; Tomasi, J.; Barone, V.; Cossi, M.; Cammi, R.; Mennucci, B.; Pomelli, C.; Adamo, C.; Clifford, S.; Ochterski, J.; Petersson, G. A.; Ayala, P. Y.; Cui, Q.; Morokuma, K.; Malick, D. K.; Rabuck, A. D.; Raghavachari, K.; Foresman, J. B.; Cioslowski, J.; Ortiz, J. V.; Stefanov, B. B.; Liu, G.; Liashenko, A.; Piskorz, P.; Komaromi, I.; Gomperts, R.; Martin, R. L.; Fox, D. J.; Keith, T.; Al-Laham, M. A.; Peng, C. Y.; Nanayakkara, A.;

Gonzalez, C.; Challacombe, M.; Gill, P. M. W.; Johnson, B. G.; Chen, W.; Wong, M. W.; Andres, J. L.; Head-Gordon, M.; Replogle, E. S.; Pople, J. A., *Gaussian 98, revision A.9*. PA: Pittsburgh, 1998.

- [17] Becke, A. D., *J. Chem. Phys.* **1993**, *98*, 5648.
- [18] Lee, C. T.; Yang, W. T.; Parr, R. G., *Physical Review B* **1988**, *37*, 785.
- [19] Reed, A. E.; Curtiss, L. A.; Weinhold, F., *Chem. Rev.* **1988**, *88*, 899.



this book is printed on 100% recycled paper
este livro está impresso em 100% papel reciclado